FUNCTIONS OF MMRN1 IN PLATELET ADHESION & THROMBUS FORMATION

FUNCTIONS OF MULTIMERIN 1 (MMRN1) IN PLATELET ADHESION AND THROMBUS FORMATION, THROUGH INTERACTIONS WITH VON WILLEBRAND FACTOR (VWF)

By: D'ANDRA PARKER, HBSc

A Thesis Submitted to the School of Graduate Studies in Partial Fulfilment of the Requirements for the Degree Doctorate of Philosophy in Health Science

McMaster University DOCTORATE OF PHILOSOPHY (2017)

Hamilton, Ontario (Health Science)

TITLE: Functions of multimerin 1 (MMRN1) in platelet adhesion and thrombus formation, through interactions with von Willebrand factor (VWF)

AUTHOR: D'Andra Parker, HBSc (McMaster University)

SUPERVISOR: Dr. Catherine P.M. Hayward

NUMBER OF PAGES: xiv, 209

ABSTRACT

Multimerin 1 (MMRN1) is a massive, homopolymeric platelet and endothelial cell protein with functions that are emerging to support platelet adhesive processes. MMRN1 supports platelet adhesion under arterial flow conditions by a mechanism dependent on interactions with von Willebrand factor (VWF). The goals of this thesis were to further define the platelet adhesive functions of MMRN1 by: 1) characterizing the molecular mechanisms of VWF interactions with MMRN1; and 2) investigating if multimerin 1 is important for platelet adhesive functions using mice with and without a selective multimerin 1 (Mmrn1) deficiency. Studies of the mechanism of MMRN1-VWF binding indicated that MMRN1 bound to shear exposed VWF, and that MMRN1 interacted with the A1 and A3 domains in the VWF A1A2A3 region. VWF A1A2A3 also bound to MMRN1 with a physiologically relevant binding affinity, and supported platelet adhesion to MMRN1 at a high shear rate. The selective loss of Mmrn1 in mice had limited effects on tail bleeding times, although it impaired collagen-induced aggregation of washed platelets, as well as high shear platelet adhesion of whole blood on collagen surfaces, *in vitro*. Additionally, the selective loss of Mmrn1 in mice was associated with impaired and delayed platelet-rich thrombus formation *in vivo,* in arterioles treated with ferric chloride. These findings provide new insights on platelet adhesive, haemostatic functions at arterial shear rates, and the involvement of the platelet and endothelial cell protein, multimerin 1, to support these processes.

ACKNOWLEDGMENTS

I would like to express my gratitude to individuals that provided me with guidance and support throughout my doctoral degree.

I would like to begin by thanking my PhD supervisor, Dr. Catherine P.M. Hayward for continued mentorship, guidance, support and encouragement throughout my graduate studies. Her drive and determination constantly inspired me.

I am grateful to my committee members, Drs. Peter Gross and William Sheffield for their continued guidance, feedback, and support. I thank my colleagues in the research laboratories of Drs. Hayward, Kelton, Sheffield, Khan, and Gross who were instrumental in the completion of my doctoral project. A special thank you is owed to Dr. Subia Tasneem for mentorship and support; her openness and willingness to help facilitated my achievements.

I would like to extend my gratitude to the collaborators that were involved in my studies. I thank Drs. J. Evan Sadler, Philip G. de Groot, Richard W. Farndale, Dominique Bihan, Eric G. Huizinga, David Lillicrap and Ms. Silvie Sebastian for providing important materials for my studies, and for their guidance with data interpretation. I am grateful to Dr. Ran Ni for providing technical guidance for flow cytometry analysis of mouse samples. A special thank you is owed to Drs. Yiming Wang and Heyu Ni for conducting ferric chloride injury studies on mice, and for providing me with guidance on data interpretation.

I also thank Dr. Lisa A. Westfield and Mrs. Nola Fuller for providing general technical guidance.

During my time at McMaster, I had the pleasure of forming lasting friendships with incredible individuals that helped bring balance to my life, and provided me with moments of comic relief. I would like to especially like to thank soon-to-be Drs. Janice Kim, Zainab Motala and Sharif Shajib for their encouragement and support throughout my graduate studies, and for the memories that I will cherish forever.

Finally, I would like to thank my family, by beginning with the woman that brought me into this world and raised me into the woman I am today. A special thank you is owed to my mom for being my rock and safe place. Thank you for pushing me to strive for more; I am forever grateful for your encouragement and support throughout this entire process. I also thank my grandma for being my shield, safe place, and prayer warrior: she kept me focused and reminded me that everything is possible, if we have faith. I owe many thanks to my little brothers D'Vantae Stewart and Enrique Parker, little sister Alecia Beckford-Stewart, and my step-father Denroy Stewart. I also thank the members of my larger than life family, including the Lewis, Hall, Seaton, Mckenzie, Osei and Odamatten clan – I hope I can make you proud. Last, but definitely not least, I need to thank the love of my life, my life partner, Kwaku Osei. Thank you Kwaku for your patience, support, and encouragement. You believe in me like no other, and I am eternally grateful for that.

TABLE OF CONTENTS

LIST OF FIGURES

LIST OF TABLES

LIST OF ABBREVIATIONS AND SYMBOLS

-/-	homozygous null
+/-	heterozygous null
+/+	wild type
ADAMTS13	a disintegrin-like metalloproteinase with thrombospondin motif type 1 member 13
ADP	adenosine diphosphate
APC	activated protein C
ATP	adenosine triphosphate
BSA	bovine serum albumin
C-terminal	carboxyl-terminal
Da	Dalton
DNA	deoxyribonucleic acid
EC	endothelial cell
ECM	extracellular matrix
EGF	epidermal growth factor
ELISA	enzyme-linked immunosorbent assay
EMILIN	elastin microfibril interface located protein
ε	Epsilon
FcR	Fc Receptor
FG	fibrinogen (human)
Fg	fibrinogen (mouse)
FN	fibronectin (human)
Fn	fibronectin (mouse)
FV	factor V (inactive cofactor)
FVa	activated factor V
FVIIa	activated factor VII
FVIII	factor VIII (inactive cofactor)
FVIIIa	activated factor VIII
FX	factor X (zymogen)
FXa	activated FX
FXIII	factor XIII
FXIIIa	activated factor XIII
g	gram
GFP	gel-filtered platelets
GP	glycoprotein
GPS	gray platelet syndrome

GT	Glanzmann's thrombasthenia
HEK	human embryonic kidney
HMWM	high molecular weight multimer
ITAM	immunoreceptor tyrosine-based activation motif
K_D	dissociation constant
L	litre
LZ	leucine zipper
M	meter or denotes the prefix milli
M	molarity
MFI	mean fluorescent intensity
min	minute
MMRN1	multimerin 1 (human)
Mmrn1	multimerin 1 (mouse)
mRNA	messenger ribonucleic acid
NSF protein	N-ethylmaleimide-sensitive fusion protein
N-terminal	amino-terminal
OCS	open canalicular system
OD	optical density
PAR	protease-activated receptor
PCR	polymerase chain reaction
PD	Parkinson’s disease
pFN	plasma fibronectin
PPP	platelet poor plasma
PRP	platelet rich plasma
PS	Phosphatidylserine
QPD	Quebec platelet disorder
RBC	red blood cell
RGD	Arginine-Glycine-Aspartic acid tripeptide
s^{-1}	per second (measure of shear rate)
SD	standard deviation
SDS-PAGE	sodium dodecyl sulfate polyacrylamide gel electrophoresis
sec	second
SEM	standard error of the mean
SNAP	soluble N-ethylmaleimide-sensitive fusion-associated proteins
SNARE	SNAP receptors
SNCA	α-synuclein (human)
Snca	α-synuclein (mouse)

SP	signalling peptide
SPR	surface plasmon resonance
TAFI	thrombin-activatable fibrinolysis inhibitor (zymogen)
TAFIa	activated thrombin-activatable fibrinolysis inhibitor
TF	tissue factor
TFPI	tissue factor pathway inhibitor
TRAP	thrombin receptor activating peptide
TSP-1	thrombospondin-1 (human)
Tsp-1	thrombospondin-1 (mice)
TxA_2	thromboxane A_2
U	unit
VAMP	vesicle/granule-associated membrane proteins
VWD	von Willebrand disease
VWF	von Willebrand factor (human)
Vwf	von Willebrand factor (mouse)
WT	wild type
α	alpha
β	beta
γ	gamma (denotes shear rate)
τ	mu (denotes viscosity or unit prefix, micro)
τ	tau (denotes shear stress)

CHAPTER 1: INTRODUCTION

Haemostasis is a physiological process that prevents excessive blood loss following vascular injury while maintaining the fluidity of blood (1-4). Haemostasis is highly regulated and involves the orchestrated actions of platelets, proteins and enzymes (1, 4-6). Genetic deficiencies of components that are crucial to this process can result in abnormal bleeding or thrombosis (7-13). Acquired dysregulation of haemostasis can lead to the formation of pathological, platelet-rich occlusive thrombi (14-17). Coronary artery occlusions and thrombotic strokes are common causes of death that reflect dysregulation of thrombogenesis at sites of atherosclerotic plaque rupture or erosion (17-23).

Plasma and platelet proteins are crucial for normal platelet adhesive processes and thrombogenesis, especially under conditions of high shear blood flow, such as in arteries, arterioles and stenotic vessels (24-27). The polymeric, shear-sensitive plasma protein, von Willebrand factor (VWF), is well-established as a crucial mediator of platelet-rich thrombus formation under arterial flow rates (24, 28-32). The platelet and endothelial cell protein, multimerin 1 (MMRN1; which is not normally in plasma (33-36)), is another large, soluble, highly polymeric protein that is released upon vascular injury, and was recently shown to support VWF-dependent platelet adhesion at high shear (37, 38). The first goal of this thesis was to further define the mechanism of VWF binding to MMRN1, and VWF-dependent platelet adhesion to MMRN1. The second aim of this thesis was to investigate the contributions of mouse multimerin 1 (Mmrn1) to platelet adhesive, haemostatic

functions *in vitro* and *in vivo*, using newly generated mice with and without a selective deficiency of Mmrn1.

The following sections provide an overview of haemostasis, with particular emphasis on the adhesive functions of platelet and plasma proteins. This is followed by a detailed review of the platelet adhesive properties of VWF, and a subsequent overview of the haemostatic properties of MMRN1.

1.1 OVERVIEW OF HAEMOSTASIS

Haemostasis is dependent on the adhesive and procoagulant functions of platelets (5, 39). Platelets are anucleate blood cells derived from megakaryocytes within the bone marrow, that in humans circulate at concentrations of 150–400 x 10^9 platelets/litre (L) with a typical lifespan of ≤ 10 days (5, 39, 40). The haemostatic functions of platelets include an important role in primary hemostasis, and a role in supporting the assembly of coagulation factor complexes that are essential to secondary haemostasis (1, 2, 5). Primary haemostasis refers to initial stages of preventing blood loss at sites of vessel injury, which involves the adhesion of platelets to damaged blood vessels and the formation of stable platelet-rich aggregates (Figure 1) (2, 5, 14, 41). Secondary haemostasis involves activation of the coagulation cascade, which results in thrombin generation and requires phospholipids that are exposed on activated platelets (1, 42). Thrombin generation leads to further platelet activation and firm adhesion, the activation of components of the

coagulation cascade, and the conversion of fibrinogen to an insoluble fibrin network (42-47). Fibrinolysis (the dissolution of fibrin clots) is also normally activated upon vascular injury to maintain vessel patency (4, 48). Most recently, haemostasis has been proposed to include an additional phase, the "protein wave" that precedes primary and secondary haemostasis (Figure 1). The "protein wave" defines the localization of plasma proteins (specifically fibronectin (49)) to the exposed subendothelium, which facilitates the subsequent platelet-dependent stages of haemostasis (49-51).

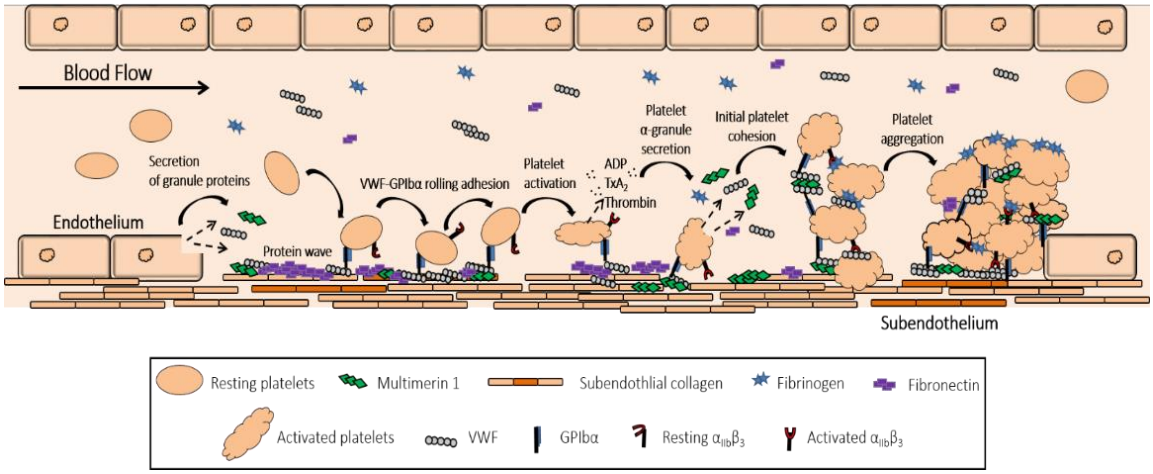

Figure 1: Schematic of platelet and protein haemostatic adhesive processes, including the protein wave and primary haemostasis. Vascular injury results in disruption of the vascular endothelium and exposure of the subendothelial proteins, including collagen. The "protein wave" allows plasma proteins (e.g., fibronectin) to localize to the exposed subendothelium. The plasma protein, von Willebrand factor (VWF), also binds to exposed collagen to initiate platelet adhesion at high shear, by binding to the platelet receptor glycoprotein (GP) Ibα on quiescent platelets. Captured platelets are activated and produce and release soluble agonists (e.g., ADP, thromboxane A_2, TxA_2), and facilitate thrombin generation, that together, further potentiate platelet activation. Activated platelets and damaged, activated endothelial cells also release intracellular stores of soluble adhesive proteins from granules. These released proteins include VWF, fibronectin, fibrinogen and multimerin 1, a number of which support platelet aggregation (primarily via $\alpha_{IIb}\beta_3$). Fibrinogen was also recently shown to localize to the surface of developing thrombus to form an extensive, non-adhesive matrix on the surface; thereby halting platelet-rich thrombogenesis. The resultant protein and platelet-rich thrombus prevents blood loss.

Haemostasis is modulated by the rheologic properties of blood (25, 52-56). Flowing blood has non-Newtonian properties that mostly originate from red blood cells that increase the viscosity of blood at low shear rates (52, 53, 57). However, blood is often assumed to behave as a Newtonian fluid, as it often does, especially at shear rates > 200 s^{-1} (53, 58). With Newtonian fluids, shear rate (γ; s^{-1}) is directly proportionate to shear stress (τ; dynes/cm^2), as per the simplified equation: $\tau = \mu \cdot \gamma$, with μ defined as the viscosity (31, 53, 59). Normal arterial shear rates are estimated to range from 500 – 5, 000 s^{-1}, under these assumptions (53, 59-61) and in this thesis. The haemostatic adhesive functions of platelets were studied under a high shear rate typical of arteries (e.g., 1500 s^{-1}) (38, 58). Also, the following sections will discuss haemostasis in the context of this specific, physiological flow condition.

Platelets also have a critical role in inflammation (62, 63). Although this not the focus of this thesis, there is evidence that platelets are immune cells that can be activated by bacterial pathogens, which releases pro-inflammatory mediators from platelets (62, 64, 65). Released platelet pro-inflammatory mediators including platelet factor 4 and P-selectin that modulate platelets-leukocyte interactions, leukocyte chemotaxis and induces the release of cytokines from neutrophils and monocytes, among other inflammatory responses (62, 66-68). Consequently, analysis of platelet functions can provide insights on inflammation, haemostasis and thrombosis.

1.1.1 Protein wave

Vascular injury disrupts the continuity of the vascular endothelium and exposes blood to proteins within the subendothelium, which then binds plasma proteins (53, 69-74). This "protein wave" (ref Figure 1) (49-51) is crucial for maximal platelet accumulation to damaged vessels under flow conditions that are typical of arterial flow (32, 49-51, 75).

Initial studies describing the "protein wave" focused on the adhesive plasma protein, fibronectin (human is abbreviated: FN; mouse is abbreviated: Fn) (49-51). In mice, fluorescently-labelled, exogenous plasma fibronectin (pFn) rapidly localizes to the luminal side of injured vessels, before the recruitment of circulating platelets (49). pFN binds to and supports *in vitro* platelet adhesion on extracellular matrix (ECM) proteins, such as collagens (49, 76-78), fibrin (79), laminin (80), and ECM-derived FN (79, 81). Therefore, pFn likely binds to exposed subendothelial proteins to participate in platelet accumulation at the site of injury *in vivo* (49). In mice, pFn may also localize to the luminal side of the injured arterioles by a mechanism independent of subendothelium exposure, as the "protein wave" was visualized using *in vivo* arterial thrombosis injury models that do not depend on vascular endothelium denudation (49, 69-74, 82-85).

Platelet adhesion to FN is independent of flow conditions (86), but VWF is necessary to support optimal, stable platelet adhesion to FN under arterial flow rates (75). Plasma VWF is a multivalent, highly polymeric protein that binds to numerous vascular

proteins exposed by vessel injury (87-94). VWF also binds to the surface receptor, glycoprotein (GP) Ibα (a subunit of the GPIb-IX-V receptor complex (5, 6, 12, 95)), on resting platelets to initiate a monolayer of platelet adhesion (25, 88, 94, 96, 97). Circulating VWF must attach to the site of vascular injury for optimal platelet adhesion to occur under physiological and pathological high shear conditions (75, 87, 88, 90-94, 98, 99). Consequently, it is likely that plasma VWF also contributes to the "protein wave" phase of haemostasis, which is proposed to support primary haemostasis (49-51).

Vascular proteins, including collagens in the subendothelium, media and adventitia support platelet adhesion independent of plasma proteins, especially under low shear rates (e.g., 100 s^{-1}), *in vitro* (56, 100). Therefore, it is possible that the "protein wave" describes a phenomenon that is dependent on flow condition, such as haemostasis in areas of high shear (i.e., arteries (61)).

1.1.2 Platelet adhesive functions (primary haemostasis)

Primary haemostasis is a multistep and multifactorial process that is dependent on adhesive ligands and surface receptors on platelets (Table 1) (2, 5, 14, 41). Circulating quiescent platelets do not adhere to the intact endothelium *in vivo*, due to repulsive forces (e.g., negatively charged glycosaminoglycans) and biochemical inhibitors of platelet adhesion and activation that are released by the vascular endothelium (e.g., nitric oxide) (3, 101, 102). However, platelets are localized at sites of vascular injury that expose the

subendothelium and deeper layers to flowing blood, as this exposes adhesive ligands for platelets (74, 103-105) (Table 2). Specific vascular membrane proteins are exposed depending on the depth of the vascular lesion, with superficial denudation of the vascular endothelium exposing the underlying subendothelial proteins, including the less platelet reactive collagens, types VI, V and VI, and laminin (103-105). Deeper lesions that extend to the media and adventitia expose more of the highly thrombogenic collagens, types I and III (74, 103-105). Collagen types I and III are also abundant in fibrous atherosclerotic plaques (103), and plaque erosion results in exposure of the circulating platelets to highly reactive constituents (17-20). Once platelet receptors bind to these exposed thrombogenic ligands, intracellular signalling activates platelets and increases its adhesive properties at the site of an injury (2, 25, 106, 107), or may cause thrombosis at plaque erosion (17-20, 103).

Table 1: Summary of abundant platelet surface receptors for haemostatic adhesive ligands. The abundant surface receptors that have well-defined roles in support platelet adhesion and aggregation.

Platelet receptor (Name & average number of receptor per platelet)	Haemostatic ligand(s)	Citation
Platelet adhesion and activation		
Glycoprotein Ib-IX-IV (specifically GPIbα) ≤ 50,000 copies	von Willebrand factor (main); thrombospondin-1; P-selectin thrombin; coagulation factors XI and XII	(6, 95, 108-113)
Glycoprotein VI ≤ 4,000 copies	Vascular collagens (e.g., collagen types I, III, and IV); fibrin; laminin	(6, 95, 114-116)
Support/stabilize platelet adhesion, activation and aggregation		
$\alpha_{IIb}\beta_3$ ≤ 80,000 copies on surface of resting platelet & 20,000 – 40,000 in platelet granules	Fibrinogen (main); fibrin; von Willebrand factor; fibronectin; multimerin 1; thrombospondin-1; vitronectin	(95, 110, 111, 117-120)
$\alpha_2\beta_1$ ≤ 4,000 copies	Vascular collagens (e.g., collagen types I, III, and IV); laminin; vitronectin	(6, 95, 117, 121, 122)

Table 2: Key vascular subendothelium proteins that support platelet accumulation and activation at sites of injury, under different conditions of shear. Particular emphasis on indirect, VWF-dependent, platelet interactions under high flow conditions.

Vascular membrane protein		Mechanism of platelet adhesion: Direct platelet interaction – Platelet receptor	Indirect platelet interaction – Platelet receptor*	Indirect platelet interaction – Shear condition	Citation
Vascular collagens	Types I and III	GPVI and $\alpha_2\beta_1$	GPIbα	≥ 500 s^{-1}	(74, 88, 100, 103-105, 121, 123)
	Type IV	GPVI and $\alpha_2\beta_1$	GPIbα	> 300 s^{-1}	(103-105, 121, 124, 125)
Laminin		GPVI, $\alpha_2\beta_1$, and $\alpha_6\beta_1$	GPIbα	> 800 s^{-1}	(88, 103, 116, 117, 126)
Fibrin		GPVI, $\alpha_{IIb}\beta_3$, and $\alpha_V\beta_3$	GPIbα	> 300 s^{-1}	(127-130)
Fibronectin†		$\alpha_{IIb}\beta_3$, $\alpha_V\beta_3$, $\alpha_5\beta_1$, and $\alpha_8\beta_1$	GPIbα	> 300 s^{-1}	(75, 79, 103, 117, 131)
Vitronectin†		$\alpha_{IIb}\beta_3$, $\alpha_V\beta_3$, $\alpha_2\beta_1$, and $\alpha_8\beta_1$	Not assessed	Not assessed	(117, 132-135)

*GPIbα bound to von Willebrand factor; †Not shown to significantly contribute to platelet activation; GP:glycoprotein

Platelet-rich thrombus formation under high shear conditions (> 600 s^{-1}), occurs as a two-step process (25). The initial phase is reversible adhesion that depends on GPIbα, and the subsequent, more stable phase of thrombus formation involves the activation of platelets and platelet integrin receptors, such as $\alpha_{IIb}\beta_3$. (25, 56) (Figure 1 and Table 1). Activated platelets and damaged, activated endothelial cells (ECs) also release various soluble agonists and proteins from their storage granules, which potentiate activation, adhesion and aggregation of platelets at sites of vessel injury (25, 56, 136, 137).

Platelet GPIbα is crucial for the initiating platelet adhesion to injured vessels, as mice deficient in this platelet receptor have a severe bleeding phenotype (138), and platelets from these mice do not adhere to injured arterioles and do not form a growing thrombus (139-141). Patients with Bernard-Soulier syndrome, a rare congenital human disease characterized by a deficiency or defect in platelet GPIbα, have a bleeding phenotype that reflects the loss of this important receptor (12, 142, 143). Interestingly, mice that are deficient in ligands for GPIbα, such as VWF and thrombospondin-1, still show platelet adhesion to injured vessels, although the adhesion is significantly less than that observed in wild type (WT) mice (72, 144, 145). It is likely that other vascular ligands, such as P-selectin (108), also participate in GPIbα-dependent platelet adhesion.

Platelet GPIbα-VWF interactions are well characterized, and reveal that GPIbα on platelets tethers to surface-captured plasma VWF (28, 94, 96, 97, 146-150). This interaction initiates reversible platelet recruitment, particularly at the high shear typical of arteries (>

500 s^{-1} in humans (100, 123), and > 2,000 s^{-1} in mice (140)) (25, 98, 100, 123, 140, 150). Reversible GPIbα-mediated platelet adhesion is characterized by rapid bond kinetics (148, 150), and "catch-slip" binding to VWF (94, 96, 97, 151-153). Catch-slip binding is defined by a reduction of the lifetime of the bond between VWF and GPIbα as the magnitude of the force acting on the bond and hydrodynamic flow increases (148, 152, 153). Consequently, the bond kinetics between VWF and GPIbα reduce platelet translocation velocity on damaged vascular endothelium, especially under elevated shear (94, 96, 97, 150-152). This interaction is like the binding kinetics that characterize selectin-dependent interactions at sites of inflammation (e.g. leukocyte-like rolling, (98, 148, 150, 154)) (Figure 1). VWF-GPIbα binding supports the adhesion of individual platelets, without significant thrombogenesis (25, 100). Platelet rolling is needed to facilitate interactions with thrombogenic proteins in the subendothelium, which lead to platelet accumulation and activation (Table 2). Interactions with thrombogenic matrix proteins are the prerequisite for integrin-mediated platelet aggregation at the vascular injury site (25, 100, 137).

Once platelets localize to the exposed subendothelium via GPIbα-dependent mechanisms (88, 123, 140), the surface platelet receptors for collagen, GPVI and $\alpha_2\beta_1$, bind to vascular collagens to promote platelet activation, recruitment and thrombogenesis (100, 115, 121, 122, 155, 156). There is contention about the importance of $\alpha_2\beta_1$ and GPVI in platelet adhesion to collagen (115, 156). The integrin $\alpha_2\beta_1$ supports and significantly modulates the adhesion of washed platelets to immobilized collagen under specific shear conditions (< 1500 s^{-1}) (156, 157). However, $\alpha_2\beta_1$ has a limited role in modulating platelet

adhesion and aggregation in the presence of plasma proteins, like VWF, which indirectly promote the platelet adhesive properties of collagen (115, 121, 155, 156, 158) (Table 2). GPVI has a more pronounced role in platelet adhesion and aggregation on collagen, irrespective of plasma proteins and fluid shear conditions (115, 121, 122, 155, 156, 158, 159). Because of this, GPVI is proposed to have a more central role in modulating platelet-collagen interactions (115, 121, 122, 155, 156). Collagen-GPVI interactions also contribute to platelet activation that enhances integrin-mediated (e.g., $\alpha_2\beta_1$ and $\alpha_{IIb}\beta_3$), firm platelet adhesion to the site of vascular injury (115, 121, 122, 155, 156).

The binding interactions between GPIbα-VWF and GPVI-collagen initiate intracellular signals that may synergistically contribute to platelet activation (160-165). VWF-GPIbα signal transduction results in tyrosine phosphorylation of Fc Receptor (FcR) γ-chain that contains an immunoreceptor tyrosine-based activation motif (ITAM) that complexes with GPVI (164, 166). VWF and collagen also bind to their respective platelet receptors and similarly induce platelet activation through the tyrosine phosphorylation of similar signalling molecules (107, 162, 167). However, platelet activation through GPVI is thought to play a bigger role in the initiation of signalling than GPIbα.

Activated platelets undergo morphological changes that facilitate rolling adhesion on the subendothelium, and form pseudopodia that increase the surface area of platelets (168-171). Activated platelets also release soluble constituents from storage granules (e.g., dense and α-granules) by a highly regulated and synchronized process (169, 171-173). The

activation-induced release of granule contents is a crucial platelet function that significantly contributes to haemostasis, and deficiencies of platelet storage granules and their constituents are associated with several bleeding diatheses (9, 174-176). The release of cargo from storage granules is defined by the: reorganization of the cytoskeleton (169, 172, 173); transportation of granules to the plasma membrane (169, 171-173); fusion of the granule and plasma membranes (169, 171-173, 177-181); and subsequent exocytosis of granule contents (169, 171-173, 178, 182). The release of soluble, abundant, adhesive α-granule proteins like MMRN1 and thrombospondin-1 (183-185) supports platelet and aggregation (25, 56, 136, 137). Released secondary modulators from dense granules, such as adenosine diphosphate (ADP) (169, 186, 187), have autocrine-like effects by binding to its respective surface receptors on platelets, to induce G-protein receptor-mediated responses (5, 6, 106). Local *de novo* production of the soluble agonist thromboxane A_2 (TxA_2) (188), and the release of ADP and serotonin and local generation of thrombin (during secondary haemostasis, which is detailed in the following section) result in secondary platelet activation. This promotes the activation of the platelet integrin, $\alpha_{IIb}\beta_3$ and stable platelet aggregate formation (25, 189-191).

ADP potentiates VWF-GPIbα mediated signal transduction (106, 162, 192), as well as collagen-GPVI-mediated platelet activation and platelet-rich thrombogenesis (186, 193-195). ADP enhances platelet activation by binding to the G-protein coupled purinergic receptors, $P2Y_1$ and $P2Y_{12}$ (168, 196, 197), to cause platelets to change shape from discoid to spiculated spheres due to actin cytoskeletal reorganization (168, 170). ADP signalling

through $P2Y_1$ and $P2Y_{12}$ also triggers other platelet activation events (198-200), including the mobilization of intracellular calcium (168, 169, 196, 201). ADP also supports stable platelet aggregate formation (25) and reduces intracellular levels of cyclic adenosine monophosphate that inhibits platelet aggregation (197, 202, 203). ADP binds to the platelet surface receptor $P2X_1$, an adenosine triphosphate-gated non-selective cation channel that contributes to ADP responses (168, 196). Signalling through $P2Y_1$, $P2X_1$ and $P2Y_{12}$ synergistically potentiates the stimulatory effects of ADP on platelet activation and aggregation (136, 168, 170, 195, 196, 204, 205).

Thrombin also enhances VWF-GPIbα and collagen-GPVI mediated platelet activation and aggregation (106, 193, 206-208), and on its own, thrombin is a very potent platelet activator. Thrombin activates platelets by cleaving the platelet surface protease-activated receptors (PAR), specifically PAR-1 and PAR-4 on human platelets (209-212), and PAR-3 and PAR-4 on mouse platelets (208, 211, 213). Thrombin irreversibly: activates PAR by cleaving the N-terminal exodomains (189, 209, 213, 214); cleaves GPIbα to potentiate platelet activation (112, 113, 215); and converts fibrinogen to insoluble fibrin that stabilizes platelet-rich thrombi (43, 45, 46, 216) (described in more detail in Section 1.2.1: Fibrinogen and fibrin). Non-physiological surrogates such as thrombin receptor activating peptide (TRAP) are used to control for the various prothrombotic actions of thrombin and specifically study PAR-mediated platelet activation (211, 212, 217). TRAP is composed of the peptides corresponding to the N-terminal end of the proteolyzed PAR that act as a tethered ligand for the receptor (209, 214). TRAP containing the sequence

SFLLRN (specific PAR-1 agonist) is primarily used to stimulate human platelets (211, 212, 217), while TRAP with the sequence AYPGKF (specific PAR-4 agonists) is mainly used for the study of mouse platelets (37, 49, 141, 193, 218).

Activation of the abundant platelet integrin, $\alpha_{IIb}\beta_3$, results from bi-directional ("inside-out" and "outside-in") intracellular signalling, which are discrete but synergistic processes for activating $\alpha_{IIb}\beta_3$ (118, 190). Inside-out activation of αIIbβ3 is triggered by: intracellular signalling; associations with cytoskeletal (e.g., talin and kindlin-3 (219)); and changes to the transmembrane-cytoplasmic domains that connect the α_{IIb} and β_3 subunits, thereby activating $\alpha_{IIb}\beta_3$ (190, 220-223). Activation of $\alpha_{IIb}\beta_3$ increases the affinity of the integrin extracellular domains for its ligands, including the abundant soluble plasma proteins, FG, VWF and FN (193, 221) (ref Table 1). Ligand binding to $\alpha_{IIb}\beta_3$ results in outside-in signalling, including tyrosine phosphorylation events (224-226), which potentiates the activation of platelets and contributes to increasing the binding of $\alpha_{IIb}\beta_3$ ligands (118, 227).

$\alpha_{IIb}\beta_3$ is crucial for firm platelet adhesion and aggregation (Figure 1 and Table 1), as evident by the bleeding diatheses associated with Glanzmann's thrombasthenia (GT) (11, 228). GT is defined as the quantitative or qualitative deficiency of $\alpha_{IIb}\beta_3$ (11, 228). Platelet aggregation, like platelet adhesion, is dependent on fluid shear rates (25, 56), and at physiological shear rates (< 10, 000 s^{-1}), activated $\alpha_{IIb}\beta_3$ binds to bi- and multi-valent haemostatic ligands to bridge adjacent activated platelets. Fibrinogen was initially

described as the main ligand crucial for stabilizing $\alpha_{IIb}\beta_3$-mediated platelet adhesion and aggregation to injured vessels (72), likely due to its high plasma concentrations (56, 229-231). At low shear (< $300s^{-1}$ (98)), fibrinogen is the preferred ligand for $\alpha_{IIb}\beta_3$ (98, 128, 193, 232), but fibrinogen has less importance in supporting $\alpha_{IIb}\beta_3$-dependent platelet aggregation under high arterial shear (98, 128, 232, 233). In mice deficient of fibrinogen, occlusive intravascular thrombi still form, despite high rates of embolization in treated arterioles (72). Platelet aggregates likely form in the injured arterioles of these mice because of the other $\alpha_{IIb}\beta_3$ ligands VWF and FN, which preferentially support platelet-rich thrombogenesis under high physiological shear (72, 193).

Primary haemostasis is spatially coordinated with secondary haemostasis, due to the bidirectional repositioning of negatively charged phospholipids (e.g., phosphatidylserine and phosphatidylethanolamine) from the inner leaflet to outer bilayer membrane of activated platelets (234-237). Negatively charged phospholipids on activated platelets are necessary for assembly of the tenase and prothrombinase complexes that ultimately result in thrombin generation that augments platelet adhesive and procoagulant functions (234, 235, 238-241). Thrombin also leads to the generation of insoluble fibrin networks, which serves as a scaffold essential for the stability of developing thrombi in the microvasculature (43-47, 216).

1.1.3 Platelet procoagulant function (secondary haemostasis) and fibrinolysis

Coagulation is self-propagating and results in the activation of circulating zymogens, which culminate in the cleavage of prothrombin to generate thrombin (42, 242, 243). Traditionally, coagulation was divided into the extrinsic, intrinsic and common pathways, but more contemporary descriptions discuss coagulation as a 3-phase overlapping process: initiation; amplification; and propagation (42, 242, 243). Initiation of coagulation (like the extrinsic pathway of coagulation) is mediated by tissue factor (TF) that is exposed with vascular injury (42, 242, 244). TF on damaged vessels binds to calcium and captures circulating activated factor VII (FVIIa (245)) to catalyze the proteolytic activation of coagulation factors IX and X (42, 242, 244). Low (picomolar) amounts of thrombin are generated during this phase of coagulation by activated FX (FXa, with "a" denoting the activated form)-mediated cleavage of prothrombin (242, 244, 246). Amplification involves positive feedback loops that augment thrombin generation, including activation of platelets and proteolytic activation of the homologous cofactors VIII and V, as well as factor XI (42, 242, 243). Propagation involves the accumulation of enzyme complexes onto the damaged endothelium and negatively charged phospholipids expressed on the surface of activated platelets and other blood cells (247), which catalyze coagulation (42, 242, 243, 248-250). FVIIIa participates in FXa generation by forming the tenase complex with factor IXa (that was activated by membrane-bound factor XIa (251)), the substrate FX, phospholipids, and calcium (42, 242, 243, 250). FVa participates in thrombin generation by forming the prothrombinase complex, which is the main source of

thrombin *in vivo* (242, 248, 249). The prothrombinase complex includes FXa, FVa, the substrate prothrombin, phospholipids and calcium (42, 242, 243, 248, 249).

Thrombin propagates coagulation and promotes the stability of platelet-rich thrombi by augmenting fibrin-rich clot formation (43, 216). Thrombin stabilizes clots by cleaving fibrinogen to fibrin that reveals polymerization sites that support the formation of fibrin networks (46, 252-254). Thrombin also activates the plasma transglutaminase FXIII to FXIIIa, which covalently links fibrin polymers to increase clot stability and strength (42, 44, 46, 47, 255). Thrombin protects against fibrinolysis by activating the thrombin-activatable fibrinolysis inhibitor, TAFI, that cleaves partially degraded fibrin and decreases the affinity of plasminogen for fibrin (42, 256-258). TAFIa also dampens fibrinolysis due to impaired tissue-type plasminogen activator-mediated conversion of plasminogen to plasmin (42, 256, 258, 259).

Several physiologic inhibitors regulate coagulation and localize thrombin generation to the site of injury (242, 260-263). Tissue factor pathway inhibitor (TFPI) is a potent proteinase inhibitor of the TF-mediated FXa generation and FXa (261, 264), and antithrombin is a serine protease inhibitor of thrombin, factors Xa and IXa (260, 265). Thrombin procoagulant activity is also downregulated by its endothelial receptor, thrombomodulin (266-268). Thrombin-thrombomodulin have anticoagulant properties and activates protein C to activated protein C (APC), a serine protease that inactivates cofactors

FVIIIa and FVa (262, 269-271). APC with its cofactor, protein S, regulate coagulation by inhibiting tenase and prothrombinase complex assembly (262, 270, 272).

Fibrinolysis is another tightly regulated process that maintains the fluidity of blood (4, 48). Fibrinolysis is mainly mediated by the action of plasmin, a serine protease that is the activated form of the circulating zymogen plasminogen (4, 48). Plasminogen is converted to plasmin by tissue-type plasminogen activator (4, 48, 273) and by urokinase plasminogen activator (4, 48). Plasmin cleaves fibrin, which generates soluble degradation products and exposes C-terminal lysine residues that are removed by TAFIa to downregulate fibrinolysis (4, 42, 48, 256-258). Fibrinolysis is also regulated by mechanisms that inhibit the activation of plasminogen (e.g., plasminogen activation inhibitor-1 (4, 48, 274)) or inhibit plasmin (e.g., α_2-plasmin inhibitor (4, 48, 275)).

1.2 OVERVIEW OF HAEMOSTATIC FUNCTIONS OF PLASMA AND PLATELET ADHESIVE PROTEINS

Haemostasis is modulated by adhesive proteins found circulating in plasma, within the storage granules of platelets and in the vascular endothelium and subendothelium (Table 2). These vascular adhesive proteins participate in every aspect of haemostasis, from the protein wave to platelet recruitment and adhesion to the damaged vessels, platelet activation, platelet-rich aggregate formation, and fibrin clot assembly (49, 50, 79, 145, 193, 218, 276). Consequently, regulation of platelet-protein interactions is crucial for normal

haemostasis (142, 228, 277-280), and its dysregulation results in bleeding (typical of deficiency states (7, 8, 10, 13, 281, 282)) or thrombosis (typical of dysregulated states (14-17)). These crucial physiological processes are protected by the numerous functional redundancies, which are often observed as single receptors interacting with several proteins (109, 120, 139, 191, 283, 284) (Table 1), or single proteins engaging several platelet receptors (75, 109, 110, 285-295) (Table 2).

Adhesive plasma proteins are typically synthesized and secreted by hepatocytes in the liver (296-298), except for VWF that is synthesized and secreted into circulation by the vascular endothelium (299-303). Some adhesive proteins stored by platelets and ECs are endogenously synthesized and stored until agonist-stimulated release, including VWF and MMRN1 (36, 183-185, 304). However, plasma fibrinogen and FN are examples of proteins in circulation that are internalized through competitive interactions with the platelet surface receptor, $\alpha_{IIb}\beta_3$ (305).

The functions of haemostatic adhesive proteins are most notably influenced by the properties of intravascular flow, and arterial shear conditions are described as having the most profound effects on protein functions (24, 54, 58, 306). The findings from studies of animal models of selective or combined deficiencies of these adhesive plasma and platelet proteins emphasize their distinct contributions to normal haemostasis (37, 49, 72, 144, 145, 193, 218, 305, 307-309). Animal models also demonstrate the collaborative action of these soluble proteins to modulate platelet functions, especially under high flow conditions (25,

75, 79, 88, 99, 128, 129, 145, 193, 200, 276, 310, 311). Within the past few decades another platelet protein, MMRN1, has been described to independently support, and collectively enhance platelet haemostatic adhesive properties (37, 38, 312), especially under high shear (37, 38). The following sections provide a detailed review of abundant plasma and platelet adhesive proteins, with particular focus on the roles of these vascular proteins in shear-mediated platelet adhesion, aggregation and thrombogenesis.

1.2.1 Fibrinogen and fibrin

Fibrinogen (human is abbreviated FG; mouse is abbreviated Fg) is an abundant, soluble, plasma glycoprotein, circulating at 1.5 – 4 mg/ml in healthy individuals (229-231). FG is converted to fibrin by thrombin-mediated proteolysis of FG N-termini fibrinopeptide sequences on the Aα and Bβ chains (46, 252-254), which removes N-terminal fibrinopeptides and reveals polymerization sites (46, 252-254). FXIIIa stabilizes fibrin networks by catalyzing a series of intermolecular ε-(γ-glutamyl) lysine covalent bonds that result in stable, insoluble fibrin networks (42, 44, 46, 47).

Plasma FG is considered the main ligand of platelet integrin $\alpha_{IIb}\beta_3$ due to its: the high affinity (represented as a low K_D) of FG for the platelet integrin, $\alpha_{IIb}\beta_3$ (K_D: < 70 x 10^{-9} M); abundance of FG in plasma; and the dimeric nature of FG engages $\alpha_{IIb}\beta_3$ to bridge platelet-platelet interactions (46, 50, 284, 313-315). The C-terminal γ chain QAGDV sequence (not RGD sequences in the Aα chain (316-318)) in FG almost exclusively

supports binding to $\alpha_{IIb}\beta_3$ (305, 316, 319, 320). This region on FG is crucial for normal $\alpha_{IIb}\beta_3$–mediated platelet aggregate formation (320), as well as $\alpha_{IIb}\beta_3$-mediated endocytosis of plasma FG (305). Fibrin binds to $\alpha_{IIb}\beta_3$ by a mechanism distinct from FG (120, 130) and it also binds to GPVI to support platelet adhesion and activation (127-129). In mice, the selective loss of Fg (and fibrin) results in a severe bleeding phenotype (320-323), likely because FG and fibrin have numerous roles in haemostasis and fibrinolysis. The availability of transgenic animals have allowed for an analysis of the independent functions of FG and fibrin, and teased out the distinct contributions of FG-$\alpha_{IIb}\beta_3$ interactions and insoluble fibrin networks (305, 322).

FG and fibrin independently support platelet adhesive functions under low shear (< 300 s^{-1}) *in vitro* (98, 128, 232, 305), but are less important for platelet adhesion and aggregation under high shear typical of the microvasculature (≥ 1500 s^{-1}), *in vitro* (98, 128, 232, 233). The shear-dependent nature of FG and fibrin are further demonstrated by *in vivo* analysis of $Fg^{-/-}$ mouse arterioles injured by superfusion of ferric chloride (72, 305). The loss of Fg (and fibrin) in these mice does not significantly impair the initial localization of platelet to injured arterioles, nor did it delay the appearance of the first large (≥ 20μm) intravascular thrombi (72, 305). Interestingly, however, the loss of the γ chain, C-terminal, QAGDV sequence for $\alpha_{IIb}\beta_3$ in FG was associated with more rapid *in vivo* thrombogenesis, in mice (305). These mice (refer to as $Fg\gamma\Delta5^{-/-}$) are characterized by an increased rate of platelet accumulation, that is attributed to the platelet adhesive properties of fibrin (127, 128, 324, 325). FG was also recently shown to halt platelet accumulation by forming an

extensive, non-adhesive matrix on the surface of developing, platelet and fibrin-rich thrombi (324). In *FgγΔ5$^{-/-}$* mice, the absence of platelet reactive FG likely prevents the formation of FG-rich, non-adhesive matrices on developing thrombi, which in turn would promote thrombogenesis (305, 324) (ref Figure 1). More rapid thrombogenesis in *FgγΔ5$^{-/-}$* mice might also be the result of increased platelet FN (due to increased $\alpha_{IIb}\beta_3$-mediated internalization of pFN (72, 305)), which promotes platelet accumulation, especially in the presence of fibrin deposition (79, 131, 305, 311, 326).

Intravascular thrombi in *Fg$^{-/-}$* mice are unstable, and consistently embolize to form occlusive thrombi downstream from the injury site (72). The inability to form insoluble fibrin networks in *Fib^{AEK}* mice (selectively mutated to eliminate complete thrombin-mediated cleavage of fibrinopeptide sequences on the Aα chain), similarly impairs *in vivo* thrombogenesis (322). This particular defect is characterized by the appearance of numerous embolization events (i.e., > 80% of injured arteries do no form occlusive thrombi at the injury site) (322). Alternatively, *FgγΔ5$^{-/-}$* mice (that form fibrin, but do not support FG-$\alpha_{IIb}\beta_3$-mediated platelet aggregation) form stable occlusive thrombi at the site of vascular injury, with small aggregates disassociating from the apex of developing thrombi (305). These findings, taken together, demonstrate that FG-$\alpha_{IIb}\beta_3$-mediated platelet aggregation contributes to platelet cohesion, albeit not significantly, under conditions of high arterial flow (56, 98, 232, 233). Additionally, fibrin generation regulates the stable attachment of platelet-rich thrombi to the vessel wall at arterial shear rates (56, 72, 305).

Tail transection assay provides a crude assessment of bleeding phenotypes in knockout and transgenic mouse models (327-330). This injury model includes transection of arteries and veins in the distal tip of the mouse tail that triggers $\alpha_{IIb}\beta_3$-mediated platelet aggregation (330, 331), and depends on the presence and functional activity of Fg, not fibrin (322). This platelet and protein adhesive process shares similarities with those observed with an automated, low shear, aggregometer, especially the involvement of FG and $\alpha_{IIb}\beta_3$ in platelet aggregation (193, 330).

In vitro aggregation assays using an automatic aggregometer (e.g., by light transmission aggregometry) and platelets from *Fg*-/- mice demonstrate the crucial roles of Fg to mediate platelet aggregate formation in response to stimulation by a panel of physiological agonists (e.g., ADP, thrombin and collagen) (193, 321, 322). In citrated plasma, complete loss of Fg is associated with no platelet aggregation response to ADP and thrombin (193, 321, 322), but the loss of fibrin polymerization (in Fib^{AEK} mice) does not abolish aggregation response to ADP (322). Defective platelet aggregation to low concentrations of collagen (2 µg/ml) is also observed with citrated samples from $Fg^{-/-}$ mice (72). In plasma free of a calcium chelator (e.g., sodium citrate), Fg loss does not abolish platelet aggregation response to any of these agonists (193), demonstrating that plasma FG and divalent cations are crucial for optimal $\alpha_{IIb}\beta_3$-mediated platelet aggregation under these conditions (193, 232, 305). These data also show that in the absence of FG, other plasma and platelet ligands, such as VWF, FN, thrombospondin-1 and MMRN1, support platelet aggregation (50, 145, 193, 218).

1.2.2 Fibronectin

Fibronectin is a disulfide-linked dimeric, ubiquitous vasculature protein that is found as a soluble form circulating in the plasma (referred to as pFN) at ≤ 400 μg/mL (332, 333). FN is also sequestered in platelet α-granules due to the internalization of pFN by platelet integrin $\alpha_{IIb}\beta_3$ (305, 334). FN is synthesized by various cells (e.g., ECs and fibroblasts (332, 335)), secreted by hepatocytes (297), and is also a regular constituent of the vascular ECM (50, 51, 332, 336). FN has platelet adhesive functions that are dependent on its localization within the vasculature, the vascular shear rates, and fibrin deposition (49-51, 75, 79, 131, 218, 326, 332).

pFN localizes to the lumen of injured arterioles by binding to ECM proteins (77, 337), such as fibrillar collagens (49, 76-78, 131), fibrin (79, 338), and laminin (80). pFN bound to damaged vessels initiates the protein wave of haemostasis and supports the subsequent adhesion of platelets, *in vivo* (49). Under high shear conditions, platelet adhesion to pFN occurs in the absence of the abundant plasma proteins, VWF and FG (49), and the absence of exposed subendothelial proteins (49). It is possible that pFN interacts with damaged ECs via integrin receptors (291), to initiate primary and secondary haemostasis.

At low shear (e.g., ≤ 300 s^{-1}), pFN supports platelet adhesion by mechanisms that involve platelet β_3 and β_1 integrin receptors (75, 79, 117, 289-291), but platelets readily detach from pFN surfaces at > 300 s^{-1}, *in vitro* (79, 339). pFN requires GPIbα or VWF for maximal thrombogenesis at arterial shear rates (75, 79, 131) (Table 2). pFN crosslinked to fibrin (via FXIIIa (79, 338)) also supports more adhesion and platelet-rich thrombogenesis of reconstituted blood, even under high flow conditions (e.g., 1250 s^{-1}) (79). Platelet adhesion to FN is limited when reconstituted blood is free of other plasma proteins (75, 79, 131), demonstrating that other haemostatic proteins are needed to support optimal platelet adhesion to pFN.

Complete global loss of *Fn* is incompatible with life (340); therefore, mice with liver-specific conditional knockout of *Fn* ($pFn^{-/-}$) or a haplodeficiency of *Fn* ($Fn^{+/-}$) are used to assess the specific contributions of Fn to haemostasis (308, 340, 341). $pFn^{-/-}$ and $Fn^{+/-}$ mice are viable, reproduce normally, and lack any overt morphological or cellular abnormalities (308, 340, 341). Bleeding time and *in vitro* plasma clot activity are also normal for $pFn^{-/-}$ and $Fn^{+/-}$ mice (340, 341), but partial and selective complete pFn loss abrogates and delays thrombotic response in mesenteric arteries treated with ferric chloride (308, 341). In these animal models, deficiencies in pFn delay the appearance of the first thrombus due to single or small platelet aggregates dissociating from the apex of the developing thrombi (308, 341). Interestingly, initial platelet localization to the vessel wall and thrombus embolization rates are normal, unlike in mice with Fg deficiency (72). This demonstrates that pFn contributes to platelet-rich thrombus growth, rather than platelet and

thrombus adherence to the injury site. Occlusive thrombi are not observed in ~ 60% of ferric chloride treated arterioles in $Fn^{+/-}$ and $pFn^{-/-}$ mice (308, 341), signifying that partial pFn loss significantly affects thrombus formation.

FG and fibrin regulate the haemostatic properties of pFN, as pFN has inhibitory effects on platelet adhesive functions in the absence of fibrin generation (218). In mice, endogenous pFn abrogates platelet aggregation when platelets are stimulated with agonists that do not convert Fg to fibrin (e.g., TRAP) (218). In Fg (and fibrin) deficient mice, endogenous pFn also reduces *in vitro* platelet adhesion and aggregation, which likely contributes to prolong bleeding and delay thrombogenesis *in vitro* and *in vivo* (218). Deficiencies in pFn ameliorate these defects to platelet adhesive functions (218), confirming that in the absence of fibrin, pFn abrogates platelet aggregation. Coincidentally, pFn assembly into developing thrombi follows a fibrin gradient at sites of vessel injury (49, 326), and it is proposed that fibrin supports the platelet adhesive properties of pFn at the vessel wall, where fibrin generation is high (49, 79, 218, 342). In this model, the platelet adhesive action of pFN switches to prevent excessive intravascular platelet aggregation further from the sites of injury, where fibrin generation is low (49).

1.2.3 Thrombospondin-1

Thrombospondin-1 (human is abbreviated TSP-1; mouse is abbreviated Tsp-1) is a trimeric glycoprotein that is a major constituent of platelets α-granules, along with FG, FN,

VWF, and MMRN1 (9, 36, 292, 343, 344). TSP-1 also circulates in plasma at relatively low concentrations (> 500 ng/mL (345)) and is a normal constituent of the ECM (343, 346). TSP-1 is released from platelet α-granules following stimulation by strong agonists like thrombin (184, 185, 292). Released TSP-1 binds to activated platelets directly via GPIbα (109), GPIV (287, 347), and β_3 and β_1 integrin receptors (292-295). TSP-1 also interacts with several other molecules on the surface of platelets (288), including the adhesive proteins, FG, fibrin and VWF, which indirectly supports the adhesion of activated platelets to TSP-1 (276, 344, 348-350). TSP-1 contributes to platelet adhesion and aggregation at sites of vessel injury, by modulating thrombogenesis under arterial flow conditions (109, 145, 348).

TSP-1 supports maximal platelet adhesion at physical high shear conditions typical of arteries (~ 1,600 s^{-1}) (109, 339), but firm platelet adhesion to TSP-1 is also observed at pathological high shear rates (e.g., 4,000 s^{-1}), *in vitro* (109). Under these *in vitro* conditions, TSP-1 interacts with the main VWF receptor GPIbα to support platelet adhesion (109), which suggested that GPIbα-TSP-1 interactions provide a redundant mechanism for supporting platelet adhesion in the absence of VWF (109). However, in mice, the selective complete loss of Tsp-1 (*Tsp-1*$^{-/-}$) does not significantly impair the initial localization of platelets to injured arteries *in vivo* (145), a process involving GPIbα-VWF binding (72, 100, 110, 144, 150). Additionally, in mice, Tsp-1 does not support platelet adhesive functions *in vivo* independent of Vwf (145). These findings suggest that the binding of

GPIbα to TSP-1 cannot substitute for the interaction of this receptor with its main ligands, VWF (145).

Tsp-1$^{-/-}$ mice have defective platelet adhesion *in vivo*, characterized by delayed thrombus growth rate, prolonged time to the first large (> 20 μm) thrombus, and prolonged total vessel occlusion times following ferric chloride-induced injury to arterioles (145, 351). These findings complement *in vitro* findings that TSP-1 contributes to the stability of platelet aggregates concomitantly with platelet activation and secretion of TSP-1, in analyses with an aggregometer (185, 288, 352). However, in mice, the loss of Tsp-1 does not significantly impair platelet aggregate formation mediated by a panel of physiological agonists (e.g., thrombin, ADP, and collagen) (145, 307, 351). It is likely that the presence of other plasma and platelet proteins compensate for the loss of Tsp-1 in mice (145). It is also likely that TSP-1 has more profound effects on shear-mediated platelet adhesive processes (109), and that platelet aggregation in an aggregometer does not adequately recapitulate the contributions of TSP-1 to platelet aggregation under arterial shear conditions (109, 339, 348).

1.3 OVERVIEW OF VON WILLEBRAND FACTOR (HUMAN, VWF; MOUSE, Vwf)

von Willebrand factor (human is abbreviated: VWF; mouse is abbreviated: Vwf) is a vascular adhesive protein that forms large polymers of dimers, which can be as large as

20 million Daltons (353, 354). The haemostatic functions of VWF are enhanced under high shear flow conditions typical of the arteries and microvasculature, where VWF is crucial for initiating and supporting normal haemostasis (24, 28-32). VWF interacts with numerous components within the vasculature, including platelets (38, 110, 111) and subendothelial proteins (87-94). The following sections provide a detailed overview of the plasma and platelet protein, VWF, its haemostatic functions, and the common bleeding diathesis that is associated with abnormalities in VWF levels and functions.

1.3.1 Background on von Willebrand factor

The expression of VWF is restricted to the vasculature (36, 299-301, 355-358), where VWF is constitutively (and basally (303)) secreted into circulation by EC (299, 303). VWF is also stored in unique storage granules in EC (300) and platelet α-granules (36, 355), until agonist stimulation causes the release of intracellular stores (302, 359). Plasma and released VWF modulate haemostatic properties by binding to: platelets, both resting and activated; (38, 110, 111); proteins in the vasculature (88-94); circulating plasma cofactor, FVIII (360-362); and numerous other vascular ligands (38, 75, 131, 310, 350). The haemostatic, adhesive properties of VWF are enhanced under high flow conditions typical of arterial flow, which transform compact VWF polymers to filamentous multimers that are more haemostatically active and support multivalent binding interactions (24, 28-32, 363). Deficiencies and mutations of VWF can result in von Willebrand disease (VWD), a common bleeding disorder that is reported to have a prevalence of ~ 1:1000 (364-368).

VWF is highly conserved among mammals (369), and the orthologous human and mouse genes are structurally similar (each with 52 exons (369)). The human *VWF* loci (on human chromosome 12 (370, 371)) and the murine *Vwf* gene (on mouse chromosome 6 (369, 372)), both encode for a 2813 residue precursor protein that shares 83% sequence identity (369, 373, 374). The regions of VWF that are mapped to support its intracellular processing, multimerization, and haemostatic functions are similarly conserved (~ 82% amino acid sequence identity (369)), suggesting functional convergence. However, subtle interspecies differences in specific regions in VWF limit interspecies cross-reactivity between plasma and platelets from different species (375, 376).

VWF is exclusively synthesized by EC and megakaryocytes (36, 299-301, 355), and is expressed in highly vascularized organs like the heart, lung, kidney and brain (356-358). In the vascular endothelium, VWF is stored in specialized granules called Weibel-Palade bodies (300, 301, 377), along with a vascular membrane protein, P-selectin (65, 378-380). The majority (> 90%) of EC-derived VWF is constitutively secreted and released basally from post-Golgi secretory organelles (likely Weibel-Palade bodies (303)), which provides the largest source of plasma VWF (302, 303). The remainder of EC-derived VWF is efficiently stored until agonist stimulation increases the release of VWF from Weibel-Palade bodies (302, 359, 377). VWF is also efficiently stored in the eccentric, electron lucent zone of platelet α-granules (381), which may contribute to ≤ 15% of circulating plasma VWF (309, 382, 383). Intracellular stores of VWF form high molecular

weight multimers (HMWM) that are more haemostatically active than plasma VWF (89, 300, 302, 384, 385), suggesting that circulating and stored VWF contribute differently to haemostasis (309, 384).

Plasma VWF levels are highly variable within the general population of healthy individuals, ranging from 5 – 15 µg of VWF per ml of plasma (386, 387). The regulation of plasma VWF levels is crucial for the maintenance of normal haemostasis, as VWF deficiencies are associated with bleeding (e.g. VWD (8)) and elevated VWF levels are associated with increased risk for thrombosis (388, 389). The level of plasma VWF is primarily regulated by genetic factors, such as intragenic mutations in the *VWF* gene (390-399) and/or extragenic causes like the *ABO* locus (387, 400-402). In mice, a few WT inbred mouse strains are significantly correlated with variabilities in the levels of plasma VWF (e.g., RIIIS/J and CASA/RkJ strains (403-407)), because of intragenic or extragenic mutations (403-408). These mutations can account for up to 63% total genetically determined variation in Vwf levels between mouse strains (404, 406), and some of these inbred mouse strains serve as naturally occurring murine models of VWD (408, 409). The level of Vwf in the commonly used C57BL/6J mouse strain is not the highest amongst laboratory mice (408), but C57BL/6J mice still serve as a commonly used mouse strain for studies of haemostasis (133, 144, 145, 341, 410, 411). C57BL/6J mice are used to investigate the haemostatic properties of Vwf because, in these mice, the phenotypic consequences associated with selective Vwf deficiencies recapitulates the resultant

bleeding diatheses due to genetic mutations to the orthologous human *VWF* locus (i.e., VWD) (144, 408, 409).

1.3.2 VWF protein structure-function relationship

The precursor VWF polypeptide (and orthologous murine protein, Vwf (369)) is composed of 2813 amino acid residues, organized as (373, 374): N-terminal signalling peptide (SP; 22 residues); pro-peptide (741 residues); and mature peptide (2050 residues) (Figure 2). Mature VWF is characterized as a pattern of repeated domains (Figure 2), which include von Willebrand A and C modules, D assemblies, and a C-terminal cysteine-knot (CK) (373, 374, 412). The D assemblies of VWF include the N-terminal pro-peptide (D1D2) and were recently identified to also possess cysteine 8 (C8) and trypsin inhibitor-like (TIL) domains, as well as E modules (412) (Figure 2). The D assemblies of VWF contribute to intercellular processing and multimerization (413-415), cofactor (FVIII) binding (360, 362, 416, 417), and modulates platelet adhesion to VWF (418, 419). The A repeats in VWF also contribute to intercellular processing and multimerization of VWF (24, 420-422), and are crucial for initiating and regulating platelet adhesion to the vessel wall (90-92, 94, 96, 97, 151, 423-427). The six C-terminal C modules in VWF contribute to the flexibility (24, 412, 428), and the C4 module supports binding to integrins on EC and platelet aggregation (111, 429, 430). The structure-function relationship of VWF has been extensively studied (24, 412), and the following section of this thesis provides a

detailed review of the distinct regions within VWF that are mapped to contribute to its intracellular processing and haemostatic functions (Figure 2).

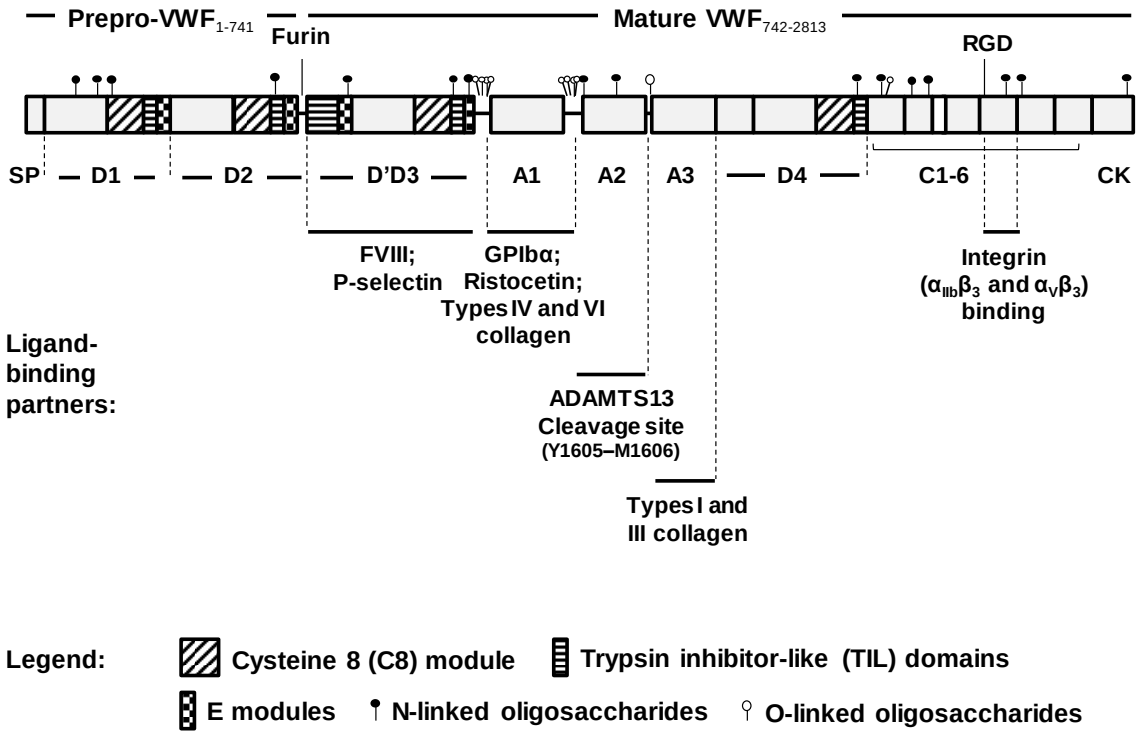

Figure 2: Structure of prepro- and mature-VWF, and the contribution of VWF domains to haemostasis. 13 N-linked and 10 O-linked glycans are respectively shown as closed and open symbols. D assemblies of VWF possess the identified domains: cysteine 8 (C8); trypsin inhibitor-like (TIL); and E modules.

Intracellular processing of precursor VWF includes proteolytic removal of the SP, dimerization, extensive glycosylation (13 N-linked and 10 O-linked oligosaccharides), multimerization, cleavage of the pro-peptide, and additional post-translational modifications (24, 354, 374). The SP of VWF localizes prepro-VWF to the endoplasmic reticulum (ER), where pro-VWF monomers undergo glycosylation and pro-VWF dimers form via intermolecule disulfide bonds at the C-terminal CK (354, 374, 431). In the ER, the D1D2 assembly of the pro-peptide also forms transient interchain disulfide bonds with the D'D3 assembly that enters the Golgi to complete glycosylation and sulfation (354, 413, 415). In the ER, VWF dimers forms multimers via intermolecule disulfide bonds at the N-terminal D'D3 assembly of mature VWF (354, 413, 414, 432). The pro-peptide is subsequently proteolytic cleaved by furin and dissociates from mature VWF multimers that are constitutively and basally secreted, or exocytosed due to cellular activation (302, 303, 359, 433, 434). In platelets and EC, VWF polymers form rod-like structures due to the D1D2 pro-peptide of VWF that is necessary for tightly packing VWF polymers during biosynthesis (354, 435). The structure of intracellular VWF filaments is crucial for the elongated shape of Weibel-Palade bodies, and the N-terminal D'D3 assembly of VWF recruits P-selectin to Weibel-Palade body-like structures in cultured cells (435, 436). Other domains within VWF also contribute to the storage of intracellular VWF, as mutations in the A1 domain can disrupt the multimerization of VWF polymers and result in degradation of intracellular VWF stores (437).

Physiological agonists (such as thrombin (110, 302, 359)) and high shear (438) result in the release of intracellular VWF from platelets and EC (110, 300, 302, 359, 438). VWF released from activated platelets contains larger polymers that support more spontaneous multivalent binding than circulating plasma VWF (385, 439), and significantly contributes to haemostasis, independent of EC-derived, plasma VWF (309). VWF released from Weibel-Palade bodies tether to surface of EC, likely through: direct interactions between the C4 module of VWF and $\alpha_V\beta_3$ on EC (440); indirect interactions between the D'D3 assembly of VWF and P-selectin that is expressed on the surface of activated EC (436, 441); and/or an uncharacterized mechanism that does not include $\alpha_V\beta_3$ or P-selectin (442). High shear unravels VWF tethered to stimulated EC (440, 442), as well as VWF captured to subendothelial proteins (32, 89, 443). High shear also promotes the self-association of VWF polymers via multiple structural regions, including the A1 and A2 domains, but not the A3 domain of VWF (30, 31, 444, 445). The resultant shear exposed VWF tethered to EC or associated with the ECM supports high-affinity binding to platelet GPIbα, and enhances the recruitment of circulating platelets to the sites of vessel injuries (152, 283, 363, 446). Tethered, shear-exposed VWF supports platelet binding by undergoing specific conformational changes that expose the binding site for GPIbα in the upper anterior surfaces of the A1 domain in VWF (96, 97, 363, 443, 447). This region of the A1 domain in VWF is typically buried within circulating, globular, plasma VWF (363), and represents a low-affinity state that does not significantly bind to the platelets (via GPIbα) (29, 152, 279). The compact, circulating form of VWF polymers regulates its interaction with GPIbα on resting platelets in circulation.

The A1 and A3 domains of VWF are homologous domains with ~ 23% residue identity (448). The A1 and A3 domains are also structurally identical, as both domains form similar loop-like structures due to intradomain disulfide bonds that link the N- and C-termini of each domain (96, 412, 425, 448). The A1 domain is more responsive to shear than the A3 domain of VWF (29, 363, 448), despite the structural similarities of these two domains in VWF. The A3 domain of VWF is constitutively exposed in circulating globular VWF and readily supports binding to exposed subendothelial proteins *in vivo* (94, 363, 423). The A3 domain also contributes to the stability of the A1A2A3 tri-domain in VWF (449) and regulates the conformational activation of the A1 domain (containing the GPIbα binding site) under high shear (447-449). Sequence homology between the A1 and A3 domains of VWF likely accounts for the functional importance of both domains in binding to vascular collagens (types I, III, IV and VI) (90-92, 423-427). The A3 domain of VWF contains the major binding site for types I and III fibrillar collagens (92, 423, 425-427), and the A1 domain of VWF preferentially binds to fibrillar collagens under high flow conditions (94, 423). The A1 domain of VWF is also essential for binding to types IV and VI non-fibrillar collagens, irrespective of haemorheology (90, 91, 424). VWF captured onto vascular collagens is crucial for initiating platelet adhesion and thrombogenesis under high shear (87, 98, 99), and dysfunctions to this process alter platelet recruitment to the exposed subendothelium of damaged vessels (99, 384, 450-452).

VWF binds to the platelet membrane receptor GPIbα, preferentially under high shear (> 500 s^{-1} in humans (100, 123), and > 2,000 s^{-1} in mice (140)), because high flow unfolds the tertiary structure of VWF A1 domain (152, 363, 446, 448). The A1 domain of VWF unfolds by a three-state mechanism that includes a stable, molten, globule intermediate (283, 363, 446, 448). This stable intermediate of VWF A1 domain contains less of secondary structure components (e.g. ~ 10% less alpha-helical structure (283)), which promotes VWF-GPIbα binding by increasing the binding affinity for GPIbα by ~ 20-fold, relative to the native conformation of VWF A1 domain (283, 446, 448). Gain-of-function mutations in VWF A1 domain can result in the pathological appearance of this stable, intermediate state, which is a characteristic of a subtype of VWD identified as type 2B (283). Type 2B VWD is defined as abnormalities in the functionality of the A1 domain that leads to spontaneous GPIbα binding without the requirement of high fluid shear to modulate VWF (8, 150). The stable intermediate of the A1 domain of VWF reveals the positively charged surface on the upper anterior surfaces, thereby supporting electrostatic "catch-slip" binding to GPIbα (94, 96, 97, 151, 152). This specialized binding interaction increases the lifetime of the A1-GPIbα bond as hydrodynamic shear increases and transitions to interactions characterized by a reduction in the lifetime of the VWF A1-GPIbα bond (152, 153). Consequently, "catch-slip" bonds between VWF and GPIbα localize platelets to the sites of vascular injury by modulating platelet translocation velocity, similar to leukocyte-like rolling adhesion (98, 148, 150, 154). This facilitates platelet activation by thrombogenic proteins in the subendothelium and integrin-mediated firm platelet adhesion and aggregation (100, 453) .

The antibiotic ristocetin (obtained from bacteria, *Amycolatopsis lurida* (454, 455)) promotes VWF-GPIbα binding by molecular mechanisms that are like the activation effects of high shear (456, 457). These molecular mechanisms include: inducing self-association of VWF polymers (456, 458); neutralizing repulsive surface charges on the A1 domain of VWF and GPIbα (459); and inducing conformational changes in the A1 domain of VWF that promote GPIbα binding (94, 455, 457). Ristocetin exerts its effect on VWF by binding to the upper face of the A1 domain (96, 97), which is adjacent to the region of the A1 domain that possesses the GPIbα binding site (96, 97). The GPIbα binding site in the A1 domain of VWF is also exposed by immobilizing VWF, either onto the subendothelial matrix or polystyrene surfaces (e.g., microtiter plates) (30, 445, 447, 460, 461). Like VWF captured by the subendothelium, VWF absorbed on polystyrene surfaces retains its biological activity by supporting the adhesion and translocation of resting platelets, preferentially under high rheologic shear (461).

VWF A1-GPIbα binding contributes to the activation of platelet integrin receptors (160-163, 462), and potentiates collagen-GPVI induced granule secretion and platelet aggregation (164). VWF binds to GPIbα to initiate integrin activation via several signalling pathways (106, 119, 162, 166, 463-465), including the ITAM signalling pathway (106, 163, 166, 463). VWF-GPIbα signalling through the ITAM signalling pathway is similar to signal transduction through the collagen receptor, GPVI (166), and VWF-GPIbα signalling may synergize collagen-GPVI induced tyrosine phosphorylation of intracellular molecules

(107, 164, 167). Recently it was shown that GPIbα directly associates with GPVI (165), and this interaction may define an alternative or complementary mechanism for how VWF-GPIbα amplifies collagen-GPVI induced platelet activation. VWF-GPIbα binding induced by ristocetin mimics conformational effects of high shear (456, 457), and results in tyrosine phosphorylation events (162, 466). These signalling events, on their own (independent of other plasma proteins (162, 466)), are not sufficient to promote the enzymatic activity of signalling molecules, platelet activation and integrin-mediated platelet aggregation (162). Released secondary mediators, such as ADP, are necessary to potentiate VWF-GPIbα-mediated activation signals and enhance platelet adhesive functions (106, 192). However, it is unclear if ADP significantly contributes to VWF-GPIbα-mediated integrin activation under flow conditions typical of arteries, in whole blood (31, 160, 453, 467, 468).

VWF binds to GPIbα and initiates platelet adhesion and activation, which enhances GPIbα and $\alpha_{IIb}\beta_3$-mediated stable platelet adhesion and aggregation (98, 160, 161, 286, 453). Activated $\alpha_{IIb}\beta_3$ binds to the RGD motif in the C4 module of VWF (110, 111, 429, 430, 469), especially under physiological or pathological high flow conditions (98, 233, 375, 469). VWF-$\alpha_{IIb}\beta_3$ binding contributes to stable, irreversible platelet adhesion and aggregation, and potentiates the activation of platelet integrins that follows ligand binding to $\alpha_{IIb}\beta_3$ (118, 162, 453, 467). However, VWF-$\alpha_{IIb}\beta_3$ binding interactions on their own are not sufficient to support maximal platelet aggregation (162, 232, 286), demonstrating that other platelet receptors (e.g., GPIbα), as well as plasma and platelet proteins, are necessary to optimize platelet aggregation at high shear.

The A1 domain and C4 module are the only regions within VWF that are reported to possess an affinity for platelet receptors (94, 110, 111, 430, 469). These regions of VWF, in addition to the collagen-binding A3 repeat of VWF (92), are highly conserved in humans and mice (sequence identity between human Vwf and murine Vwf: 85% in the A1 domain (369, 375); 82% in the A3 domain (369)). Despite this, subtle interspecies differences exist between the A1 domain of VWF in humans and mice that significantly limit the ability of murine A1 domain to support the GPIbα-dependent adhesion of human platelets (375, 376). This interspecies incompatibility is due to a single, complementary substitution at residue 1326 in the A1 domain (murine Vwf A1: R1326; human VWF A1: H1326 (375)), which causes an electrostatic clash between the positive charge of R1326 in murine Vwf and a single residue in human GPIbα (375). This electrostatic clash disrupts the formation of a single salt-bridge and shortens bond lifetime between murine Vwf-GPIbα complexes (375, 470). This salt-bridge is not formed between human VWF-GPIbα complexes (375).

The A2 domain of VWF is homologous to the A1 and A3 domains but is structurally distinct because VWF A2 domain lacks the intradomain disulfide bond that links the N- and C-termini (24, 471). VWF A2 domain is also under regulation by shear, like the A1 domain, and the A2 domain of VWF possesses unique structural features that regulate its conformation (363, 471-473). One of the unique structural features in the A2 domain of VWF is a vicinal disulfide loop in its C-terminal (between C1669 and C1670), which forms a “molecular plug” that stabilizes the structure of VWF A2 domain and

protects it from readily unfolding under high flow conditions (471-473). This structural feature may have evolved as a mechanism to protect the functionality of VWF, as the A2 domain also has a cryptic scissile bond that is cleaved by the plasma and platelet metalloproteinase, ADAMTS13 (a disintegrin and metalloprotease with thrombospondin type 1 repeats) (474-476). ADAMTS13 cleaves the scissile bond in the A2 domain of VWF (between Y1605–M1606; (350, 474, 477)), which fragments VWF polymers and reduces the haemostatic properties of VWF.

The importance of VWF A domains in regulating platelet adhesion to vascular collagens was described by *in vitro* protein binding studies that used full-length domain deleted VWF protein mutants (92, 94, 474) and inhibitory antibodies that block the proposed functional activity of the A domains of VWF (426, 427, 478-480). The A1A2A3 tri-domain of VWF, on its own, as well as isolated A1, A2, or A3 domain protein mutants (without neighbouring N- or C-terminal regions) have been useful for estimating binding kinetics for some VWF ligands (310, 480-482). These peptides were also used to elucidate the functional importance of this region to modulate the haemostatic, platelet adhesive properties of VWF (310, 449, 482, 483). VWF A1A2A3 tri-domain also independently supports GPIbα-dependent platelet adhesion (310, 449, 482), platelet activation in the presence of whole blood (449), and binds to vascular collagens (although weakly due to the importance of multimerization to enhance the avidity of this interaction) (385, 480).

VWF contributes to coagulation, as circulating VWF binds to FVIII with high affinity (K_D: 0.2 – 0.4 x 10^{-9} M (362, 385, 484)) through the D'D3 assembly of VWF (360, 362, 385, 416). There is a significant correlation between plasma VWF levels and FVIII cofactor activity (361, 485), as plasma VWF is an *in vivo* carrier protein for FVIII (361, 362, 484). VWF also protects FVIII from degradation by APC, a proteolytic inhibitor of FVIII (262, 417, 486, 487). VWF may also synergize thrombin-catalyzed activation of FVIII (488), and FVIIIa readily dissociates from VWF to participate in tenase (361, 489, 490).

1.3.3 Deficiencies in von Willebrand factor, in humans and mice, and its effect on haemostasis

VWF supports the various phases of haemostasis, as it is an abundant, adhesive plasma protein that: likely supports and promotes the "protein wave" (refer to Section 1.1.1); initiates platelet adhesion to the subendothelium (38, 87-94, 110, 111); and is the carrier protein for FVIII (361, 362, 484). The haemostatic importance of VWF is exemplified by the pathological consequences of the congenital bleeding disorder, VWD, which is characterized by quantitative and qualitative deficiencies of VWF (8, 390-399, 491). Almost a century after the first index case described in 1924, VWD is one of the most commonly diagnosed bleeding disorders and is reported to affect ~ 1:1000 persons (364-368, 492). VWD often results in abnormalities in platelet adhesion and when severe, can

also cause haemophilia-like symptoms because of the associated deficiency of FVIII (395, 397, 493, 494).

VWD is divided into 3 subgroups (8): types 1 and 3 describe the respective partial or complete quantitative deficiency of VWF; and type 2 describes mutated VWF with abnormal haemostatic functions. Type 1 VWD, the most common form (affecting ~ 70% of VWD patients (367, 495)), is typically an inherited, autosomal dominant, milder form of VWD (390, 392). Type 1 VWD is characterized by varied decrease in the level of functional VWF (VWF levels ranging from 5 – 40% (390)). Type 1 can be associated with changes in: transcriptional activation (496); decreased synthesis (497); intracellular retention and impaired secretion (498); and/or accelerated clearance of VWF (391, 497, 499). Type 3 is another quantitative deficiency of VWF, characterized by the almost complete deficiencies of VWF (VWF levels typically < 5% (8)) in both plasma and platelets (8, 397). Type 3 is the least common form of VWD (affecting ~ 5% of VWD patients (8, 367)) and is often a congenital recessive disorder (396-398, 491). ~ 65% of index cases of type 1 VWD and ~ 90% of index cases of type 3 VWD are associated with mutations in the *VWF* gene, including missense mutations, insertions and/or deletions (390-399). The remainder of index cases (of types 1 or 3 VWD) are likely defined by mutations in other loci (that are distinct from locus for VWF) that also regulate VWF levels (390, 402, 404, 407, 500-502).

Type 2 VWD is characterized by discordance in VWF functionality and levels, unlike types 1 and 3 VWD, because this subgroup is defined by abnormal VWF haemostatic functions relative to the level of VWF protein (8). Type 2 VWD is also a more heterogeneous disease subgroup that is further divided into four categories, namely types 2A, 2B, 2M or 2N, depending on the resultant pathological phenotype (8). Types 2A, 2B and 2M VWD are defined by numerous mutations within the A1A2A3 domains of VWF (503). Some forms of type 2M VWD indirectly and directly impair platelet adhesion to VWF due to mutations to the vascular collagen binding sites in the A1 and A3 domains of VWF (90, 91, 399, 450, 451, 504, 505), or loss of function mutations in the GPIbα binding site in VWF A1 domain (399, 450). Gain-of-function mutations in the GPIbα binding site in the A1 repeat of VWF is associated with type 2B, which is marked by increased affinity of VWF A1 domain for GPIbα (8, 96, 97, 151, 481). Type 2N VWD is defined by mutations in the D'D3 assembly of VWF that result in defective binding to FVIII (399, 491, 493). Type 2N VWD can cause a mild haemophilia-like disorder because VWF cannot bind to and protect plasma FVIII from proteolytic degradation (493, 494). Knowledge is constantly emerging on type 2 VWD because new haemostatic ligands for VWF are continuously being described. It is interesting to characterize the binding interactions between VWF and other mediators of haemostasis, as this knowledge may further define the dysfunctions observed in type 2 VWD. This information may lead to the development of novel therapies and alternative screening methods for diagnosing this heterogeneous subgroup of VWD.

In mice, the partial or complete deficiency of Vwf results in a mild to severe bleeding diathesis that is comparable to the various forms of VWD (8, 144, 390, 392, 408, 409). Deficiencies in murine Vwf significantly prolong bleeding times and increase blood loss following transection of the distal tip of the mouse tail (144, 309), abrogate high shear platelet adhesion to collagen *in vitro* (309) and severely impair platelet adhesive functions *in vivo* (72, 144). The loss of Vwf is also associated with deficiencies in FVIII (144, 309). Defects to *in vivo* platelet function from Vwf defiviency include the delayed appearance of occlusive thrombi in injured arterioles due to significantly impaired platelet localization to the damaged vessels, which prolongs the formation of large (> 20 μm) thrombi (72, 144). Vwf deficient mice also have defective thrombogenesis due to impaired high shear-induced platelet aggregation *in vivo* (72, 144), a process that involves plasma VWF binding to GPIbα and $\alpha_{IIb}\beta_3$ (31, 285, 506). Interestingly, platelet aggregates still form in mice deficient of Vwf (72, 144), implying that other plasma and platelet proteins contribute to support platelet adhesive functions in the absence of Vwf (72).

1.4 OVERVIEW OF MULTIMERIN 1 (HUMAN, MMRN1; MOUSE, MMRN1)

Multimerin 1 (human is abbreviated: MMRN1; mouse is abbreviated: Mmrn1) is one of the largest polymeric, vascular adhesive proteins, aside from VWF (33, 34, 507, 508); MMRN1 forms large, variably-sized, disulfide-linked polymers of trimers that range from 400, 000 to several million Daltons (33, 34, 507, 508). The expression of MMRN1 is restricted to megakaryocytes and the vasculature (33, 35, 509-512), suggesting that

MMRN1 has roles in modulating vascular biology. MMRN1 is efficiently stored in platelets and EC where it remains until agonist stimulation causes the release of intracellular stores (33, 35, 38, 312, 507). Released MMRN1 is detected on the surface of activated platelets and EC (33-35, 183), and it associates with the extracellular matrix (33, 35). MMRN1 is postulated to support platelet haemostatic, adhesive functions (38, 312, 513, 514). The following section provides an overview of the current knowledge on the platelet and vascular protein, MMRN1, and its haemostatic properties.

1.4.1 Background on multimerin 1

MMRN1 was discovered through the use of an antibody (known as JS-1 (33)) raised by immunizing mice against human platelets and was initially designated "p-155" due to its average reduced mobility (33, 507). p-155 was later renamed multimerin to reflect the multimeric structure of the protein (507), and designated multimerin 1 to differentiate from the homolog multimerin 2 (MMRN2), another vascular protein with anti-angiogenic properties (515, 516), but uncharacterized haemostatic functions (508, 509, 511, 517). MMRN1 is not detected in plasma, as it is efficiently stored in platelets and EC (34-36, 183); however, physiological agonists (e.g. thrombin and ADP) cause the activation-induced release of intracellular stores of MMRN1 (33, 35, 38, 312, 507). Because of this, MMRN1 is an "activation protein" (508), that is detected on the surface of these haemostatic adhesive cells following cellular activation (33, 35, 38, 183, 312, 507), a process that potentially localizes the activity of MMRN1 within the vasculature.

The gene for multimerin 1 is highly conserved among mammals (508, 509), and is located on human chromosome 4 and murine chromosome 6 (508, 509, 511, 518). MMRN1 is found in highly vascularized tissue (e.g. placenta, lung, and liver (509)), due to its restricted expression by megakaryocytes and platelets (33, 36, 183, 386, 507, 519) and the vascular endothelium and subendothelium (35, 509). MMRN1 is not detected in other blood cellular components, such as peripheral blood lymphocytes, T-cells, granulocytes, monocytes, and RBC (33). Similarly, MMRN1 is not normally detected in plasma (33), nor is it detected in liver lysates (33). This finding indicates that MMRN1 is likely synthesized endogenously by megakaryocytes and the vascular endothelium, and is likely not endocytosed from plasma like a number of platelet proteins, such as FV, FG and FN (35, 36, 183, 509).

The biosynthesis of MMRN1 includes (183, 304, 509): extensive complex N-linked glycosylation (there are 23 potential N-glycosylation sites (183, 509)); O-linked glycosylation; formation of interchain disulfide bonds that form homotrimers (likely before N-linked oligosaccharides are converted to complex forms (304)); and proteolysis of its N-terminal precursor peptide (without disrupting the multimeric structure of MMRN1 (509)). MMRN1 trimers are predicted to assemble at the C-terminus of MMRN1, a region that includes a C1q-like globular domain (a motif that participates in trimerization in other proteins (509, 520)), but it is still unclear how MMRN1 trimers are assembled into large, disulfide-linked polymers. In platelets, the subunits contained in MMRN1 polymers are

processed to 155 and 170 kDa forms (33, 183, 507). MMRN1 subunits are highly glycosylated: N-glycosylation accounts for > 30 % MMRN1 molecular mass (183, 509), and the 170 kDa subunit contains a larger polypeptide sequence of the 1228 residue precursor protein that is cleaved at a more N-terminal, uncharacterized site than the 155 kDa subunit (183, 304, 509). proMMRN1 is rarely detected in platelets (183, 304, 508, 509).

MMRN1 belongs to the EMILIN family of structurally similar, disulfide-linked polymeric proteins (508, 521-523). MMRN1 possesses the typical EMILIN domains (Figure 3), including: N-terminal cysteine-rich domain EMI domain (508, 521-523); long, central coiled-coil region (with leucine zipper (LZ) sequences) (509, 521, 523) and C-terminal C1q-like globular domain (509, 520, 521, 523). MMRN1 also contains a C-terminal cysteine-rich epidermal growth factor (EGF)-like domain (509) (Figure 3), unlike other EMILIN proteins (521-523). How all these structural features contribute to the functionality of MMRN1 is not clearly defined (508); however, the N-terminal region of mature MMRN1 includes an integrin binding motif, RGD tripeptide (509) that supports the platelet adhesive properties of MMRN1 (38, 312). Most of the structural features of multimerin 1 are conserved among mammals (508, 509), except the N-terminal RGD motif, central LZ sequences and C-terminal C1q-like globular domain that are not present in all mammals and chickens (508) (Figure 3). Structural conservation among mammals suggests that MMRN1 has an important physiological role. As mentioned earlier, due to the restricted expression of MMRN1 in platelets and EC, and its release into the plasma upon

vessel injury (37, 38, 312, 513, 514), suggest that MMRN1 is likely to support vascular homoeostasis.

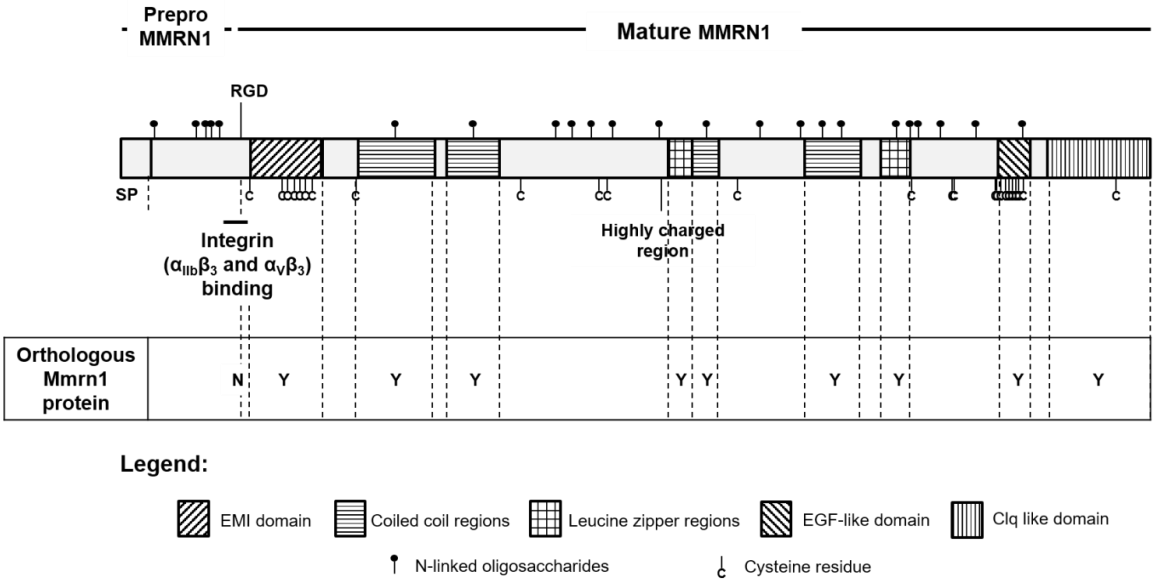

Figure 3: Structure of human MMRN1 and the ortholog murine Mmrn1. Most of the structural features of multimerin 1 are conserved among humans and mice (67% sequence similarity), except for the N-terminal integrin-binding RGD motif. 23 putative N-linked and 21 cysteine residues are respectively shown as closed symbols and "C".

Platelets contain ~ 16 µg of MMRN1 per 10^9 platelets (524), and store MMRN1 within the eccentric, electron lucent zone of platelet α-granules, along with VWF and FV (34, 183, 386, 510). MMRN1 storage in α-granules is independent of VWF and FV, as demonstrated by the normal retention of MMRN1 in platelet α-granules deficient of either VWF or FV (36, 175, 386, 525). EC also independently store MMRN1 and VWF (35), and MMRN1 mainly sorts to granules in EC that are distinct from the Weibel-Palade bodies that contain both VWF and P-selectin (35). Cultured EC constitutively secrete low levels of MMRN1 that associates with the ECM, and it is possible that it binds to ECs or is cleared from the circulation (33, 35) as MMRN1 is not detected in normal plasma (33). MMRN1 retained in the storage granules of cultured EC contains a lower proportion of HMWM of MMRN1 than is stored in platelet α-granules (36, 304, 507). Recombinant MMRN1 for *in vitro* studies, produced from stably transfected human embryonic kidney (HEK) 293 cells resembles EC-derived MMRN1 in polymerization and mobility (nonreduced and reduced) (35, 304). However, recombinant MMRN1 is functionally comparable to platelet-derived MMRN1 (37, 38, 304, 312, 513, 514, 526), and it is likely that EC- and platelet-derived MMRN1 are functionally similar, despite the differences in multimerization.

1.4.2 MMRN1, the main FV/Va binding protein in platelets, and its functions in coagulation

MMRN1 co-localizes and forms a complex with FV *in vivo,* in the α-granules of resting platelets (34, 524). MMRN1 supports physiologically relevant, high-affinity

binding to FV and Va (respective affinity estimations, K_D: 2 and 7 x 10^{-9} M; (514)), and it is estimated that the majority (> 98 %) of platelet FV/Va is complexed with MMRN1 in α-granules (514). Consequently, MMRN1 is likely the main binding protein for platelet-FV (34, 513, 514, 524, 526), and like the relationship between VWF and FVIII (361, 362), it is postulated that MMRN1 is the *in vivo* carrier protein for FV (34, 304, 514, 524).

Affinity chromatography was used to initially demonstrate that MMRN1 non-covalently interacts with the light chain, not the heavy chain of FV/Va (34), and later, it was identified that ~25% of platelet-FV is covalently bound to MMRN1 via disulfide bonds between the B domain of FV and MMRN1 (34, 524). The B domain of FV is not essential for MMRN1-FV binding, but it influences non-covalent MMRN1 binding to the homologous C1 and C2 domains in the light chain of FV/Va (513, 514, 526). Mutations and autoantibodies against the C2 domain of FV/Va have deleterious effects on MMRN1 binding (526, 527); therefore, it is likely that this region contains the main binding site for MMRN1. MMRN1 is mapped to overlap with phosphatidylserine (PS) binding sites in the C1 and C2 domains of FV/Va (513, 526), and regions within FV/Va C2 domain that are necessary for the procoagulant function of FVa (513). However, MMRN1 does not detectably impair FV/Va localization on PS because MMRN1 also binds to phospholipids *in vitro* (513), and it is likely that MMRN1 that is bound to PS supports FV/Va binding and indirectly localizes FV/Va to the surface of activated platelets (513). MMRN1-FV complexes are also functionally active and participate in thrombin generation *in vitro* (513, 514), although the addition of MMRN1 impairs FV activation by both FXa and low levels

of thrombin (reflective of thrombin concentrations during the initial stages of TF-initiated thrombin generation (514)). Delayed FVa generation (due to exogenous MMRN1 (514)) consequently reduces prothrombinase activity and thrombin generation *in vitro* (514), and MMRN1 also reduces *in vitro* thrombin generation when added to pre-formed FVa (514).

1.4.3 MMRN1 functions in platelet adhesion

MMRN1 was initially discovered associated with the surface of activated platelets (33), and since its initial discovery more than two decades ago (33), there is emerging evidence that it has roles in supporting and enhancing platelet adhesive functions (37, 38, 312). MMRN1 supports platelet adhesion by distinct molecular mechanisms that are dependent on physiological shear rates and the plasma protein, VWF (37, 38, 312) (Table 3). The N-terminal RGD-integrin binding motif of MMRN1 is also necessary for platelet adhesion under specific flow conditions (38, 312) (Table 3).

Table 3: Platelet adhesive properties of MMRN1 under varying vascular flow conditions (38, 312).

Vascular flow condition	Platelet adhesion		MMRN1 RGD	Molecular mechanism requires:	
	Resting	**Activated**		**Platelet receptors**	**VWF**
Stasis (absence of flow)	No	Yes	Dependent	$\alpha_{IIb}\beta_3$ and $\alpha_v\beta_3$	No
Venous shear rate (150 s^{-1})	No	Yes	Dependent and independent	$\alpha_v\beta_3$ and GPIbα, not $\alpha_{IIb}\beta_3$	No
Arterial shear rate (1500 s^{-1})	Yes	Yes	Independent	GPIbα, not $\alpha_{IIb}\beta_3$ or $\alpha_V\beta_3$	Yes

MMRN1 matrices support the adhesion of thrombin- and ADP-activated platelets via platelet β_3 integrin(s), under low shear rates (38, 312) (Table 3). However, activated GT (β_3 deficient (11)) platelets still support detectable, albeit significantly lower, adhesion to MMRN1 (312), suggesting that platelets adhere to MMRN1 via β_3-(in)dependent mechanisms. Washed, resting platelets do not directly adhere to untreated MMRN1 matrices, demonstrating that the platelet receptors that bind MMRN1 require activation (38, 312) (Table 3). MMRN1 binds to PS *in vitro* (513), and it is possible that in addition to β_3 integrins (312), MMRN1 might interact with PS on the surface of activated platelets.

Platelet GPIbα participates in platelet adhesion to MMRN1 under low and high physiological shear rates, but MMRN1 does not directly bind to GPIbα (38) (Table 3). It is likely that another plasma or platelet protein (e.g., VWF) interacts with GPIbα, and that MMRN1 indirectly supports GPIbα-dependent platelet adhesion (38). This molecular mechanism is like other vascular proteins that do not directly bind to GPIbα (e.g., FG and FN) (88, 99), although this platelet receptor is required for normal platelet recruitment and adhesion, especially under high flow conditions (139). The main plasma GPIbα-ligand, VWF, is essential for platelet adhesion to numerous vascular proteins at arterial shear rates (24, 41, 88, 99), and is also crucial for platelet adhesion to MMRN1 under similar flow conditions (38) (Table 3). Pretreating MMRN1 matrices with plasma levels of exogenous VWF supports GPIbα-dependent platelet adhesion at arterial shear rates *in vitro,* which does not require the N-terminal RGD motif in MMRN1 or β_3 integrin(s) on activated platelets (38) (Table 3). Platelet activation is also not necessary for platelet adhesion to

MMRN1 under these flow conditions, since MMRN1 surfaces capture shear-exposed VWF to support the adhesion of resting platelets (38). Interestingly, plasma VWF does not detectably bind to MMRN1 under conditions of no or low flow, as observed in static protein binding assays and surface plasmon resonance (38). These findings suggest that shear exposure may modulate VWF binding to MMRN1. In addition to plasma VWF, platelet VWF likely also contributes to high shear platelet adhesion on MMRN1 matrices, as activated platelets completely deficient of VWF (e.g., type 3 VWD platelets (8)) do not adhere to untreated MMRN1 matrices (38). VWF is also required to support and enhance *in vitro* platelet adhesion to subendothelial collagen types I and III pretreated with MMRN1, under arterial flow conditions (38).

1.4.4 MMRN1 deficiencies in inherited and acquired disease states

Platelet activation is crucial for normal haemostasis, and activation of platelets and EC releases MMRN1 onto these cells (34, 183), suggesting that MMRN1 localizes to the surface of these haemostatic cells to modulate events at sites of vascular injury. To date, there are no human diseases associated with selective deletions at the *MMRN1* locus (508). Platelet MMRN1 is deficient in several types of platelet disorders, including gray platelet syndrome (GPS) and Quebec platelet disorder (QPD) (175, 525, 528-530). GPS is a mild to moderate inherited bleeding disorder characterized by macrothrombocytopenia and the absence of α-granules that gives platelets a gray appearance by light microscope (174, 175). In GPS, the failure to retain megakaryocyte-synthesized α-granule proteins (including

MMRN1) results in abnormal plasma levels of MMRN1 and MMRN1-FV complexes (175). In QPD, the platelet MMRN1 deficiency has a different cause: QPD is a moderate to severe, autosomal dominant bleeding disorder, associated with a duplication mutation of the gene for urokinase plasminogen activator, *PLAU* (525, 528-533). In QPD, platelet MMRN1 and other platelet α-granule proteins are degraded by plasmin due to increased expression and storage of urokinase plasminogen activator in megakaryocytes and platelets (525, 528, 529, 531-533). Acquired defects in MMRN1 regulation have been reported in malignant disorders that may alter vascular homoeostasis (e.g. angiogenesis). MMRN1 expression has been suggested as a predictive biomarker of cancer prognosis (534), as its elevated expression is detected in patients with ovarian carcinoma (535), non-small cell lung cancer (536), and acute myelogenous leukaemia (534, 537). Additionally, reduced expression of MMRN1 is associated with anti-angiogenic chemotherapy (538).

1.4.5 Haemostatic functions of Mmrn1 in mice with spontaneous tandem deletion of genes for multimerin 1 and α-synuclein

The platelet adhesive, haemostatic functions of human and mouse multimerin 1 appear to be similar, as demonstrated by studies using mice with spontaneous tandem deletions of the two adjacent genes for Mmrn1 and α-synuclein (human abbreviation: *SNCA*; mouse abbreviation: *Snca*) (37). In humans and mice, the chromosomal region that includes the adjacent multimerin 1 and α-synuclein loci is hypothesized to be vulnerable to recombination events (511, 539). Variations at the *SNCA* locus contributes to the etiology

of several diseases, including the common neurodegenerative disorder, Parkinson's disease (PD) (511, 539-541). Mutations and deletions at the *MMRN1* locus and the associated consequences have not been described (508). Assessing the functional consequences of a deficiency of Mmrn1 in mice might provide insights of the consequences of *MMRN1* deficiency in humans. With this knowledge, new diagnostics and applicable therapeutics could be derived due to a better understanding of the specific contributions of MMRN1 to haemostasis.,

The genetic instability at the *Mmrn1* and *Snca* loci contributed to a spontaneous deletion of this chromosomal region in an inbred strain of mice (C57BL/6JOlaHsd from Harlan, Bicester, UK) (37, 511, 542, 543). C57BL/6JOlaHsd mice are missing ~ 365 kb of chromosome 6 (without significant insertion of DNA at the deletion junction (511)), which deletes the eight exons of *Mmrn1* and six exons of *Snca* (511). The phenotype of C57BL/6JOlaHsd mice was initially assessed for the pathological consequences of Snca loss on neuronal phenotypes (544), since α-synuclein, unlike MMRN1 (509, 511, 512), is expressed in the presynaptic terminals of neurons (511, 540, 541, 545). However, recent studies on these mice looked at the effect of combined Mmrn1 and Snca (referred to as Mmrn1/Snca) loss on platelet function and platelet-dependent thrombus formation (37). In mice, spontaneous tandem deletion of the *Mmrn1* and *Snca* genes does not alter fertility nor does it result in an overt phenotype that reduced viability (37, 511, 543). However, Mmrn1/Snca double deficient mice have reduced platelet adhesion, *in vitro* and *in vivo*, and have prolonged vessel occlusion times in mesenteric arteries treated with ferric chloride,

with unstable thrombus formation (37). Mmrn1/Snca double deficient mice also have defects in several aspects of platelet function *in vitro*, including impaired platelet adhesion to collagen (at an arterial shear rate) and reduced maximal aggregation in response to thrombin and a selective PAR4 agonist (37). The addition of recombinant MMRN1, by transfusion before ferric chloride-induced injury or the addition of MMRN1 to *in vitro* experiments, ameliorates the observed *in vivo* and *in vitro* defects in platelet haemostatic functions in Mmrn1/Snca double-deficient mice (37). How much functional convergence exists between human and mouse multimerin 1 is still unclear; however, this finding suggests that selective knockout mice might provide insights on human MMRN1 functions, despite the differences between the human and murine forms of multimerin 1 (37, 508) (Figure 3).

The concomitant loss of α-synuclein in Mmnr1/Snca double deficient mice likely contributes to the phenotype of these mice, because the vasculature expresses both proteins (509, 511, 546, 547). Exogenous α-synuclein inhibits thrombin-induced platelet α-granule release and platelet activation, *in vitro* (540), without detectable effects on dense or lysosomal granule release (540). Exogenous α-synuclein penetrates platelets and associates with the membrane of α-granules to directly inhibit α-granule release (540, 546). The inhibitory effect of α-synuclein on platelet response to thrombin *in vitro* (540) suggests that the loss of the *Snca* locus, in mice, might result in abnormally accelerated platelet α-granule release in response to agonist stimulation. This was observed in Mmrn1/Snca double deficient platelets (measured by the increased detection of platelet granule protein, P-

selectin on the platelet surface after activation with low thrombin concentrations) (37). Functional studies have not assessed whether MMRN1 alters platelet responses to thrombin. Accelerated α-granule release due to Snca deficiency could be prothrombotic because platelets store proteins that enhance platelet adhesive functions, such as VWF, TSP1, FN, and FG. Thus, the analysis of Mmrn1 functions using Mmrn1/Snca deficient mice could have underestimated the contributions of Mmrn1 to platelet haemostatic functions. Therefore, there is a need to directly address the effects of selective Mmrn1 loss on platelet adhesive functions in mice.

1.5 THESIS HYPOTHESIS AND OBJECTIVES

1.5.1. Rationale

Activated platelets and vascular endothelium release two distinct massive polymeric proteins, MMRN1 and VWF (35, 183, 508) with several interesting functional similarities (38, 508, 509). Like VWF, MMRN1 binds to subendothelial collagens (types I and III), and enhances platelet adhesion to collagen at a high shear rate by a mechanism that requires both VWF and the platelet receptor, GPIbα (38). As MMRN1 does not detectably bind to GPIbα, this suggests that MMRN1 indirectly supports VWF-GPIbα-dependent platelet adhesion at a high shear rate by binding VWF (38). As shear exposed VWF localizes to MMRN1 matrices (38), this suggests that high shear exposes cryptic sites within VWF that are involved in MMRN1 binding; however, the mechanism underlying VWF interactions with MMRN1 has not been directly evaluated.

Mice with spontaneous tandem loss of *Mmrn1* and *Snca* genes have defective platelet function *in vivo*, characterized by reduced platelet adhesion, the formation of unstable thrombi that readily dissociate, and prolonged vessel occlusion times in mesenteric arteries treated with ferric chloride (37). Mmrn1/Snca double deficient mice also have defective *in vitro*, platelet function, such as impaired platelet adhesion to collagen at high shear and reduced maximal aggregation responses to thrombin and a selective PAR4 agonist (37). As SNCA inhibits platelet α-granule release *in vitro* (540), its loss in Mmrn1/Snca deficient mice could explain the increased α-granule release of P-selectin at low thrombin concentrations in the double-deficient compared to WT mice (37). As increased α-granule release could be pro-thrombotic, the phenotypes observed in these double deficient mice could have underestimated Mmrn1 contributions to platelet adhesive hemostatic functions.

To further elucidate how platelets contribute to haemostasis and thrombosis, the primary objective of my thesis was to assess the contributions of the platelet protein, multimerin 1, to *in vitro* platelet functions, and to *in vivo* platelet-rich thrombus formation in mice. The original research presented in the following chapters details the specific hypotheses and research objectives that aimed to define the contributions of multimerin 1 to platelet haemostatic functions *in vitro* and *in vivo.*

1.5.2 Hypotheses

1. MMRN1 binds to the shear-sensitive A1A2A3 region of VWF (which is critical for GPIbα-dependent platelet adhesion), and this region of VWF is required for platelet adhesion to MMRN1 at high shear.

2. Mmrn1 loss impairs platelet adhesion and platelet-mediated thrombus formation in mice with a selective Mmrn1 deficiency.

1.5.3 Research objectives

To test these hypotheses, my specific research objectives were to:

1. Characterize the interaction between MMRN1 and VWF by evaluating:
    i. the roles of specific VWF domains in supporting binding to MMRN1;
    ii. whether VWF binding to other ligands for VWF A1A2A3 (specifically GPIbα and collagen) alters interactions between VWF and MMRN1;
    iii. the binding affinity of VWF-MMRN1 interactions; and
    iv. whether VWF A1A2A3 domains can support platelet adhesion to MMRN1, at a high shear rate.

2. Define the contributions of Mmrn1 to platelet adhesive functions in mice with a selective Mmrn1 deficiency, by defining the consequences of Mmrn1 loss on:
    i. bleeding phenotype;
    ii. platelet aggregation, *in vitro*;
    iii. platelet adhesion at high shear, *in vitro*; and
    iv. platelet adhesion and thrombus formation, *in vivo.*

CHAPTER 2: MATERIALS AND METHODS

2.1 MATERIALS

2.1.1 Reagents

Reagents and supplies included: CNBr-activated Sepharose™ 4B (GE Healthcare Bio-Sciences AB, Uppsala Sweden); EZ-Link Sulfo-NHS-LC Biotin (spacer arm length 22.4 Å; Pierce, Rockford, IL, USA); One Shot® Top10 Chemically Competent *Escherichia coli* (Invitrogen Canada Inc., Burlington, ON, Canada); PureLink™ Hipure Plasmid Midiprep Kit (Invitrogen Canada Inc.); Maxiprep Plasmid Kit (Qiagen Inc., Toronto, ON, Canada); EcoRI (Fermentas, Burlington, ON, Canada); HindIII (Promega, Madison, WI, USA); Opti-MEM Reduced Serum® (Invitrogen Canada Inc.); Ultroser™ Serum Substitute (Pall Canada Ltd, Mississauga, ON, Canada); Ni-NTA Agarose (Sigma-Aldrich Canada, Oakville, ON, Canada); and bicinchoninic acid (BCA) assay (Thermo Scientific, Waltham, MA, USA).

Other supplies and reagents included: microtitre plates (Costar® # 3695; Corning Inc., Kennebunk, ME, USA); chromogenic substrate tetramethylbenzidine (TMB, ALerCHEK, Inc. Colorburst™ Blue, Portland, ME, USA); 0.45 μm nitrocellulose membrane (Whatman® Protran® Dassel, Germany); EMD Millipore Immobilon™ Western Chemiluminescent horseradish peroxidase (HRP) Substrate (Thermo Fisher Scientific Inc., Mississauga, ON, Canada); Lipofectamine 2000® (Invitrogen Canada Inc.);

ristocetin (American Biochemical & Pharmaceuticals Ltd., NJ, USA); dalteparin sodium (Pfizer Canada Inc., Mississauga, ON, Canada); calcein acetoxymethyl ester (calcein-AM; Invitrogen Canada Inc.); Halt™ Protease Inhibitor Cocktail (Thermo Fisher Scientific Inc.); Vena8Fluoro+ Biochips (Cellix, Dublin, Ireland); Accustart™ II GelTrack PCR SuperMix (Quanta Biosciences, Beverly, MA, USA); ketamine (Ketaset, Wyeth, Guelph, ON); xylazine (Rompun™, BayerDVM, Shawnee Mission, KS, USA); atropine (Arto-SA, Rafter8, Calgary, AB, Canada); 3.2% sodium citrate (BD Biosciences); Heparin (Sandoz, Boucherville, QC, Canada); Phe-Pro-Arg-chloromethylketone (PPACK; Calbiochem/EMD, San Diego, CA, USA); polyethylene tubing (PE10; Becton Dickinson and Company, Franklin Lakes, NJ, USA); and Zap-oglobin II Lytic Reagent (Beckman Coulter, Mississauga, ON, Canada).

Additional reagents from Sigma-Aldrich Canada included: 2-Mercaptoethanol (2-ME); 3,3′-dihexyloxacarbocyanine iodide ($DICO_6$); Extract-N-AMP™ Tissue Polymerase Chain Reaction (PCR) Kit; prostaglandin E1 (PGE_1); Prostacyclin (PGI_2); apyrase; and ethylenediaminetetraacetic acid (EDTA); Tween® 20 (P-20); and Triton X-100; Sepharose 2B; thrombin; PAR4 agonist (TRAP, AYPGKF-NH_2); and ADP.

2.1.2 Antibody sources

Antibodies against MMRN1 included: commercial rabbit polyclonal anti-Mmrn1, sc-367225 (epitope in the C-terminal region of Mmrn1, residues 1051-1228; Santa Cruz

Biotechnology, Inc., Dallas, TX, USA); in-house prepared murine monoclonal anti-MMRN1, JS-1 (epitope in the C-terminal region of MMRN1, residues 961-1139 (38, 509)); and in-house prepared rabbit polyclonal anti-MMRN1, P155 (175, 312).

Antibodies against VWF included: rabbit polyclonal anti-VWF, A0082 (Dako, Glostrup, Denmark); HRP-conjugated rabbit polyclonal anti-VWF, P0226 (Dako); mouse monoclonal anti-VWF, MCA4683 (functional inhibitor of VWF A1-GPIbα binding (478, 479); AbD Serotec, Raleigh, NC, USA); and monoclonal anti-VWF, RU5 (functional inhibitor of VWF A3-collagen binding (480); generously provided by Dr. P.G. de Groot).

Fluorescently-labelled antibodies against mouse platelet receptors included: fluorescein isothiocyanate (FITC)-labelled anti-CD42b, (M040-1; Emfret Analytics GmbH & Co. KG, Eibelstadt, Germany); phycoerythrin (PE)-labelled anti-CD61 and FITC-labelled anti-CD29 (BD Biosciences, Mississauga, ON, Canada); and FITC-labelled anti-CD62P and PE-labelled anti-activated CD41/CD61 (JON/A; Emfret Analytics GmbH & Co. KG).

Other antibodies included: HRP-conjugated donkey anti-rabbit and donkey anti-mouse immunoglobulin G (IgG; Jackson ImmunoResearch, West Grove, PA, USA); normal mouse IgG (mIgG; Jackson ImmunoResearch); rabbit polyclonal anti- β-actin (Cell Signaling, Danvers, MA, USA); and FITC or PE-labelled isotype-matched, control immunoglobulins (Emfret Analytics GmbH & Co. KG; BD Biosciences).

2.1.3 Recombinant proteins

2.1.3.1 Recombinant MMRN1

WT recombinant MMRN1 from stably transfected human embryonic kidney (HEK) 293 cells (304, 312) was affinity purified from culture media using JS-1 conjugated to CNBr-activated Sepharose (312). Biotin-labelled MMRN1 was prepared as described (514), using a 20-fold molar excess of biotin. MMRN1 concentrations were determined by an enzyme-linked immunosorbent assay (ELISA), as described (175, 312), using: JS-1 (5 μg/ml); P155 (1:2,000 dilution); and HRP-conjugated donkey anti-rabbit IgG (1:1,000 dilution). Pooled, normal platelet lysate (prepared as described (525)), was used to quantify recombinant MMRN1, with 1 unit (U) of MMRN1 defined as the amount in 10^9 pooled normal platelets (524, 525), an amount previously shown to be equivalent to 18.5 μg of recombinant MMRN1 (524). Each preparation of purified MMRN1 was analysed for acceptable purity (>95%) and appropriate mobility as follows: samples were denatured and reduced using Laemmli sample buffer ((548); final: 2.5% 2-ME), followed by separation on 6% polyacrylamide gels containing sodium dodecyl sulfate (SDS-PAGE; (312)) and evaluations by silver staining (524), and immunoblotting after transfer to nitrocellulose (549). Immunoblots were probed for MMRN1 with P155 (1:5,000 dilution), followed by HRP-conjugated donkey anti-rabbit IgG (1:25,000 dilution).

2.1.3.2 Recombinant VWF sources

VWF mutant proteins that were tested for MMRN1 binding are depicted in Figure 4, and were generously provided by Drs. J.E. Sadler, P.G. de Groot, and E. Huizinga.

VWF cDNA of domain deleted truncates inserted into a pSVH 1.1 vector (550) were received from Dr. J.E. Sadler, and included: WT-VWF; and VWF lacking the A1A2A3 residues 497-1111 of mature VWF (ΔA1A2A3). VWF plasmid DNA were transformed into One Shot® Top10 Chemically Competent *E. coli* (following manufacture's guidelines), isolated using Plasmid Midiprep and Maxiprep Kits (following manufacture's protocols), and were subsequently digested with EcoRI and HindIII to confirm truncate identity. Restriction digested DNA fragments were resolved on a 1% agarose gel. Recombinant WT and VWF mutant protein were produced by HEK 293 cells transiently transfected using Lipofectamine 2000® (following manufacture's guidelines) and 26 µg of isolated VWF plasmid DNA.

VWF mutants from Dr. P.G. de Groot were received as stably transfected baby hamster kidney (BHK) 21 cells that overexpress furin (92, 474), and included: WT-VWF; VWF lacking the A1 domain (ΔA1; 478-716 (94)); VWF lacking the A2 domain (ΔA2; 729-910 (474)); VWF lacking the A3 domain (ΔA3; 911-1113 (92)); and a VWF protein mutant possessing the A1A2A3 domains with a C-terminal Hexa-histidine tag (498-1111

(551)). VWF mutant proteins lacked or possessed the indicated residues (in parentheses) of mature VWF.

HEK 293 and BHK 21/furin cells that respectively transiently or stably expressed VWF protein mutants were similarly cultured in media free of serum by the use of Opti-MEM Reduced Serum® or the addition of 1 % Ultroser™ Serum Substitute to culture media (111). Collected conditioned media was treated with 1 mM benzamidine and 0.01% sodium azide, and stored at -80°C until assayed. Recombinant VWF A1A2A3 expressed by BHK 21/furin cells was purified from conditioned media using Ni-NTA Agarose (following manufacture's protocols).

The concentrations of WT-VWF and VWF mutant proteins were determined by a sandwich ELISA (94), using: A0082 (1:600 dilution); P0226 (HRP-conjugated; 1:4000 dilution); and pooled, normal plasma (George King Bio-Medical Inc., Overland Park, KS, USA) taken as containing 1 U/ml VWF (equivalent to ~ 10 µg/ml VWF). VWF subunits were resolved by reduced (final: 2.5% 2-ME) SDS-PAGE (4-6% polyacrylamide) followed by immunoblotting with P0026 to assess the mobilities of WT-VWF and VWF mutant proteins.

Purified monomeric VWF mutant proteins that were tested for MMRN1 binding (generously provided by Drs. P.G. de Groot and E. Huizinga) included: VWF A1 domain (498-705 (552)), VWF A2 domain (717-915 (553)) and VWF A3 domain (911-1113 (425)).

The concentrations of provided purified monomeric VWF mutant proteins (including the A1A2A3 protein mutant) were confirmed by BCA assay, with assessment for protein purity and integrity by silver staining, as previously described in the methods of this thesis. VWF mutant proteins possessed the indicated residues (in parentheses) of mature VWF.

Other sources of VWF tested included: human plasma purified VWF (generously provided by Dr. P.G. de Groot); and recombinant mouse Vwf (generously provided by Dr. D. Lillicrap). Recombinant Vwf, received as conditioned media from stably transfected HEK 293 cells (554, 555), was quantified as previously described, except that pooled citrated (3.2% buffered sodium citrate, 1:9, v/v) platelet poor plasma from 8 week old, WT (n = 25, mixed genders) C57BL/6 mice was used as the standard and was presumed to contain 1 U/ml Vwf (554, 555).

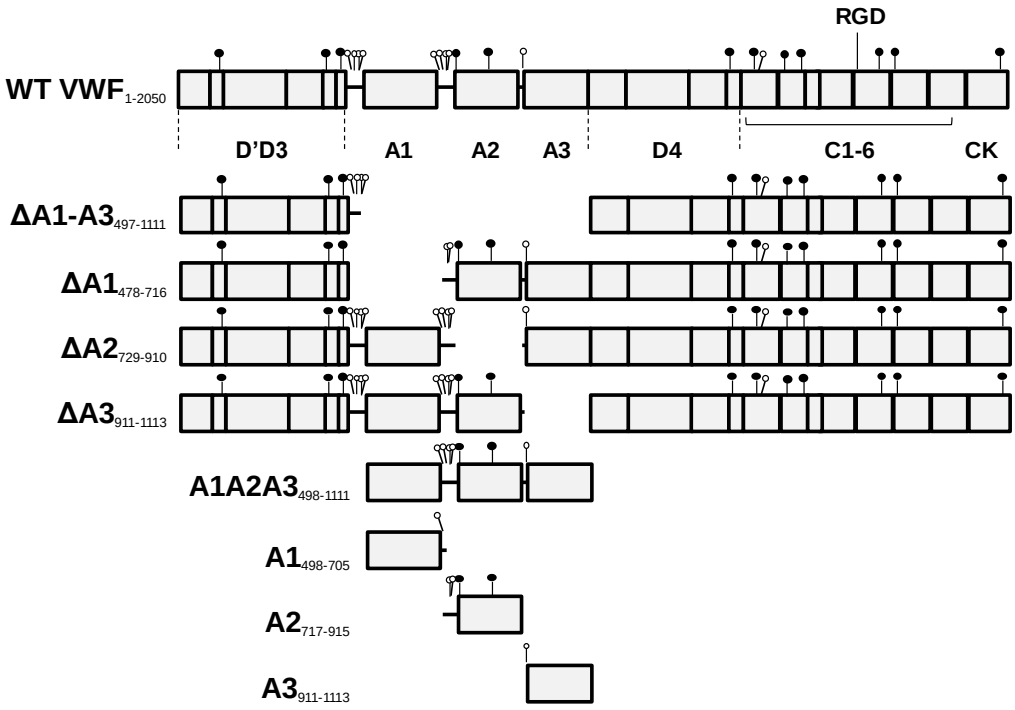

Figure 4: Recombinant VWF protein mutants used for screening MMRN1 binding. Mature VWF mutant proteins either lacked or possessed the indicated residues of mature VWF A domain(s). 13 N-linked and 10 O-linked glycans are respectively shown as closed and open symbols.

2.1.3.3 Other protein sources

Triple-helical type III collagen peptides tested were provided by Dr. R. Farndale (480) and included: VWF-binding peptide III-23, GPC-$(GPP)_5$-GPOGPSGPRGQOGVMGFOGPKGNDGAO-$(GPP)_5$-GPC-NH_2; a smaller VWF-binding peptide designated GPRGQOGVMGFO, GPC-$(GPP)_5$-GPRGQOGVMGFO-$(GPP)_5$-GPC-NH_2; and negative control peptide GPP, GPC-$(GPP)_{10}$-GPC-NH_2, that does not bind VWF (480). All of these collagen peptides were verified to not bind to MMRN1 (data included in this thesis).

Other proteins used included: Horm collagen (Nycomed Linz, Austria); and the negative control protein, bovine serum albumin (BSA; Sigma-Aldrich Canada).

2.2. METHODS

2.2.1 Helsinki Declaration on human research

This study was performed with approval from McMaster University Research Ethics Board (REB; REB# 01-268) and was conducted in accordance with the revised Helsinki Declaration on human research. For platelet adhesion experiments, venipuncture blood (5 – 30 ml) was collected after obtaining written informed consent from 3 healthy individuals, and from an individual with type 3 VWD and undetectable plasma and platelet VWF (8, 38)).

2.2.2 VWF-MMRN1 protein binding assays

2.2.2.1 Modified enzyme-linked immunosorbent assay (ELISA)

Modified ELISAs (38) were used to assess the ability of immobilized MMRN1 (microtitre plates incubated with 0.5 μg per well) to support the binding of: WT-VWF (0 – 0.2 μg per well), VWF lacking individual A domains (0.05 – 0.1 μg per well), and the mutant protein VWF A1A2A3 (0 – 0.3 μg per well). WT-VWF and VWF protein mutants were tested: untreated; after pre-treatment with ristocetin (1 mg/ml); or after exposure to shear on a mini vortex mixer for 20-30 seconds (2500 – 3200 rotations per minute (RPM); VWR, Radnor, PA, USA) (556). Other assays were performed to assess the ability of immobilized plasma purified VWF or VWF A1A2A3 (0.5 μg incubated per well) to support MMRN1 binding (0 – 0.4 μg per well). Microtitre plates were coated with the desired proteins diluted in carbonate buffer (14.2 mM Na_2CO_3, 35 mM $NaHCO_3$, pH 9.6) and incubated overnight at 4°C, then plates were blocked with 2% BSA in HEPES-Tyrode buffer (5 mM HEPES, 137 mM NaCl, 2 mM KCl, 0.3 mM NaH_2PO_4,1 mM $MgCl_2$, 12 mM $NaHCO_3$, pH 7.4, supplemented with 2 mM $CaCl_2$) for 2 hours at room temperature, and VWF-MMRN1 binding was assessed after incubation for 2 hours at room temperature. For all protein binding assays, purified test proteins were diluted in HEPES-Tyrode buffer containing 2 mM $CaCl_2$. VWF bound to immobilized MMRN1 was detected with P0226 (1: 4,000 dilution), and MMRN1 bound to immobilized VWF was detected with JS-1 (2 μg/ml), followed by HRP-conjugated donkey anti-mouse (1:1,000 dilution). Bound HRP-

conjugated antibodies were detected using the chromogenic substrate TMB, and reaction was stopped with 1 M H_2SO_4 before measuring the optical density (OD) at 450 nm on a microplate reader (ELx808, with KC4 software version 3.4; Bio Tek Instruments, Winooski, VT, USA) (38). The OD reading for the negative control (wells precoated with BSA) was subtracted from the test reading to correct for nonspecific binding (~ 10% of the OD reading for the positive control, WT-VWF). Binding assays were done three times with each sample, each tested in duplicate or triplicate.

For some assays, VWF binding to MMRN1 was assessed by the simultaneous addition (without preincubation) of 2 μg/ml of an inhibitory antibody against VWF A1 domain (MCA4683 (478, 479)), A3 domain (RU5; (480)), or control mIgG. For other experiments, VWF binding to MMRN1 was assessed by the simultaneous addition (without preincubation) of 250 μg/ml of the VWF binding collagen peptides III-23, GPRGQOGVMGFO, or the control peptide, GPP. Inhibitory antibodies and peptides were used at concentrations that were confirmed to inhibit VWF binding to GPIbα and collagen (480), respectively.

2.2.2.2 Surface plasmon resonance (SPR)

SPR was used to estimate the binding affinity of VWF for biotinylated MMRN1 that was immobilized onto streptavidin-coated sensorchips (GE Healthcare Canada, Mississauga, ON, Canada) at levels ranging from 500 – 1000 resonance units (RU; 1000

RU is equivalent to ~1 ng protein/mm^2 (514)). BIAcoreX instrument and software (BIAcore, Uppsala, Sweden) was used to monitor the real-time association and dissociation of VWF A domains (in HEPES-Tyrode-$CaCl_2$ buffer, with 0.005% P-20) to captured biotinylated MMRN1. The analytes, VWF A1A2A3, A1, A2, and A3 protein mutants, were perfused at different contact times (2 – 10 minutes (min)) and injected at varying flow rates (10 – 40 μl/min) to avoid mass transfer effects (557, 558). MMRN1 could not be tested as the analyte in SPR experiments because fluid-phase MMRN1 has high non-specific binding to biochips and BIAcore instrument tubing (514).

Full-length VWF was previously noted to have varied and inconsistent binding to MMRN1 by SPR (38), likely because the shear rates are low during these experiments (556). The polymeric nature of both VWF and MMRN1 also confound affinity estimations because of the erroneous measurements of avidity instead of affinity (559, 560). Consequently, the binding affinities of MMRN1 for VWF were defined by using VWF A domain(s) mutant proteins, as described for other VWF ligands (310, 481, 482). VWF A domain mutant proteins can also form polymers (444) due to interactions between VWF A1 and A2 domains (30, 444), but not the A3 domain (30). We controlled the self-association of VWF A domain mutants by testing VWF A1A2A3 and A1 at concentrations well below those reported to induce self-association (< 500 nM; (31)). VWF mutant proteins were tested at various concentrations (≤ 250 nM for A1; ≤ 25 nM for A1A2A3; ≤ 2000 nM for A3). The baseline MMRN1 surface was confirmed to be restored by a 30 – 60 second pulse (flow rate: 20 μl/min) with 1 M NaCl containing 50 mM NaOH (514). The

MMRN1-VWF binding to a negative control (surface treated with biotinylated albumin) was subtracted to correct for changes in the bulk refractive index of buffers and nonspecific binding of VWF A domain protein mutants (557). SPR experiments were repeated 2 or more times for each analyte, using different preparations of biotinylated MMRN1 and VWF A1A2A3. Data were analysed using recommended global curve-fitting procedures (561) and binding affinities were determined using BIAEvaluation software (version 4.1) and best-fit models for data (determined by visual inspection of residuals and Chi^2 values) (514). The simplest model that fit the data were used to define the binding affinity (557, 558): the two state conformational model ($K_D = (k_{d1} \cdot k_{d2})/k_{a1}(k_{d2}+k_{a2})$) was used for VWF A1A2A3 and A1 domain binding to MMRN1; whereas the 1:1 Langmuir binding model ($K_D = k_d/k_a$) was used for VWF A3 binding to MMRN1.

2.2.3 Human platelet preparation

Venipuncture blood was collected into low molecular weight heparin anticoagulant (final concentration: 20 U/ml dalteparin sodium) to prepare calcein-labelled, washed platelets for adhesion assays (38, 562). Platelet-rich plasma (PRP) was prepared by centrifugation (120 x g for 10 min at room temperature; (38, 562)), followed by incubation of the platelets with calcein-AM (2.5 μg/ml, 30 min at 37°C), centrifugation at 1,500 x g for 10 min to remove plasma proteins, followed by two sequential washes in buffer containing platelet activation inhibitors (36 mM citric acid, 103 mM NaCl, 5 mM glucose, 5 mM KCl, 1 mM $MgCl_2$, pH 6.5, with 0.1 U/ml apyrase and 1 μM PGE_1) (38). Washed

platelets were resuspended in HEPES-Tyrode buffer with 2 mM $CaCl_2$ (38). Red blood cells (RBC) from the collected blood were washed in buffer containing 10 mM HEPES, 140 mM NaCl, 5 mM glucose, pH 7.4, with 0.1 U/ml apyrase (38), before being mixed with platelet resuspensions (final: 300 x 10^6 platelets/ml; haematocrit 45%).

2.2.4 *In vitro* platelet adhesion to MMRN1, under high shear (1, 500 s^{-1})

High shear (1500s^{-1}) platelet adhesion assays were performed to determine the regions of VWF that are important for supporting platelet adhesion to MMRN1. Vena8Fluoro+ Biochips were precoated with MMRN1 or BSA (50 μg/ml, overnight at 4°C), blocked with 2% BSA in HEPES-Tyrode buffer (supplemented with 2 mM $CaCl_2$; 2 hours at room temperature), before pre-treatment with: VWF A1A2A3 (40 nM, estimated based on a ~ 73 kDa monomer size (8)); WT-VWF (40 nM, positive control; estimated based on a ~ 250 kDa monomer size (354, 374)); or buffer only as a negative control (0.2% BSA in HEPES-Tyrode-$CaCl_2$ buffer). Pre-treatments were done by perfusing proteins at a high shear rate (1500 s^{-1}, 6 min), using Mirus™ 2.0 Nanopump (Cellix) and VenaFluxAssay™ Software (Cellix). Subsequently, calcein-labelled platelets (in reconstituted blood) were perfused at a high shear rate (1500 s^{-1}, 3 min), before washing unbound platelets from the surfaces using 0.2% BSA in HEPES-Tyrode supplemented with 2 mM $CaCl_2$ and 1 U/ml heparin (750 s^{-1}, 2 min).

For some assays, MMRN1 precoated chambers were perfused with WT-VWF that was preincubated (15 min at 37°C) with 20 μg/ml of MCA4683 (inhibitory antibody against VWF A1; (478, 479)) or control, mouse IgG.

Adherent platelets were quantified by endpoint analysis of 10 or more microscope field images (acquired with 40 X objective), visualized with a Zeiss Axiovert 200 inverted epifluorescence microscope and AXIOVISION software (Carl Zeiss Canada Ltd., Toronto, ON, Canada) (38) with comparison of fluorescently labelled platelets (white) to background (dark area with no adherent platelets). Data were reported as the percentage (%) of an area (circle: 15 x 15 cm) that was covered by platelets (38). Platelet adhesion assays were conducted at least two times with different protein preparations and control donor samples.

2.2.5 Animal handling

This study met the regulations set by the Canadian Council of Animal Care, and were performed with approval from McMaster University Animal Research Ethics Board (Animal Utilization Protocol #13-02-02) and the Animal Care Committee (ACC) at St. Michael's Hospital (ACC #437). Mmrn1 mice were interbred and maintained at the animal vivaria at: McMaster University Medical Centre; the Thrombosis and Arteriosclerosis Research Institute in Hamilton; and St. Michael's Hospital's Keenan Research Centre. Mmrn1 mice were housed in specific pathogen-free facilities with a 12-hour dark-light

cycle, and were kept in sterilized filter-top cages. Mmrn1 mice were fed, ad libitum, sterile water and irradiated regular chow (18 % protein rodent diet; Teklad Global Diets, Madison, WI, USA) or a breeder diet (19% protein extruded rodent diet; Teklad Global Diets), whenever applicable. Studies on platelet function were conducted with gender-mixed, age-matched, littermates (WT, $Mmrn1^{+/+}$; $Mmrn1^{-/-}$; and $Mmrn1^{+/-}$), and whenever possible, researchers were blinded to mouse genotypes for experimental animals.

2.2.6 Generating mice with a selective Mmrn1 deficiency

Mmrn1 knockout mice were generated by Dr. Subia Tasneem, as part of collaborative studies between the laboratories of Drs. Bradley Doble and Catherine Hayward, using mice possessing a *Mmrn1* "knockout first allele" ($Mmrn1^{flnxeo/+}$, (563) obtained from European Mutant Mouse Archive (EMMA), Neuherberg/Munich, Germany; EM:05337; http://www.informatics.jax.org). Figure 5 details the strategy for generating *Mmrn1* deficient mice.

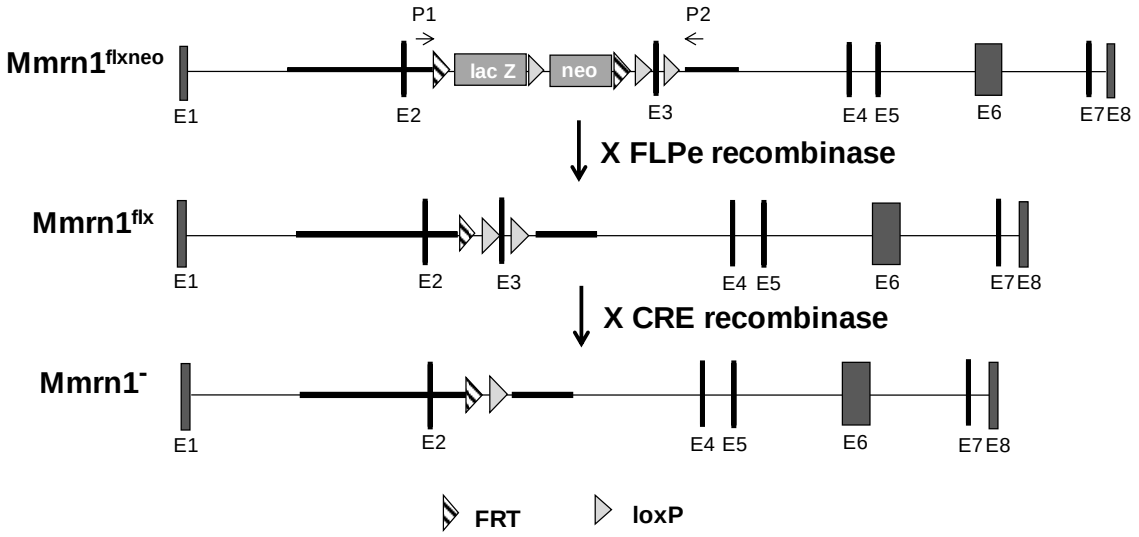

Figure 5: Creating mice with a selective Mmrn1 deficiency. Breeding schematic for creating mice with a selective Mmrn1 deficiency, beginning with mice heterozygous for a 'knockout-first allele' ((563); shown as $Mmrn1^{flxneo}$ allele). $Mmrn1^{flnxeo}$ allele possess a gene trapped Mmrn1 gene with: flippase recombinase target (FRT) sequences flanking an internal ribosomal entry site (IRES):lacZ trapping cassette and a floxed (by loxP sites) promoter-driven Neomycin (neo) cassette inserted into the second intron; and the third exon (E3) flanked by loxP sites. FLPe-FRT and subsequent Cre-loxP site-specific recombination created a null allele ($Mmrn1^{-}$) due to removal of cassettes and deletion of the third exon (E3), which generated a frameshift mutation that produced a severely truncated gene product possessing only E1-2. Primer pairs (P1 and P2) that were used to verify and distinguish $Mmrn1^{+}$ and $Mmrn1^{-}$ alleles are shown.

2.2.7 Genotyping Mmrn1 deficient mice

Genomic DNA was extracted from mouse tails (0.5 – 1 cm of distal tip) using Extract-N-AMP^{TM} Tissue PCR Kit as per the manufacture's protocol, followed by PCR using the oligonucleotide primers: forward (5'-TCTTTCTCTCCCTCTCACCCT-3'); and reverse (5'-GGCTCCTTTCATTCACAGCC-3'). PCR fragments were resolved on a 2% agarose gel. The respective size of the PCR products for mice of different genotypes were: 1038 base pairs (bp) for WT (Mmrn1$^{+/+}$); 336 bp for homozygous null (Mmrn1$^{-/-}$); and 1038 bp and 336 bp for heterozygous (Mmrn1$^{+/-}$) mice.

2.2.8 Mouse blood collection and cell count analysis

Whole blood was collected into citrate-anticoagulant (1:9, v/v) from anaesthetized (125 μg/g ketamine; 12.5 μg/g xylazine; 0.25 μg/g atropine) Mmrn1 mice by cannulating the carotid artery (9). The right common carotid artery was exteriorized by blunt dissection, permanently occluded inferior to bifurcation of carotid artery with a 5-0 silk surgical suture, and temporarily occluded superior to bifurcation of brachiocephalic artery with an artery clip, before subsequently cannulation using PE10 tubing. After removing the artery clip, 800-900 μl of arterial blood was collected into syringes pre-filled with 100-200 μl of sodium citrate.

Complete blood counts of collected samples were determined on an automatic veterinarian cell counter (Hemavet 950FS, Drew Scientific Group, Waterbury, CT, USA) and were corrected for dilution with anticoagulant.

2.2.9 Mouse platelet lysate and plasma preparation

Platelet lysate was prepared after isolating platelets from citrate-anticoagulated whole blood (9, 562). Briefly, whole blood samples were centrifuged at 180 x g for 6 minutes at room temperature to obtain PRP, then inhibitors of platelet activation (0.5 μM PGI_2 and 0.02 U/ml apyrase) were added (9). PRP samples were then centrifuged at 500 x g for 6 minutes to pellet platelets, and the platelet pellet was washed twice with a modified Tyrode buffer (20 mM HEPES, 134 mM NaCl, 0.34 mM Na_2HPO_4, 2.9 mM KCl, 12 mM $NaHCO_3$, 5 mM glucose, 0.35% (w/v) BSA, pH 7.0) containing inhibitors of platelet activation (0.5 μM PGI_2 and 0.02 U/ml apyrase). Washed platelets were pelleted and lysed (final: 1 x 10^{10} platelets/ml) in TBS (20 mM Tris, 137 mM NaCl, pH 7.4) containing (final: 0.5% Triton X-100, 1X Halt™ Protease Inhibitor Cocktail and 5 mM EDTA) (564).

Platelet poor plasma (PPP) was harvested from 3.2% sodium citrate anticoagulated whole blood (1:9, v/v) after centrifugation at 1,500 x g for 20 minutes, followed by a second centrifugation at 10,000 x g for 5 minutes to ensure removal of platelets (37).

2.2.10 Immunoblot analysis of mouse platelet and plasma proteins

Platelet lysates (2.5 µl of 10^{10} platelets/ml) were separated by reduced SDS-PAGE (5% polyacrylamide gels for Mmrn1 and Vwf; 10% gels for β-actin) for immunoblot analysis of Mmrn1 (sc-367225, 1:200) and Vwf (P0226, 1:2,500), with the β-actin (rabbit anti- β-actin, 1:5,000) immunoblot used to verify equivalent sample loading.

2.2.11 Analysis of mouse Vwf levels in plasma and platelet lysates

Vwf levels in PPP and platelet lysate samples were quantified as previously described in this thesis (refer to Section 2.1.3.2 Recombinant VWF sources) and elsewhere (554, 555, 565), with the Vwf content of pooled plasma from WT, 8-12 weeks old, gender-mixed littermates (n = 10) arbitrarily defined as 100% plasma Vwf.

2.2.12 Mouse tail transect bleeding model

6-8 weeks old gender-mixed mice (maintained on a thermal blanket, temperature: 37°C) were anaesthetized using ketamine-atropine-xylazine cocktail, as previously detailed (9, 330), and the distal tip of the tail was transected at a constant diameter (1.5 mm) (329, 330, 566, 567). Transected tails were immediately immersed in isotonic saline (0.9% NaCl, ~40 ml) maintained at 37°C with a thermoblanket (330, 567). Bleeding time was recorded for a maximum of 15 min (900 seconds), at which point tails were cauterized to prevent

further bleeding. RBC were lysed with 2 drops of Zap-oglobin II Lytic Reagent (~70 µl in 1000 µl of blood/saline mixture) and the amount of blood loss was determined by measuring the OD at 405 or 492 nm (depending on the volume of blood loss) (330, 566, 567). Blood loss ($\mu l_{blood}/ml_{saline}$) was determined using a standard curve from samples with pre-defined volumes of blood, then the total blood loss (μl_{blood}) was determined by considering the total volume of saline (ml_{saline}) used in tail transect studies.

2.2.13 *In vitro* platelet aggregation by physiological agonists

Aggregation responses were assessed using PRP and gel-filtered platelets (GFP), respectively adjusted to 2.5 x 10^8 platelets/ml using autologous and genotype, gender-matched PPP, or PIPES buffer (37, 193). Each PRP (from 2% sodium citrate anticoagulated whole blood (1:9, v/v)) and GFP sample for testing was prepared by pooling samples from 2-3 genotype-matched mice. GFP was prepared by using a Sepharose 2B chromatography column equilibrated with PIPES buffer (5 mM PIPES, 137 mM NaCl, 4 mM KCl, 0.1% glucose, pH 7.0) (37, 193). For aggregation responses to collagen or thrombin, platelet suspensions were supplemented with 2 mM $MgCl_2$ or 1 mM $CaCl_2$, respectively as described (139, 193, 307, 568, 569). Aggregation responses were monitored for 15-20 min using a Chrono-Log aggregometer (set at 1000 RPM, 37°C), 250 µl of PRP or GFP, and a panel of agonists that included: TRAP (500 µM, PRP only), thrombin (0.5 and 1.0 U/ml, GFP), Horm collagen (5, 10 and 20 µg/ml, PRP and GFP) and ADP (10 and 20 µM, PRP

only). 100% aggregation was set using PPP for PRP, and PIPES buffer for GFP samples (37, 193).

2.2.14 *In vitro* platelet adhesion to collagen and Vwf, under high shear

Perfusion studies were performed using Vena8Fluoro+ Biochips (Cellix) precoated with Horm collagen (100 µg/ml; (100)) or murine Vwf (10 U/ml; (98, 570)) to assess the consequences of platelet Mmrn1 loss on platelet adhesion at a high shear rate (1500 s^{-1}).

Whole blood was collected in 93 µM PPACK for these perfusion studies, with an additional 2 U/ml of heparin added for testing adhesion to collagen. Mouse platelets (≥ 5 x 10^8/ml for whole blood) were labelled by incubating whole blood with $DIOC_6$ (4 µM, 10 minutes at 37°C), and samples were perfused over pre-coated surfaces for 3 min, before removal of unbound platelets by washing as previously described (37, 38, 571). Adherent platelets (quantified as % area covered by platelets and the numbers of adherent platelets) were estimated using microscope field images. Adhesion to collagen was estimated as previously detailed in this thesis (refer to Section 2.2.4 In vitro platelet adhesion to MMRN1, under high shear (1, 500 s-1) and elsewhere (37). The adhesion of individual resting platelets on Vwf surfaces are associated with smaller aggregates than on collagen surfaces (570). Therefore, adhesion of resting platelets (in whole blood) to Vwf was estimated by analyzing the entire chamber at 20X magnification (w: 1300; h: 860). As described in this thesis (refer to Section 2.2.4 In vitro platelet adhesion to MMRN1, under

high shear (1, 500 s-1) and elsewhere (37, 38, 571), threshold settings were standardized with fluorescently labelled platelets (white), relative to a dark background (area with no adherent platelets).

2.2.15 Surface expression of receptors on resting and thrombin-activated platelets

Resting washed mouse platelets for flow cytometry were prepared from heparinized (final concentration: 4 U/ml) blood as described (9). Washed platelets were prepared as described in this thesis (refer to Section 2.2.9 Mouse platelet lysate and plasma preparation), and were then resuspended in Tyrode buffer which was then supplemented with 1 mM $CaCl_2$ (final) before quantifying surface expression of the following proteins by flow cytometry: GPIbα (anti-CD42b, M040-1, Emfret Analytics GmbH & Co. KG); $\alpha_{IIb}\beta_3$ (anti-CD61,BD Biosciences); and $\alpha_2\beta_1$ (anti-CD29; BD Biosciences). Antibodies (5 µl M040-1; 1 µl BD antibodies, and 5 or 1 µl isotype controls) were incubated with 26 or 100 µl resting platelets (10^6 platelets/ml) for 15 – 30 min at room temperature (9, 37).

For assessing markers of platelet activation, washed mouse platelets were resuspended in Tyrode buffer supplemented with 1 mM $CaCl_2$, then activated with thrombin (0 – 96.4 mU/ml; 15 min at room temperature) before evaluating activation-induced changes in $\alpha_{IIb}\beta_3$ (anti-CD41/CD61; JON/A, Emfret Analytics GmbH & Co. KG) and platelet surface expression of P-selectin (anti-CD62P; Emfret Analytics GmbH & Co. KG). 2.5 µl of each antibody was simultaneously incubated with thrombin-stimulated

platelets (final: 10^6 platelets in 26 µl) for 15 min at room temperature (9). Platelets were fixed with 1% formaldehyde as described (9), and labelled platelets (in fixate) were immediately evaluated by flow cytometry (total: 10^4 events; mean fluorescent intensities, MFI, quantified as medians) on a BD FACSCalibur instrument, using previously established instrument settings (9), with comparison to isotype control antibodies, whenever possible.

2.2.16 Intravital microscopy – ferric chloride injury model

Intravital microscopy was performed collaboratively with Dr. Y. Wang, in the research laboratory of Dr. H. Ni, to evaluate *in vivo* platelet adhesion and thrombus formation in mesenteric arterioles treated with ferric chloride (37, 49, 218). I genotyped ear clippings from experimental animals, and Dr. Wang prepared GFP from genotype-matched, gender-mixed donor mice as described in this thesis (refer to Section 2.2.13 In vitro platelet aggregation by physiological agonists) and elsewhere (37, 193). GFP were fluorescently labelled with calcein-AM (1 µg/mL for 30-60 min at 37°C) for injection into the tail vein of 3-4 weeks old genotyped-matched mice, whose mesenteric vascular bed was exteriorized for intravital microscopy through a midline abdominal incision (37). A single arteriole was chosen for analysis, based on vessel diameter (~ 80 – 120 µm), shear rate (~1500 s^{-1}) and vessel exposure (free of adipose tissue) (37). Dr. Wang induced thrombus formation by superfusion of 30 µL of 250 mM ferric chloride onto the target vessel, and recorded using a Zeiss Axiovert 135-inverted fluorescent microscope (Zeiss Oberkochen,

Germany). Thrombus formation was collaboratively assessed by myself and Dr. Wang, by analysis of: 1) number of fluorescently labelled platelets deposited on the vessel wall 5-7 min after initiation of ferric chloride injury; 2) time required for the formation of the first 20 μm thrombus; and 3) vessel occlusion time, defined as the complete cessation of blood flow for at least 10 seconds (37).

2.3 STATISTICAL ANALYSIS

Data from protein binding assays was reported as the mean (with non-specific binding subtracted) ± standard deviation (SD) for representative experiments, unless otherwise stated.

Data from animal studies were reported as mean ± standard error of the mean (SEM), unless data failed to pass normality tests ($p < 0.05$, Shapiro-Wilk or D'Agostino-Pearson Omnibus Normality test; GraphPad Prism 6, La Jolla, CA, USA), in which case non-parametric data were expressed as the median, range (min-max). Typically, 5 or more mice were tested, per genotype, as this sample size is the accepted minimum to obtain statistical significance with a minimum of 80% power.

Comparative data with two groups were evaluated by an unpaired two-tailed Student's *t* test or Mann-Whitney test (for non-parametric data). Comparative data for three

or more groups were evaluated by one-way analysis of variance (ANOVA) or Kruskal-Wallis test (for non-parametric data), followed by post hoc analyses (GraphPad Prism 6).

Best-fit, nonlinear, stimulation four parameter curves were generated to analyze the surface expression of receptors on thrombin-activated platelets. MFI were plotted relative to thrombin concentrations (log, mU/ml), assuming a bottom of 0 because MFI of resting platelets were subtracted (9). Data were analyzed with the null hypothesis that the other 3 parameters (top of curve, logEC50 and hill/slope) are similar for each genotype compared if the extra sum of squares F test was $p \geq 0.05$, generating a single curve for the different genotypes (9). Alternatively, if the F test was $p < 0.05$, separate curves were generated for each genotype compared (9).

Proportional data were analyzed using the Fisher's exact test when two groups were compared, or the Chi^2 test when three groups were compared (i.e., observed versus expected Mendelian ratios for litters of heterozygous mice; (572)).

For all statistical analyses, *p* values < 0.05 were considered statistically significant.

CHAPTER 3: RESULTS

The following chapter details the findings from studies that aimed to: 1) define the MMRN1 binding region in the shear-sensitive protein, VWF; 2) gain insights on the molecular mechanisms of platelet adhesion to MMRN1 at high shear; and 3) define Mmrn1 contributions to platelet adhesive, haemostatic functions in mice with selective Mmrn1 deficiency.

The data displayed in sections 3.1 and 3.2 of this chapter were previously published (571) and are reproduced with permission from *Thrombosis and Haemostasis*. The senior author of this manuscript is Dr. Catherine P.M. Hayward. Dr. Hayward supervised the study design, experimental work and writing of the manuscript. I contributed to the study design, experimental work, data analysis, and manuscript writing. Dr. Subia Tasneem contributed to the study design, provided guidance with data interpretation, manuscript writing, and provided technical guidance. Drs. Richard W. Farndale and Dominique Bihan created and provided triple-helical type III collagen peptides for these studies, guidance with data interpretation, and helped with writing the manuscript. Drs. J. Evan Sadler, Philip G. de Groot, Eric G. Huizinga, and Ms. Silvie Sebastian provided important VWF mutant proteins and inhibitory antibodies for these studies, guidance with data interpretation, and helped with writing the manuscript. Dr. Lisa A. Westfield and Mrs. Nola Fuller provided technical guidance.

3.1 MECHANISM OF VWF BINDING TO MMRN1

As VWF binds to MMRN1 matrices and is required for platelet adhesion to MMRN1 under high shear (38), I explored the mechanisms of VWF-MMRN1 binding, and the need for fluid shear to modulate this binding interaction. In modified ELISA, WT-VWF exposed to shear or ristocetin (which mimics the effects of shear (457)) showed more binding to MMRN1 than untreated VWF ($p < 0.05$, Figure 6A). The binding of ristocetin or shear exposed WT-VWF to MMRN1 matrices was also saturable and concentration-dependent (Figure 6A), unlike the inconsistent and often undetectable binding of untreated VWF. Immobilized VWF also supported concentration-dependent and saturable MMRN1 binding ($p < 0.001$, relative to negative control, BSA surface; Figure 6B).

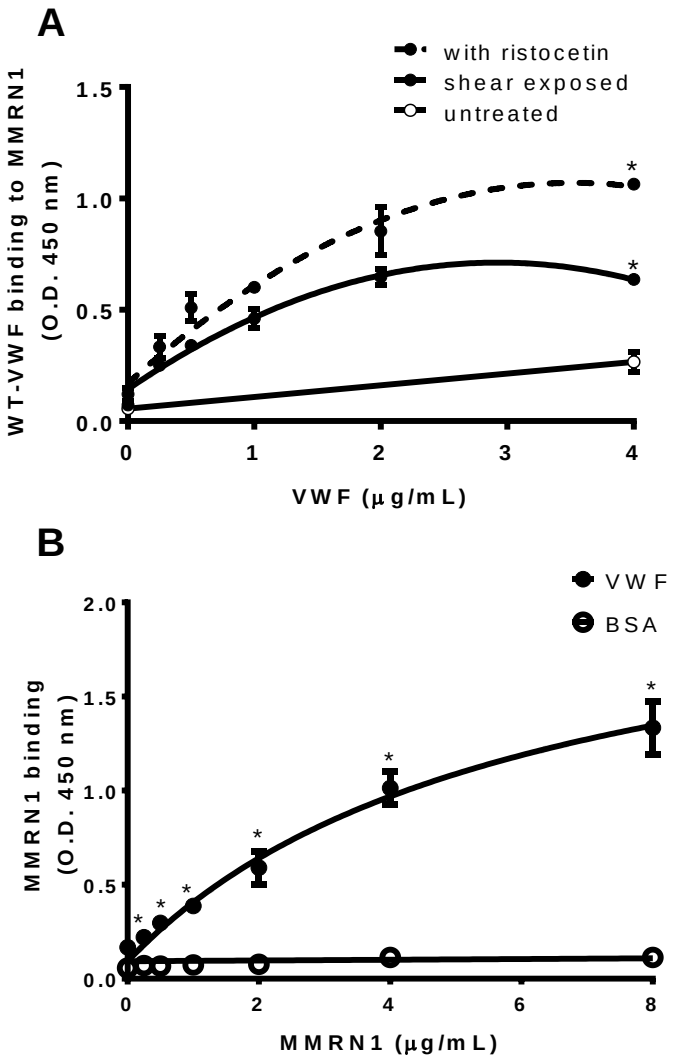

Figure 6: VWF-MMRN1 binding curves, in modified ELISA. A) Binding of untreated (open circles, solid line), shear-exposed (closed circles, solid line) and ristocetin-treated (closed circles, dashed line) WT-VWF to immobilized MMRN1. * indicates different from untreated VWF ($p < 0.05$). B) Binding of MMRN1 to immobilized WT-VWF (closed circles) and to the negative control protein BSA (open circles) were compared. * indicates different ($p < 0.001$) from BSA coated surfaces. Binding data shown were representative of 3 separate experiments, expressed as the mean OD 450 nm ± SD. Reproduced with permission from Thrombosis and Haemostasis 2016. 116(1): 87-95.

As the functions of the VWF A domains are known to be influenced by shear (24, 29, 152, 363, 446, 448, 471), I next evaluated the mechanism of VWF binding to MMRN1 using mutated VWF constructs, which were expressed *in vitro*.

VWF mutant proteins lacking all A domains (ΔA1A2A3) showed impaired binding to MMRN1 ($p < 0.01$, relative to WT-VWF), as did VWF mutant proteins lacking the A1 (ΔA1) or A3 domains (ΔA3) ($p < 0.01$, relative to WT-VWF) (Figure 7A). However, the VWF construct lacking the A2 domain (ΔA2) showed binding to MMRN1 that was indistinguishable from WT-VWF (Figure 7A).

Further analyses were done to determine if monoclonal antibodies and peptides that bind to VWF A1 or A3 domain inhibited VWF-MMRN1 binding. In modified ELISA, WT-VWF binding to immobilized MMRN1 was reduced (~55% reduction) by monoclonal antibodies that inhibit ristocetin-induced VWF A1 domain binding to GPIbα (MCA4683) or VWF A3 domain binding to collagen (RU5) ($p < 0.05$, relative to VWF alone; Figure 7B-C), whereas mIgG had no effect. VWF binding to MMRN1 was inhibited by type III collagen peptides III-23 (sequence: GPOGPSGPRGQOGVMGFOGPKGNDGAO) and by the smaller peptide GPRGQOGVMGFO that binds to the A3 region of VWF (~70% reduction; $p < 0.01$, relative to VWF alone), but not by the control collagen peptide GPP (Figure 7D).

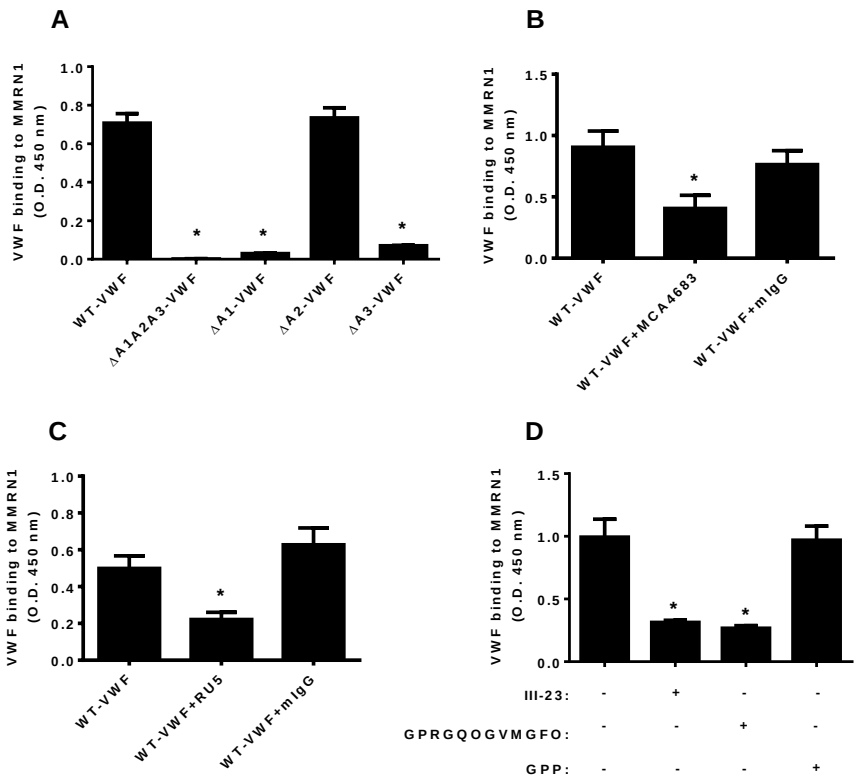

Figure 7: Binding of WT-VWF and VWF mutant proteins to immobilized MMRN1, with or without functional inhibitors, in modified ELISA. A) The binding of 0.5 μg/ml shear-exposed WT-VWF, and VWF mutant proteins lacking all or one A domain (ΔA1A2A3, ΔA1, ΔA2, ΔA3), to MMRN1. * indicate reduced binding ($p < 0.01$), relative to WT-VWF. B) Effect of MCA4683 (2 μg/ml, a VWF A1 domain antibody that inhibits GPIbα binding (478, 479)) or negative control mIgG (2 μg/ml) on VWF-MMRN1 binding in the presence of ristocetin. * indicates reduced ($p < 0.05$), relative to WT-VWF without inhibitory antibody. C) Effect of RU5 (2 μg/ml) a VWF A3 domain antibody that inhibits collagen binding (480), and mIgG (2 μg/ml; negative control) on VWF-MMRN1 binding is compared. * indicates reduced binding ($p < 0.05$), relative to WT-VWF without inhibitory antibody. D) Effect of type III collagen peptides that bind to VWF A3 domain (III-23: GPOGPSGPRGQOGVMGFOGPKGNDGAO, and GPRGQOGVMGFO (480)) and the negative control peptide, GPP, on VWF-MMRN1 binding. * indicates reduced, ($p < 0.01$), relative to WT-VWF without inhibitory peptide. Panels show representative (D; expressed as the mean OD 450 nm ± SD) or pooled (A-C; expressed as the mean OD 450 nm ± SEM) data for 3 separate independent experiments. Reproduced with permission from Thrombosis and Haemostasis 2016. 116(1): 87-95.

Next, the mechanism of VWF binding to MMRN1 was further explored using VWF domain peptides. In modified ELISA, VWF A1A2A3 (tested without exposure to shear or ristocetin) showed saturable, concentration-dependent binding to immobilized MMRN1 ($p < 0.001$, relative to BSA coated surfaces; Figure 8A) whereas the individual VWF A1, A2, and A3 domains showed inconsistent binding to immobilized MMRN1.

Next, SPR was performed to further assess for stable and/or transient binding of individual A domains to MMRN1, and to compare the association and dissociation profiles (Figure 8B). In SPR experiments, the A1, A3, and A1A2A3 domains showed binding to MMRN1, unlike the A2 domain (Figure 8B). VWF A1A2A3 binding to MMRN1 showed some features of VWF A1 domain and A3 domain binding to MMRN1 (Figure 8B). Like VWF A1 domain, VWF A1A2A3 showed rapid initial association to MMRN1, followed by an initial rapid dissociation from MMRN1 (Figure 8B). This was then followed by a second slower phase of dissociation that resembled dissociation of the VWF A3 domain from MMRN1, as well as the later phase of VWF A1 domain dissociation from MMRN1 (Figure 8B). VWF A3 domain showed apparently slower association and dissociation from MMRN1 than the A1 and A1A2A3 protein mutants (Figure 8B).

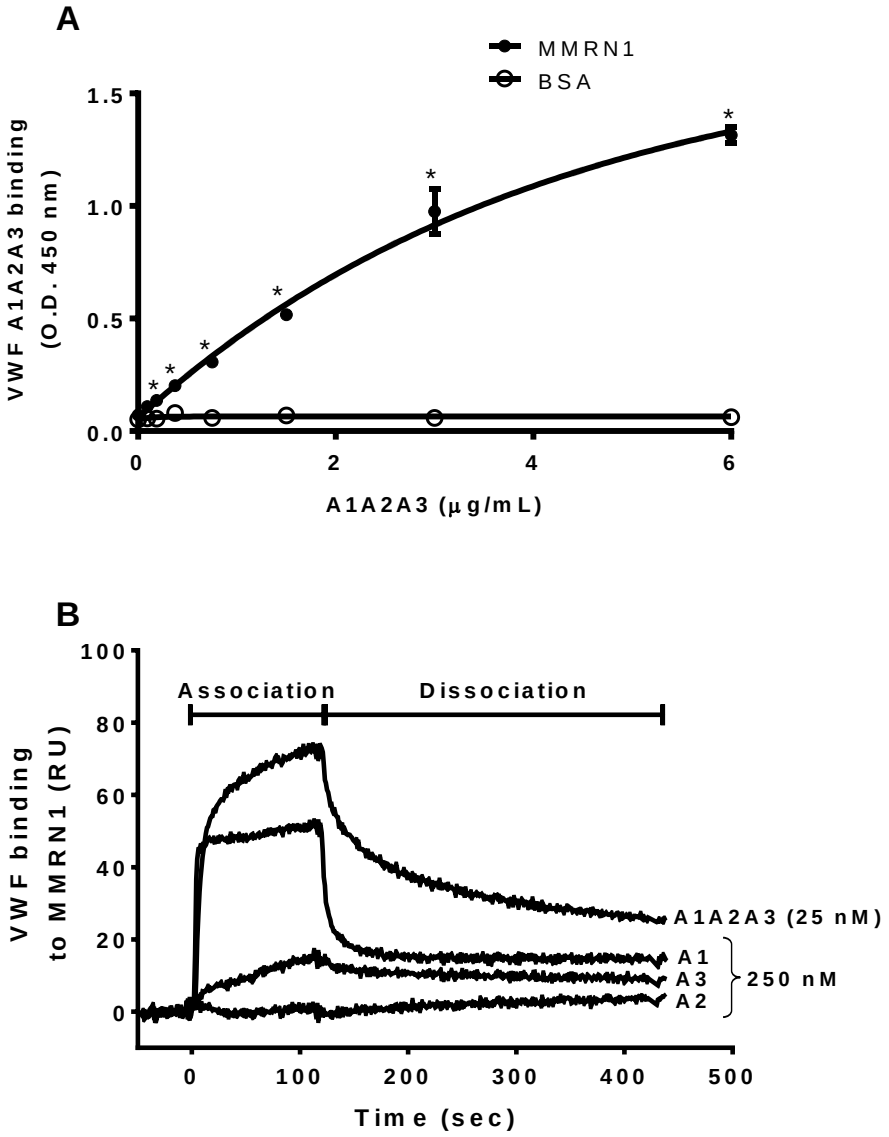

Figure 8: VWF A domain binding to MMRN1, in modified ELISA and SPR. A) Binding of VWF A1A2A3 to immobilized MMRN1 (closed circles) is compared to the negative control protein BSA (open circles). * indicates different ($p < 0.001$) from BSA. Panel B shows a representative plot of the association and dissociation profiles for VWF: A1A2A3 (25 nM); and A1, A2, and A3 domain (250 nM) binding to MMRN1-coated sensor chips (~1000 RU immobilized MMRN1). Binding data shown were representative of 2-3 separate experiments, with ELISA data expressed as the mean OD 450 nm ± SD. Reproduced with permission from Thrombosis and Haemostasis 2016. 116(1): 87-95.

SPR findings were further evaluated to assess VWF-MMRN1 binding. Table 4 summarizes the binding kinetic estimations for the binding of VWF A1A2A3, A1, and A3 domains to MMRN1.

SPR analyses indicated that VWF A1, A3 and A1A2A3 binding to immobilized MMRN1 was concentration-dependent (Figure 9A-C). The binding of VWF A1A2A3 and the A1 domain to MMRN1 showed best fit (Chi^2: 2.32 - 9.34) to a two-state, conformational change binding model ($A+L \leftrightarrow AL \leftrightarrow AL^*$), where A (analyte: A1A2A3 or A1) and L (Ligand: MMRN1) form two stable complexes (AL and AL*). The binding of VWF A3 domain to MMRN1 showed best fit (Chi^2: 1.07 – 3.19) to a simple 1:1 Langmuir binding model ($A+L \leftrightarrow AL$).

VWF A1A2A3 had higher apparent affinity (represented by a lower K_D) for MMRN1 (K_D: 2.0 ± 0.4 x 10^{-9} M) than the VWF A1 domain (K_D: 39.3 ± 7.7 x 10^{-9} M, $p < 0.01$). VWF A1A2A3 (k_{a1}: 2.6 ± 0.9 x 10^6 $M^{-1}s^{-1}$; k_{a2}: 4.2 ± 0.3 x 10^{-3} s^{-1}) and VWF A1 domain (k_{a1}: 1.2 ± 0.8 x 10^6 $M^{-1}s^{-1}$; k_{a2}: 1.0 ± 0.5 x 10^{-2} s^{-1}) had similar on-rates for binding to MMRN1 (respectively: $p = 0.35$ and 0.28). VWF A1A2A3 had a slower initial off-rate (k_{d1}: 2.7 ± 0.3 x 10^{-2} s^{-1}) than the VWF A1 domain (k_{d1}: 1.3 ± 0.2 x 10^{-1} s^{-1}, $p < 0.01$). A second slower phase of the dissociation was evident with both VWF A1A2A3 and the VWF A1 domain (respectively: k_{d2}: 1.1 ± 0.5 x 10^{-3} s^{-1} vs k_{d2}: 3.2 ± 2.1 x 10^{-3} s^{-1}, $p = 0.31$).

Compared to VWF A1A2A3, the VWF A3 domain bound to MMRN1 with a relatively low affinity (represented by a high K_D: 229 ± 114 x 10^{-9} M), and with slow on-rates (k_a: 8.8 ± 2.1 x 10^3 $M^{-1}s^{-1}$) and slow off-rates (k_d: 1.8 ± 0.5 x 10^{-3} s^{-1}).

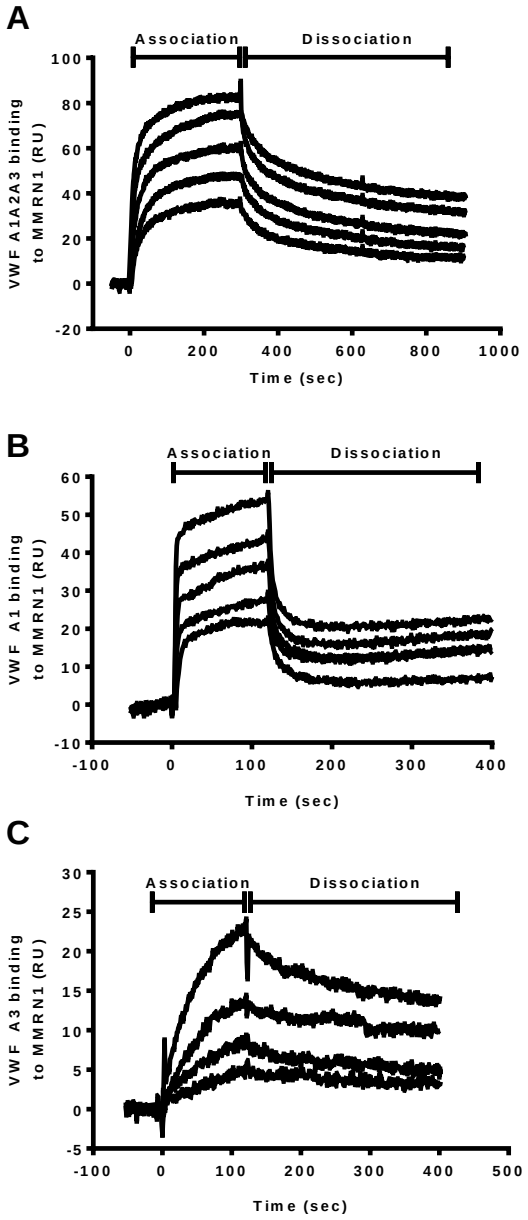

Figure 9: Real-time association and dissociation curves for VWF A domains binding to MMRN1, evaluated by SPR. Panels A, B, and C show SPR sensorgrams for the real-time binding of different analytes (tested at analyte concentrations: nM, top to bottom) to MMRN1-coated sensor chips (data for chips with ~1000 RU immobilized MMRN1 are shown): A) VWF A1A2A3: 25, 18.8, 9.4, 4.7 and 3.1; B) VWF A1 domain: 250, 125, 62.5, 31.3 and 15.6; and C) VWF A3 domain: 2000, 1000, 500 and 250. All data shown were representative of 2-3 experiments. Reproduced with permission from Thrombosis and Haemostasis 2016. 116(1): 87-95.

Table 4: Binding kinetic estimations for the binding between VWF A1A2A3, A1, and A3 binding to MMRN1, as measured by SPR. Reproduced with permission from Thrombosis and Haemostasis 2016. 116(1): 87-95.

VWF Analyte	Binding model	Estimated affinity	Estimated association rate constant	Estimated dissociation rate constant
A1A2A3	2-State	K_D: 2.0 ± 0.4 x 10^{-9} M	k_{a1}: 2.6 ± 0.9 x 10^{6} $M^{-1}s^{-1}$ k_{a2}: 4.2 ± 0.3 x 10^{-3} s^{-1}	k_{d1}: 2.7 ± 0.3 x 10^{-2} s^{-1} k_{d2}: 1.1 ± 0.5 x 10^{-3} s^{-1}
A1	2-State	K_D: 39.3 ± 7.7 x 10^{-9} M	k_{a1}: 1.2 ± 0.8 x 10^{6} $M^{-1}s^{-1}$ k_{a2}: 1.0 ± 0.5 x 10^{-2} s^{-1}	k_{d1}: 1.3 ± 0.2 x 10^{-1} s^{-1} k_{d2}: 3.2 ± 2.1 x 10^{-3} s^{-1}
A3	1:1 Langmuir	K_D: 229 ± 114 x 10^{-9} M	k_a: 8.8 ± 2.1 x 10^{3} $M^{-1}s^{-1}$	k_d: 1.8 ± 0.5 x 10^{-3} s^{-1}

3.2 EFFECT OF VWF A DOMAINS ON PLATELET ADHESION TO MMRN1, AT HIGH SHEAR (1500 S^{-1})

The ELISA and SPR findings led me to investigate the interactions between VWF and MMRN1 at high shear. MMRN1 surfaces that were treated with WT-VWF supported more adhesion of resting control platelets than MMRN1 surfaces pre-treated with negative control BSA ($p < 0.001$). This enhancing effect of WT-VWF on platelet adhesion to MMRN1 was abrogated by an inhibitory antibody MCA4683, that blocks VWF A1-GPIbα binding (478, 479) ($p < 0.001$) (Figure 10); unlike mIgG (which was tested as a negative control), MCA4683 reduced platelet adhesion down to the level seen with MMRN1 surfaces pre-treated with the negative control, BSA (Figure 10).

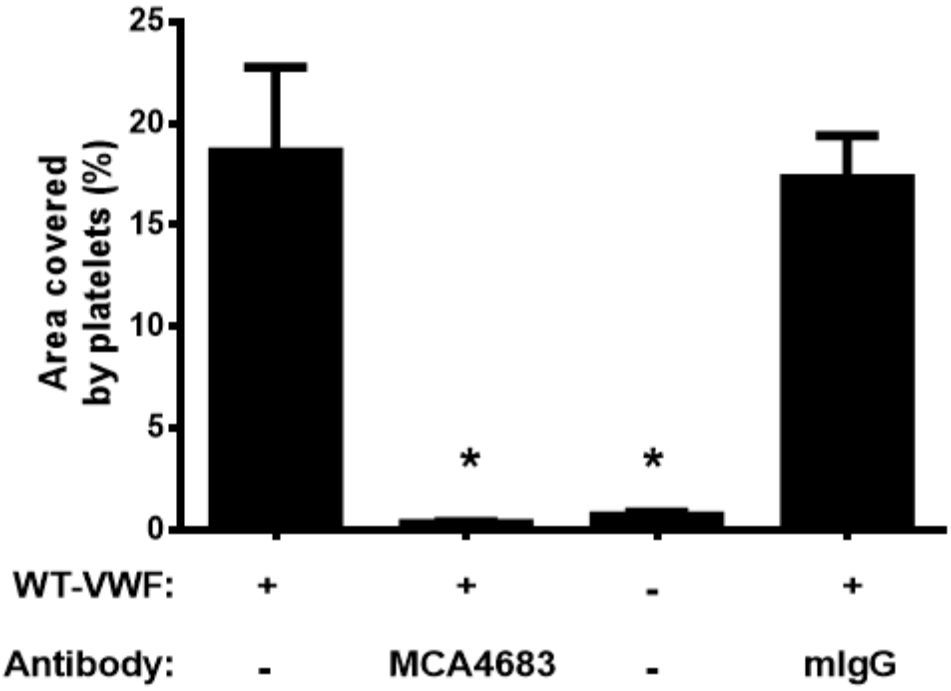

Figure 10: Effect of inhibitory antibodies on the ability of VWF to support high shear platelet adhesion to immobilized MMRN1. The adhesion of platelets (expressed as mean ± SEM for the percentage, %, area covered by platelets) in reconstituted blood (final: platelets: 300 x 10^6/ml; haematocrit: 45%) to immobilized MMRN1 was tested at a shear rate of 1500 s^{-1} after pre-treatment with: WT-VWF (40 nM, positive control); WT-VWF + MCA4683 (20 μg/mL, inhibits VWF-GPIbα binding); BSA (negative control); or WT-VWF + mIgG (20 μg/mL, negative control). Reduced platelet adhesion to MMRN1 is indicated (*; $p < 0.001$, relative to MMRN1 pre-treated with WT-VWF alone). Data shown were representative of 2-3 independent experiments. Reproduced with permission from Thrombosis and Haemostasis 2016. 116(1): 87-95.

My next set of experiments were designed to test if VWF A1A2A3 could enhance platelet adhesion to MMRN1, like WT-VWF. This testing was done with platelets from healthy controls and from an individual with VWD (lacking platelet and plasma VWF), as platelet-released VWF is known to aid platelet adhesion at high shear (309). MMRN1 surfaces that were pre-treated with equimolar (40×10^{-9} M) amounts of WT-VWF or VWF A1A2A3 supported the adhesion of both control and type 3 VWD platelets, better than MMRN1 surfaces that were pretreated with BSA ($p < 0.001$, Figure 11). BSA-coated surfaces that were similarly pre-treated with VWF A1A2A3, supported < 5 % of the platelet adhesion observed with VWF A1A2A3-treated MMRN1 surfaces, confirming that the enhancing effects of VWF A1A2A3 on platelet adhesion reflected attachment to MMRN1.

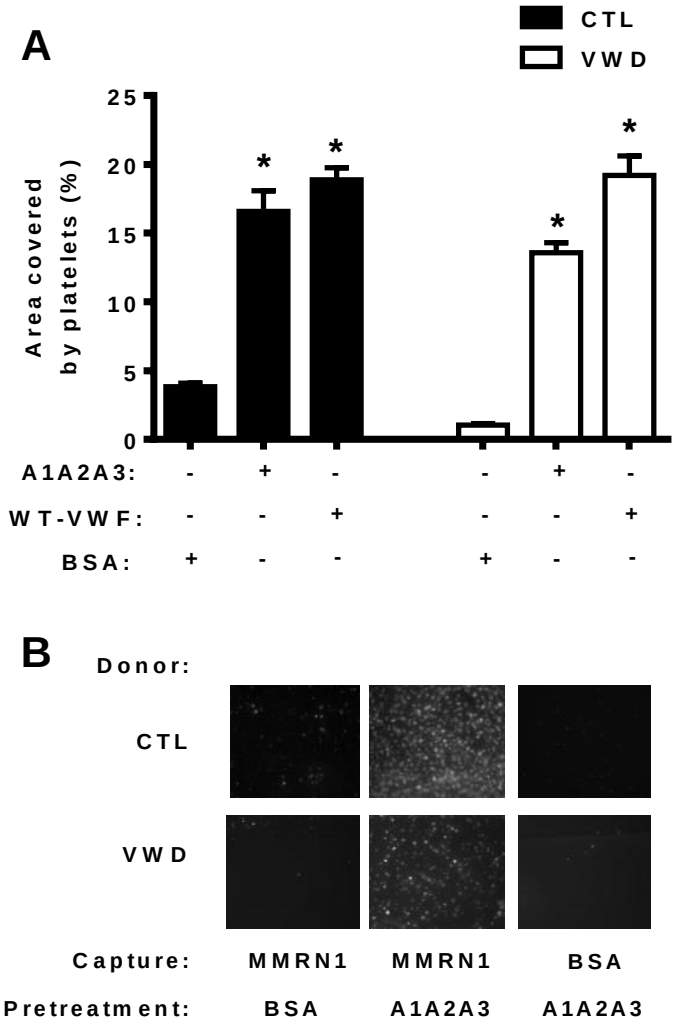

Figure 11: Effect of VWF A1A2A3 on platelet adhesion to MMRN1, under high shear ($1500s^{-1}$). The adhesion (expressed as mean ± SEM for the percentage, %, area covered by platelets) of control (CTL) and type 3 VWD reconstituted blood (platelets: 300 x 10^6/ml; haematocrit: 45%) to immobilized MMRN1, tested at a shear rate of 1500 s^{-1} after pre-treatment with: BSA (negative control); VWF A1A2A3 (40 nM); or WT-VWF (40 nM; positive control). A) Pre-treatments that increased platelet adhesion to MMRN1 are indicated (*; $p < 0.001$, relative to MMRN1 pre-treated with BSA). B) Representative microscope field images comparing the adhesion of control (CTL) and type 3 VWD platelets (white) to MMRN1 and BSA-coated surfaces (black background) that were pre-treated with BSA or VWF A1A2A3 (40 nM). Data shown were representative of 2-3 independent experiments. Reproduced with permission from Thrombosis and Haemostasis 2016. 116(1): 87-95.

3.3 ANALYSES OF MULTIMERIN 1 DEFICIENT MICE

Deficiencies in the *MMRN1* gene and the pathogenic consequences on vascular biology are largely uncharacterized (175, 525, 528). As a result, I further evaluated the platelet adhesive functions of multimerin 1 by exploring the consequences of a selective Mmrn1 loss, in mice.

Genomic DNA analysis of *Mmrn1*$^{-/-}$ and *Mmrn1*$^{+/-}$ mice (Figure 12A-B) confirmed the deletion of the exon 3 in the *Mmrn1* gene, which resulted in the desired null genotype for the Mmrn1 deficient mice (refer to Figure 5 in the Material and Methods Chapter). *Mmrn1*$^{-/-}$ mice were viable and fertile, and *Mmrn1*$^{+/-}$ mice reproduced with expected Mendelian frequency ($p = 0.88$). Mmrn1$^{-/-}$ and *Mmrn1*$^{+/-}$ mice also had normal blood cell counts, compared to WT mice: platelets (values in 10^6/ml: WT, 523 ± 73; *Mmrn1*$^{-/-}$, 617 ± 66; *Mmrn1*$^{+/-}$, 684 ± 79; $p = 0.32$; Figure 13A); white blood cells (values in 10^6/ml: WT, 7.0 ± 1.0; *Mmrn1*$^{-/-}$, 5.6 ± 0.9; *Mmrn1*$^{+/-}$, 4.4 ± 0.8; $p = 0.18$; Figure 13B); and red blood cells (values in 10^9/ml: WT, 7.8 ± 0.3; *Mmrn1*$^{-/-}$, 7.6 ± 0.2; *Mmrn1*$^{+/-}$, 8.7 ± 0.3; $p \geq 0.05$; Figure 13C). Mmnr1$^{-/-}$ mice also did not show any overt morphological abnormalities or phenotype.

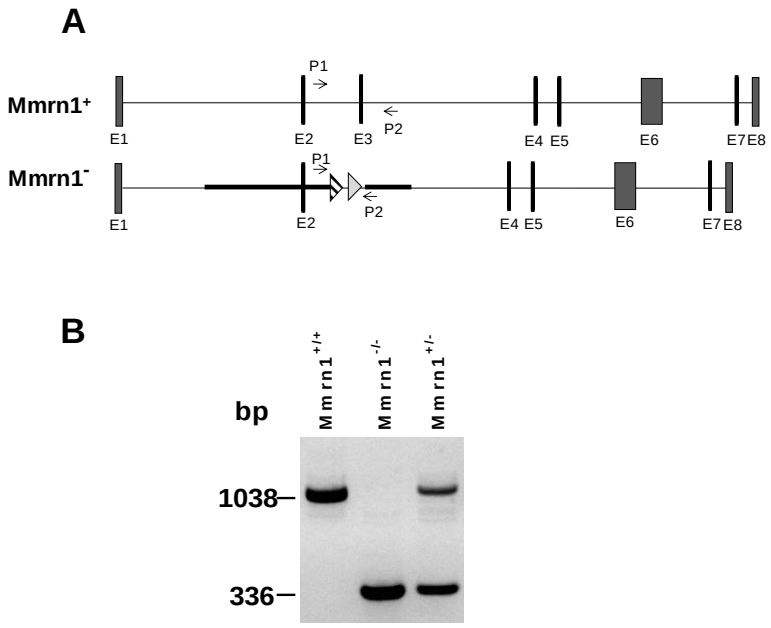

Figure 12: Generation of mice with a selective Mmrn1 deficiency. Mice with a selective Mmrn1 deficiency were generated that lacked the third exon (E3), which generates a frameshift mutation that is predicted to yield a severely truncated gene product, possessing only E1-2. Panel A shows primer pairs (P1 and P2) that were used to verify and distinguish $Mmrn1^{+}$ and $Mmrn1^{-}$ alleles. Panel B shows resolved PCR fragments from genotyping using P1 and P2 that verified genotypes for: wild type (WT, $Mmrn1^{+/+}$; 1038 base pair (bp) PCR product), $Mmrn1^{-/-}$ (336 bp PCR product), and $Mmrn1^{+/-}$ (336 and 1038 bp PCR products) mice.

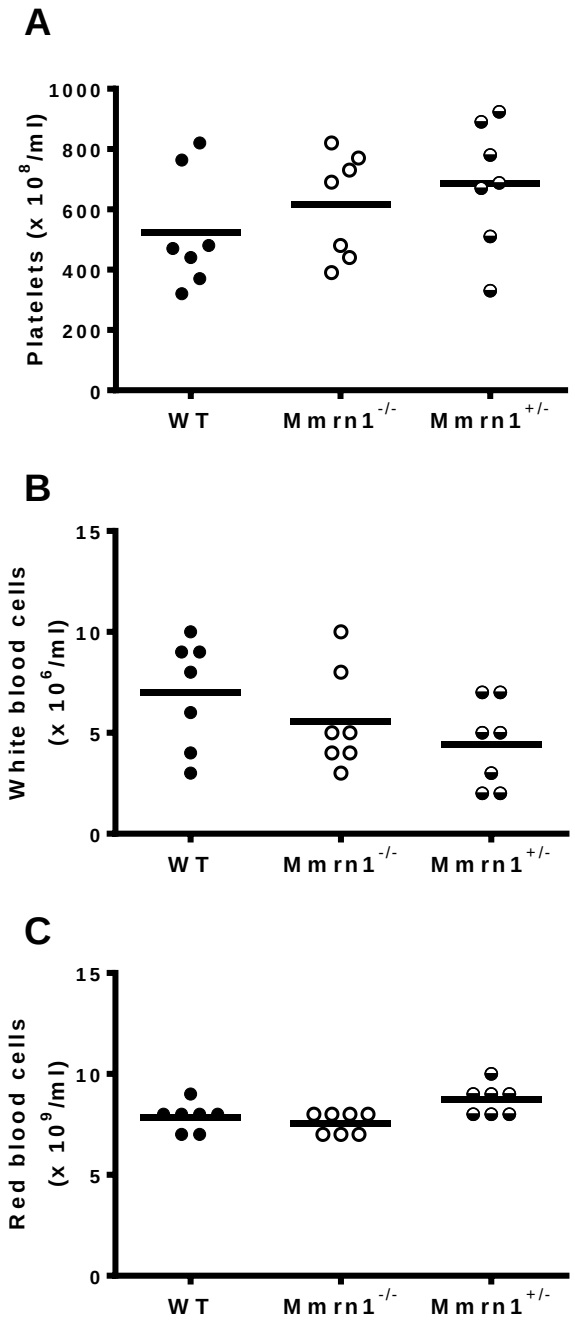

Figure 13: Blood cell counts of WT, Mmrn1$^{-/-}$ and Mmrn1$^{+/-}$ mice, assessed using an automated veterinarian cell counter. Blood cell counts (mean depicted by a solid line) were obtained for blood anticoagulated with sodium citrate (1:9, v/v) from WT (closed circles), Mmrn1$^{-/-}$ (open circles), and Mmrn1$^{+/-}$ (half-closed circles) mice (n = 8) for: platelets (A); white blood cells (B); and red blood cells (C).

3.3.1 Mouse plasma and platelet protein content

To confirm the loss of Mmrn1 in mouse platelets, Western blot analysis of reduced platelet lysate samples indicated that Mmrn1 subunits were detectable in platelets from WT and *Mmrn1*$^{+/-}$ mice, but not *Mmrn1*$^{-/-}$ mice (Figure 14). In WT and *Mmrn1*$^{+/-}$ mice, reduced Mmrn1 migrated as two distinct bands, with reduced mobilities > 155 kD (Figure 15). Like MMRN1 in human platelets (33, 183, 507, 508), the reduced mobilities of Mmrn1 in mouse platelets are likely suggestive of differential processing of polypeptide subunits (Figure 14).

Next, I investigated if the loss of platelet MMRN1 alters the levels of VWF in platelets and plasma. ELISA and Western blot analysis indicated that platelets from WT and *Mmrn1*$^{-/-}$ mice contained similar amounts of Vwf (WT: 100 ± 10% vs *Mmrn1*$^{-/-}$: 103 ± 16%; p = 0.89,) as did *Mmrn1*$^{+/-}$ mice (106 ± 15%, p = 0.74, relative to WT) (Figure 15C-D). WT and *Mmrn1*$^{-/-}$ plasma also contained similar amounts of Vwf (WT: 100 ± 7 % vs *Mmrn1*$^{-/-}$: 108 ± 6 %; p = 0.41), as did *Mmrn1*$^{+/-}$ mice (95 ± 8 %, p = 0.67) (Figure 15A-B).

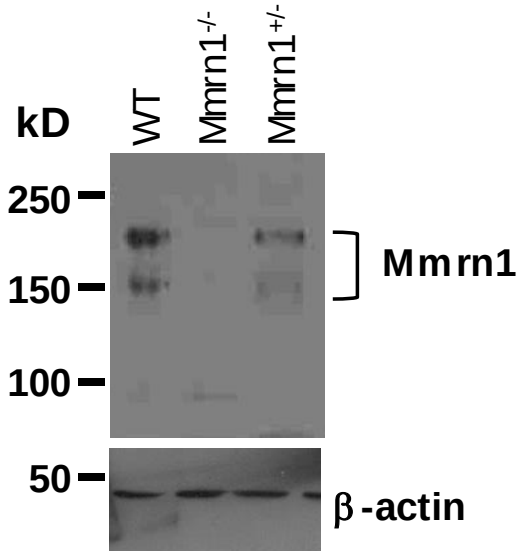

Figure 14: Western blot analysis of reduced Mmrn1 in platelet lysates from WT, Mmrn1$^{-/-}$, and Mmrn1$^{+/-}$ mice. A representative immunoblot is shown, comparing proteins in 2.5 µl of platelet lysate, prepared at a concentration of 1 x 10^{10} platelets/ml). The lower portion of the gel was probed for β-actin to confirm sample loading.

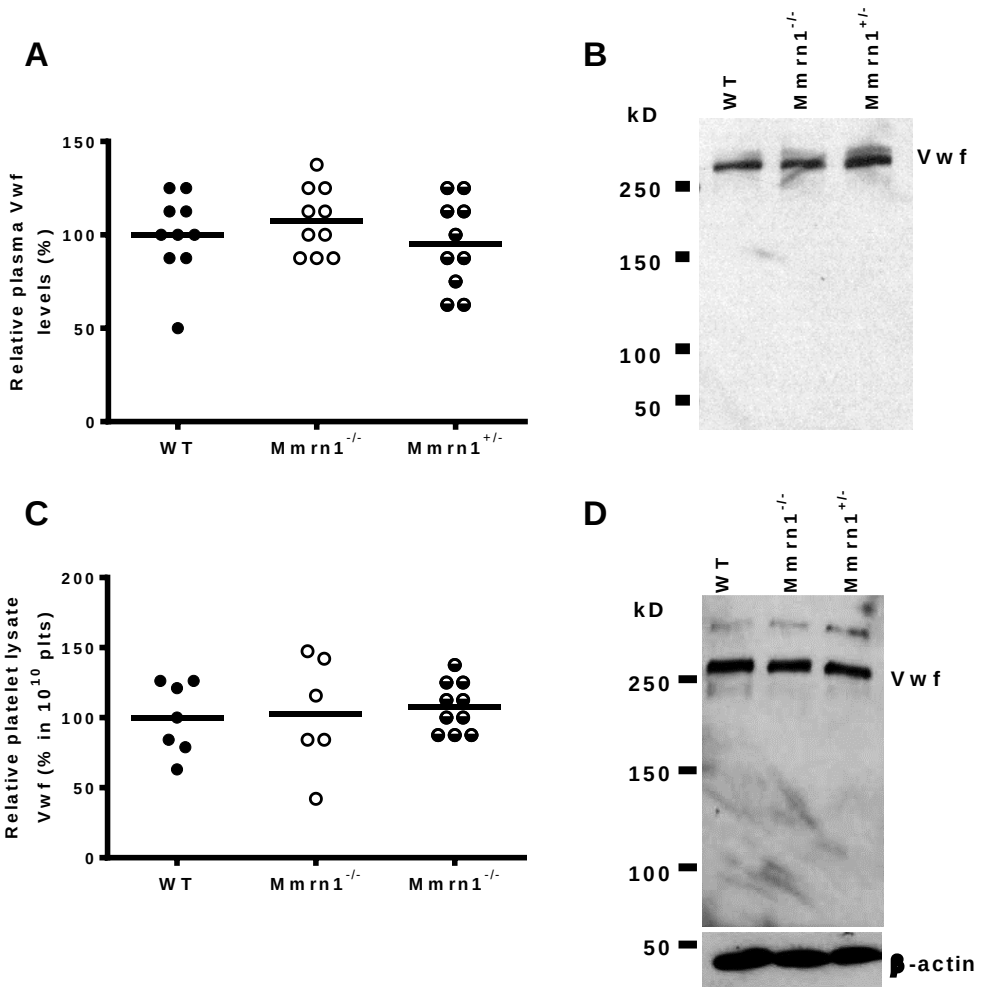

Figure 15: Vwf levels in plasma and platelet lysate samples from WT, Mmrn1$^{-/-}$ and Mmrn1$^{+/-}$ mice. Vwf levels were measured by ELISA (solid lines show means; results shown as % of the corresponding WT sample) from: A) citrated plasma (1:9, v/v) samples (n = 10, per genotype); and C) platelet lysate (1 x 10^{10}/ml) samples (n = 6 – 7, per genotype). Symbols indicate: Mmrn1$^{-/-}$: open circles; and Mmrn1$^{+/-}$: half-closed circles; WT: closed circles. Panels B and D show representative images of immunoblot detection of Vwf in plasma (2.5 µl of citrated plasma, (B)) and platelet lysate (2.5 µl from 1 x 10^{10}/ml, (D)) samples from WT, Mmrn1$^{-/-}$, and Mmrn1$^{+/-}$ mice. Protein loading for platelet samples was confirmed by Western blot analysis for β-actin (D).

3.4 EFFECT OF MMRN1 DEFICIENCY ON BLEEDING TIMES

Bleeding times were evaluated to determine if Mmrn1 deficiency altered either the amount or duration of bleeding with tail transection. The proportion of WT and Mmrn1 deficient mice that bled for more than 600 sec, the typical time allotted for measuring duration of bleeding in a mouse tail transection model (37, 144, 328), was not significantly different (WT: 1 out of 22 (0.05 %); *Mmrn1*$^{-/-}$: 6 out of 22 (~27 %); p = 0.09) (Figure 16A) Moreover, complete loss of *Mmrn1* did not significantly prolong bleeding times after tail transection compared to WT mice (values in sec: WT, 300, 60-900; *Mmrn1*$^{-/-}$, 330, 90-900; p = 0.07, Figure 16A), nor did it increase total blood loss after tail transection (values in µl: WT, 60, 0-570; *Mmrn1*$^{-/-}$, 65, 10-1120; p = 0.21, Figure 16B). Similar results were reported for *Mmrn1*$^{+/-}$ mice, relative to WT mice (*Mmrn1*$^{+/-}$: 6 out of 22 (~27 %), p = 0.09, Figure 16A; bleeding time in sec: *Mmrn1*$^{+/-}$: 225, 60-900, p = 0.60, Figure 16A; total blood loss in µl: Mmrn1$^{+/-}$: 15, 0-500, p = 0.09, Figure 16B).

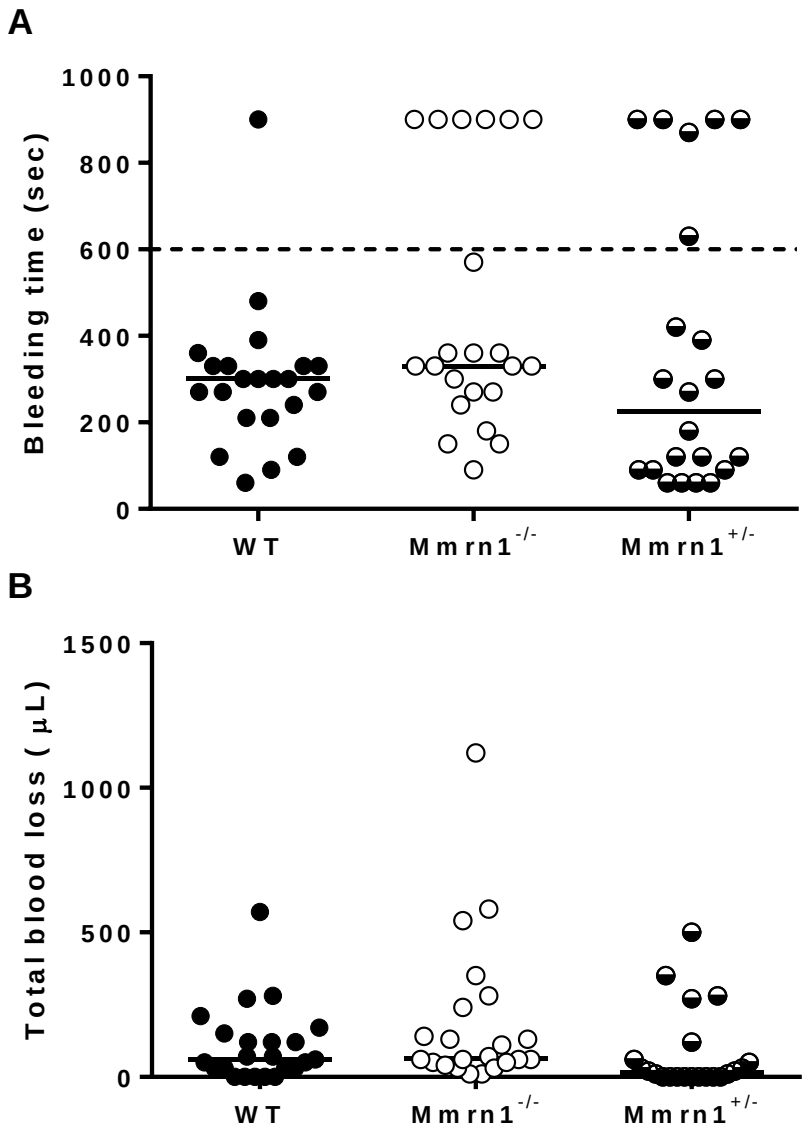

Figure 16: Duration and total blood loss following tail transection for WT, Mmrn1$^{-/-}$ and Mmrn1$^{+/-}$ mice. Panels show data (medians depicted by solid lines) for WT (closed circles), Mmrn1$^{-/-}$ (open circles), and Mmrn1$^{+/-}$ (half-closed circles) mice (n = 22) for: (A) bleeding times (sec); and (B) total blood loss (µl) following transection of the distal tip of the tail.

3.5 *IN VITRO* PLATELET AGGREGATION RESPONSES OF WT AND MMRN1 DEFICIENT MICE

In the next set of experiments, I focused my investigations on determining the effect of complete Mmrn1 loss on platelet adhesive properties, using WT mice as the comparison. Heterozygous Mmrn1 deficient mice were investigated when the homozygous null mice showed altered platelet function (> 30% difference from WT).

I found that platelets from WT and Mmrn1 deficient mice showed very similar aggregation profiles in their aggregation response to TRAP (using PRP, Figure 18A), thrombin (using GFP, 0.5 – 1.0 U/ml; Figure 17C and E), and ADP (using PRP, 10 – 20 μM; Figure 18A and C). Additionally, the maximal aggregation obtained with these agonists was not significantly different for *Mmrn1*$^{-/-}$ compared WT mice (TRAP: $p = 0.65$, Figure 17B; 0.5 – 1.0 U/ml thrombin: $p \geq 0.37$, Figure 17D and F; 10-20 μM ADP: $p \geq 0.13$, Figure 18B and D).

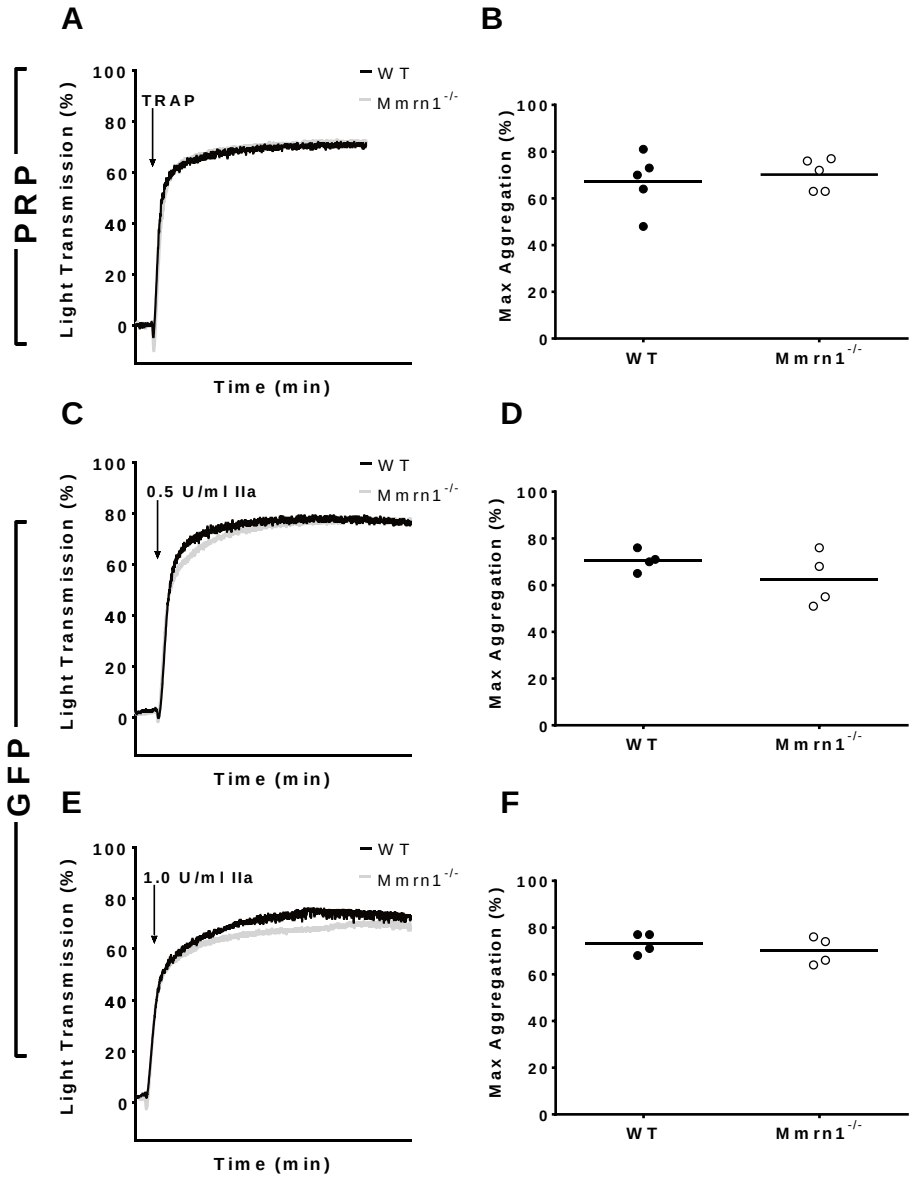

Figure 17: Aggregation of WT and Mmrn1$^{-/-}$ mouse platelets in response to TRAP and thrombin stimulation. Aggregation responses (A, C, E show representative samples; arrows indicate time of addition of agonist) compare findings for WT and Mmrn1 deficient PRP (A) and GFP samples, (C and E) stimulated with 500 µM TRAP (A, B) or with 0.5 U/ml (C, D) or 1.0 U/ml thrombin (E, F). Black and gray lines in tracings respectively show data for WT and Mmrn1$^{-/-}$ mice. Panels on the right summarize percent maximal aggregation (means depicted by solid lines) responses for WT (closed circles) and Mmrn1$^{-/-}$ (open circles) mice for 5 independent experiments with PRP (B), and 4 independent experiments with GFP (D, F), each using pooled samples from 2-3 mice.

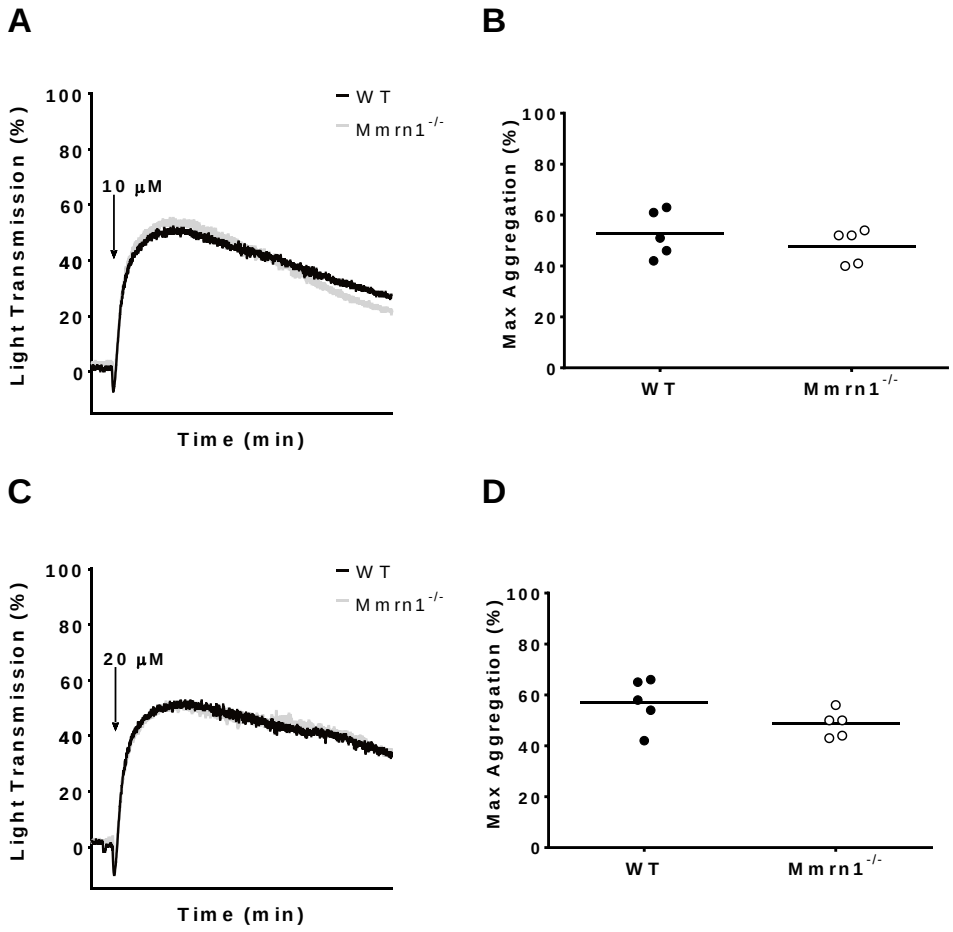

Figure 18: Aggregation of WT and Mmrn1$^{-/-}$ mouse platelets in response to ADP. Panels A and C show representative, PRP aggregation responses to the indicated concentrations of ADP and the corresponding percent maximal aggregation data for each concentration of ADP (means depicted by solid lines, n = 5 samples of each genotype, each pooled from 2-3 mice) for WT (black lines; closed circles) and Mmrn1$^{-/-}$ (gray lines; open circles) mice. Arrows indicate the addition of ADP.

With collagen (5 – 20 µg/ml), GFP from WT and *Mmrn1*$^{-/-}$ mice showed similar initial aggregation responses (Figure 19A, C), however, the maximal aggregation responses were significantly lower (20 – 30 % reduction) for the Mmrn1 deficient GFP ($p < 0.05$) relative to WT GFP for all concentrations of collagen tested; Figure 19B, D). This reduction in maximal aggregation was not evident when collagen-induced aggregation was tested with PRP and the same concentrations of collagen ($p \geq 0.15$, relative to WT PRP; Figure 19A-D).

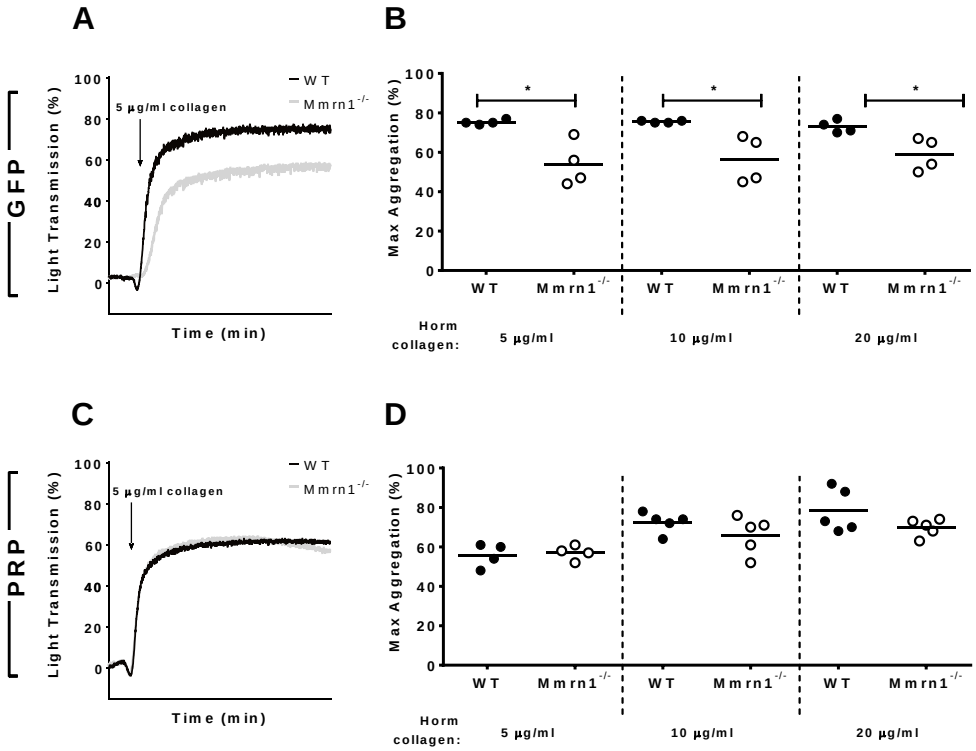

Figure 19: Aggregation of WT and Mmrn1$^{-/-}$ platelets in response to collagen. Panels A and C show representative aggregation responses after addition (arrow) of 5 µg/ml Horm collagen. Panels B and D show the percent maximal aggregation responses to the indicated final concentrations of Horm collagen (5, 10, and 20 µg/ml; means depicted by solid lines). Findings for WT (black line; closed circles) and Mmrn1$^{-/-}$ (gray lines; open circles) mice are compared for GFP (panels A, B) and PRP (panels C, D). * indicate significantly less percent maximal aggregation ($p < 0.05$) compared to WT platelets. Data are shown for 5 independent experiments for PRP and 4 independent experiments for GFP, each with pooled samples from 2-3 mice per genotype.

3.6 *IN VITRO* ANALYSIS OF MOUSE PLATELET ADHESION

Subsequent studies were used to further explore the effect of Mmrn1 loss on platelet adhesion to collagen, under high shear conditions of flow using whole blood samples from WT and Mmrn1 deficient mice. Mmrn1$^{-/-}$ platelets showed reduced adhesion to collagen (~ 50% reduction) relative to WT platelets, as did Mmrn1$^{+/-}$ platelets (values as percent surface area covered, p values indicate comparisons with WT: WT: 37 ± 3 %; *Mmrn1*$^{-/-}$: 18 ± 2 %, $p < 0.001$; *Mmrn1*$^{+/-}$: 15 ± 3 %, $p < 0.001$; Figure 20A). Both Mmrn1$^{-/-}$ and *Mmrn1*$^{+/-}$ platelets also formed smaller aggregates on collagen than WT platelets (Figure 20B). There were no significant differences in the amount of platelet adhesion to collagen for *Mmrn1*$^{-/-}$ and *Mmrn1*$^{+/-}$ platelets.

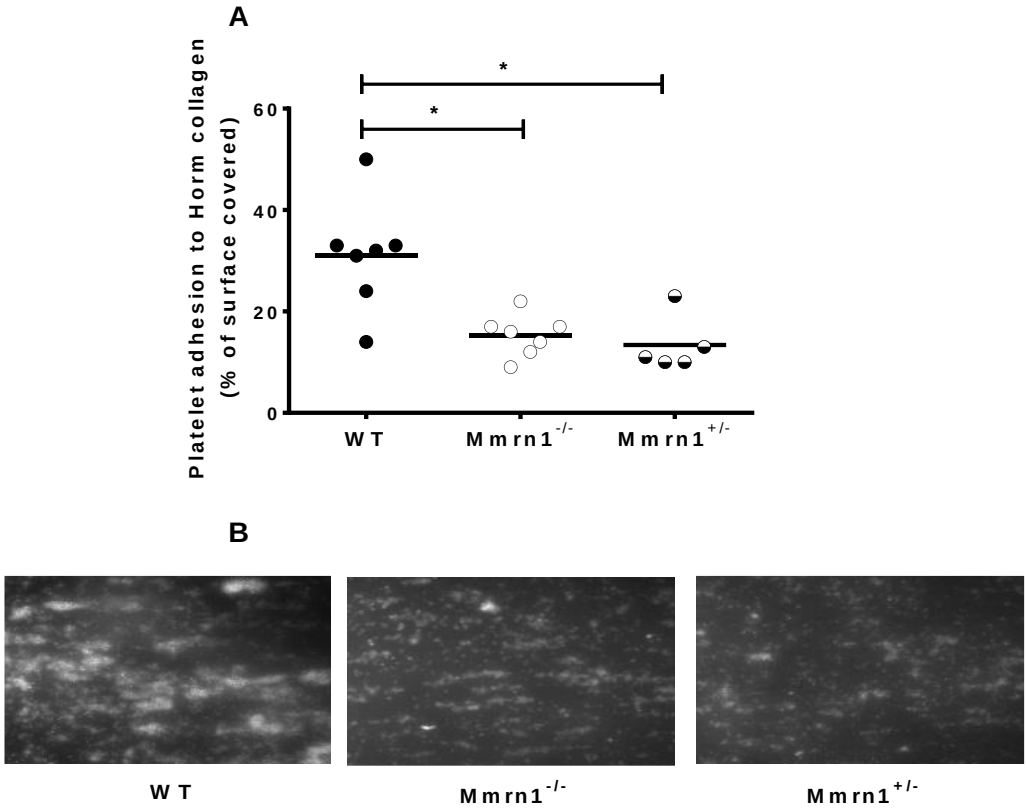

Figure 20: Comparison of WT and Mmrn1 deficient platelet adhesion to Horm collagen. Testing was performed at high shear (1500 s^{-1}) with fluorescently labeled platelets that were reconstituted in whole blood. Panel A compares quantitative data on the percentage of the collagen surface that was covered by platelets (means depicted as solid lines) for WT (closed circles; n = 7), $Mmrn1^{-/-}$ (open circles; n = 7) and $Mmrn1^{+/-}$ (half-closed circles; n = 4) samples. * indicate reduced platelet adhesion ($p < 0.01$) compared to WT samples. Panel B images compare representative microscope fields images, illustrating differences in the number of adherent platelets, and the size of platelet aggregates attached to collagen, for WT compared to $Mmrn1^{-/-}$ and $Mmrn1^{+/-}$ samples.

As platelet adhesion to collagen at high shear is dependent on VWF (74, 88, 100, 103-105, 121, 123) (ref to Table 2), I investigated if the loss of Mmrn1 alters platelet adhesion to VWF. In analyses of platelet adhesion to immobilised Vwf at high shear, Mmrn1 deficient platelets did not show significantly reduced adhesion (data as the percentage of surface area covered by platelets: WT: 18.5 ± 3.5 %; *Mmrn1*$^{-/-}$: 11.0 ± 1.6 %; p=0.08; Figure 21A; data as the numbers of adherent platelets: WT: 1480, 1200 – 1910; *Mmrn1*$^{-/-}$: 1200, 900 – 1900; p=0.08; Figure 21B).

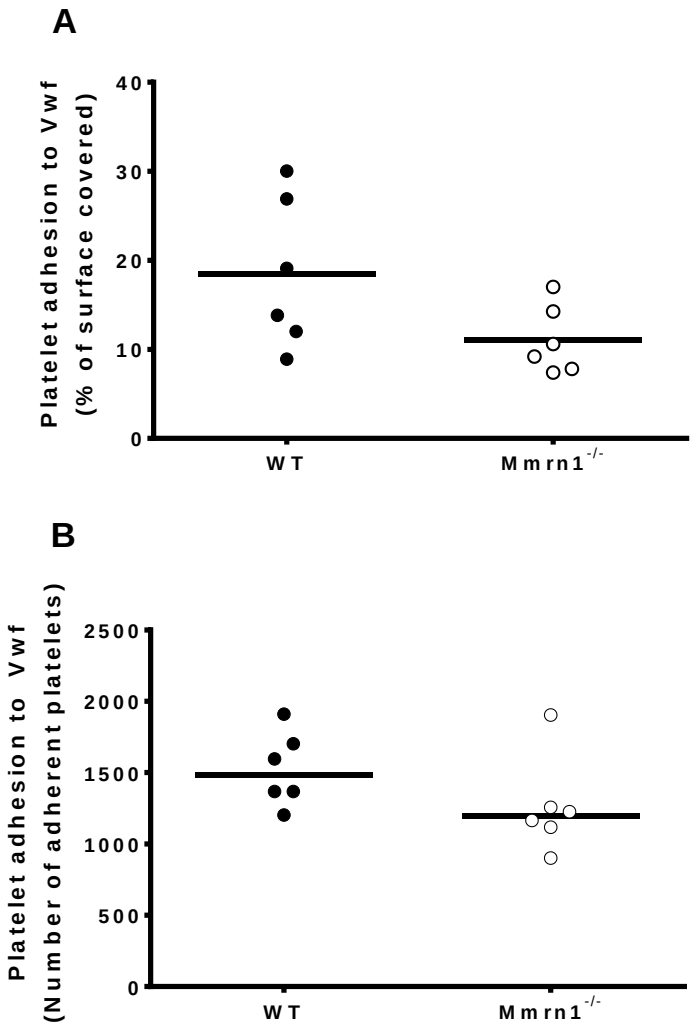

Figure 21: Comparison of WT and Mmrn1 deficient platelet adhesion to Vwf at high shear. Adhesion was assessed at high shear (1500 s^{-1}), using whole blood samples from WT (closed circles) and Mmrn1$^{-/-}$ (open circles) mice (n = 6). Endpoints evaluated included: area covered by platelets (%, mean depicted as a solid line; A) and the number of adherent platelets (median depicted as a solid line; B).

3.7 SURFACE EXPRESSION OF PLATELET RECEPTORS

I also assessed the expression of receptors involved in VWF and collagen-dependent platelet adhesion and aggregation on both resting and thrombin-activated platelets from WT, *Mmrn1*$^{-/-}$, and *Mmrn1*$^{+/-}$ mice. The resting platelets from WT, *Mmrn1*$^{-/-}$, and *Mmrn1*$^{+/-}$ mice showed similar levels of GPIbα, the cell surface receptor for VWF, (CD42b, $p = 0.33$, Figure 22A), and of integrin receptors for collagen and fibrinogen (respective p-values: β_1, CD29, $p = 0.16$; and β_3, CD61, $p = 0.43$, Figure 22B-C). Also, prior to and after thrombin stimulation, the platelets from WT, *Mmrn1*$^{-/-}$, and *Mmrn1*$^{+/-}$ mice showed similar increases in surface expression of the α-granule protein, P-selectin with platelet activation ($p = 0.14$) (Figure 23A). With thrombin stimulation, the amount of activated $\alpha_{IIb}\beta_3$ detected on the platelet surface was greater for *Mmrn1*$^{-/-}$ and *Mmrn1*$^{+/-}$ mice compared to WT mice ($p < 0.01$; Figure 23B).

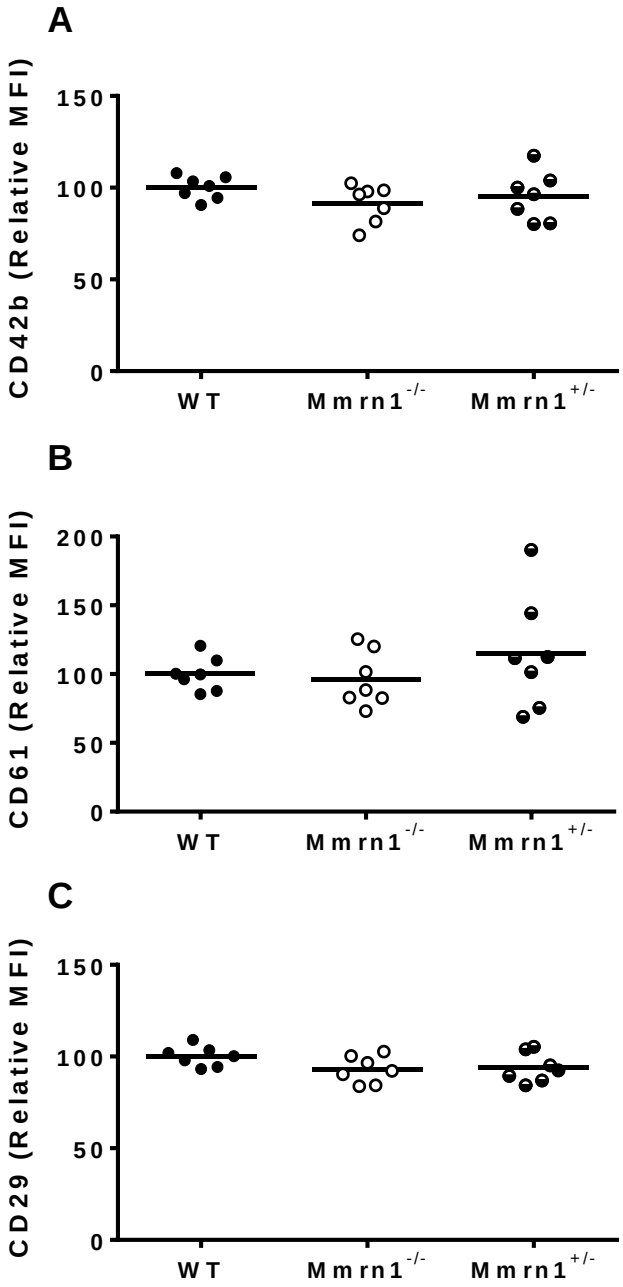

Figure 22: Surface expression of platelet receptors on washed resting platelets from WT, Mmrn1$^{-/-}$ and Mmrn1$^{+/-}$ mice, assessed by flow cytometry. Resting platelets were assessed for expression of: (A) GPIbα (receptor for VWF, CD42b); (B-C) $\alpha_{IIb}\beta_3$ (receptor for fibrinogen, CD61) and $\alpha_2\beta_1$ (integrin receptor for collagen, CD29). Relative median fluorescent intensity (MFI; mean depicted by a solid line) are displayed, with MFI from WT platelets arbitrarily defined as 100%.

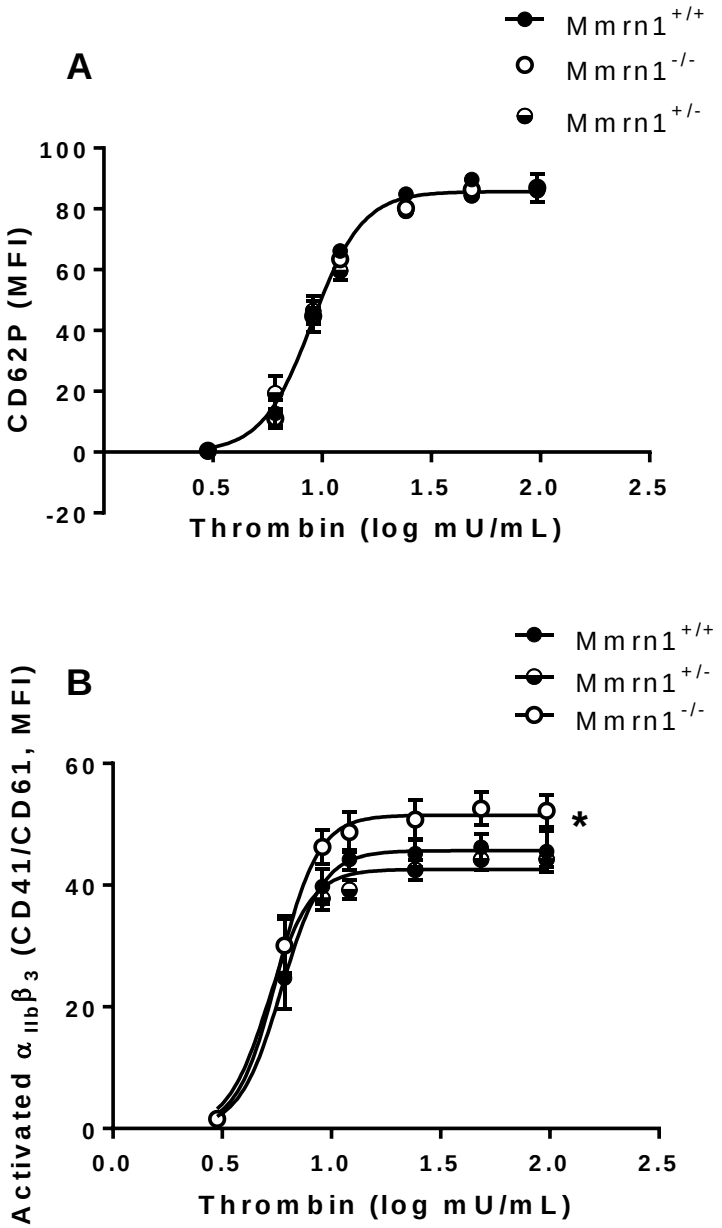

Figure 23: Surface expression of platelet receptors on washed thrombin-activated platelets from WT, Mmrn1$^{-/-}$ and Mmrn1$^{+/-}$ mice, assessed by flow cytometry. Thrombin-activated (0 – 96.4 mU/ml) washed platelets were assessed for expression of: (A) α-granule release of P-selectin (CD62P); and B) activated $\alpha_{IIb}\beta_3$ (CD41/CD61). Relative median fluorescent intensity (MFI; mean depicted by a solid line) ± SEM are displayed.

3.8 *IN VIVO* PLATELET ADHESION AND THROMBUS FORMATION IN RESPONSE TO FERRIC CHLORIDE INJURY

Intravital microscopy was performed to assess if Mmrn1 deficiency altered platelet-rich thrombus formation, following ferric chloride-induced injury to mesenteric arterioles in mice. These results were generated through a collaboration with Dr. Wang from the research laboratory of Dr. Ni, as previous detailed in this thesis (refer to Section 2.2.16 Intravital microscopy – ferric chloride injury model). In these studies, *in vivo* thrombogenesis was visualized in real-time, and representative microscopy images from these experiments are depicted in Figure 24, with the quantitative analyses shown in Figure 25.

Compared to WT mice, *Mmrn1*$^{-/-}$ and *Mmrn1*$^{+/-}$ mice showed a visible delay in the thrombotic response to ferric chloride injury of mesenteric arterioles (Figure 24A-D). While large platelet-rich intravascular thrombi were visible in mesenteric arteries of WT mice by 8-10 min after ferric chloride injury (Figure 24A), only single platelets or small platelet aggregates were visible in the arterioles of *Mmrn1*$^{-/-}$ and *Mmrn1*$^{+/-}$ mice, even by 20 min (Figure 24B-D). In WT mice, occlusive thrombi had formed by 15 min in almost all mice (Figure 24A and 25A) whereas in the *Mmrn1*$^{-/-}$ deficient mice, thrombi often formed later (e.g., by ~28 min, Figure 24B) or not at all (Figure 24C). Injured vessels from *Mmrn1*$^{+/-}$ mice did not form occlusive thrombi (Figure 24D).

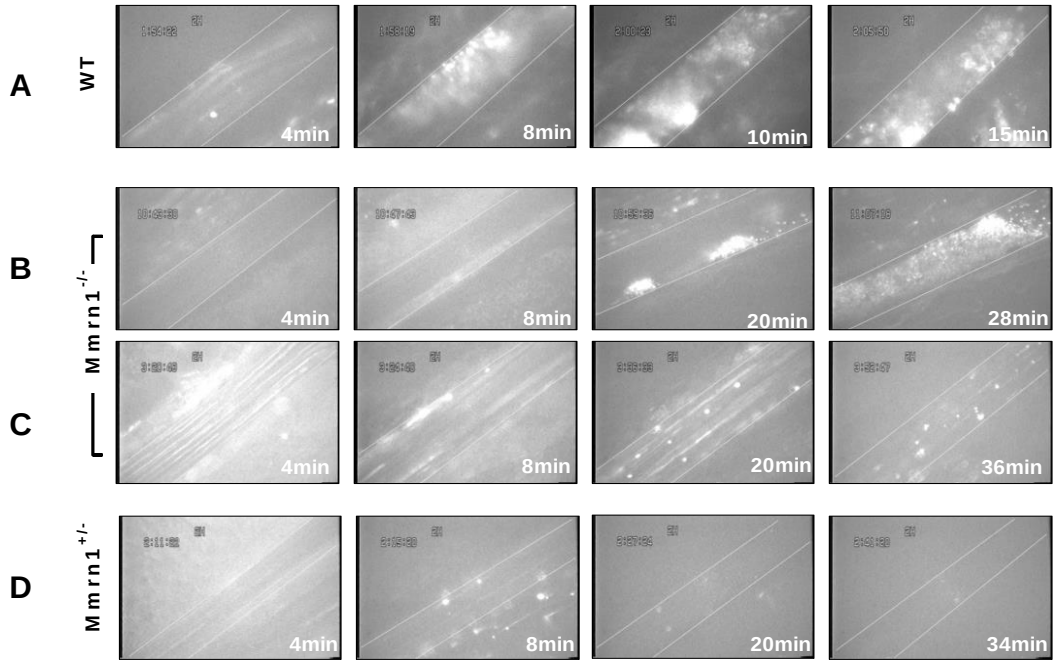

Figure 24: In vivo, platelet adhesion and thrombus formation in WT and Mmrn1 deficient mice, following exposure of mesenteric arteries to ferric chloride. Representative microscope field images show adherent platelets and platelet-rich thrombi (white; blood flow is from right to left) in mesenteric arterioles of mice after ferric chloride injury (time after injury, in min, is indicated on bottom right of images) for: WT (A), $Mmrn1^{-/-}$ (B-C), and $Mmrn1^{+/-}$ (D) mice.

Compared to WT mice, both *Mmrn1*$^{-/-}$ and *Mmrn1*$^{-/+}$ mice showed significantly less initial platelet localization to the damaged vessel following ferric chloride injury (values, as number of adherent platelets, 3-5 min after injury, p values indicate comparisons to WT: WT: 82 ± 4, *Mmrn1*$^{-/-}$: 42 ± 6; *Mmrn1*$^{+/-}$: 28 ± 7; $p < 0.001$; Figure 25A). There was no significant difference in the initial localization of platelets for *Mmrn1*$^{-/-}$ and *Mmrn1*$^{+/-}$ mice.

In WT mice, stable platelet aggregates formed and typically a thrombus ≥ 20 μm was evident by 10.1 ± 1.1 min after ferric chloride injury (Figure 25B). However, in both *Mmrn1*$^{-/-}$ and *Mmrn1*$^{+/-}$ mice, thrombi were much smaller and readily dissociated into smaller platelet aggregates that were removed by flowing blood. When a ≥ 20 μm thrombus formed in the arterioles of Mmrn1 deficient mice, smaller platelet aggregates dissociated from the apex of the developing thrombus, and flowed away from the site of injury, without re-associating downstream from the injury. WT mice always formed a thrombus in response to ferric chloride injury, and Mmrn1 deficient mice often failed to form a thrombus (number of injured arterioles that did not form a ≥ 20 μm thrombus: *Mmrn1*$^{-/-}$: 2 out of 9 (~22%); and *Mmrn1*$^{+/-}$: 3 out of 7 (~43%)), but there was no significant difference in the frequency of observed ≥ 20 μm thrombus in WT and Mmrn1 deficient mice ($p = 0.15$). There was also a pronounced delay in the time to the appearance of the first ≥ 20 μm thrombus in Mmrn1 deficient compared to WT mice (*Mmrn1*$^{-/-}$: 27.4 ± 3.7 min; *Mmrn1*$^{+/-}$: 36.5 ± 1.4 min, $p < 0.001$, relative to WT; Figure 25B), but there was no significant difference in the findings for *Mmrn1*$^{-/-}$ and *Mmrn1*$^{+/-}$mice.

The thrombi that formed in WT arterioles after ferric chloride injury grew to occlude the injured vessels rapidly (median 15 min, range: 10-35; Figure 25C), whereas in Mmrn1 deficient mice, the time to occlusion was slower (median, range, p value compared to WT mice: *Mmrn1*$^{-/-}$: 37, 22-40 min; *Mmrn1*$^{+/-}$: 40, 40-40 min, $p < 0.001$; Figure 25C). While occlusive thrombi always formed in the injured arterioles of WT mice, occlusive thrombi did not consistently form in the injured arterioles of Mmrn1 deficient mice (number of injured arterioles that did not form occlusive thrombi 40 min after exposure to ferric chloride: *Mmrn1*$^{-/-}$: 5 out of 11; *Mmrn1*$^{+/-}$: 7 out of 7, $p < 0.01$ relative to WT mice; Figure 25C). There was no significant difference in the occlusion times for *Mmrn1*$^{-/-}$ and *Mmrn1*$^{+/-}$ mice, although significantly more injured vessels in *Mmrn1*$^{+/-}$ mice did not form occlusive thrombi (100%, $p < 0.05$), when compared to injured vessels in *Mmrn1*$^{-/-}$ mice (~45 %).

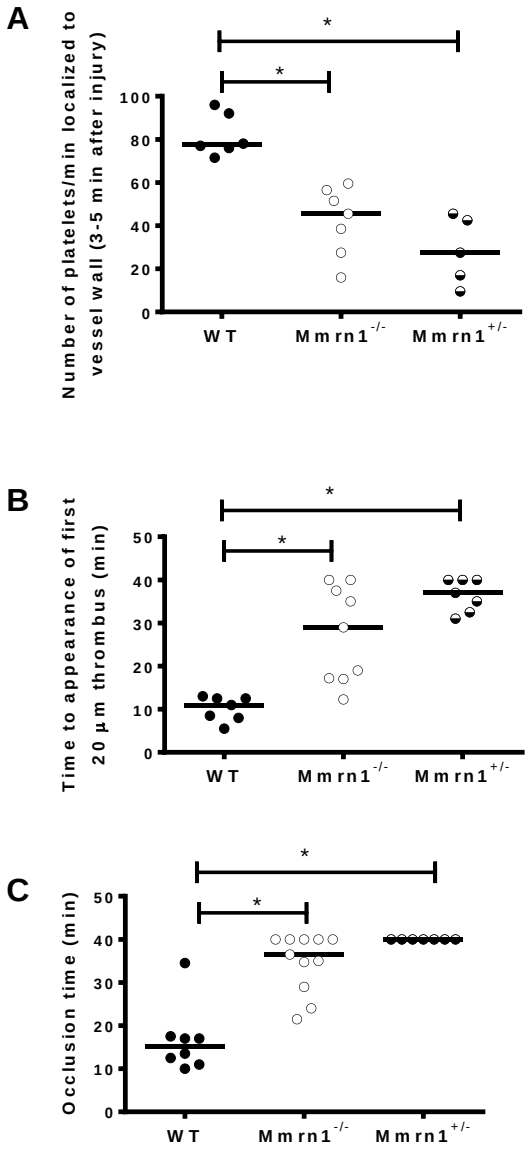

Figure 25: In vivo, platelet adhesion and thrombus formation in WT and Mmrn1 deficient mice, following exposure of mesenteric arteries to ferric chloride. Quantitative data (mean and median depicted as a solid line) of: (A) the number of fluorescently labelled adherent platelets, 3-5 min after injury; (B) the time (in min) required to form the first thrombus ≥ 20 µm; (C) vessel occlusion time (in min), defined as the complete cessation of blood flow for at least 10 seconds. * indicates statistical significant differences ($p < 0.001$) for Mmrn1$^{-/-}$ (open circles; $n \geq 7$) and Mmrn1$^{+/-}$ (half-closed circles; $n \geq 5$) mice, relative to WT (closed circles; $n \geq 6$) mice.

CHAPTER 4: DISCUSSION

MMRN1 is a platelet protein that supports and enhances VWF-dependent platelet adhesion at high shear rates *in vitro* (38), and is implicated in modulating platelet adhesive, haemostatic functions *in vivo* (37). This thesis aimed to extend the current knowledge on the platelet adhesive functions of MMRN1 by addressing some unanswered questions about: 1) the molecular mechanisms of MMRN1-VWF binding that support the *in vitro* platelet adhesive properties of MMRN1 under arterial shear rates; and 2) the consequences of a selective Mmrn1 loss, in mice, on platelet adhesive, haemostatic functions *in vitro* and *in vivo*. The first goal of this thesis was achieved and published (571), and investigated the molecular basis of VWF-MMRN1 binding that supports platelet adhesion to MMRN1 at high shear, *in vitro*. The second goal was to describe the contributions of Mmrn1 to *in vitro* and *in vivo* platelet adhesive functions by evaluating the phenotype of mice with a selective Mmrn1 deficiency.

The main findings from studies of the mechanism of MMRN1-VWF binding were that shear exposed (and ristocetin-treated) VWF binds to MMRN1 matrices, and that VWF A1A2A3 region, specifically the structurally homologous VWF A1 and A3 domains are important for MMRN1 binding. VWF A1A2A3 binds to MMRN1 with a high binding affinity (K_D: 2.0 ± 0.4 x 10^{-9} M), and the individual A1 (K_D: 39.3 ± 7.7 x 10^{-9} M) and A3 (K_D: 229 ± 114 x 10^{-9} M) domains of VWF supported lower affinity binding to MMRN1. VWF A1A2A3 tri-domain, like full-length WT-VWF, also supported GPIbα-dependent platelet adhesion to MMRN1 at an arterial shear rate. The selective loss of Mmrn1 in mice

had modest yet not significant effects on tail bleeding times, but the loss of platelet Mmrn1 significantly impaired collagen-induced aggregation of washed platelets and high shear adhesion of platelets (in whole blood) onto collagen surfaces, *in vitro*. The selective loss of Mmrn1 in mice was also associated with delayed platelet localization to the site of vascular injury, and impaired and prolonged platelet-rich thrombus formation *in vivo*, in arterioles treated with ferric chloride. Collectively, the findings in this thesis provide novel insights on the involvement of the platelet and endothelial cell protein, MMRN1, to support platelet adhesive, haemostatic functions, especially under arterial flow conditions.

The following section discusses in detail these key findings and future work that could be considered to address new questions that have been raised by the studies in this thesis.

4.1 INSIGHTS INTO THE MOLECULAR MECHANISM OF VWF BINDING TO MMRN1

The platelet adhesive functions of VWF have been extensively investigated (detailed in Section 1.3 Overview of von Willebrand factor), and are influenced by mechanisms that expose cryptic sites in VWF, including: VWF exposure to high shear (24, 30-32, 148, 279, 285, 457, 460, 469, 573) and to the non-physiological agonist ristocetin (mimics effects of high shear (457)); and VWF immobilization onto the subendothelial matrix or surfaces (e.g., microtiter plates) (30, 445, 447, 460, 461). My thesis studies

determined that VWF binding to MMRN1 is similarly enhanced by these mechanisms (571), suggesting that MMRN1 binds to cryptic regions in VWF. The regulated exposure of ligand binding sites controls the adhesive properties of VWF, and localizes its functionality to areas of high fluid shear and denudation of the vascular endothelium, where VWF is crucial for normal haemostasis (25, 98, 100, 123, 140, 150). The regulation of MMRN1-VWF binding is likely also important for modulating the interaction between these two massive, highly polymeric, platelet adhesive proteins, especially under physiologic and pathological conditions that lead to platelet adhesion at the sites of vessel injury (24, 25, 98, 100, 123, 140, 150, 477). The regulated exposure of the homologous, shear-sensitive A domains of VWF controls its binding to several haemostatic ligands that modulate the platelet-dependent adhesive functions of VWF at arterial shear rates (29, 148, 279, 310, 483, 573). Ligands known to bind to the A domains of VWF include: the platelet receptor, GPIbα (28, 29, 148, 279); the VWF-cleaving metalloproteinase, ADAMTS13 (573-575); and an enhancer of high shear platelet adhesion, vimentin (310). I show that MMRN1 also interacts with the A1A2A3 domains of VWF to support the platelet adhesive properties of VWF, at a high shear rate (571). Removal of this region in full-length VWF impairs MMRN1 binding (571), further confirming that VWF A1A2A3 domains are necessary to support binding to MMRN1. Interestingly, I noted that the mutant protein possessing only the A1A2A3 tri-domain of VWF binds to MMRN1 independent of shear or ristocetin, which are required for optimal MMRN1 binding of full-length WT-VWF (571). The absence of neighbouring N- and C-terminal regions in VWF influences the conformation and exposure of cryptic sites in VWF A1A2A3 region (418, 423, 449, 482,

576, 577), and likely attributed to the ability of VWF A1A2A3 tri-domain to bind MMRN1 without exposure to shear or ristocetin.

The roles of VWF A domains in MMRN1 binding were evaluated in a complementary fashion, by using VWF mutant proteins (i.e. domain deleted and truncated mutant proteins), and functional inhibitors (i.e. antibodies and collagen peptides) (571). I found that VWF lacking the A1 or A3 does not detectably bind to MMRN1 (571), which suggests that both domains are critical for normal MMRN1 binding. As VWF lacking the A2 domain binds to MMRN1 similarly to WT-VWF (571), this suggests that the A2 domain in VWF does not significantly modulate MMRN1 binding. My investigations also illustrated that MMRN1-VWF binding is only partially impaired (≥ 55% reduction) by functional inhibitory antibodies and peptides that abolish GPIbα and collagen binding to the A1 and A3 domains of VWF, respectively (571). These additional findings suggest that MMRN1 independently binds to the structurally homologous VWF A1 and A3 domains, and that both domains are needed for optimal MMRN1 binding. These findings also suggest that the MMRN1 binding sites in VWF may overlap (at least partially) with the binding region for GPIbα in the A1 domain of VWF, and with the regions that binds to fibrillar collagens in the VWF A3 domain. I provide evidence that monomeric VWF A1A2A3 tri-domain enhances platelet adhesion to MMRN1 at high shear, which requires VWF A1A2A3 to bind MMRN1 and the A1 domain of VWF to bind to GPIbα (38, 571). Also, VWF A1-GPIbα binding is important for normal platelet adhesion to collagen at arterial shear rates (30, 88, 100, 123), a process that is enhanced by MMRN1, likely due to VWF-

MMRN1 binding on collagen surfaces (38). Therefore, it is possible that overlap in MMRN1 binding to VWF A1-GPIbα and VWF A3-collagen binding sites does not negatively modulate the native, multivalent adhesive properties of polymeric VWF, in circulation. It is also possible that the inhibitory antibodies and collagen peptides reduce MMRN1-VWF binding by steric hindrance of MMRN1 binding to sites that are near, but distinct from the VWF A1-GPIbα and VWF A3-collagen binding sites. Regardless, the direct or indirect inhibition of MMRN1-VWF binding by antibodies and collagen peptides confirms that MMRN1 interacts with the A1 and A3 domains of VWF (571). VWF A domains regulate the exposure and conformation of neighbouring domains in VWF (423, 444, 447, 449, 482, 550), and this could explain why the lack of the A1 or A3 domains drastically reduces the binding to MMRN1 to VWF constructs (571). My observations that the exposure of VWF to shear (or ristocetin) enhanced VWF-MMRN1 binding (571), provides further evidence that the conformation of VWF controls its interactions with MMRN1.

I noted that the A1 and A3 domains of VWF independently bound to MMRN1 in SPR experiments, unlike the homologous A2 domain of VWF that showed low or undetectable MMRN1 binding in these studies (571). These findings further suggest that MMRN1 specifically and independently interacts with the structurally homologous A1 and A3 domains, but not with the A2 domain of VWF that shares a primary sequence identity of > 20% with the homologous neighbouring A1 and A3 domains (448, 573, 578). Similar findings are reported for types I and III collagens (92, 423, 425, 427) and snake venom

bitiscetin (426, 447, 579, 580) that interact with the A1 and A3 domains of VWF, but not with the VWF A2 domain. It is possible that large polymeric (and hence multivalent) proteins like collagen and MMRN1 simultaneously bind to the structurally homologous A1 and A3 domains of VWF because of the proximity of these sites (423, 576).

VWF A1A2A3 tri-domain mutant protein binds to MMRN1 with high physiologically relevant binding affinity (K_D: 2.0 ± 0.4 x 10^{-9} M) (571), that is ~5% of the normal plasma levels of VWF (40 x 10^{-9} M, based on ~ 250 kD subunits) (386, 387). This finding suggests that MMRN1-VWF binding likely occurs in vivo at sites where MMRN1 is released from platelets and endothelium and encounters plasma VWF. It was interesting that the individual A1 and A3 domains of VWF, but not the A2 domain, independently supported lower affinity binding to MMRN1 (respective K_D: 39.3 ± 7.7 x 10^{-9} M and 229 ± 114 x 10^{-9} M) (571). A two-step conformational change model best described the binding of VWF A1A2A3 tri-domain and individual A1 domain to MMRN1 (571), which raises the possibility that VWF and/or MMRN1 undergo a change in conformation after their initial binding as reported for the interaction between FV and MMRN1 (514). As multiple domains within VWF contribute to MMRN1 binding (571), and individual A domains influence the conformation of the A1A2A3 region (423, 444, 447, 449, 482, 550), it is not surprising that affinity estimations confirm that the entire A1A2A3 region of VWF is needed for optimal, stable, high-affinity binding to MMRN1. Affinity estimations implicate the A1 domain of VWF as the key MMRN1 binding region; however, the lower affinity binding observed with the VWF A3 domain could be the result of an altered conformation

due to the absence of the neighbouring structural regions (425). VWF A domain mutant proteins are noted to underestimate the binding affinity of full-length, WT-VWF to other haemostatic ligands by several orders of magnitude (425, 480, 481, 581), and it is similarly possible that WT-VWF binds to MMRN1 with an even higher affinity than VWF A1A2A3 tri-domain. As the polymeric structure of WT-VWF also enhances the binding of VWF to other ligands (384, 425, 505, 582), it may further augment the binding of WT-VWF for MMRN1 by increasing the avidity.

These data on the mechanisms of VWF-MMRN1 binding have implications for when and how these proteins interact *in vivo*. At the site of vascular injury, MMRN1 that is released from platelets and EC (as perhaps also the exposure of MMRN1 in the vascular subendothelium) (33, 35, 183, 509) may serve to help localize platelet-reactive VWF in order to promote platelet adhesion. This is similar to the action of other haemostatic proteins, including TSP-1, FN, and subendothelial collagens (90-92, 94, 99, 124, 423-425, 447, 583). This hypothesis was tested by *in vitro* assays that were designed to quantify platelet adhesion to MMRN1 at an arterial shear rate. These studies revealed that MMRN1 requires pretreatment with physiological amounts of VWF A1A2A3 tri-domain (or full-length WT-VWF (38, 571)) to optimally support platelet adhesion at a high shear rate (571). These observations, in conjunction with the stable, higher affinity binding of VWF A1A2A3 tri-domain to MMRN1 (571), suggest that the tri-A domain is sufficient and likely the smallest region of VWF that supports high shear platelet adhesion to MMRN1 under physiological conditions. This is supported by my observation that the VWF A1A2A3 tri-

domain even supports platelet adhesion to MMRN1 in the absence of platelet-released VWF (in experiments that I conducted using type 3 VWD platelets, (571)), which is known to promote platelet adhesion at arterial shear rates (309). The observation that VWF A1A2A3 tri-domain supports platelet adhesion to MMRN1 is interesting, as this tri-domain contains the binding site of GPIbα, but not the C-terminal $\alpha_{IIb}\beta_3$ binding site in VWF (310, 449, 482). This finding is consistent with the prior observation that platelets adhere to MMRN1 by a VWF-dependent mechanism that involves GPIbα, but is independent of β_3 integrins (38). The finding that inhibition of VWF A1-GPIbα binding abolished platelet adhesion to MMRN1 (571), and prior observations that MMRN1 does not bind GPIbα (38), suggest that MMRN1 needs to bind VWF and does not independently support GPIbα-dependent platelet adhesion at high shear (38). It is possible that in damaged arteries, MMRN1 optimizes VWF localization via the shear-sensitive A domains of VWF, while still allowing VWF to bind to the platelet receptor, GPIbα. As MMRN1 is normally sequestered in storage granules, its release could be important to upregulate VWF-platelet interactions at sites of vessel injury.

Polymeric VWF localizes to sites of vessel injury to support multivalent binding with several hemostatic ligands (24, 75, 88, 384, 581, 582, 584). Overlap in the VWF A1 and A3 binding sites for MMRN1, GPIbα, and collagen (which can also bind both VWF and MMRN1) could work cooperatively to optimize the capture of multivalent VWF at sites of vessel injury, as postulated for other haemostatic ligands of VWF (75, 88). Importantly, VWF A1A2A3 tri-domain captured on MMRN1 still supports VWF-GPIbα

binding (571), despite the potential overlap between the MMRN1 and GPIbα binding sites in the A1 domain of VWF. I postulate that the site in the A1 domain of VWF that binds to MMRN1 does not completely overlap with GPIbα binding to the front and upper faces of VWF A1 domain (96, 97). MMRN1 likely binds to adjacent or distal sites or faces in VWF A1 domain, similar to ristocetin that binds to the upper face of the A1 domain of VWF (96), or botrocetin (96, 585), heparin (96), and types IV and VI collagens (90, 91) that bind to the right-hand face of VWF A1 domain. Further insights might be gained by mapping of the region in the A1 domain that binds MMRN1 (refer to Section 4.3.1 Mapping MMRN1 binding to VWF A1 and A3 domains).

Exposure to shear enhances VWF binding to MMRN1 (571), suggesting that the mechanism of MMRN1 binding to the A1 domain is under shear-regulation, similar to the undefined binding of types I and III collagens to the A1 domain of VWF under fluid shear (423). Types I and III collagens primarily bind to the lower anterior surfaces of VWF A3 domain (425-427), which is a conserved ligand-binding region that may also support MMRN1 binding. Additional insights would be obtained by mapping the faces of VWF A1 and A3 domains that directly support MMRN1 binding (refer to Section 4.3.1 Mapping MMRN1 binding to VWF A1 and A3 domains), which may highlight similarities for VWF binding to fibrillar collagens and MMRN1.

VWF A2 domain contributes to the conformation of VWF A1A2A3 domains, and binds to VWF A1 domain to regulate its platelet adhesive properties (310, 363, 444, 474).

The A2 domain of VWF interacts with its neighbouring A1 domain by a mechanism regulated by fluid shear (and ristocetin) (444), similar to what I describe for MMRN1 binding to VWF (571). VWF A2 domain interacts with the GPIbα binding site in VWF A1 domain to impair platelet adhesion (310, 444), and likewise, the absence of VWF A2 domain supports enhanced VWF-GPIbα binding (474). In this thesis, I show that VWF A2 domain does not significantly support MMRN1 binding, nor does its absence significantly modulate VWF-MMRN1 binding (571). These findings, taken together, suggest that MMRN1 interacts with VWF at sites that are not regulated by the A2 domain of VWF, such as the GPIbα binding site in VWF A1 (310, 444, 474). It is also interesting to note that the absence of VWF A2 domain does not impair VWF interactions with heparin and botrocetin (474), which are mapped to the upper and right-hand faces of the A1 domain (96, 585). These findings complement my hypothesis that MMRN1 may bind to these surfaces in VWF A1 domain, at sites that are distinct from the GPIbα binding site.

Ligand binding to VWF A1 domain regulates the neighbouring A2 domain of VWF and promotes ADAMTS13-mediated proteolysis of VWF A2 domain (550, 575). Additionally, ADAMTS13 fragments VWF polymers to reduce its haemostatic properties, including platelet adhesion and collagen-binding (384, 477, 586). It would be interesting to assess whether ADAMTS13 also regulates VWF binding to MMRN1, and if MMRN1 binding to VWF A1A2A3 region modulates the activity of ADAMTS13 on VWF polymers.

My thesis study illustrates that MMRN1 is a novel ligand for the shear-sensitive A domains of VWF. Mutations in the A1A2A3 region of VWF occur in some forms of type 2 VWD that impair the platelet adhesive functions of VWF, including VWF A1 domain binding to GPIbα (279, 481, 587, 588), and the collagen binding properties of VWF A1 and A3 domains (90, 91, 450, 451, 504, 505). Likewise, defective MMRN1 binding to the A1 and A3 domains of VWF could abrogate or modulate the platelet adhesive functions of VWF, specifically GPIbα-dependent platelet adhesion at arterial shear rates. As detailed in the introduction of my thesis, there are a few platelet disorders that are associated with deficiencies in platelet MMRN1 (175, 525, 528), but conditions associated with mutations in the *MMRN1* gene, and the pathogenic consequences, are not yet described. Consequently, I further evaluated multimerin 1 functions by exploring the implications of a selective Mmrn1 loss in mice on platelet adhesive functions, *in vitro* and *in vivo*.

4.2 INSIGHTS INTO THE CONTRIBUTIONS OF MMRN1 TO PLATELET ADHESIVE FUNCTIONS IN MICE

In humans and mice, the multimerin 1 and α-synuclein genes are adjacent and encode proteins that modulate platelet functions, *in vitro* (37, 38, 312, 511, 540, 543). In mice, spontaneous tandem loss of the *Mmrn1* and *Snca* genes impairs a number of platelet adhesive, haemostatic functions (37), but the phenotypes of these mice are likely influenced by the dual protein deficiency. The loss of the *Snca* gene could accelerate α-granule release and augment platelet response to thrombin (37, 540), as observed in Mmrn1/Snca double

deficient mice (37), which could result in a prothrombotic phenotype. Consequently, studies of the dual deficient mice could have underestimated the importance of Mmrn1 to platelet adhesive functions. To specifically explore the specific contributions of Mmrn1 to platelet haemostatic functions, mice with a selective loss of the *Mmrn1* gene were generated and I worked to characterize several aspects of their platelet, adhesive haemostatic functions, *in vitro* and *in vivo* (Table 5).

Table 5: Platelet adhesive properties/functions of Mmrn1/Snca double deficient mice (37), compared to the mice assessed in this thesis, with selective Mmrn1 deficiency.

Platelet function analyses			Mmrn1/Snca double deficient mice*	Mmrn1 deficient mice*†
Tail bleeding phenotype			NS	NS
Platelet aggregation (with PRP)	**TRAP**	**500 µM**	20% reduction in maximal aggregation	NS
	ADP	**10 µM**	NS	NS
		20 µM	NS	NS
	Collagen	**5 µg/ml**	NT	NS
		10 µg/ml	NS	NS
		20 µg/ml	NS	NS
Platelet aggregation (with GFP)	**Thrombin**	**0.5 U/ml**	25-50% reduction in maximal aggregation	NS
		1.0 U/ml		NS
	Collagen	**5 µg/ml**	NT	20-30 % reduction in maximal aggregation
		10 µg/ml	NS	
		20 µg/ml	NS	
High shear platelet adhesion	**Collagen**		~30% reduced platelet adhesion	~ 50% reduced platelet adhesion
	Vwf		NT	NS
Surface expression of platelet receptors and granule proteins	**Resting platelets**	**GPIbα, CD42b; β_1, CD29; and β_3, CD61**	NS	NS
	Thrombin-activated platelets	**P-selectin, CD62P**	More detection of P-selectin at lower (0.125-0.25 U/mL), but not higher (0.5 – 1.0 U/mL) concentrations	NS
		Activated $\alpha_{IIb}\beta_3$, CD41/CD61	NS	Slight increase in the overall detection of $\alpha_{IIb}\beta_3$
Ferric chloride injury model of arterial thrombosis	**Initial platelet localization to the damaged vessel**		Impaired	Impaired
	Appearance of first large (≥ 20 µm) thrombus		Delayed	Delayed
	Vessel occlusion times		Prolonged, and occlusive thrombi did not always form	Prolonged, and occlusive thrombi did not always form

NS indicates no significant differences between WT and deficient mice; Not tested (NT); *Comparison to WT mice; †Mmrn1 deficient mice includes both *Mmrn1*$^{-/-}$ and *Mmrn1*$^{+/-}$ mice

Selective Mmrn1 deficiency, like Mmrn1/Snca double deficiency (37), resulted in fertile, viable mice, with normal cell counts. The selective loss of Mmrn1 also did not result in an overt bleeding phenotype (evaluated by distal tail transection), although there was a trend suggesting that proportionally more *Mmrn1*$^{-/-}$ mice bleed for longer than 10 min – this difference was not statistically significant. The lack of an overt bleeding phenotype in these mice resembles observations for mice with combined Mmrn1/Snca deficiency (37) (Table 5), as well as mice deficient in TSP-1 and pFN that have significant defects in platelet adhesive, haemostatic functions, despite normal bleeding times (37, 133, 307, 340). This contrasts with the effects of a loss of Vwf (144, 309) and/or Fg (321, 322) that result in a severe bleeding diathesis in mice, likely because these abundant plasma proteins have crucial roles in supporting platelet aggregate formation during wound haemostasis (144, 193, 286, 309, 321, 322). It is important to note that the tail transection model does not detect all deficits to platelet adhesive functions, especially those that are modulated by high arterial shear conditions (133, 141, 307, 340, 341) or that are dependent on platelet adhesion to collagen (115, 589, 590). Consequently, these findings do not preclude the possibility that the loss of Mmrn1 impairs platelet adhesion and platelet-rich thrombogenesis. For subsequent studies on platelet function, I mainly focused on comparing *Mmrn1*$^{-/-}$ to WT mice, due to the lack of an overt bleeding phenotype in mice deficient of Mmrn1. I also assessed heterozygous (*Mmrn1*$^{+/-}$) mice in experiments where homozygous (*Mmrn1*$^{-/-}$) null mice had drastically (> 30%) altered platelet function.

Bleeding models that incorporate arterial injury, as was chosen for analyzing mice with selective Mmrn1 deficiency (Section 2.2.12 Mouse tail transect bleeding model), are reportedly more responsive to mild alterations in $\alpha_{IIb}\beta_3$-dependent platelet aggregation (330). Aggregometry studies with ADP and thrombin also involve $\alpha_{IIb}\beta_3$-dependent platelet aggregation (193, 331), and showed normal responses for *Mmrn1*$^{-/-}$ platelets, coinciding with the lack of an overt bleeding phenotype in *Mmrn1*$^{-/-}$ mice. Interestingly, however, the monoclonal antibody JON/A detected more functionally active $\alpha_{IIb}\beta_3$ on thrombin-activated platelets from Mmrn1 deficient mice, although the increase in active $\alpha_{IIb}\beta_3$ was small (~ 10% more with maximal activation) relative to wild-type platelets. This raises the possibility that Mmrn1 loss modulates the activation of $\alpha_{IIb}\beta_3$, despite the normal $\alpha_{IIb}\beta_3$-dependent platelet function of *Mmrn1*$^{-/-}$ mice. Alternatively, Mmrn1 loss may merely modulate the accessibility of this integrin to JON/A, as is reported for mouse platelets deficient in GPIbα (IL4Rα/GPIbα-tg) (139). Thrombin-activated platelets release MMRN1 that binds to activated $\alpha_{IIb}\beta_3$ (33, 38, 183, 312), and JON/A similarly binds to activated $\alpha_{IIb}\beta_3$ (591). As MMRN1 is a large homopolymer (33, 507), it is possible that Mmrn1 binding to activated $\alpha_{IIb}\beta_3$ sterically hinders the binding of the equally large PE-labelled JON/A antibody (> 600 kD) (591). Mmrn1 loss in mice, likely does not significantly alter platelet activation, as thrombin stimulation led to similar levels of platelet activation as assessed by the expression of P-selection on *Mmrn1*$^{-/-}$ and WT platelets. As resting platelets lacking Mmrn1 had normal surface levels of $\alpha_{IIb}\beta_3$, this excludes the possibility that Mmrn1 loss reduces the surface expression of this integrin receptor. I had not anticipated that selective Mmrn1 deficiency would have an effect on the activation of $\alpha_{IIb}\beta_3$, given that mice

with combined Mmrn1/Snca loss had normal JON/A detection of activated $\alpha_{IIb}\beta_3$ (37) (Table 5).

In this thesis, I showed that GFP, but not PRP, from *Mmrn1*$^{-/-}$ mice had impaired collagen-induced platelet aggregation, despite the normal aggregation responses to all other agonists tested. It is possible that abundant plasma proteins, such as VWF and FG, limited the contributions of platelet Mmrn1 to collagen-induced aggregation response of PRP from *Mmrn1*$^{-/-}$ mice. Similarly, integrin $\alpha_2\beta_1$, which is important for supporting the adhesion of washed platelets to collagen (156, 157), has a limited role in modulating platelet adhesion and aggregation in the presence of plasma proteins that can indirectly support and enhance the adhesive properties of collagen (121, 155, 156). These findings, taken together with my other results, suggest that platelet Mmrn1 has limited effects on platelet aggregation to collagen, that are dependent on the presence of plasma proteins. While Mmrn1/Snca dual deficient platelets (both PRP and GFP) have normal aggregation response to collagen (37) (Table 5), it is possible that the presumed prothrombotic effects of Snca loss compensate for the loss of platelet Mmrn1 in Mmnr1/Snca double deficient mice.

In mice, concomitant loss of Mmrn1 and Snca alters platelet response to thrombin by increasing α-granule release of P-selectin at low thrombin concentrations, and reducing maximal platelet aggregation response to thrombin or TRAP, *in vitro* (37). However, I show that the selective loss of Mmrn1 did not increase thrombin-induced release of P-selectin from platelet granules, nor did it reduce thrombin (or TRAP)-induced platelet

aggregation (Table 5). These data suggest that a selective Mmrn1 deficiency does not modulate platelet granule release or platelet aggregation responses to thrombin. It is possible and likely that the Snca loss alters thrombin-induced granule release and platelet aggregation responses to thrombin and TRAP in mice with combined Mmrn1/Snca deficiency (37, 540), as α-synuclein modulates thrombin-stimulated platelet response, *in vitro* (540). Mice with a selective Snca deficiency have not been assessed for defects in platelet haemostatic functions (540, 592), which could clarify the effect of Snca loss on platelet responses to thrombin in mice.

Combined Mmrn1 and Snca loss reduces high shear platelet adhesion to collagen (37), and the selective loss of Mmrn1 similarly impaired platelet adhesion to collagen at high shear *in vitro* (Table 5). These findings corroborate observations that MMRN1 supports platelet adhesion to types I and III collagens, *in vitro* (38), a process that is also dependent on plasma and platelet VWF (38, 88, 100, 309, 593). I show that WT and *Mmrn1*$^{-/-}$ mice had similar Vwf levels in plasma and platelets, and comparable membrane expression of platelet receptors that participate in thrombogenesis (e.g., GPIbα, $\alpha_2\beta_1$, and $\alpha_{IIb}\beta_3$). These findings reduce the likelihood that changes to these aspects contributed to platelets from *Mmrn1*$^{-/-}$ mice having defective platelet-rich thrombus formation on collagen. As a result, it is likely that the specific loss of Mmrn1 is responsible for impaired platelet adhesion to collagen, and that in mice, Mmrn1 is necessary for the normal platelet adhesive properties of collagen, specifically under arterial flow conditions. While it is still unclear how MMRN1 contributes to this adhesive process, Mmrn1 loss may reduce platelet

adhesion to collagen directly due to loss of direct collagen-Mmrn1 interactions, or indirectly due to loss of Mmrn1 interactions with other platelet/plasma proteins (e.g., Vwf).

The loss of Mmrn1, in mice, did not significantly impair platelet adhesion to Vwf matrices, under arterial flow conditions. This platelet adhesive process depends on the platelet receptor, GPIbα, that binds to captured/immobilized VWF to initiate a monolayer of adhesive platelets (25, 88, 94, 96, 97). This finding suggests that the loss of platelet Mmrn1 does not significantly modulate GPIbα-dependent platelet adhesion to Vwf, at arterial shear rates. However, it is possible that unlike the highly thrombogenic nature of fibrillar collagen that induces platelet activation and secretion of granule contents (93, 121, 570), GPIbα-mediated platelet adhesion to VWF may not induce complete release of soluble granule proteins (25, 162, 466, 570), like MMRN1. Inadequate release of Mmrn1 from WT platelets would underestimate its contributions to platelet adhesion on Vwf. Platelet adhesion to collagen at high shear (> 300 s^{-1}) is similarly dependent on both VWF and GPIbα (74, 88, 100, 103-105, 121, 123) (Table 2). MMRN1 supports VWF-GPIbα-dependent platelet adhesion under arterial shear rates *in vitro* (38, 571), and also enhances high shear, VWF-dependent platelet adhesion to collagen *in vitro* (38), likely through its combined interactions with VWF and collagen (37, 38). Future studies are required to assess if platelet released Mmrn1 participates in Vwf-dependent platelet adhesive functions, in mice (refer to Section 4.3.2 Contributions of Mmrn1 to platelet aggregation and thrombogenesis at arterial shear rates), and whether this interaction directly modulates

platelet adhesion to collagen under similar haemodynamic conditions (refer to Section 4.3.3 Contributions of Mmrn1 to platelet adhesion on collagen).

Immunoblots demonstrated that Mmrn1 and Vwf are stored in mouse platelets, suggesting that like VWF, there is a conserved role for MMNR1 in modulating platelet function. MMRN1 and VWF co-localize to platelet α-granules in humans (183), but it is unclear if this is preserved in mouse platelets. Future studies are needed to determine the precise localization of intracellular Mmrn1 in mouse platelets. It is anticipated that Mmrn1 similarly sorts to mouse platelet α-granules, as there is conserved retention of other proteins to mouse platelets, including P-selectin (9, 594), FV (595, 596), and TSP-1 (9, 307, 597). Type 3 VWD (complete VWF deficiency (8, 386)) does not alter MMRN1 levels in human platelets (386), and in mice, I show that Mmrn1 loss did not reduce platelet (and plasma) Vwf levels. I also show that shear is required to expose the A1A2A3 tri-domain of VWF that supports MMRN1 binding (571). These findings, taken together suggest that platelet stores of VWF and MMRN1 do not interact (likely because VWF A1A2A3 are not adequately exposed), and that MMRN1 and VWF are independently retained in platelets. In platelets, MMRN1 is the main binding protein for FV/Va (34, 513, 514, 524, 527), and further studies are needed to determine if Mmrn1 loss modulates levels of platelet FV in mice. Platelet MMRN1 is not shown to interact with other platelet and plasma proteins (38, 508); therefore, it is not anticipated that the loss of Mmrn1 would alter the levels of these blood proteins.

Platelet adhesive function, *in vivo*, is conventionally analyzed by the ferric chloride arteriole injury model (37, 49, 72, 144, 145, 598). This model was used previously to investigate Mmrn1/Snca double deficient mice, and this provided the first evidence that Mmrn1 contributes to platelet adhesive functions, *in vivo* (37) (Table 5). Hence, this injury model was used to study mice with a selective Mmrn1 loss, as the concomitant Snca loss in Mmrn1/Snca double deficient mice may have underestimated of the platelet adhesive functions of Mmrn1 (37, 540). Like Snca/Mmrn1 double deficient mice (37), mice with selective Mmrn1 loss had impaired *in vivo* platelet adhesion and platelet-rich thrombus formation in arterioles exposed to ferric chloride (Table 5). In Mmrn1 deficient mice, there was delayed localization and recruitment of circulating platelets to the ferric chloride injury site, as measured by the number of individual adherent platelets per minute, during the interval 3 to 5 min after ferric chloride injury. This stage of the ferric chloride injury model is also defective in mice with combined Mmrn1 and Snca loss (37) (Table 5), and is similarly impaired in mice with selective Vwf loss (72, 144), or combined loss of Vwf with either Tsp-1 (145) or Fg (72). By comparison, the selective loss of another platelet protein, Tsp-1 (145), or the abundant plasma protein, Fg (72), does not alter the platelet adhesive functions during initial stage of the ferric chloride injury model. These findings, and the findings in this thesis, suggest that like Vwf, Mmrn1 has crucial roles in localizing and recruiting circulating platelets to the ferric chloride injury site.

Mice with selective Mmrn1 loss had defective platelet aggregate formation *in vivo*, resulting in the delayed appearance of the first intravascular thrombus. When a $\geq$ 20 μm

thrombus formed in Mmrn1 deficient mice, there was dissociation of smaller platelet aggregates from the top of developing platelet-rich thrombi. This observation is similar to those reported for mice deficient in Vwf and Fn (72, 144, 308, 341), and *FgγΔ5*$^{-/-}$ mice (form fibrin, but do not support FG-$\alpha_{IIb}\beta_3$-mediated platelet aggregation) (305), that have small aggregates disassociate from the apex of developing thrombi (72, 144, 305, 308, 341). This observation is unlike mice deficient of Fg (and fibrin) that form large unstable thrombi that readily dissociate from the injury site (72, 305). These findings, in conjunction with my observations, suggest that Mmrn1 participates in platelet-rich aggregate formation and growth *in vivo*, but has minor roles in stabilizing the attachment of platelet-rich thrombi to the vessel wall, a process that requires fibrin generation (56, 72, 305).

Vessel occlusion times were significantly delayed in Mmrn1 deficient mice, and in some cases, the loss of Mmrn1 had deleterious effects on the formation of occlusive thrombi during the 40-min observation period. These findings are similar to the defective thrombogenesis that results in the delayed formation, or absence of intravascular occlusive thrombi in mice with double deficiency of Mmrn1 and Snca (37) (Table 5). Similar observations are also reported in mice deficient of Vwf and Fg (72), or a selective loss of Vwf (72) or pFn (308, 341). Mice with selective deficiencies of Fg (72, 305) or Tsp-1 (145) have only prolonged occlusion times, and loss of these proteins do not abolish *in vivo* thrombus formation in mice. These findings, taken together with my observations, suggests that Mmrn1, like Vwf and Fn (69, 72, 144, 308, 341), is a crucial modulator of platelet-rich thrombogenesis at arterial shear rates, *in vivo*.

The precise mechanism underlying ferric chloride-induced thrombosis remains controversial (69-71, 82, 83), despite its widespread use as an experimental model. Ferric chloride was traditionally thought to denude the endothelium by iron-induced oxidative stress in the arterial lumen (70, 71, 73) that exposes proteins in the subendothelial basal lamina (69-72) or deeper within the vasculature (74). Circulating platelets were thought to adhere and aggregate on the exposed subendothelium (69, 70, 74); however, current studies suggest that ferric chloride induces the localization of platelets to the vessel walls by complex, multifaceted mechanisms (69, 71, 82, 83). These mechanisms are mediated by RBC hemolysis and oxidation of hemoglobin (71, 83), as well as colloidal chemistry, whereby intravascular aggregate formation is dependent on the charge of cells and proteins (69, 82). These mechanisms may also be independent of platelet adhesion mediated by endothelial dysfunction (82, 83), but are similarly ameliorated by the haemostatic adhesive functions of Vwf (72, 83, 144). As MMRN1 binds to VWF and supports platelet adhesion *in vitro* (38, 571), in the mouse ferric chloride injury model, Mmrn1 may similarly modulate the platelet localization to damaged vessels by supporting the adhesive properties of VWF *in vivo*.

Ferric chloride may also initiate intravascular thrombogenesis by mechanisms that may not depend on the haemostatic adhesive properties of vascular proteins (71). In fact, ferric chloride may actually decrease the functionality of adhesive vascular proteins, like collagen, VWF and FG at the injury site (69), thereby limiting the platelet adhesive

properties of these proteins. These new insights raise questions about the validity of this injury model to accurately recapitulate physiological platelet adhesive processes; thus, future studies are needed to further assess the haemostatic, platelet adhesive functions of Mmrn1 *in vivo* (refer to Section 4.3.6 Other animal and injury models).

This thesis has focused on exploring the platelet adhesive properties of MMRN1 at arterial shear rates, which requires both VWF and GPIbα (38, 312). However, studies are still needed to fully describe the contributions of MMRN1 to other aspects of platelet adhesion that may involve VWF-MMRN1 binding, such as shear-induced platelet aggregation (31, 233, 285, 506) (refer to Section 4.3.2 Contributions of Mmrn1 to platelet aggregation and thrombogenesis at arterial shear rates). MMRN1 also supports platelet function under venous shear rates by molecular mechanisms that involve β_3 integrins and GPIbα, but not VWF (38, 312). Therefore, it is possible that the loss of Mmrn1 modulates thrombogenesis in veins, like its effect on arterioles treated with ferric chloride. MMRN1 is also the main binding protein for FV in platelets (34, 513, 524, 526, 527), and its loss could have impact on FV/Va localization and thrombin generation (514). Consequently, further studies are needed to explore if the loss of Mmrn1, in mice, has impacts on other aspects of haemostasis (refer to Section 4.3.6 Other animal and injury models).

It is worthwhile to consider the strategy used to generate Mmrn1 deficient mice when evaluating phenotypic findings. Mmrn1 deficient (*Mmrn1*$^{-/-}$ and *Mmrn1*$^{+/-}$) mice are generated by removing exon 3, which produces a frameshift mutation and a severely

truncated gene product possessing only the first two exons (~20 % of full-length transcribed mRNA: 942 out of 4636 base pairs). Translated, exons 1-2 in *Mmrn1* would produce a functionally null, aberrant protein that possesses ~20 % of preproMmrn1 (232 out of 1210 residues), including < 60 % of the N-terminal, cysteine-rich EMI domain (38 out of 67-76 residues). I was unable to determine if *Mmrn1*$^{-/-}$ mice store an N-terminal truncated form of Mmrn1 in their platelets, as there are currently no antibodies available that detect this region of Mmrn1. Using an antibody that recognizes the C-terminus of Mmrn1, I confirmed that Mmrn1 was detectable in platelet lysate samples from WT mice, as expected based on MMRN1 findings for humans (33, 183, 507). I also found that Mmrn1 was reduced in platelets of *Mmrn1*$^{+/-}$ mice, based on Western blot analyses as there are presently no immunoassays available to quantify Mmrn1.

Haplodeficiencies often results in milder phenotypes than complete deficiencies, as one WT allele is present to compensate for the deficits due to the mutant/null allele (144, 331, 341, 589, 599). Surprisingly, the WT allele in *Mmrn1*$^{+/-}$ mice did not rescue the impaired platelet adhesion and thrombus formation of *Mmrn1*$^{-/-}$ mice. *Mmrn1*$^{+/-}$ mice had the expected reduced level of Mmrn1 in Western blots of platelet lysate samples, and it is possible that the abnormal phenotype in *Mmrn1*$^{+/-}$ mice could be the result of a reduction in threshold levels of Mmrn1 necessary for normal platelet function. This would suggest that normal levels of Mmrn1 (as in the WT mice) are need to support platelet adhesive, haemostatic functions, like the importance of normal levels of VWF to properly modulate haemostasis (8, 409, 497). It is also possible that the null allele leads to synthesis of a partial

Mmrn1 protein that inhibits the functionality of Mmrn1 polymers in a dominant-negative manner (599, 600). As MMRN1 is assembled as polymers of its trimers (34, 304, 509, 510), the integration of truncated Mmrn1 subunits could create a dysfibrinogenemia-like defect (13), and explain the similar phenotypes for *Mmrn1*$^{+/-}$ and *Mmrn1*$^{-/-}$ mice. In some forms of type 2 VWD, synthesis of an abnormal subunit similarly antagonizes VWF polymerization and function (420, 421). There was detectable WT-Mmrn1 in platelets from *Mmrn1*$^{+/-}$ mice, and there is no evidence that a null allele produces an aberrant protein that causes degradation of WT-Mmrn1, as occurs in some forms of type 1 VWD (422). Future studies are needed to determine if *Mmrn1*$^{+/-}$ mice produce a truncated N-terminal protein that compromises the integrity and functionality of Mmrn1 polymers (refer to Section 4.3.5 Studies of haploinsuffuciency in *Mmrn1*$^{+/-}$ mice).

The addition of recombinant MMRN1 prior to ferric chloride-induced injury or to *in vitro* perfusion studies, ameliorates the observed defects in platelet haemostatic functions in mice with combined Mmrn1 and Snca deficiency (37). This suggests that murine and human multimerin 1 are functionally similar, despite the sequence differences (i.e., ~67% sequence similarity) (37, 508). The data presented in this thesis demonstrates that, in mice, Mmrn1 significantly contributes to platelet adhesive, haemostatic functions, especially at high shear rates. These findings, taken together, provides unique insights that may clarify the potential consequences of *MMRN1* deficiency in humans. The data presented here suggest that the loss of *MMRN1* may cause platelet function defects and contribute to abnormal arterial bleeds.

The expression of MMRN1 is restricted to megakaryocytes and platelets (33, 36, 183, 386, 507, 519) and the vascular endothelium and subendothelium (35, 509). MMRN1 is not detected in other blood cellular components (33), nor is it normally detected in plasma (33). Mice with selective loss of Mmrn1 likely have deficiencies of both platelet and the EC-derived Mmrn1, and the resultant *in vivo* phenotype of *Mmrn1*$^{-/-}$ mice was likely attributed to combined deficiency of both sources of Mmrn1. It is unknown how platelet vs. endothelial Mmrn1 contribute differentially to haemostasis; therefore, future studies could assess this (refer to Section 4.3.6 Other animal and injury models).

MMRN1 supports platelet adhesion irrespective of fluid shear (38, 312), and at low shear ($\leq 150\ s^{-1}$) MMRN1 supports platelet adhesion via a mechanism dependent on the N-terminal RGD-integrin binding motif of MMRN1 and platelet β_3-integrins (38, 312). Additional studies are also needed to assess the contributions of MMRN1 to platelet adhesive functions under these specific haemodynamic conditions, *in vivo* (refer to Section 4.3.6 Other animal and injury models).

The findings in this thesis describe the functional importance of multimerin 1 as a unique, haemostatic adhesive protein that modulates platelet-rich thrombogenesis, especially at shear rates typical of arteries. MMRN1 likely exerts its effect on platelet adhesive properties, under these flow conditions, by binding to VWF and supporting GPIbα-dependent platelet adhesion (571). Using the findings from this thesis, I constructed

a schematic to illustrate the platelet adhesive functions of MMRN1 (Figure 26). I propose that at the sites of arterial endothelium dysfunction, MMRN1 released from platelets and ECs (33, 35, 183, 507, 508) supports platelet adhesive functions by: 1) capturing the shear-exposed VWF A domains to support GPIbα-dependent platelet adhesion; 2) enhancing VWF-dependent platelet adhesion to subendothelial collagens; and 3) promoting platelet-rich aggregate formation (Figure 26).

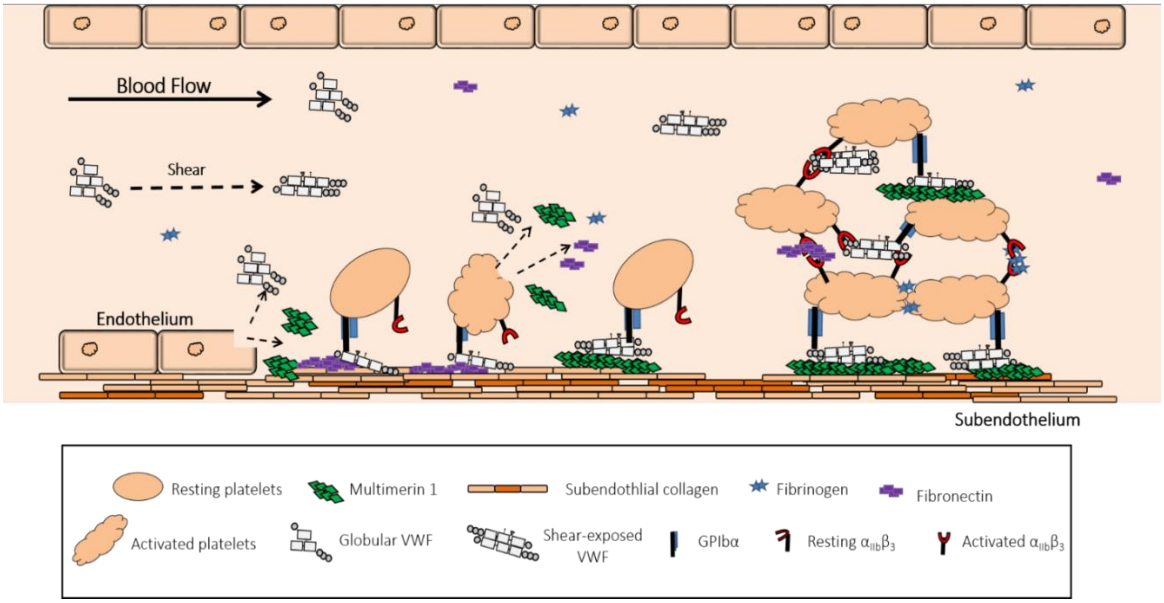

Figure 26: Schematic of MMRN1 supporting VWF-dependent platelet adhesive functions at arterial shear rates. Released MMRN1 binds to subendothelial collagen and supports the binding of shear exposed VWF A1A2A3 domains. VWF captured on MMRN1 matrices supports GPIbα-dependent platelet adhesion, that is important for the initial localization of platelets to the exposed subendothelium under arterial flow conditions. Platelets localized to the subendothelium are activated and release more MMRN1 that supports platelet recruitment to the injury site, as well as platelet-rich thrombogenesis.

4.3 CONCLUSION AND FUTURE DIRECTIONS

In this thesis I provide complementary evidence demonstrating that multimerin 1 supports platelet adhesive functions at arterial shear rates *in vitro* and *in vivo*, likely through its interactions with VWF (571). The results described in this thesis provide clear evidence that MMRN1 interacts with shear exposed VWF, and that the entire shear sensitive A1A2A3 tri-domains in VWF are crucial for MMRN1 binding (571). VWF A1A2A3 tri-domain, like WT-full, also supports GPIbα-dependent, but β_3 integrin-independent platelet adhesion to MMRN1 matrices at an arterial shear rate (571). Collectively, these findings demonstrate that the A1A2A3 of VWF is the minimum region required to support platelet adhesion to MMRN1 under physiological conditions typical of arteries.

Human and murine multimerin 1 are conserved (37, 508) and have platelet adhesive functions that are emerging to be similar, as evident from previous studies with Mmrn1/Snca double deficient mice (37) and studies in this these with *Mmrn1*$^{-/-}$ mice. Deficiencies in Mmrn1 significantly impaired platelet adhesive processes, including VWF-dependent platelet adhesion, aggregation, and thrombogenesis at arterial shear rates *in vitro* and *in vivo.* Mmrn1 loss also reduced collagen-induced platelet aggregation of washed platelets *in vitro* and the adhesion of platelets (in whole blood) to collagen. Even partial loss of Mmrn1, as observed in *Mmrn1*$^{+/-}$ mice, resulted in haploinsufficiency that abrogated platelet adhesive processes *in vitro* and *in vivo.* These studies, taken together, address the functional importance of multimerin 1 as a unique, haemostatic adhesive protein that

significantly contributes to normal platelet-rich thrombogenesis at arterial flow rates. This information importantly contributes to the understanding of platelet adhesive, haemostatic functions at arterial shear rates, and the roles of the vascular protein, multimerin 1, to support these processes. This knowledge may also further our understanding of the pathology of platelet-rich arterial thrombosis in coronary artery disease and thrombotic strokes.

During these studies, new questions arose that require additional studies to further explore the molecular mechanisms underlying the contributions of MMRN1 to normal platelet adhesion and thrombogenesis. The following section summarizes some approaches for future studies that will address these new questions.

4.3.1 Mapping MMRN1 binding to VWF A1 and A3 domains

The adjacent right-hand face of VWF A1 domain is the main ligand binding site for several modulators of VWF-GPIbα binding (90, 91, 96, 585), including bitiscetin (579), and is also implicated in binding to types I and III collagens after exposure of cryptic sites (423). Similarly, MMRN1 likely directly interacts with the right-hand face of the A1 domain of VWF, and may also interact with additional sites in the neighbouring front and upper faces of VWF A1 domain due to the large size of MMRN1 subunits (33, 507, 508, 510). This would be like the larger binding site of MMRN1 for the C1 and C2 domains in FV/Va (513, 526). It is not anticipated that MMRN1 directly overlaps with ristocetin

binding to the upper face of VWF A1 domain (96), as ristocetin is needed to enhance MMRN1-VWF binding (571). The left-hand and back face of the A1 domain of VWF are not implicated in ligand binding, nor is the bottom face of VWF A1 domain (96), suggesting that these regions may not directly support MMRN1 binding. In the A3 domain of VWF, MMRN1 likely binds to the conserved ligand binding region in the bottom and front surfaces, which are also implicated in supporting binding to types I and III collagens (425-427).

Further insights on the mechanism of MMRN1-VWF binding could come from mapping the residues in the A1 and A3 domains of VWF that support MMRN1 binding using a panel of scanning mutagenesis protein mutants (Table 6). I anticipate that such experiments might confirm my hypothesis that MMRN1 interacts with the right-hand surface of VWF A1 domain (residues of pre-pro-VWF: 1358 – 1431 (96)), as well as the two lower anterior surfaces of VWF A3 domain (residues of pre-pro-VWF: 1725 – 1790 (426, 427)). Scanning mutagenesis of these regions does not disrupt the global structure of VWF (90, 91, 426, 427), and has proven useful in mapping the sites for type IV collagen binding to the A1 domain of VWF (90) and for types I and III collagen binding to the A3 domain of VWF (426, 427). There are also naturally occurring type 2M VWD mutations localized to the right-hand surface of the A1 domain of VWF and the lower anterior surface of the A3 domain of VWF, which impair VWF-collagen binding and indirectly impair VWF binding to GPIbα (summarized in Table 6). It would be interesting to see if these mutants have defective VWF-MMRN1 binding. Such experiments would help to further

define the molecular contributions of MMRN1 to support the normal haemostatic, adhesive functions of VWF.

Table 6: Common naturally occurring type 2M VWD mutations in VWF A1 and A3 domains for defining the MMRN1 binding site in VWF.

	Type 2M VWD mutants**	Functional defect	Citation(s)
VWF A1 domain	S1358N (type 2M VWD)	Reduced binding to type IV collagen	(90)
	F1369I (type 2M VWD)	Reduced binding to GPIbα; Normal binding to collagen	(97)
	S1387I (type 2M VWD)	Reduced binding to types I, III and VI collagens	(91, 450)
	R1399H (type 1 VWD)	No detectable binding to types IV and VI collagens	(90, 91)
	Q1402P (type 2M VWD)	No detectable binding to type IV collagen; Reduced binding to type VI collagens	(90, 91)
	I1416N/T (type 2M VWD)	Reduced binding to GPIbα at $\geq 600\ s^{-1}$; Normal binding to GPIbα and type I and III collagen under static conditions	(278)
	I1425F	Reduced binding to GPIbα; Normal binding to collagen	(601)
	I1425F and R1399H (type 2M VWD)	Reduced binding to GPIbα and type IV collagen	(90, 601)
	Δ1392-1402 (type 2M)	No detectable binding to types IV and VI collagens; Defective binding to platelets	(90, 91, 277)
VWF A3 domain	L1696R* (type 2M)	No detectable binding to types I and III collagens; Reduced binding to GPIbα and $\alpha_{IIb}\beta_3$	(452)
	S1731T (type 2M)	Impaired binding to types I collagen	(504, 602)
	W1745C (type 2M)	No detectable binding to types I and III collagens	(602)
	S1783A (type 2M)	No detectable binding to types I and III collagens	(602)
	H1786D (type 2M)	No detectable binding to types I and III collagens	(423, 504, 602)
	P1824H* (type 2M)	No detectable binding to types I and III collagens; Reduced binding to GPIbα and $\alpha_{IIb}\beta_3$	(452, 603)

*Located outside the collagen-binding surfaces of VWF A3 domain.
** VWF numbering with 1, the start of prepro-VWF and residue 2714 the C-terminal end.

4.3.2 Contributions of Mmrn1 to platelet aggregation at arterial shear rates

MMRN1 may be an important mediator of the platelet adhesive functions of VWF under high shear and future studies could evaluate the contributions of MMRN1 to shear-induced platelet aggregation (SIPA), using a cone-and-plate viscometer. SIPA is dependent on plasma VWF (31, 233, 285), GPIbα (31, 233, 285, 506) and $\alpha_{IIb}\beta_3$ (233, 285, 506), but not FG (233). SIPA may also involve platelet activation at > 75 dynes/cm^2 threshold shear stress (31, 233). Platelet activation is necessary to release α-granule proteins, like MMRN1 that could contribute to this SIPA. Pathologically high flow conditions (> 10, 000 s^{-1}, 400 dyn/cm^2) do not significantly activate platelets (25, 27), and would likely underestimate the contributions of platelet proteins (like MMRN1) to platelet adhesive processes under conditions reported in severely stenotic arteries (27, 604, 605).

Alternative to SIPA, the snake venom protein botrocetin induces the aggregation of washed platelet by a biphasic mechanism that first depends on VWF-GPIbα agglutination, then VWF-$\alpha_{IIb}\beta_3$ aggregation (192, 606). VWF-GPIbα binding stimulated by botrocetin activates platelets, resulting in the granule secretion of intracellular stores (192, 606), and may similarly release intracellular MMRN1 from platelet α-granules. However, it is important to note that botrocetin promotes VWF-GPIbα binding by a mechanism that is distinct from ristocetin- and shear-induced platelet adhesion to VWF (146, 192, 457, 607), and ristocetin and shear are needed to promote VWF-MMRN1 binding (571). Ristocetin mimics the effects of shear on VWF-dependent platelet aggregation (141, 459, 608) and

mainly induces VWF-GPIbα-dependent agglutination (162). Ristocetin-induced platelet agglutination results in limited activation of washed platelets and may not significantly promote secretion of granule proteins (162, 466), like MMRN1. Limited release of platelet MMRN1 would underestimate its contributes to VWF-dependent platelet aggregation, under these conditions.

4.3.3 Contributions of Mmrn1 to platelet adhesion on collagen at arterial shear rates

It is still unclear how MMRN1 augments platelet adhesion to collagen under high shear (38), and additional studies are required to assess theses molecular mechanism. High shear perfusion studies could directly assess if impaired MMRN1-VWF binding abrogates platelet adhesion to collagen. These studies could include the use of VWF site-directed mutagenesis protein mutants (detailed in Section 4.3.1 Mapping MMRN1 binding to VWF A1 and A3 domains) that reduce VWF-MMRN1 binding, without modulating VWF interactions with collagen and GPIbα. However, the MMRN1 binding site in VWF may functionally overlap with the collagen binding site in VWF A3 domain, which may make it problematic to significantly reduce VWF binding to MMRN1 without also impairing VWF binding to collagen. This would be like the overlapped binding of MMRN1 and PS to the C1 and C2 domains of FV/Va (513, 526). Alternatively, MMRN1 protein mutations could prove useful, providing that collagen and VWF bind to distinct sites in MMRN1. Functional inhibitory antibodies against GPIbα would not be useful in these studies, as the

loss and functional block of GPIbα had deleterious effects on platelet adhesion and platelet-rich thrombogenesis at arterial shear rates (100, 139).

4.3.5 Studies of haploinsuffuciency in *Mmrn1*$^{+/-}$ mice

Mmrn1$^{+/-}$ mice could have abnormal phenotypes due to haploinsufficiency caused by a reduction in the amount of Mmrn1 protein biologically available to modulate platelet functions; similar mechanisms are reported for mice haploinsufficient in VWF and pFN (that is important for normal haemostasis) (341, 409). This assumption is supported by the reduced detection of Mmrn1 in platelet lysate samples from *Mmrn1*$^{+/-}$ mice, but needs to be confirmed by quantifying ELISA.

Mmrn1$^{-/-}$ and *Mmrn1*$^{+/-}$ mice possess severely truncated *Mmrn1* gene product(s) that includes the first two exons, which if translated produces a functionally null, aberrant protein that is ~20 % of preproMmrn1. Polymers in *Mmrn1*$^{+/-}$ mice with WT-Mmrn1 and this truncated, aberrant protein could antagonize the functionality of Mmrn1 multimers in a dominant-negative manner (600); thereby explain the abnormal phenotype of *Mmrn1*$^{+/-}$ mice. To test this hypothesis, studies will need to assess the presence of a truncated N-terminal Mmrn1 protein in platelet lysate samples of *Mmrn1*$^{-/-}$ and *Mmrn1*$^{+/-}$ mice. Multimers with the truncated N-terminal Mmrn1 subunit would have modified polymerization patterns, relative to WT mice, much like the defects in VWF that abrogate multimerization (420, 421). If there is a difference in the multimerization between WT and

Mmrn1$^{-/-}$ mice, then additional studies may also co-transfect specific cell lines with the WT and this severely truncated Mmrn1 protein and assess: 1) Mmrn1 multimerization patterns (to confirm observations in *Mmrn1*$^{+/-}$ mice); 2) intracellular storage/retention; 3) secretion of Mmrn1; and 4) functionality of Mmrn1 polymers (via protein binding and platelet adhesion assays (38, 571)). These studies would use cell lines like HEK293 cells that are shown to produce and store MMRN1 like platelets, and generate functional active recombinant MMRN1 (37, 38, 304, 312, 513, 514). These studies would collectively assess the various mechanisms that could describe the abnormal phenotype in *Mmrn1*$^{+/-}$ mice.

4.3.6 Other animal and injury models

There are two commonly used models that use intravital microscopy to study arterial thrombosis: laser-induced injury to cremaster arterioles; and ferric chloride-induced injury to mesenteric arterioles. These injury models cause *in vivo* arterial thrombosis that are initiated by distinct processes, with varied dependency on endothelial dysfunction (69-74, 82, 83, 609, 610). In this thesis, I analyzed ferric chloride induced arterial thrombosis, which involves the adhesive functions of platelets, plasma and platelet proteins, as well as RBCs (69-71, 82, 83). In this injury model, thrombosis is dependent on platelet receptors and involves adhesive proteins that support platelet-rich occlusive thrombus formation to the luminal side of the injured vessel (72, 74, 84, 85, 105, 133, 144, 145, 610-614), regardless of the absence or extent of vascular endothelium dysfunction (74). The laser injury model does not result in complete occlusion of the injured vessel, but leads to the

development of multiple independent thrombi (105, 613-615). Additionally, laser injury is primarily mediated by thrombin generation (TF–mediated pathway; (74, 85, 613)), and involves (depending on the depth of the vascular injury (105, 613-615)) haemostatic adhesive proteins or platelet receptors that interact on the luminal side of the injured vessel (74, 85, 105, 613). MMRN1 delays FV activation (513, 514), especially at thrombin levels observed during the initiation stages of TF-mediated coagulation (514), and inhibits plasma and platelet-FVa dependent thrombin generation *in vitro* (514). As a result, the loss of Mmrn1, in mice, may modulate laser-induced injury response, *in vivo*, which may demonstrate that MMRN1 modulates thrombin generation after its release from activated platelets.

There are other vascular injury models that try to recapitulate human vascular trauma or disease, such as arterial and venous thrombosis in response to: inflammation (e.g. laser injury (74, 84, 85, 105, 610, 612-614)); atherosclerotic plaque rupture (e.g. photochemical injury; (611, 614, 616-619)); or physical injury (e.g. mechanical injury (609, 620-626)). The injury models provide insight into various aspects of haemostasis, such as mechanical injury that provides detailed information on vascular remodeling, including neointimal hyperplasia (620, 621, 623-626). Each model has its advantages and disadvantages, such as mechanical injury typically provides less information on the various stages of thrombogenesis because of the limited analysis of the haemostatic adhesive functions of platelets (620, 621, 623-626). Some injury models cannot employ the use of fluorophores because the primary endpoint is death by systematic thrombosis (as is the case

with intravenous bolus injection of epinephrine and collagen (589, 627)), which makes it difficult to determine the precise location of developing intravascular thrombi. This inability to monitor *in vivo* platelet function limits the real-time visualization and simultaneous monitoring of the dynamics of thrombogenesis and describe the complexities of the hemostatic system. Using complementary injury models (e.g. models that denude the vascular endothelium, like ferric chloride and Rose Bengal), will provide critical *in vivo* evidence of the contributions of vascular proteins, like MMRN1, to haemostasis and the pathological mechanisms of thrombosis.

The expression of MMRN1 is restricted to megakaryocytes and the vasculature (33, 35, 509-512), and mice with selective loss of Mmrn1 likely have deficiencies of Mmrn1 in both platelets and the endothelium. Therefore, it is unclear whether platelet or EC-derived Mmrn1 differentially contribute to haemostasis. Future studies could assess platelet and endothelial Mmrn1 functions, using tissue-specific knockouts, to characterize the functional importance of either form of MMRN1. This has been described for several other animal models (49, 218, 308, 309, 340, 341, 628).

REFERENCE

1. Monagle P, Massicotte P. Developmental haemostasis: secondary haemostasis. Semin Fetal Neonatal Med 2011; 16(6): 294-300.
2. Berndt MC, Metharom P, Andrews RK. Primary haemostasis: newer insights. Haemophilia 2014; 20 Suppl 4: 15-22.
3. Aird WC. Endothelium and haemostasis. Hamostaseologie 2015; 35(1): 11-6.
4. Chapin JC, Hajjar KA. Fibrinolysis and the control of blood coagulation. Blood Rev 2015; 29(1): 17-24.
5. Cimmino G, Golino P. Platelet biology and receptor pathways. J Cardiovasc Transl Res 2013; 6(3): 299-309.
6. Kauskot A, Hoylaerts MF. Platelet receptors. Handb Exp Pharmacol 2012(210): 23-57.
7. Mannucci PM, Duga S, Peyvandi F. Recessively inherited coagulation disorders. Blood 2004; 104(5): 1243-52.
8. Sadler JE, Budde U, Eikenboom JC, et al. Update on the pathophysiology and classification of von Willebrand disease: a report of the Subcommittee on von Willebrand Factor. J Thromb Haemost 2006; 4(10): 2103-14.
9. Kahr WH, Lo RW, Li L, et al. Abnormal megakaryocyte development and platelet function in Nbeal2(-/-) mice. Blood 2013; 122(19): 3349-58.
10. Goodeve AC, Perry DJ, Cumming T, et al. Genetics of haemostasis. Haemophilia 2012; 18 Suppl 4: 73-80.
11. Nair S, Ghosh K, Kulkarni B, et al. Glanzmann's thrombasthenia: updated. Platelets 2002; 13(7): 387-93.
12. Andrews RK, Berndt MC. Bernard-Soulier syndrome: an update. Semin Thromb Hemost 2013; 39(6): 656-62.
13. Casini A, Neerman-Arbez M, Ariëns RA, et al. Dysfibrinogenemia: from molecular anomalies to clinical manifestations and management. J Thromb Haemost 2015; 13(6): 909-19.
14. Franchini M, Lippi G. Von Willebrand factor and thrombosis. Ann Hematol 2006; 85(7): 415-23.
15. Zheng XL. ADAMTS13 and von Willebrand factor in thrombotic thrombocytopenic purpura. Annu Rev Med 2015; 66: 211-25.
16. Marchi R, Walton BL, McGary CS, et al. Dysregulated coagulation associated with hypofibrinogenaemia and plasma hypercoagulability: implications for identifying coagulopathic mechanisms in humans. Thromb Haemost 2012; 108(3): 516-26.
17. Stakos DA, Tziakas DN, Stellos K. Mechanisms of platelet activation in acute coronary syndromes. Curr Vasc Pharmacol 2012; 10(5): 578-88.
18. Shah PK. Mechanisms of plaque vulnerability and rupture. J Am Coll Cardiol 2003; 41(4 Suppl S): 15S-22S.
19. Langer HF, Gawaz M. Platelet-vessel wall interactions in atherosclerotic disease. Thromb Haemost 2008; 99(3): 480-6.

20. Schulz C, Massberg S. Platelets in atherosclerosis and thrombosis. Handb Exp Pharmacol 2012(210): 111-33.
21. Gaziano TA, Bitton A, Anand S, et al. Growing epidemic of coronary heart disease in low- and middle-income countries. Curr Probl Cardiol 2010; 35(2): 72-115.
22. Mozaffarian D, Benjamin EJ, Go AS, et al. Executive Summary: Heart Disease and Stroke Statistics--2016 Update: A Report From the American Heart Association. Circulation 2016; 133(4): 447-54.
23. Dai X, Wiernek S, Evans JP, et al. Genetics of coronary artery disease and myocardial infarction. World J Cardiol 2016; 8(1): 1-23.
24. Springer TA. von Willebrand factor, Jedi knight of the bloodstream. Blood 2014.
25. Maxwell MJ, Westein E, Nesbitt WS, et al. Identification of a 2-stage platelet aggregation process mediating shear-dependent thrombus formation. Blood 2007; 109(2): 566-76.
26. Tran R, Myers DR, Ciciliano J, et al. Biomechanics of haemostasis and thrombosis in health and disease: from the macro- to molecular scale. J Cell Mol Med 2013; 17(5): 579-96.
27. Ruggeri ZM, Orje JN, Habermann R, et al. Activation-independent platelet adhesion and aggregation under elevated shear stress. Blood 2006; 108(6): 1903-10.
28. Miyata S, Goto S, Federici AB, et al. Conformational changes in the A1 domain of von Willebrand factor modulating the interaction with platelet glycoprotein Ibalpha. JBiolChem 1996; 271(15): 9046-53.
29. Miyata S, Ruggeri ZM. Distinct structural attributes regulating von Willebrand factor A1 domain interaction with platelet glycoprotein Ibalpha under flow. JBiolChem 1999; 274(10): 6586-93.
30. Savage B, Sixma JJ, Ruggeri ZM. Functional self-association of von Willebrand factor during platelet adhesion under flow. ProcNatlAcadSciUSA 2002; 99(1): 425-30.
31. Shankaran H, Alexandridis P, Neelamegham S. Aspects of hydrodynamic shear regulating shear-induced platelet activation and self-association of von Willebrand factor in suspension. Blood 2003; 101(7): 2637-45.
32. Colace TV, Diamond SL. Direct observation of von Willebrand factor elongation and fiber formation on collagen during acute whole blood exposure to pathological flow. Arterioscler Thromb Vasc Biol 2013; 33(1): 105-13.
33. Hayward CP, Smith JW, Horsewood P, et al. p-155, a multimeric platelet protein that is expressed on activated platelets. JBiolChem 1991; 266(11): 7114-20.
34. Hayward CP, Furmaniak-Kazmierczak E, Cieutat AM, et al. Factor V is complexed with multimerin in resting platelet lysates and colocalizes with multimerin in platelet alpha-granules. J Biol Chem 1995; 270(33): 19217-24.
35. Hayward CP, Cramer EM, Song Z, et al. Studies of multimerin in human endothelial cells. Blood 1998; 91(4): 1304-17.
36. Veljkovic DK, Cramer EM, Alimardani G, et al. Studies of alpha-granule proteins in cultured human megakaryocytes. Thromb Haemost 2003; 90(5): 844-52.
37. Tasneem S, Reheman A, Ni H, et al. Mice with deleted multimerin 1 and alpha-synuclein genes have impaired platelet adhesion and impaired thrombus formation that is corrected by multimerin 1. ThrombRes 2010; 125(5): e177-e83.

38. Tasneem S, Adam F, Minullina I, et al. Platelet adhesion to multimerin 1 in vitro: influences of platelet membrane receptors, von Willebrand factor and shear. JThrombHaemost 2009; 7(4): 685-92.
39. Machlus KR, Italiano JE. The incredible journey: From megakaryocyte development to platelet formation. J Cell Biol 2013; 201(6): 785-96.
40. Harker LA, Finch CA. Thrombokinetics in man. J Clin Invest 1969; 48(6): 963-74.
41. Bryckaert M, Rosa JP, Denis CV, et al. Of von Willebrand factor and platelets. Cell Mol Life Sci 2015; 72(2): 307-26.
42. Palta S, Saroa R, Palta A. Overview of the coagulation system. Indian J Anaesth 2014; 58(5): 515-23.
43. Wolberg AS. Thrombin generation and fibrin clot structure. Blood Rev 2007; 21(3): 131-42.
44. Pisano JJ, Finlayson JS, Peyton MP. [Cross-link in fibrin polymerized by factor 13: epsilon-(gamma-glutamyl)lysine]. Science 1968; 160(3830): 892-3.
45. Ryan EA, Mockros LF, Weisel JW, et al. Structural origins of fibrin clot rheology. Biophys J 1999; 77(5): 2813-26.
46. Mosesson MW. Fibrinogen and fibrin structure and functions. J Thromb Haemost 2005; 3(8): 1894-904.
47. Undas A, Ariëns RA. Fibrin clot structure and function: a role in the pathophysiology of arterial and venous thromboembolic diseases. Arterioscler Thromb Vasc Biol 2011; 31(12): e88-99.
48. Cesarman-Maus G, Hajjar KA. Molecular mechanisms of fibrinolysis. Br J Haematol 2005; 129(3): 307-21.
49. Wang Y, Reheman A, Spring CM, et al. Plasma fibronectin supports hemostasis and regulates thrombosis. J Clin Invest 2014; 124(10): 4281-93.
50. Hou Y, Carrim N, Wang Y, et al. Platelets in hemostasis and thrombosis: Novel mechanisms of fibrinogen-independent platelet aggregation and fibronectin-mediated protein wave of hemostasis. J Biomed Res 2015; 29.
51. Wang Y, Carrim N, Ni H. Fibronectin orchestrates thrombosis and hemostasis. Oncotarget 2015; 6(23): 19350-1.
52. Zwaginga JJ, Nash G, King MR, et al. Flow-based assays for global assessment of hemostasis. Part 1: Biorheologic considerations. J Thromb Haemost 2006; 4(11): 2486-7.
53. Ruggeri ZM. Platelet adhesion under flow. Microcirculation 2009; 16(1): 58-83.
54. Szymczak P, Cieplak M. Proteins in a shear flow. J Chem Phys 2007; 127(15): 155106.
55. Nesbitt WS, Westein E, Tovar-Lopez FJ, et al. A shear gradient-dependent platelet aggregation mechanism drives thrombus formation. Nat Med 2009; 15(6): 665-73.
56. Jackson SP. The growing complexity of platelet aggregation. Blood 2007; 109(12): 5087-95.
57. Turitto VT, Baumgartner HR. Platelet interaction with subendothelium in a perfusion system: physical role of red blood cells. Microvasc Res 1975; 9(3): 335-44.
58. Wolberg AS, Aleman MM, Leiderman K, et al. Procoagulant activity in hemostasis and thrombosis: Virchow's triad revisited. Anesth Analg 2012; 114(2): 275-85.

59. Papaioannou TG, Stefanadis C. Vascular wall shear stress: basic principles and methods. Hellenic J Cardiol 2005; 46(1): 9-15.
60. Sakariassen KS, Orning L, Turitto VT. The impact of blood shear rate on arterial thrombus formation. Future Sci OA 2015; 1(4): FSO30.
61. Tangelder GJ, Slaaf DW, Arts T, et al. Wall shear rate in arterioles in vivo: least estimates from platelet velocity profiles. Am J Physiol 1988; 254(6 Pt 2): H1059-64.
62. Thomas MR, Storey RF. The role of platelets in inflammation. Thromb Haemost 2015; 114(3): 449-58.
63. Totani L, Evangelista V. Platelet-leukocyte interactions in cardiovascular disease and beyond. Arterioscler Thromb Vasc Biol 2010; 30(12): 2357-61.
64. McNicol A, Agpalza A, Jackson EC, et al. Streptococcus sanguinis-induced cytokine release from platelets. J Thromb Haemost 2011; 9(10): 2038-49.
65. Stenberg PE, McEver RP, Shuman MA, et al. A platelet alpha-granule membrane protein (GMP-140) is expressed on the plasma membrane after activation. J Cell Biol 1985; 101(3): 880-6.
66. Deuel TF, Senior RM, Chang D, et al. Platelet factor 4 is chemotactic for neutrophils and monocytes. Proc Natl Acad Sci U S A 1981; 78(7): 4584-7.
67. Petersen F, Bock L, Flad HD, et al. A chondroitin sulfate proteoglycan on human neutrophils specifically binds platelet factor 4 and is involved in cell activation. J Immunol 1998; 161(8): 4347-55.
68. Spertini O, Cordey AS, Monai N, et al. P-selectin glycoprotein ligand 1 is a ligand for L-selectin on neutrophils, monocytes, and CD34+ hematopoietic progenitor cells. J Cell Biol 1996; 135(2): 523-31.
69. Eckly A, Hechler B, Freund M, et al. Mechanisms underlying FeCl3-induced arterial thrombosis. JThrombHaemost 2011; 9(4): 779-89.
70. Tseng MT, Dozier A, Haribabu B, et al. Transendothelial migration of ferric ion in FeCl3 injured murine common carotid artery. Thromb Res 2006; 118(2): 275-80.
71. Woollard KJ, Sturgeon S, Chin-Dusting JP, et al. Erythrocyte hemolysis and hemoglobin oxidation promote ferric chloride-induced vascular injury. J Biol Chem 2009; 284(19): 13110-8.
72. Ni H, Denis CV, Subbarao S, et al. Persistence of platelet thrombus formation in arterioles of mice lacking both von Willebrand factor and fibrinogen. J Clin Invest 2000; 106(3): 385-92.
73. Li W, McIntyre TM, Silverstein RL. Ferric chloride-induced murine carotid arterial injury: A model of redox pathology. Redox Biol 2013; 1: 50-5.
74. Dubois C, Panicot-Dubois L, Merrill-Skoloff G, et al. Glycoprotein VI-dependent and -independent pathways of thrombus formation in vivo. Blood 2006; 107(10): 3902-6.
75. Beumer S, Heijnen HF, IJsseldijk MJ, et al. Platelet adhesion to fibronectin in flow: the importance of von Willebrand factor and glycoprotein Ib. Blood 1995; 86(9): 3452-60.
76. Nievelstein PF, D'Alessio PA, Sixma JJ. Fibronectin in platelet adhesion to human collagen types I and III. Use of nonfibrillar and fibrillar collagen in flowing blood studies. Arteriosclerosis 1988; 8(2): 200-6.

77. Bastida E, Escolar G, Ordinas A, et al. Fibronectin is required for platelet adhesion and for thrombus formation on subendothelium and collagen surfaces. Blood 1987; 70(5): 1437-42.
78. Houdijk WP, Sakariassen KS, Nievelstein PF, et al. Role of factor VIII-von Willebrand factor and fibronectin in the interaction of platelets in flowing blood with monomeric and fibrillar human collagen types I and III. J Clin Invest 1985; 75(2): 531-40.
79. Cho J, Mosher DF. Enhancement of thrombogenesis by plasma fibronectin cross-linked to fibrin and assembled in platelet thrombi. Blood 2006; 107(9): 3555-63.
80. Cho J, Mosher DF. Characterization of fibronectin assembly by platelets adherent to adsorbed laminin-111. J Thromb Haemost 2006; 4(5): 943-51.
81. Beumer S, Heijnen-Snyder GJ, IJsseldijk MJ, et al. Fibronectin in an extracellular matrix of cultured endothelial cells supports platelet adhesion via its ninth type III repeat : A comparison with platelet adhesion to isolated fibronectin. Arterioscler Thromb Vasc Biol 2000; 20(4): E16-25.
82. Ciciliano JC, Sakurai Y, Myers DR, et al. Resolving the multifaceted mechanisms of the ferric chloride thrombosis model using an interdisciplinary microfluidic approach. Blood 2015.
83. Barr JD, Chauhan AK, Schaeffer GV, et al. Red blood cells mediate the onset of thrombosis in the ferric chloride murine model. Blood 2013; 121(18): 3733-41.
84. Furie B, Furie BC. Thrombus formation in vivo. J Clin Invest 2005; 115(12): 3355-62.
85. Falati S, Gross P, Merrill-Skoloff G, et al. Real-time in vivo imaging of platelets, tissue factor and fibrin during arterial thrombus formation in the mouse. Nat Med 2002; 8(10): 1175-81.
86. Polanowska-Grabowska R, Simon CG, Gear AR. Platelet adhesion to collagen type I, collagen type IV, von Willebrand factor, fibronectin, laminin and fibrinogen: rapid kinetics under shear. Thromb Haemost 1999; 81(1): 118-23.
87. Sakariassen KS, Bolhuis PA, Sixma JJ. Human blood platelet adhesion to artery subendothelium is mediated by factor VIII-Von Willebrand factor bound to the subendothelium. Nature 1979; 279(5714): 636-8.
88. Inoue O, Suzuki-Inoue K, Ozaki Y. Redundant mechanism of platelet adhesion to laminin and collagen under flow: involvement of von Willebrand factor and glycoprotein Ib-IX-V. J Biol Chem 2008; 283(24): 16279-82.
89. Sporn LA, Marder VJ, Wagner DD. von Willebrand factor released from Weibel-Palade bodies binds more avidly to extracellular matrix than that secreted constitutively. Blood 1987; 69(5): 1531-4.
90. Flood VH, Schlauderaff AC, Haberichter SL, et al. Crucial role for the VWF A1 domain in binding to type IV collagen. Blood 2015; 125(14): 2297-304.
91. Flood VH, Gill JC, Christopherson PA, et al. Critical von Willebrand factor A1 domain residues influence type VI collagen binding. J Thromb Haemost 2012; 10(7): 1417-24.
92. Lankhof H, van Hoeij M, Schiphorst ME, et al. A3 domain is essential for interaction of von Willebrand factor with collagen type III. Thromb Haemost 1996; 75(6): 950-8.

93. Zangari M, Kaplan KL, Glanville RW, et al. Reduced thrombogenicity of type VI collagen as compared to type I collagen. Thromb Res 1995; 79(5-6): 429-36.
94. Sixma JJ, Schiphorst ME, Verweij CL, et al. Effect of deletion of the A1 domain of von Willebrand factor on its binding to heparin, collagen and platelets in the presence of ristocetin. Eur J Biochem 1991; 196(2): 369-75.
95. Saboor M, Ayub Q, Ilyas S, et al. Platelet receptors; an instrumental of platelet physiology. Pak J Med Sci 2013; 29(3): 891-6.
96. Emsley J, Cruz M, Handin R, et al. Crystal structure of the von Willebrand Factor A1 domain and implications for the binding of platelet glycoprotein Ib. JBiolChem 1998; 273(17): 10396-401.
97. Cruz MA, Diacovo TG, Emsley J, et al. Mapping the glycoprotein Ib-binding site in the von willebrand factor A1 domain. JBiolChem 2000; 275(25): 19098-105.
98. Savage B, Saldivar E, Ruggeri ZM. Initiation of platelet adhesion by arrest onto fibrinogen or translocation on von Willebrand factor. Cell 1996; 84(2): 289-97.
99. Wu YP, Vink T, Schiphorst M, et al. Platelet thrombus formation on collagen at high shear rates is mediated by von Willebrand factor-glycoprotein Ib interaction and inhibited by von Willebrand factor-glycoprotein IIb/IIIa interaction. Arterioscler Thromb Vasc Biol 2000; 20(6): 1661-7.
100. Savage B, Almus-Jacobs F, Ruggeri ZM. Specific synergy of multiple substrate-receptor interactions in platelet thrombus formation under flow. Cell 1998; 94(5): 657-66.
101. Tousoulis D, Kampoli AM, Tentolouris C, et al. The role of nitric oxide on endothelial function. Curr Vasc Pharmacol 2012; 10(1): 4-18.
102. Yau JW, Teoh H, Verma S. Endothelial cell control of thrombosis. BMC Cardiovasc Disord 2015; 15: 130.
103. Voss B, Rauterberg J. Localization of collagen types I, III, IV and V, fibronectin and laminin in human arteries by the indirect immunofluorescence method. Pathol Res Pract 1986; 181(5): 568-75.
104. Murata K, Motayama T, Kotake C. Collagen types in various layers of the human aorta and their changes with the atherosclerotic process. Atherosclerosis 1986; 60(3): 251-62.
105. Hechler B, Nonne C, Eckly A, et al. Arterial thrombosis: relevance of a model with two levels of severity assessed by histologic, ultrastructural and functional characterization. JThrombHaemost 2010; 8(1): 173-84.
106. Li Z, Delaney MK, O'Brien KA, et al. Signaling during platelet adhesion and activation. Arterioscler Thromb Vasc Biol 2010; 30(12): 2341-9.
107. Suzuki-Inoue K, Wilde JI, Andrews RK, et al. Glycoproteins VI and Ib-IX-V stimulate tyrosine phosphorylation of tyrosine kinase Syk and phospholipase Cgamma2 at distinct sites. Biochem J 2004; 378(Pt 3): 1023-9.
108. Romo GM, Dong JF, Schade AJ, et al. The glycoprotein Ib-IX-V complex is a platelet counterreceptor for P-selectin. J Exp Med 1999; 190(6): 803-14.
109. Jurk K, Clemetson KJ, de Groot PG, et al. Thrombospondin-1 mediates platelet adhesion at high shear via glycoprotein Ib (GPIb): an alternative/backup mechanism to von Willebrand factor. FASEB J 2003; 17(11): 1490-2.

110. Ruggeri ZM, De Marco L, Gatti L, et al. Platelets have more than one binding site for von Willebrand factor. J Clin Invest 1983; 72(1): 1-12.
111. Lankhof H, Wu YP, Vink T, et al. Role of the glycoprotein Ib-binding A1 repeat and the RGD sequence in platelet adhesion to human recombinant von Willebrand factor. Blood 1995; 86(3): 1035-42.
112. Yamamoto N, Greco NJ, Barnard MR, et al. Glycoprotein Ib (GPIb)-dependent and GPIb-independent pathways of thrombin-induced platelet activation. Blood 1991; 77(8): 1740-8.
113. Jandrot-Perrus M, Clemetson KJ, Huisse MG, et al. Thrombin interaction with platelet glycoprotein Ib: effect of glycocalicin on thrombin specificity. Blood 1992; 80(11): 2781-6.
114. Kehrel B, Wierwille S, Clemetson KJ, et al. Glycoprotein VI is a major collagen receptor for platelet activation: it recognizes the platelet-activating quaternary structure of collagen, whereas CD36, glycoprotein IIb/IIIa, and von Willebrand factor do not. Blood 1998; 91(2): 491-9.
115. Nieswandt B, Brakebusch C, Bergmeier W, et al. Glycoprotein VI but not alpha2beta1 integrin is essential for platelet interaction with collagen. EMBO J 2001; 20(9): 2120-30.
116. Inoue O, Suzuki-Inoue K, McCarty OJ, et al. Laminin stimulates spreading of platelets through integrin alpha6beta1-dependent activation of GPVI. Blood 2006; 107(4): 1405-12.
117. Ni H, Freedman J. Platelets in hemostasis and thrombosis: role of integrins and their ligands. Transfus Apher Sci 2003; 28(3): 257-64.
118. Du XP, Plow EF, Frelinger AL, et al. Ligands "activate" integrin alpha IIb beta 3 (platelet GPIIb-IIIa). Cell 1991; 65(3): 409-16.
119. Phillips DR, Charo IF, Scarborough RM. GPIIb-IIIa: the responsive integrin. Cell 1991; 65(3): 359-62.
120. Litvinov RI, Farrell DH, Weisel JW, et al. The Platelet Integrin αIIbβ3 Differentially Interacts with Fibrin Versus Fibrinogen. J Biol Chem 2016; 291(15): 7858-67.
121. Jarvis GE, Atkinson BT, Snell DC, et al. Distinct roles of GPVI and integrin alpha(2)beta(1) in platelet shape change and aggregation induced by different collagens. Br J Pharmacol 2002; 137(1): 107-17.
122. Kuijpers MJ, Schulte V, Bergmeier W, et al. Complementary roles of glycoprotein VI and alpha2beta1 integrin in collagen-induced thrombus formation in flowing whole blood ex vivo. FASEB J 2003; 17(6): 685-7.
123. Weiss HJ, Turitto VT, Baumgartner HR. Effect of shear rate on platelet interaction with subendothelium in citrated and native blood. I. Shear rate--dependent decrease of adhesion in von Willebrand's disease and the Bernard-Soulier syndrome. J Lab Clin Med 1978; 92(5): 750-64.
124. Henrita van Zanten G, Saelman EU, Schut-Hese KM, et al. Platelet adhesion to collagen type IV under flow conditions. Blood 1996; 88(10): 3862-71.

125. Saelman EU, Nieuwenhuis HK, Hese KM, et al. Platelet adhesion to collagen types I through VIII under conditions of stasis and flow is mediated by GPIa/IIa (alpha 2 beta 1-integrin). Blood 1994; 83(5): 1244-50.
126. Hindriks G, Ijsseldijk MJ, Sonnenberg A, et al. Platelet adhesion to laminin: role of Ca2+ and Mg2+ ions, shear rate, and platelet membrane glycoproteins. Blood 1992; 79(4): 928-35.
127. Alshehri OM, Hughes CE, Montague S, et al. Fibrin activates GPVI in human and mouse platelets. Blood 2015; 126(13): 1601-8.
128. Hantgan RR, Hindriks G, Taylor RG, et al. Glycoprotein Ib, von Willebrand factor, and glycoprotein IIb:IIIa are all involved in platelet adhesion to fibrin in flowing whole blood. Blood 1990; 76(2): 345-53.
129. Endenburg SC, Hantgan RR, Lindeboom-Blokzijl L, et al. On the role of von Willebrand factor in promoting platelet adhesion to fibrin in flowing blood. Blood 1995; 86(11): 4158-65.
130. Podolnikova NP, Yakovlev S, Yakubenko VP, et al. The interaction of integrin αIIbβ3 with fibrin occurs through multiple binding sites in the αIIb β-propeller domain. J Biol Chem 2014; 289(4): 2371-83.
131. Cho J, Mosher DF. Impact of fibronectin assembly on platelet thrombus formation in response to type I collagen and von Willebrand factor. Blood 2006; 108(7): 2229-36.
132. Asch E, Podack E. Vitronectin binds to activated human platelets and plays a role in platelet aggregation. J Clin Invest 1990; 85(5): 1372-8.
133. Fay WP, Parker AC, Ansari MN, et al. Vitronectin inhibits the thrombotic response to arterial injury in mice. Blood 1999; 93(6): 1825-30.
134. Reheman A, Gross P, Yang H, et al. Vitronectin stabilizes thrombi and vessel occlusion but plays a dual role in platelet aggregation. J Thromb Haemost 2005; 3(5): 875-83.
135. Xu J, Shi GP. Vascular wall extracellular matrix proteins and vascular diseases. Biochim Biophys Acta 2014; 1842(11): 2106-19.
136. Jones S, Evans RJ, Mahaut-Smith MP. Ca2+ influx through P2X1 receptors amplifies P2Y1 receptor-evoked Ca2+ signaling and ADP-evoked platelet aggregation. Mol Pharmacol 2014; 86(3): 243-51.
137. Jackson SP, Nesbitt WS, Westein E. Dynamics of platelet thrombus formation. J Thromb Haemost 2009; 7 Suppl 1: 17-20.
138. Ware J, Russell S, Ruggeri ZM. Generation and rescue of a murine model of platelet dysfunction: the Bernard-Soulier syndrome. Proc Natl Acad Sci U S A 2000; 97(6): 2803-8.
139. Bergmeier W, Piffath CL, Goerge T, et al. The role of platelet adhesion receptor GPIbalpha far exceeds that of its main ligand, von Willebrand factor, in arterial thrombosis. ProcNatlAcadSciUSA 2006; 103(45): 16900-5.
140. Konstantinides S, Ware J, Marchese P, et al. Distinct antithrombotic consequences of platelet glycoprotein Ibalpha and VI deficiency in a mouse model of arterial thrombosis. J Thromb Haemost 2006; 4(9): 2014-21.

141. Lei X, Reheman A, Hou Y, et al. Anfibatide, a novel GPIb complex antagonist, inhibits platelet adhesion and thrombus formation in vitro and in vivo in murine models of thrombosis. Thromb Haemost 2014; 111(2): 279-89.
142. Savoia A, Kunishima S, De Rocco D, et al. Spectrum of the mutations in Bernard-Soulier syndrome. Hum Mutat 2014; 35(9): 1033-45.
143. Boeckelmann D, Hengartner H, Greinacher A, et al. Patients with Bernard-Soulier syndrome and different severity of the bleeding phenotype. Blood Cells Mol Dis 2017.
144. Denis C, Methia N, Frenette PS, et al. A mouse model of severe von Willebrand disease: defects in hemostasis and thrombosis. Proc Natl Acad Sci U S A 1998; 95(16): 9524-9.
145. Prakash P, Kulkarni PP, Chauhan AK. Thrombospondin 1 requires von Willebrand factor to modulate arterial thrombosis in mice. Blood 2015; 125(2): 399-406.
146. Girma JP, Takahashi Y, Yoshioka A, et al. Ristocetin and botrocetin involve two distinct domains of von Willebrand factor for binding to platelet membrane glycoprotein Ib. Thromb Haemost 1990; 64(2): 326-32.
147. Uff S, Clemetson JM, Harrison T, et al. Crystal structure of the platelet glycoprotein Ib(alpha) N-terminal domain reveals an unmasking mechanism for receptor activation. JBiolChem 2002; 277(38): 35657-63.
148. Kumar RA, Dong JF, Thaggard JA, et al. Kinetics of GPIbalpha-vWF-A1 tether bond under flow: effect of GPIbalpha mutations on the association and dissociation rates. Biophys J 2003; 85(6): 4099-109.
149. Coller BS, Peerschke EI, Scudder LE, et al. Studies with a murine monoclonal antibody that abolishes ristocetin-induced binding of von Willebrand factor to platelets: additional evidence in support of GPIb as a platelet receptor for von Willebrand factor. Blood 1983; 61(1): 99-110.
150. Doggett TA, Girdhar G, Lawshé A, et al. Selectin-like kinetics and biomechanics promote rapid platelet adhesion in flow: the GPIb(alpha)-vWF tether bond. Biophys J 2002; 83(1): 194-205.
151. Matsushita T, Sadler JE. Identification of amino acid residues essential for von Willebrand factor binding to platelet glycoprotein Ib. Charged-to-alanine scanning mutagenesis of the A1 domain of human von Willebrand factor. J Biol Chem 1995; 270(22): 13406-14.
152. Auton M, Sedlák E, Marek J, et al. Changes in thermodynamic stability of von Willebrand factor differentially affect the force-dependent binding to platelet GPIbalpha. Biophys J 2009; 97(2): 618-27.
153. Ju L, Dong JF, Cruz MA, et al. The N-terminal flanking region of the A1 domain regulates the force-dependent binding of von Willebrand factor to platelet glycoprotein Ibα. J Biol Chem 2013; 288(45): 32289-301.
154. Fredrickson BJ, Dong JF, McIntire LV, et al. Shear-dependent rolling on von Willebrand factor of mammalian cells expressing the platelet glycoprotein Ib-IX-V complex. Blood 1998; 92(10): 3684-93.
155. Grüner S, Prostredna M, Aktas B, et al. Anti-glycoprotein VI treatment severely compromises hemostasis in mice with reduced alpha2beta1 levels or concomitant aspirin therapy. Circulation 2004; 110(18): 2946-51.

156. Nieswandt B, Watson SP. Platelet-collagen interaction: is GPVI the central receptor? Blood 2003; 102(2): 449-61.
157. Inoue O, Suzuki-Inoue K, Dean WL, et al. Integrin alpha2beta1 mediates outside-in regulation of platelet spreading on collagen through activation of Src kinases and PLCgamma2. J Cell Biol 2003; 160(5): 769-80.
158. Savage B, Ginsberg MH, Ruggeri ZM. Influence of fibrillar collagen structure on the mechanisms of platelet thrombus formation under flow. Blood 1999; 94(8): 2704-15.
159. Nieswandt B, Schulte V, Bergmeier W, et al. Long-term antithrombotic protection by in vivo depletion of platelet glycoprotein VI in mice. J Exp Med 2001; 193(4): 459-69.
160. Yap CL, Hughan SC, Cranmer SL, et al. Synergistic adhesive interactions and signaling mechanisms operating between platelet glycoprotein Ib/IX and integrin alpha IIbbeta 3. Studies in human platelets ans transfected Chinese hamster ovary cells. J Biol Chem 2000; 275(52): 41377-88.
161. Feng S, Reséndiz JC, Lu X, et al. Filamin A binding to the cytoplasmic tail of glycoprotein Ibalpha regulates von Willebrand factor-induced platelet activation. Blood 2003; 102(6): 2122-9.
162. Marshall SJ, Asazuma N, Best D, et al. Glycoprotein IIb-IIIa-dependent aggregation by glycoprotein Ibalpha is reinforced by a Src family kinase inhibitor (PP1)-sensitive signalling pathway. Biochem J 2002; 361(Pt 2): 297-305.
163. Yanabu M, Ozaki Y, Nomura S, et al. Tyrosine phosphorylation and p72syk activation by an anti-glycoprotein Ib monoclonal antibody. Blood 1997; 89(5): 1590-8.
164. Baker J, Griggs RK, Falati S, et al. GPIb potentiates GPVI-induced responses in human platelets. Platelets 2004; 15(4): 207-14.
165. Arthur JF, Gardiner EE, Matzaris M, et al. Glycoprotein VI is associated with GPIb-IX-V on the membrane of resting and activated platelets. Thromb Haemost 2005; 93(4): 716-23.
166. Gardiner EE, Arthur JF, Shen Y, et al. GPIbalpha-selective activation of platelets induces platelet signaling events comparable to GPVI activation events. Platelets 2010; 21(4): 244-52.
167. Mangin P, Yuan Y, Goncalves I, et al. Signaling role for phospholipase C gamma 2 in platelet glycoprotein Ib alpha calcium flux and cytoskeletal reorganization. Involvement of a pathway distinct from FcR gamma chain and Fc gamma RIIA. J Biol Chem 2003; 278(35): 32880-91.
168. Jin J, Daniel JL, Kunapuli SP. Molecular basis for ADP-induced platelet activation. II. The P2Y1 receptor mediates ADP-induced intracellular calcium mobilization and shape change in platelets. J Biol Chem 1998; 273(4): 2030-4.
169. Rendu F, Brohard-Bohn B. The platelet release reaction: granules' constituents, secretion and functions. Platelets 2001; 12(5): 261-73.
170. Hardy AR, Hill DJ, Poole AW. Evidence that the purinergic receptor P2Y12 potentiates platelet shape change by a Rho kinase-dependent mechanism. Platelets 2005; 16(7): 415-29.
171. Pokrovskaya ID, Aronova MA, Kamykowski JA, et al. STEM tomography reveals that the canalicular system and α-granules remain separate compartments during early secretion stages in blood platelets. J Thromb Haemost 2016; 14(3): 572-84.

172. Woronowicz K, Dilks JR, Rozenvayn N, et al. The platelet actin cytoskeleton associates with SNAREs and participates in alpha-granule secretion. Biochemistry 2010; 49(21): 4533-42.
173. Koseoglu S, Peters CG, Fitch-Tewfik JL, et al. VAMP-7 links granule exocytosis to actin reorganization during platelet activation. Blood 2015; 126(5): 651-60.
174. Nurden AT, Nurden P. The gray platelet syndrome: clinical spectrum of the disease. Blood Rev 2007; 21(1): 21-36.
175. Hayward CP, Weiss HJ, Lages B, et al. The storage defects in grey platelet syndrome and alphadelta-storage pool deficiency affect alpha-granule factor V and multimerin storage without altering their proteolytic processing. Br J Haematol 2001; 113(4): 871-7.
176. Deppermann C, Nurden P, Nurden AT, et al. The Nbeal2(-/-) mouse as a model for the gray platelet syndrome. Rare Dis 2013; 1: e26561.
177. Chen D, Bernstein AM, Lemons PP, et al. Molecular mechanisms of platelet exocytosis: role of SNAP-23 and syntaxin 2 in dense core granule release. Blood 2000; 95(3): 921-9.
178. Lemons PP, Chen D, Whiteheart SW. Molecular mechanisms of platelet exocytosis: requirements for alpha-granule release. Biochem Biophys Res Commun 2000; 267(3): 875-80.
179. Ren Q, Barber HK, Crawford GL, et al. Endobrevin/VAMP-8 is the primary v-SNARE for the platelet release reaction. Mol Biol Cell 2007; 18(1): 24-33.
180. Ye S, Karim ZA, Al Hawas R, et al. Syntaxin-11, but not syntaxin-2 or syntaxin-4, is required for platelet secretion. Blood 2012; 120(12): 2484-92.
181. Golebiewska EM, Harper MT, Williams CM, et al. Syntaxin 8 regulates platelet dense granule secretion, aggregation, and thrombus stability. J Biol Chem 2015; 290(3): 1536-45.
182. Polgár J, Reed GL. A critical role for N-ethylmaleimide-sensitive fusion protein (NSF) in platelet granule secretion. Blood 1999; 94(4): 1313-8.
183. Hayward CP, Bainton DF, Smith JW, et al. Multimerin is found in the alpha-granules of resting platelets and is synthesized by a megakaryocytic cell line. JClinInvest 1993; 91(6): 2630-9.
184. Hourdillé P, Hasitz M, Belloc F, et al. Immunocytochemical study of the binding of fibrinogen and thrombospondin to ADP- and thrombin-stimulated human platelets. Blood 1985; 65(4): 912-20.
185. Legrand C, Thibert V, Dubernard V, et al. Molecular requirements for the interaction of thrombospondin with thrombin-activated human platelets: modulation of platelet aggregation. Blood 1992; 79(8): 1995-2003.
186. Holmsen H, Weiss HJ. Hereditary defect in the platelet release reaction caused by a deficiency in the storage pool of platelet adenine nucleotides. Br J Haematol 1970; 19(5): 643-9.
187. Fogelson AL, Wang NT. Platelet dense-granule centralization and the persistence of ADP secretion. Am J Physiol 1996; 270(3 Pt 2): H1131-40.
188. Arita H, Nakano T, Hanasaki K. Thromboxane A2: its generation and role in platelet activation. Prog Lipid Res 1989; 28(4): 273-301.

189. Liu L, Freedman J, Hornstein A, et al. Binding of thrombin to the G-protein-linked receptor, and not to glycoprotein Ib, precedes thrombin-mediated platelet activation. J Biol Chem 1997; 272(3): 1997-2004.
190. Mehrbod M, Trisno S, Mofrad MR. On the activation of integrin αIIbβ3: outside-in and inside-out pathways. Biophys J 2013; 105(6): 1304-15.
191. Fullard JF. The role of the platelet glycoprotein IIb/IIIa in thrombosis and haemostasis. Curr Pharm Des 2004; 10(14): 1567-76.
192. Liu J, Pestina TI, Berndt MC, et al. The roles of ADP and TXA in botrocetin/VWF-induced aggregation of washed platelets. J Thromb Haemost 2004; 2(12): 2213-22.
193. Yang H, Reheman A, Chen P, et al. Fibrinogen and von Willebrand factor-independent platelet aggregation in vitro and in vivo. J Thromb Haemost 2006; 4(10): 2230-7.
194. Remijn JA, Wu YP, Jeninga EH, et al. Role of ADP receptor P2Y(12) in platelet adhesion and thrombus formation in flowing blood. Arterioscler Thromb Vasc Biol 2002; 22(4): 686-91.
195. Oury C, Toth-Zsamboki E, Thys C, et al. The ATP-gated P2X1 ion channel acts as a positive regulator of platelet responses to collagen. Thromb Haemost 2001; 86(5): 1264-71.
196. Daniel JL, Dangelmaier C, Jin J, et al. Molecular basis for ADP-induced platelet activation. I. Evidence for three distinct ADP receptors on human platelets. J Biol Chem 1998; 273(4): 2024-9.
197. Yang J, Wu J, Jiang H, et al. Signaling through Gi family members in platelets. Redundancy and specificity in the regulation of adenylyl cyclase and other effectors. J Biol Chem 2002; 277(48): 46035-42.
198. Gachet C. ADP receptors of platelets and their inhibition. Thromb Haemost 2001; 86(1): 222-32.
199. Dorsam RT, Kunapuli SP. Central role of the P2Y12 receptor in platelet activation. J Clin Invest 2004; 113(3): 340-5.
200. Andre P, Delaney SM, LaRocca T, et al. P2Y12 regulates platelet adhesion/activation, thrombus growth, and thrombus stability in injured arteries. J Clin Invest 2003; 112(3): 398-406.
201. Hallam TJ, Rink TJ. Responses to adenosine diphosphate in human platelets loaded with the fluorescent calcium indicator quin2. J Physiol 1985; 368: 131-46.
202. Mills DC, Smith JB. The control of platelet responsiveness by agents that influence cyclic AMP metabolism. Ann N Y Acad Sci 1972; 201: 391-9.
203. Macfarlane DE, Mills DC. The effects of ATP on platelets: evidence against the central role of released ADP in primary aggregation. Blood 1975; 46(3): 309-20.
204. Larson MK, Chen H, Kahn ML, et al. Identification of P2Y12-dependent and -independent mechanisms of glycoprotein VI-mediated Rap1 activation in platelets. Blood 2003; 101(4): 1409-15.
205. Mahaut-Smith MP, Jones S, Evans RJ. The P2X1 receptor and platelet function. Purinergic Signal 2011; 7(3): 341-56.

206. Adam F, Guillin MC, Jandrot-Perrus M. Glycoprotein Ib-mediated platelet activation. A signalling pathway triggered by thrombin. Eur J Biochem 2003; 270(14): 2959-70.
207. Estevez B, Kim K, Delaney MK, et al. Signaling-mediated cooperativity between glycoprotein Ib-IX and protease-activated receptors in thrombin-induced platelet activation. Blood 2016; 127(5): 626-36.
208. Bynagari-Settipalli YS, Cornelissen I, Palmer D, et al. Redundancy and interaction of thrombin- and collagen-mediated platelet activation in tail bleeding and carotid thrombosis in mice. Arterioscler Thromb Vasc Biol 2014; 34(12): 2563-9.
209. Vu TK, Hung DT, Wheaton VI, et al. Molecular cloning of a functional thrombin receptor reveals a novel proteolytic mechanism of receptor activation. Cell 1991; 64(6): 1057-68.
210. Xu WF, Andersen H, Whitmore TE, et al. Cloning and characterization of human protease-activated receptor 4. Proc Natl Acad Sci U S A 1998; 95(12): 6642-6.
211. Kahn ML, Zheng YW, Huang W, et al. A dual thrombin receptor system for platelet activation. Nature 1998; 394(6694): 690-4.
212. Arachiche A, Mumaw MM, de la Fuente M, et al. Protease-activated receptor 1 (PAR1) and PAR4 heterodimers are required for PAR1-enhanced cleavage of PAR4 by α-thrombin. J Biol Chem 2013; 288(45): 32553-62.
213. Nakanishi-Matsui M, Zheng YW, Sulciner DJ, et al. PAR3 is a cofactor for PAR4 activation by thrombin. Nature 2000; 404(6778): 609-13.
214. Vu TK, Wheaton VI, Hung DT, et al. Domains specifying thrombin-receptor interaction. Nature 1991; 353(6345): 674-7.
215. Greco NJ, Tandon NN, Jones GD, et al. Contributions of glycoprotein Ib and the seven transmembrane domain receptor to increases in platelet cytoplasmic [Ca2+] induced by alpha-thrombin. Biochemistry 1996; 35(3): 906-14.
216. Duong H, Wu B, Tawil B. Modulation of 3D fibrin matrix stiffness by intrinsic fibrinogen-thrombin compositions and by extrinsic cellular activity. Tissue Eng Part A 2009; 15(7): 1865-76.
217. Derian CK, Santulli RJ, Tomko KA, et al. Species differences in platelet responses to thrombin and SFLLRN. receptor-mediated calcium mobilization and aggregation, and regulation by protein kinases. Thromb Res 1995; 78(6): 505-19.
218. Reheman A, Yang H, Zhu G, et al. Plasma fibronectin depletion enhances platelet aggregation and thrombus formation in mice lacking fibrinogen and von Willebrand factor. Blood 2009; 113(8): 1809-17.
219. Moser M, Nieswandt B, Ussar S, et al. Kindlin-3 is essential for integrin activation and platelet aggregation. Nat Med 2008; 14(3): 325-30.
220. Vinogradova O, Velyvis A, Velyviene A, et al. A structural mechanism of integrin alpha(IIb)beta(3) "inside-out" activation as regulated by its cytoplasmic face. Cell 2002; 110(5): 587-97.
221. Tadokoro S, Shattil SJ, Eto K, et al. Talin binding to integrin beta tails: a final common step in integrin activation. Science 2003; 302(5642): 103-6.
222. Li A, Guo Q, Kim C, et al. Integrin αII b tail distal of GFFKR participates in inside-out αII b β3 activation. J Thromb Haemost 2014; 12(7): 1145-55.

223. Lau TL, Kim C, Ginsberg MH, et al. The structure of the integrin alphaIIbbeta3 transmembrane complex explains integrin transmembrane signalling. EMBO J 2009; 28(9): 1351-61.
224. Law DA, Nannizzi-Alaimo L, Phillips DR. Outside-in integrin signal transduction. Alpha IIb beta 3-(GP IIb IIIa) tyrosine phosphorylation induced by platelet aggregation. J Biol Chem 1996; 271(18): 10811-5.
225. Phillips DR, Nannizzi-Alaimo L, Prasad KS. Beta3 tyrosine phosphorylation in alphaIIbbeta3 (platelet membrane GP IIb-IIIa) outside-in integrin signaling. Thromb Haemost 2001; 86(1): 246-58.
226. Law DA, DeGuzman FR, Heiser P, et al. Integrin cytoplasmic tyrosine motif is required for outside-in alphaIIbbeta3 signalling and platelet function. Nature 1999; 401(6755): 808-11.
227. Naik UP, Naik MU. Association of CIB with GPIIb/IIIa during outside-in signaling is required for platelet spreading on fibrinogen. Blood 2003; 102(4): 1355-62.
228. Tomiyama Y. Glanzmann thrombasthenia: integrin alpha IIb beta 3 deficiency. Int J Hematol 2000; 72(4): 448-54.
229. Oswald MW, Hunt HH, Lazarchick J. Normal range of plasma fibrinogen. Am J Med Technol 1983; 49(1): 57-9.
230. Ceriello A, Taboga C, Giacomello R, et al. Fibrinogen plasma levels as a marker of thrombin activation in diabetes. Diabetes 1994; 43(3): 430-2.
231. Laharrague PF, Cambus JP, Fillola G, et al. Plasma fibrinogen and physiological aging. Aging (Milano) 1993; 5(6): 445-9.
232. Ruggeri ZM, Dent JA, Saldívar E. Contribution of distinct adhesive interactions to platelet aggregation in flowing blood. Blood 1999; 94(1): 172-8.
233. Ikeda Y, Handa M, Kawano K, et al. The role of von Willebrand factor and fibrinogen in platelet aggregation under varying shear stress. J Clin Invest 1991; 87(4): 1234-40.
234. Bevers EM, Comfurius P, Zwaal RF. Changes in membrane phospholipid distribution during platelet activation. Biochim Biophys Acta 1983; 736(1): 57-66.
235. Lentz BR. Exposure of platelet membrane phosphatidylserine regulates blood coagulation. Prog Lipid Res 2003; 42(5): 423-38.
236. Lhermusier T, Chap H, Payrastre B. Platelet membrane phospholipid asymmetry: from the characterization of a scramblase activity to the identification of an essential protein mutated in Scott syndrome. J Thromb Haemost 2011; 9(10): 1883-91.
237. Fujii T, Sakata A, Nishimura S, et al. TMEM16F is required for phosphatidylserine exposure and microparticle release in activated mouse platelets. Proc Natl Acad Sci U S A 2015; 112(41): 12800-5.
238. Rosing J, van Rijn JL, Bevers EM, et al. The role of activated human platelets in prothrombin and factor X activation. Blood 1985; 65(2): 319-32.
239. Monroe DM, Roberts HR, Hoffman M. Platelet procoagulant complex assembly in a tissue factor-initiated system. Br J Haematol 1994; 88(2): 364-71.
240. Ahmad SS, Walsh PN. Coordinate binding studies of the substrate (factor X) with the cofactor (factor VIII) in the assembly of the factor X activating complex on the activated platelet surface. Biochemistry 2002; 41(37): 11269-76.

241. Ahmad SS, London FS, Walsh PN. The assembly of the factor X-activating complex on activated human platelets. J Thromb Haemost 2003; 1(1): 48-59.
242. Mann KG, Brummel-Ziedins K, Orfeo T, et al. Models of blood coagulation. Blood Cells Mol Dis 2006; 36(2): 108-17.
243. Triplett DA. Coagulation and bleeding disorders: review and update. Clin Chem 2000; 46(8 Pt 2): 1260-9.
244. Eilertsen KE, Østerud B. Tissue factor: (patho)physiology and cellular biology. Blood Coagul Fibrinolysis 2004; 15(7): 521-38.
245. Morrissey JH, Macik BG, Neuenschwander PF, et al. Quantitation of activated factor VII levels in plasma using a tissue factor mutant selectively deficient in promoting factor VII activation. Blood 1993; 81(3): 734-44.
246. Butenas S, van 't Veer C, Mann KG. Evaluation of the initiation phase of blood coagulation using ultrasensitive assays for serine proteases. J Biol Chem 1997; 272(34): 21527-33.
247. Ivanciu L, Krishnaswamy S, Camire RM. New insights into the spatiotemporal localization of prothrombinase in vivo. Blood 2014; 124(11): 1705-14.
248. Haynes LM, Bouchard BA, Tracy PB, et al. Prothrombin activation by platelet-associated prothrombinase proceeds through the prethrombin-2 pathway via a concerted mechanism. J Biol Chem 2012; 287(46): 38647-55.
249. Wood JP, Silveira JR, Maille NM, et al. Prothrombin activation on the activated platelet surface optimizes expression of procoagulant activity. Blood 2011; 117(5): 1710-8.
250. Swieringa F, Kuijpers MJ, Lamers MM, et al. Rate-limiting roles of the tenase complex of factors VIII and IX in platelet procoagulant activity and formation of platelet-fibrin thrombi under flow. Haematologica 2015; 100(6): 748-56.
251. Walsh PN, Bradford H, Sinha D, et al. Kinetics of the Factor XIa catalyzed activation of human blood coagulation Factor IX. J Clin Invest 1984; 73(5): 1392-9.
252. Blombäck B, Gröndahl NJ, Hessel B, et al. Primary structure of human fibrinogen and fibrin. II. Structural studies on NH2-terminal part of gamma chain. J Biol Chem 1973; 248(16): 5806-20.
253. Collen D, Kudryk B, Hessel B, et al. Primary structure of human fibrinogen and fibrin. Isolation and partial characterization of chains of fragment D. J Biol Chem 1975; 250(15): 5808-17.
254. Hessel B, Makino M, Iwanaga S, et al. Primary structure of human fibrinogen and fibrin. Structural studies on NH2-terminal part of B beta chain. Eur J Biochem 1979; 98(2): 521-34.
255. Nikolajsen CL, Dyrlund TF, Poulsen ET, et al. Coagulation factor XIIIa substrates in human plasma: identification and incorporation into the clot. J Biol Chem 2014; 289(10): 6526-34.
256. Miljić P, Heylen E, Willemse J, et al. Thrombin activatable fibrinolysis inhibitor (TAFI): a molecular link between coagulation and fibrinolysis. Srp Arh Celok Lek 2010; 138 Suppl 1: 74-8.

257. Nesheim M, Wang W, Boffa M, et al. Thrombin, thrombomodulin and TAFI in the molecular link between coagulation and fibrinolysis. Thromb Haemost 1997; 78(1): 386-91.
258. Wang W, Boffa MB, Bajzar L, et al. A study of the mechanism of inhibition of fibrinolysis by activated thrombin-activable fibrinolysis inhibitor. J Biol Chem 1998; 273(42): 27176-81.
259. Bajzar L, Manuel R, Nesheim ME. Purification and characterization of TAFI, a thrombin-activable fibrinolysis inhibitor. J Biol Chem 1995; 270(24): 14477-84.
260. Quinsey NS, Greedy AL, Bottomley SP, et al. Antithrombin: in control of coagulation. Int J Biochem Cell Biol 2004; 36(3): 386-9.
261. Wood JP, Ellery PE, Maroney SA, et al. Biology of tissue factor pathway inhibitor. Blood 2014; 123(19): 2934-43.
262. Koedam JA, Meijers JC, Sixma JJ, et al. Inactivation of human factor VIII by activated protein C. Cofactor activity of protein S and protective effect of von Willebrand factor. J Clin Invest 1988; 82(4): 1236-43.
263. Esmon CT. The protein C pathway. Chest 2003; 124(3 Suppl): 26S-32S.
264. Wood JP, Bunce MW, Maroney SA, et al. Tissue factor pathway inhibitor-alpha inhibits prothrombinase during the initiation of blood coagulation. Proc Natl Acad Sci U S A 2013; 110(44): 17838-43.
265. Izaguirre G, Zhang W, Swanson R, et al. Localization of an antithrombin exosite that promotes rapid inhibition of factors Xa and IXa dependent on heparin activation of the serpin. J Biol Chem 2003; 278(51): 51433-40.
266. Esmon CT, Esmon NL, Harris KW. Complex formation between thrombin and thrombomodulin inhibits both thrombin-catalyzed fibrin formation and factor V activation. J Biol Chem 1982; 257(14): 7944-7.
267. Esmon NL, Carroll RC, Esmon CT. Thrombomodulin blocks the ability of thrombin to activate platelets. J Biol Chem 1983; 258(20): 12238-42.
268. Fuentes-Prior P, Iwanaga Y, Huber R, et al. Structural basis for the anticoagulant activity of the thrombin-thrombomodulin complex. Nature 2000; 404(6777): 518-25.
269. Suzuki K, Stenflo J, Dahlbäck B, et al. Inactivation of human coagulation factor V by activated protein C. J Biol Chem 1983; 258(3): 1914-20.
270. Gale AJ, Cramer TJ, Rozenshteyn D, et al. Detailed mechanisms of the inactivation of factor VIIIa by activated protein C in the presence of its cofactors, protein S and factor V. J Biol Chem 2008; 283(24): 16355-62.
271. Cramer TJ, Griffin JH, Gale AJ. Factor V is an anticoagulant cofactor for activated protein C during inactivation of factor Va. Pathophysiol Haemost Thromb 2010; 37(1): 17-23.
272. Hackeng TM, van 't Veer C, Meijers JC, et al. Human protein S inhibits prothrombinase complex activity on endothelial cells and platelets via direct interactions with factors Va and Xa. J Biol Chem 1994; 269(33): 21051-8.
273. Hoylaerts M, Rijken DC, Lijnen HR, et al. Kinetics of the activation of plasminogen by human tissue plasminogen activator. Role of fibrin. J Biol Chem 1982; 257(6): 2912-9.
274. Gils A, Declerck PJ. Plasminogen activator inhibitor-1. Curr Med Chem 2004; 11(17): 2323-34.

275. Carpenter SL, Mathew P. Alpha2-antiplasmin and its deficiency: fibrinolysis out of balance. Haemophilia 2008; 14(6): 1250-4.
276. Bale MD, Westrick LG, Mosher DF. Incorporation of thrombospondin into fibrin clots. J Biol Chem 1985; 260(12): 7502-8.
277. Mancuso DJ, Kroner PA, Christopherson PA, et al. Type 2M:Milwaukee-1 von Willebrand disease: an in-frame deletion in the Cys509-Cys695 loop of the von Willebrand factor A1 domain causes deficient binding of von Willebrand factor to platelets. Blood 1996; 88(7): 2559-68.
278. McKinnon TA, Nowak AA, Cutler J, et al. Characterisation of von Willebrand factor A1 domain mutants I1416N and I1416T: correlation of clinical phenotype with flow-based platelet adhesion. J Thromb Haemost 2012; 10(7): 1409-16.
279. Yago T, Lou J, Wu T, et al. Platelet glycoprotein Ibalpha forms catch bonds with human WT vWF but not with type 2B von Willebrand disease vWF. J Clin Invest 2008; 118(9): 3195-207.
280. Tosetto A, Castaman G. How I treat type 2 variant forms of von Willebrand disease. Blood 2015; 125(6): 907-14.
281. de Moerloose P, Casini A, Neerman-Arbez M. Congenital fibrinogen disorders: an update. Semin Thromb Hemost 2013; 39(6): 585-95.
282. Lebreton A, Casini A. Diagnosis of congenital fibrinogen disorders. Ann Biol Clin (Paris) 2016; 74(4): 405-12.
283. Auton M, Zhu C, Cruz MA. The mechanism of VWF-mediated platelet GPIbalpha binding. Biophys J 2010; 99(4): 1192-201.
284. Smyth SS, Parise LV. Regulation of ligand binding to glycoprotein IIb-IIIa (integrin alpha IIb beta 3) in isolated platelet membranes. Biochem J 1993; 292 (Pt 3): 749-58.
285. Peterson DM, Stathopoulos NA, Giorgio TD, et al. Shear-induced platelet aggregation requires von Willebrand factor and platelet membrane glycoproteins Ib and IIb-IIIa. Blood 1987; 69(2): 625-8.
286. Naimushin YA, Mazurov AV. Von Willebrand factor can support platelet aggregation via interaction with activated GPIIb-IIIa and GPIb. Platelets 2004; 15(7): 419-25.
287. Asch AS, Barnwell J, Silverstein RL, et al. Isolation of the thrombospondin membrane receptor. J Clin Invest 1987; 79(4): 1054-61.
288. Bonnefoy A, Moura R, Hoylaerts MF. The evolving role of thrombospondin-1 in hemostasis and vascular biology. Cell Mol Life Sci 2008; 65(5): 713-27.
289. Beumer S, IJsseldijk MJ, de Groot PG, et al. Platelet adhesion to fibronectin in flow: dependence on surface concentration and shear rate, role of platelet membrane glycoproteins GP IIb/IIIa and VLA-5, and inhibition by heparin. Blood 1994; 84(11): 3724-33.
290. Akiyama SK, Yamada SS, Chen WT, et al. Analysis of fibronectin receptor function with monoclonal antibodies: roles in cell adhesion, migration, matrix assembly, and cytoskeletal organization. J Cell Biol 1989; 109(2): 863-75.
291. Huynh KC, Stoldt VR, Scharf RE. Contribution of distinct platelet integrins to binding, unfolding, and assembly of fibronectin. Biol Chem 2013; 394(11): 1485-93.

292. Asch AS, Leung LL, Polley MJ, et al. Platelet membrane topography: colocalization of thrombospondin and fibrinogen with the glycoprotein IIb-IIIa complex. Blood 1985; 66(4): 926-34.
293. Calzada MJ, Annis DS, Zeng B, et al. Identification of novel beta1 integrin binding sites in the type 1 and type 2 repeats of thrombospondin-1. J Biol Chem 2004; 279(40): 41734-43.
294. Krutzsch HC, Choe BJ, Sipes JM, et al. Identification of an alpha(3)beta(1) integrin recognition sequence in thrombospondin-1. J Biol Chem 1999; 274(34): 24080-6.
295. Tuszynski GP, Kowalska MA. Thrombospondin-induced adhesion of human platelets. J Clin Invest 1991; 87(4): 1387-94.
296. Sugiyama K, Emori T, Nagase S. Synthesis and secretion of plasma proteins by isolated hepatocytes of analbuminemic rats. J Biochem 1982; 92(3): 775-9.
297. Tamkun JW, Hynes RO. Plasma fibronectin is synthesized and secreted by hepatocytes. J Biol Chem 1983; 258(7): 4641-7.
298. Grieninger G, Hertzberg KM, Pindyck J. Fibrinogen synthesis in serum-free hepatocyte cultures: stimulation by glucocorticoids. Proc Natl Acad Sci U S A 1978; 75(11): 5506-10.
299. Jaffe EA, Hoyer LW, Nachman RL. Synthesis of antihemophilic factor antigen by cultured human endothelial cells. J Clin Invest 1973; 52(11): 2757-64.
300. Ewenstein BM, Warhol MJ, Handin RI, et al. Composition of the von Willebrand factor storage organelle (Weibel-Palade body) isolated from cultured human umbilical vein endothelial cells. J Cell Biol 1987; 104(5): 1423-33.
301. Wagner DD, Olmsted JB, Marder VJ. Immunolocalization of von Willebrand protein in Weibel-Palade bodies of human endothelial cells. J Cell Biol 1982; 95(1): 355-60.
302. Sporn LA, Marder VJ, Wagner DD. Inducible secretion of large, biologically potent von Willebrand factor multimers. Cell 1986; 46(2): 185-90.
303. Giblin JP, Hewlett LJ, Hannah MJ. Basal secretion of von Willebrand factor from human endothelial cells. Blood 2008; 112(4): 957-64.
304. Hayward CP, Song Z, Zheng S, et al. Multimerin processing by cells with and without pathways for regulated protein secretion. Blood 1999; 94(4): 1337-47.
305. Ni H, Papalia JM, Degen JL, et al. Control of thrombus embolization and fibronectin internalization by integrin alpha IIb beta 3 engagement of the fibrinogen gamma chain. Blood 2003; 102(10): 3609-14.
306. Di Stasio E, De Cristofaro R. The effect of shear stress on protein conformation: Physical forces operating on biochemical systems: The case of von Willebrand factor. Biophys Chem 2010; 153(1): 1-8.
307. Lawler J, Sunday M, Thibert V, et al. Thrombospondin-1 is required for normal murine pulmonary homeostasis and its absence causes pneumonia. J Clin Invest 1998; 101(5): 982-92.
308. Ni H, Yuen PS, Papalia JM, et al. Plasma fibronectin promotes thrombus growth and stability in injured arterioles. Proc Natl Acad Sci U S A 2003; 100(5): 2415-9.
309. Kanaji S, Fahs SA, Shi Q, et al. Contribution of platelet vs. endothelial VWF to platelet adhesion and hemostasis. J Thromb Haemost 2012; 10(8): 1646-52.

310. Da Q, Behymer M, Correa JI, et al. Platelet adhesion involves a novel interaction between vimentin and von Willebrand factor under high shear stress. Blood 2014; 123(17): 2715-21.
311. Cho J, Degen JL, Coller BS, et al. Fibrin but not adsorbed fibrinogen supports fibronectin assembly by spread platelets. Effects of the interaction of alphaIIb beta3 with the C terminus of the fibrinogen gamma-chain. J Biol Chem 2005; 280(42): 35490-8.
312. Adam F, Zheng S, Joshi N, et al. Analyses of cellular multimerin 1 receptors: in vitro evidence of binding mediated by alphaIIbbeta3 and alphavbeta3. ThrombHaemost 2005; 94(5): 1004-11.
313. Cahill M, Mistry R, Barnett DB. The human platelet fibrinogen receptor: clinical and therapeutic significance. Br J Clin Pharmacol 1992; 33(1): 3-9.
314. Mistry R, Cahill M, Chapman C, et al. 125I-fibrinogen binding to platelets in myeloproliferative disease. Thromb Haemost 1991; 66(3): 329-33.
315. Phillips DR, Baughan AK. Fibrinogen binding to human platelet plasma membranes. Identification of two steps requiring divalent cations. J Biol Chem 1983; 258(17): 10240-6.
316. Smith JW, Ruggeri ZM, Kunicki TJ, et al. Interaction of integrins alpha v beta 3 and glycoprotein IIb-IIIa with fibrinogen. Differential peptide recognition accounts for distinct binding sites. J Biol Chem 1990; 265(21): 12267-71.
317. Farrell DH, Thiagarajan P, Chung DW, et al. Role of fibrinogen alpha and gamma chain sites in platelet aggregation. Proc Natl Acad Sci U S A 1992; 89(22): 10729-32.
318. Mohri H, Okubo T. Affinity of Fibrinogen Binding to Platelet Membrane Glycoprotein IIb/IIIa Increases with RGDS and gamma Chain Fibrinogen Peptide Hybrid. J Thromb Thrombolysis 1996; 3(1): 45-9.
319. Kloczewiak M, Timmons S, Lukas TJ, et al. Platelet receptor recognition site on human fibrinogen. Synthesis and structure-function relationship of peptides corresponding to the carboxy-terminal segment of the gamma chain. Biochemistry 1984; 23(8): 1767-74.
320. Holmbäck K, Danton MJ, Suh TT, et al. Impaired platelet aggregation and sustained bleeding in mice lacking the fibrinogen motif bound by integrin alpha IIb beta 3. EMBO J 1996; 15(21): 5760-71.
321. Suh TT, Holmbäck K, Jensen NJ, et al. Resolution of spontaneous bleeding events but failure of pregnancy in fibrinogen-deficient mice. Genes Dev 1995; 9(16): 2020-33.
322. Prasad JM, Gorkun OV, Raghu H, et al. Mice expressing a mutant form of fibrinogen that cannot support fibrin formation exhibit compromised antimicrobial host defense. Blood 2015; 126(17): 2047-58.
323. Iwaki T, Sandoval-Cooper MJ, Paiva M, et al. Fibrinogen stabilizes placental-maternal attachment during embryonic development in the mouse. Am J Pathol 2002; 160(3): 1021-34.
324. Owaynat H, Yermolenko IS, Turaga R, et al. Deposition of fibrinogen on the surface of in vitro thrombi prevents platelet adhesion. Thromb Res 2015; 136(6): 1231-9.
325. Mammadova-Bach E, Ollivier V, Loyau S, et al. Platelet glycoprotein VI binds to polymerized fibrin and promotes thrombin generation. Blood 2015; 126(5): 683-91.
326. Zhai Z, Wu J, Xu X, et al. Fibrinogen controls human platelet fibronectin internalization and cell-surface retention. J Thromb Haemost 2007; 5(8): 1740-6.

327. Jirouskova M, Shet AS, Johnson GJ. A guide to murine platelet structure, function, assays, and genetic alterations. J Thromb Haemost 2007; 5(4): 661-9.
328. Greene TK, Schiviz A, Hoellriegl W, et al. Towards a standardization of the murine tail bleeding model. JThrombHaemost 2010; 8(12): 2820-2.
329. Liu Y, Jennings NL, Dart AM, et al. Standardizing a simpler, more sensitive and accurate tail bleeding assay in mice. World JExpMed 2012; 2(2): 30-6.
330. Vaezzadeh N, Ni R, Kim PY, et al. Comparison of the effect of coagulation and platelet function impairments on various mouse bleeding models. Thromb Haemost 2014; 112(2): 412-8.
331. Hodivala-Dilke KM, McHugh KP, Tsakiris DA, et al. Beta3-integrin-deficient mice are a model for Glanzmann thrombasthenia showing placental defects and reduced survival. J Clin Invest 1999; 103(2): 229-38.
332. To WS, Midwood KS. Plasma and cellular fibronectin: distinct and independent functions during tissue repair. Fibrogenesis Tissue Repair 2011; 4: 21.
333. Stathakis NE, Fountas A, Tsianos E. Plasma fibronectin in normal subjects and in various disease states. J Clin Pathol 1981; 34(5): 504-8.
334. Maurer LM, Tomasini-Johansson BR, Mosher DF. Emerging roles of fibronectin in thrombosis. Thromb Res 2010; 125(4): 287-91.
335. Mao Y, Schwarzbauer JE. Fibronectin fibrillogenesis, a cell-mediated matrix assembly process. Matrix Biol 2005; 24(6): 389-99.
336. Cho J, Mosher DF. Role of fibronectin assembly in platelet thrombus formation. J Thromb Haemost 2006; 4(7): 1461-9.
337. Houdijk WP, de Groot PG, Nievelstein PF, et al. Subendothelial proteins and platelet adhesion. von Willebrand factor and fibronectin, not thrombospondin, are involved in platelet adhesion to extracellular matrix of human vascular endothelial cells. Arteriosclerosis 1986; 6(1): 24-33.
338. Matsuka YV, Migliorini MM, Ingham KC. Cross-linking of fibronectin to C-terminal fragments of the fibrinogen alpha-chain by factor XIIIa. J Protein Chem 1997; 16(8): 739-45.
339. Agbanyo FR, Sixma JJ, de Groot PG, et al. Thrombospondin-platelet interactions. Role of divalent cations, wall shear rate, and platelet membrane glycoproteins. J Clin Invest 1993; 92(1): 288-96.
340. Sakai T, Johnson KJ, Murozono M, et al. Plasma fibronectin supports neuronal survival and reduces brain injury following transient focal cerebral ischemia but is not essential for skin-wound healing and hemostasis. Nat Med 2001; 7(3): 324-30.
341. Matuskova J, Chauhan AK, Cambien B, et al. Decreased plasma fibronectin leads to delayed thrombus growth in injured arterioles. Arterioscler Thromb Vasc Biol 2006; 26(6): 1391-6.
342. Mosher DF. Cross-linking of cold-insoluble globulin by fibrin-stabilizing factor. J Biol Chem 1975; 250(16): 6614-21.
343. Wight TN, Raugi GJ, Mumby SM, et al. Light microscopic immunolocation of thrombospondin in human tissues. J Histochem Cytochem 1985; 33(4): 295-302.

344. Legrand C, Dubernard V, Kieffer N, et al. Use of a monoclonal antibody to measure the surface expression of thrombospondin following platelet activation. Eur J Biochem 1988; 171(1-2): 393-9.
345. Choi KY, Kim DB, Kim MJ, et al. Higher plasma thrombospondin-1 levels in patients with coronary artery disease and diabetes mellitus. Korean Circ J 2012; 42(2): 100-6.
346. Adams JC, Bentley AA, Kvansakul M, et al. Extracellular matrix retention of thrombospondin 1 is controlled by its conserved C-terminal region. J Cell Sci 2008; 121(Pt 6): 784-95.
347. Asch AS, Liu I, Briccetti FM, et al. Analysis of CD36 binding domains: ligand specificity controlled by dephosphorylation of an ectodomain. Science 1993; 262(5138): 1436-40.
348. Bonnefoy A, Hantgan R, Legrand C, et al. A model of platelet aggregation involving multiple interactions of thrombospondin-1, fibrinogen, and GPIIbIIIa receptor. J Biol Chem 2001; 276(8): 5605-12.
349. Bacon-Baguley T, Ogilvie ML, Gartner TK, et al. Thrombospondin binding to specific sequences within the A alpha- and B beta-chains of fibrinogen. J Biol Chem 1990; 265(4): 2317-23.
350. Wang A, Liu F, Dong N, et al. Thrombospondin-1 and ADAMTS13 competitively bind to VWF A2 and A3 domains in vitro. ThrombRes 2010; 126(4): e260-e5.
351. Bonnefoy A, Daenens K, Feys HB, et al. Thrombospondin-1 controls vascular platelet recruitment and thrombus adherence in mice by protecting (sub)endothelial VWF from cleavage by ADAMTS13. Blood 2006; 107(3): 955-64.
352. Dixit VM, Haverstick DM, O'Rourke KM, et al. A monoclonal antibody against human thrombospondin inhibits platelet aggregation. Proc Natl Acad Sci U S A 1985; 82(10): 3472-6.
353. Hoyer LW, Shainoff JR. Factor VIII-related protein circulates in normal human plasma as high molecular weight multimers. Blood 1980; 55(6): 1056-9.
354. Sadler JE. Biochemistry and genetics of von Willebrand factor. AnnuRevBiochem 1998; 67: 395-424.
355. Nachman R, Levine R, Jaffe EA. Synthesis of factor VIII antigen by cultured guinea pig megakaryocytes. J Clin Invest 1977; 60(4): 914-21.
356. Yamamoto K, de Waard V, Fearns C, et al. Tissue distribution and regulation of murine von Willebrand factor gene expression in vivo. Blood 1998; 92(8): 2791-801.
357. Page C, Rose M, Yacoub M, et al. Antigenic heterogeneity of vascular endothelium. Am J Pathol 1992; 141(3): 673-83.
358. Pusztaszeri MP, Seelentag W, Bosman FT. Immunohistochemical expression of endothelial markers CD31, CD34, von Willebrand factor, and Fli-1 in normal human tissues. J Histochem Cytochem 2006; 54(4): 385-95.
359. Reinders JH, de Groot PG, Dawes J, et al. Comparison of secretion and subcellular localization of von Willebrand protein with that of thrombospondin and fibronectin in cultured human vascular endothelial cells. Biochim Biophys Acta 1985; 844(3): 306-13.

360. Yee A, Gildersleeve RD, Gu S, et al. A von Willebrand factor fragment containing the D'D3 domains is sufficient to stabilize coagulation factor VIII in mice. Blood 2014; 124(3): 445-52.
361. Terraube V, O'Donnell JS, Jenkins PV. Factor VIII and von Willebrand factor interaction: biological, clinical and therapeutic importance. Haemophilia 2010; 16(1): 3-13.
362. Vlot AJ, Koppelman SJ, van den Berg MH, et al. The affinity and stoichiometry of binding of human factor VIII to von Willebrand factor. Blood 1995; 85(11): 3150-7.
363. Auton M, Cruz MA, Moake J. Conformational stability and domain unfolding of the Von Willebrand factor A domains. J Mol Biol 2007; 366(3): 986-1000.
364. Mannucci PM, Bloom AL, Larrieu MJ, et al. Atherosclerosis and von Willebrand factor. I. Prevalence of severe von Willebrand's disease in western Europe and Israel. Br J Haematol 1984; 57(1): 163-9.
365. Rodeghiero F, Castaman G, Dini E. Epidemiological investigation of the prevalence of von Willebrand's disease. Blood 1987; 69(2): 454-9.
366. Werner EJ, Broxson EH, Tucker EL, et al. Prevalence of von Willebrand disease in children: a multiethnic study. J Pediatr 1993; 123(6): 893-8.
367. Rodeghiero F, Castaman G. Congenital von Willebrand disease type I: definition, phenotypes, clinical and laboratory assessment. Best Pract Res Clin Haematol 2001; 14(2): 321-35.
368. Flood VH, Gill JC, Friedman KD, et al. Von Willebrand disease in the United States: a perspective from Wisconsin. Semin Thromb Hemost 2011; 37(5): 528-34.
369. Chitta MS, Duhé RJ, Kermode JC. Cloning of the cDNA for murine von Willebrand factor and identification of orthologous genes reveals the extent of conservation among diverse species. Platelets 2007; 18(3): 182-98.
370. Mancuso DJ, Tuley EA, Westfield LA, et al. Structure of the gene for human von Willebrand factor. J Biol Chem 1989; 264(33): 19514-27.
371. Ginsburg D, Handin RI, Bonthron DT, et al. Human von Willebrand factor (vWF): isolation of complementary DNA (cDNA) clones and chromosomal localization. Science 1985; 228(4706): 1401-6.
372. Barrow LL, Simin K, Mohlke K, et al. Conserved linkage of neurotrophin-3 and von Willebrand factor on mouse chromosome 6. Mamm Genome 1993; 4(6): 343-5.
373. Verweij CL, Diergaarde PJ, Hart M, et al. Full-length von Willebrand factor (vWF) cDNA encodes a highly repetitive protein considerably larger than the mature vWF subunit. EMBO J 1986; 5(8): 1839-47.
374. Titani K, Kumar S, Takio K, et al. Amino acid sequence of human von Willebrand factor. Biochemistry 1986; 25(11): 3171-84.
375. Chen J, Tan K, Zhou H, et al. Modifying murine von Willebrand factor A1 domain for in vivo assessment of human platelet therapies. Nat Biotechnol 2008; 26(1): 114-9.
376. Magallon J, Chen J, Rabbani L, et al. Humanized mouse model of thrombosis is predictive of the clinical efficacy of antiplatelet agents. Circulation 2011; 123(3): 319-26.
377. Reinders JH, De Groot PG, Gonsalves MD, et al. Isolation of a storage and secretory organelle containing Von Willebrand protein from cultured human endothelial cells. Biochim Biophys Acta 1984; 804(3): 361-9.

378. Berman CL, Yeo EL, Wencel-Drake JD, et al. A platelet alpha granule membrane protein that is associated with the plasma membrane after activation. Characterization and subcellular localization of platelet activation-dependent granule-external membrane protein. J Clin Invest 1986; 78(1): 130-7.
379. Bonfanti R, Furie BC, Furie B, et al. PADGEM (GMP140) is a component of Weibel-Palade bodies of human endothelial cells. Blood 1989; 73(5): 1109-12.
380. Hattori R, Hamilton KK, Fugate RD, et al. Stimulated secretion of endothelial von Willebrand factor is accompanied by rapid redistribution to the cell surface of the intracellular granule membrane protein GMP-140. J Biol Chem 1989; 264(14): 7768-71.
381. Cramer EM, Meyer D, le Menn R, et al. Eccentric localization of von Willebrand factor in an internal structure of platelet alpha-granule resembling that of Weibel-Palade bodies. Blood 1985; 66(3): 710-3.
382. Howard MA, Montgomery DC, Hardisty RM. Factor-VIII-related antigen in platelets. Thromb Res 1974; 4(5): 617-24.
383. Nichols WL, Hultin MB, James AH, et al. von Willebrand disease (VWD): evidence-based diagnosis and management guidelines, the National Heart, Lung, and Blood Institute (NHLBI) Expert Panel report (USA). Haemophilia 2008; 14(2): 171-232.
384. Stockschlaeder M, Schneppenheim R, Budde U. Update on von Willebrand factor multimers: focus on high-molecular-weight multimers and their role in hemostasis. Blood Coagul Fibrinolysis 2014; 25(3): 206-16.
385. Fischer BE, Kramer G, Mitterer A, et al. Effect of multimerization of human and recombinant von Willebrand factor on platelet aggregation, binding to collagen and binding of coagulation factor VIII. Thromb Res 1996; 84(1): 55-66.
386. Chen CI, Federici AB, Cramer EM, et al. Studies of multimerin in patients with von Willebrand disease and platelet von Willebrand factor deficiency. BrJHaematol 1998; 103(1): 20-8.
387. Gill JC, Endres-Brooks J, Bauer PJ, et al. The effect of ABO blood group on the diagnosis of von Willebrand disease. Blood 1987; 69(6): 1691-5.
388. Bongers TN, de Maat MP, van Goor ML, et al. High von Willebrand factor levels increase the risk of first ischemic stroke: influence of ADAMTS13, inflammation, and genetic variability. Stroke 2006; 37(11): 2672-7.
389. Payne AB, Miller CH, Hooper WC, et al. High factor VIII, von Willebrand factor, and fibrinogen levels and risk of venous thromboembolism in blacks and whites. Ethn Dis 2014; 24(2): 169-74.
390. Lillicrap D. von Willebrand disease: advances in pathogenetic understanding, diagnosis, and therapy. Blood 2013; 122(23): 3735-40.
391. James PD, Notley C, Hegadorn C, et al. The mutational spectrum of type 1 von Willebrand disease: Results from a Canadian cohort study. Blood 2007; 109(1): 145-54.
392. Goodeve A, Eikenboom J, Castaman G, et al. Phenotype and genotype of a cohort of families historically diagnosed with type 1 von Willebrand disease in the European study, Molecular and Clinical Markers for the Diagnosis and Management of Type 1 von Willebrand Disease (MCMDM-1VWD). Blood 2007; 109(1): 112-21.

393. Cumming A, Grundy P, Keeney S, et al. An investigation of the von Willebrand factor genotype in UK patients diagnosed to have type 1 von Willebrand disease. Thromb Haemost 2006; 96(5): 630-41.
394. Bellissimo DB, Christopherson PA, Flood VH, et al. VWF mutations and new sequence variations identified in healthy controls are more frequent in the African-American population. Blood 2012; 119(9): 2135-40.
395. Johnsen JM, Auer PL, Morrison AC, et al. Common and rare von Willebrand factor (VWF) coding variants, VWF levels, and factor VIII levels in African Americans: the NHLBI Exome Sequencing Project. Blood 2013; 122(4): 590-7.
396. Ngo KY, Glotz VT, Koziol JA, et al. Homozygous and heterozygous deletions of the von Willebrand factor gene in patients and carriers of severe von Willebrand disease. Proc Natl Acad Sci U S A 1988; 85(8): 2753-7.
397. Eikenboom JC. Congenital von Willebrand disease type 3: clinical manifestations, pathophysiology and molecular biology. Best Pract Res Clin Haematol 2001; 14(2): 365-79.
398. Baronciani L, Cozzi G, Canciani MT, et al. Molecular defects in type 3 von Willebrand disease: updated results from 40 multiethnic patients. Blood Cells Mol Dis 2003; 30(3): 264-70.
399. Hampshire DJ, Goodeve AC. The international society on thrombosis and haematosis von Willebrand disease database: an update. Semin Thromb Hemost 2011; 37(5): 470-9.
400. Orstavik KH, Magnus P, Reisner H, et al. Factor VIII and factor IX in a twin population. Evidence for a major effect of ABO locus on factor VIII level. Am J Hum Genet 1985; 37(1): 89-101.
401. Jenkins PV, O'Donnell JS. ABO blood group determines plasma von Willebrand factor levels: a biologic function after all? Transfusion 2006; 46(10): 1836-44.
402. Franchini M, Capra F, Targher G, et al. Relationship between ABO blood group and von Willebrand factor levels: from biology to clinical implications. Thromb J 2007; 5: 14.
403. Sa Q, Hart E, Hill AE, et al. Quantitative trait locus analysis for hemostasis and thrombosis. Mamm Genome 2008; 19(6): 406-12.
404. Mohlke KL, Nichols WC, Westrick RJ, et al. A novel modifier gene for plasma von Willebrand factor level maps to distal mouse chromosome 11. Proc Natl Acad Sci U S A 1996; 93(26): 15352-7.
405. Lemmerhirt HL, Shavit JA, Levy GG, et al. Enhanced VWF biosynthesis and elevated plasma VWF due to a natural variant in the murine Vwf gene. Blood 2006; 108(9): 3061-7.
406. Mohlke KL, Purkayastha AA, Westrick RJ, et al. Mvwf, a dominant modifier of murine von Willebrand factor, results from altered lineage-specific expression of a glycosyltransferase. Cell 1999; 96(1): 111-20.
407. Lemmerhirt HL, Broman KW, Shavit JA, et al. Genetic regulation of plasma von Willebrand factor levels: quantitative trait loci analysis in a mouse model. J Thromb Haemost 2007; 5(2): 329-35.

408. Shavit JA, Manichaikul A, Lemmerhirt HL, et al. Modifiers of von Willebrand factor identified by natural variation in inbred strains of mice. Blood 2009; 114(26): 5368-74.
409. Pendu R, Christophe OD, Denis CV. Mouse models of von Willebrand disease. J Thromb Haemost 2009; 7 Suppl 1: 61-4.
410. Barrios M, Rodríguez-Acosta A, Gil A, et al. Comparative hemostatic parameters in BALB/c, C57BL/6 and C3H/He mice. Thromb Res 2009; 124(3): 338-43.
411. White TA, Pan S, Witt TA, et al. Murine strain differences in hemostasis and thrombosis and tissue factor pathway inhibitor. Thromb Res 2010; 125(1): 84-9.
412. Zhou YF, Eng ET, Zhu J, et al. Sequence and structure relationships within von Willebrand factor. Blood 2012; 120(2): 449-58.
413. Purvis AR, Gross J, Dang LT, et al. Two Cys residues essential for von Willebrand factor multimer assembly in the Golgi. ProcNatlAcadSciUSA 2007; 104(40): 15647-52.
414. Voorberg J, Fontijn R, van Mourik JA, et al. Domains involved in multimer assembly of von willebrand factor (vWF): multimerization is independent of dimerization. EMBO J 1990; 9(3): 797-803.
415. Wise RJ, Pittman DD, Handin RI, et al. The propeptide of von Willebrand factor independently mediates the assembly of von Willebrand multimers. Cell 1988; 52(2): 229-36.
416. Chiu PL, Bou-Assaf GM, Chhabra ES, et al. Mapping the interaction between factor VIII and von Willebrand factor by electron microscopy and mass spectrometry. Blood 2015; 126(8): 935-8.
417. Koppelman SJ, van Hoeij M, Vink T, et al. Requirements of von Willebrand factor to protect factor VIII from inactivation by activated protein C. Blood 1996; 87(6): 2292-300.
418. Madabhushi SR, Shang C, Dayananda KM, et al. von Willebrand factor (VWF) propeptide binding to VWF D'D3 domain attenuates platelet activation and adhesion. Blood 2012; 119(20): 4769-78.
419. Madabhushi SR, Zhang C, Kelkar A, et al. Platelet GpIba binding to von Willebrand Factor under fluid shear:contributions of the D′D3-domain, A1-domain flanking peptide and O-linked glycans. J Am Heart Assoc 2014; 3(5): e001420.
420. Casari C, Pinotti M, Lancellotti S, et al. The dominant-negative von Willebrand factor gene deletion p.P1127_C1948delinsR: molecular mechanism and modulation. Blood 2010; 116(24): 5371-6.
421. Yadegari H, Driesen J, Pavlova A, et al. Insights into pathological mechanisms of missense mutations in C-terminal domains of von Willebrand factor causing qualitative or quantitative von Willebrand disease. Haematologica 2013; 98(8): 1315-23.
422. Bodó I, Katsumi A, Tuley EA, et al. Type 1 von Willebrand disease mutation Cys1149Arg causes intracellular retention and degradation of heterodimers: a possible general mechanism for dominant mutations of oligomeric proteins. Blood 2001; 98(10): 2973-9.
423. Bonnefoy A, Romijn RA, Vandervoort PA, et al. von Willebrand factor A1 domain can adequately substitute for A3 domain in recruitment of flowing platelets to collagen. J Thromb Haemost 2006; 4(10): 2151-61.

424. Hoylaerts MF, Yamamoto H, Nuyts K, et al. von Willebrand factor binds to native collagen VI primarily via its A1 domain. Biochem J 1997; 324 (Pt 1): 185-91.
425. Huizinga EG, Martijn vdP, Kroon J, et al. Crystal structure of the A3 domain of human von Willebrand factor: implications for collagen binding. Structure 1997; 5(9): 1147-56.
426. Romijn RA, Bouma B, Wuyster W, et al. Identification of the collagen-binding site of the von Willebrand factor A3-domain. J Biol Chem 2001; 276(13): 9985-91.
427. Romijn RA, Westein E, Bouma B, et al. Mapping the collagen-binding site in the von Willebrand factor-A3 domain. J Biol Chem 2003; 278(17): 15035-9.
428. Zhou YF, Eng ET, Nishida N, et al. A pH-regulated dimeric bouquet in the structure of von Willebrand factor. EMBO J 2011; 30(19): 4098-111.
429. Denis C, Williams JA, Lu X, et al. Solid-phase von Willebrand factor contains a conformationally active RGD motif that mediates endothelial cell adhesion through the alpha v beta 3 receptor. Blood 1993; 82(12): 3622-30.
430. Perrault C, Lankhof H, Pidard D, et al. Relative importance of the glycoprotein Ib-binding domain and the RGD sequence of von Willebrand factor for its interaction with endothelial cells. Blood 1997; 90(6): 2335-44.
431. Voorberg J, Fontijn R, Calafat J, et al. Assembly and routing of von Willebrand factor variants: the requirements for disulfide-linked dimerization reside within the carboxy-terminal 151 amino acids. J Cell Biol 1991; 113(1): 195-205.
432. Huang RH, Wang Y, Roth R, et al. Assembly of Weibel-Palade body-like tubules from N-terminal domains of von Willebrand factor. Proc Natl Acad Sci U S A 2008; 105(2): 482-7.
433. van de Ven WJ, Voorberg J, Fontijn R, et al. Furin is a subtilisin-like proprotein processing enzyme in higher eukaryotes. Mol Biol Rep 1990; 14(4): 265-75.
434. Haberichter SL. von Willebrand factor propeptide: biology and clinical utility. Blood 2015; 126(15): 1753-61.
435. Wagner DD, Saffaripour S, Bonfanti R, et al. Induction of specific storage organelles by von Willebrand factor propolypeptide. Cell 1991; 64(2): 403-13.
436. Michaux G, Pullen TJ, Haberichter SL, et al. P-selectin binds to the D'-D3 domains of von Willebrand factor in Weibel-Palade bodies. Blood 2006; 107(10): 3922-4.
437. Siguret V, Ribba AS, Christophe O, et al. Characterization of recombinant von Willebrand factors mutated on cysteine 509 or 695. Thromb Haemost 1996; 76(3): 453-9.
438. Galbusera M, Zoja C, Donadelli R, et al. Fluid shear stress modulates von Willebrand factor release from human vascular endothelium. Blood 1997; 90(4): 1558-64.
439. Arya M, Anvari B, Romo GM, et al. Ultralarge multimers of von Willebrand factor form spontaneous high-strength bonds with the platelet glycoprotein Ib-IX complex: studies using optical tweezers. Blood 2002; 99(11): 3971-7.
440. Huang J, Roth R, Heuser JE, et al. Integrin alpha(v)beta(3) on human endothelial cells binds von Willebrand factor strings under fluid shear stress. Blood 2009; 113(7): 1589-97.
441. Padilla A, Moake JL, Bernardo A, et al. P-selectin anchors newly released ultralarge von Willebrand factor multimers to the endothelial cell surface. Blood 2004; 103(6): 2150-6.

442. Chauhan AK, Goerge T, Schneider SW, et al. Formation of platelet strings and microthrombi in the presence of ADAMTS-13 inhibitor does not require P-selectin or beta3 integrin. J Thromb Haemost 2007; 5(3): 583-9.
443. Schneider SW, Nuschele S, Wixforth A, et al. Shear-induced unfolding triggers adhesion of von Willebrand factor fibers. Proc Natl Acad Sci U S A 2007; 104(19): 7899-903.
444. Martin C, Morales LD, Cruz MA. Purified A2 domain of von Willebrand factor binds to the active conformation of von Willebrand factor and blocks the interaction with platelet glycoprotein Ibalpha. JThrombHaemost 2007; 5(7): 1363-70.
445. Ulrichts H, Vanhoorelbeke K, Girma JP, et al. The von Willebrand factor self-association is modulated by a multiple domain interaction. J Thromb Haemost 2005; 3(3): 552-61.
446. Tischer A, Madde P, Blancas-Mejia LM, et al. A molten globule intermediate of the von Willebrand factor A1 domain firmly tethers platelets under shear flow. Proteins 2014; 82(5): 867-78.
447. Obert B, Houllier A, Meyer D, et al. Conformational changes in the A3 domain of von Willebrand factor modulate the interaction of the A1 domain with platelet glycoprotein Ib. Blood 1999; 93(6): 1959-68.
448. Zimmermann MT, Tischer A, Whitten ST, et al. Structural origins of misfolding propensity in the platelet adhesive von Willebrand factor A1 domain. Biophys J 2015; 109(2): 398-406.
449. Auton M, Sowa KE, Smith SM, et al. Destabilization of the A1 domain in von Willebrand factor dissociates the A1A2A3 tri-domain and provokes spontaneous binding to glycoprotein Ibalpha and platelet activation under shear stress. JBiolChem 2010; 285(30): 22831-9.
450. Larsen DM, Haberichter SL, Gill JC, et al. Variability in platelet- and collagen-binding defects in type 2M von Willebrand disease. Haemophilia 2013; 19(4): 590-4.
451. Flood VH, Gill JC, Friedman KD, et al. Collagen binding provides a sensitive screen for variant von Willebrand disease. Clin Chem 2013; 59(4): 684-91.
452. Legendre P, Navarrete AM, Rayes J, et al. Mutations in the A3 domain of von Willebrand factor inducing combined qualitative and quantitative defects in the protein. Blood 2013; 121(11): 2135-43.
453. Chow TW, Hellums JD, Moake JL, et al. Shear stress-induced von Willebrand factor binding to platelet glycoprotein Ib initiates calcium influx associated with aggregation. Blood 1992; 80(1): 113-20.
454. Koutts J, Stott L, Firkin BG. Actions of ristocetin on platelets. Am J Hematol 1976; 1(3): 313-7.
455. Howard MA, Firkin BG. Ristocetin--a new tool in the investigation of platelet aggregation. Thromb Diath Haemorrh 1971; 26(2): 362-9.
456. Di Stasio E, Romitelli F, Lancellotti S, et al. Kinetic study of von Willebrand factor self-aggregation induced by ristocetin. Biophys Chem 2009; 144(3): 101-7.
457. Dong JF, Berndt MC, Schade A, et al. Ristocetin-dependent, but not botrocetin-dependent, binding of von Willebrand factor to the platelet glycoprotein Ib-IX-V complex correlates with shear-dependent interactions. Blood 2001; 97(1): 162-8.

458. Papi M, Maulucci G, De Spirito M, et al. Ristocetin-induced self-aggregation of von Willebrand factor. Eur Biophys J 2010; 39(12): 1597-603.
459. Coller BS. The effects of ristocetin and von Willebrand factor on platelet electrophoretic mobility. J Clin Invest 1978; 61(5): 1168-75.
460. Dayananda KM, Singh I, Mondal N, et al. von Willebrand factor self-association on platelet GpIbalpha under hydrodynamic shear: effect on shear-induced platelet activation. Blood 2010; 116(19): 3990-8.
461. Tronic EH, Yakovenko O, Weidner T, et al. Differential surface activation of the A1 domain of von Willebrand factor. Biointerphases 2016; 11(2): 029803.
462. Kasirer-Friede A, Cozzi MR, Mazzucato M, et al. Signaling through GP Ib-IX-V activates alpha IIb beta 3 independently of other receptors. Blood 2004; 103(9): 3403-11.
463. Wu Y, Suzuki-Inoue K, Satoh K, et al. Role of Fc receptor gamma-chain in platelet glycoprotein Ib-mediated signaling. Blood 2001; 97(12): 3836-45.
464. Mu FT, Cranmer SL, Andrews RK, et al. Functional association of phosphoinositide-3-kinase with platelet glycoprotein Ibalpha, the major ligand-binding subunit of the glycoprotein Ib-IX-V complex. J Thromb Haemost 2010; 8(2): 324-30.
465. Li Z, Xi X, Du X. A mitogen-activated protein kinase-dependent signaling pathway in the activation of platelet integrin alpha IIbbeta3. J Biol Chem 2001; 276(45): 42226-32.
466. Asazuma N, Ozaki Y, Satoh K, et al. Glycoprotein Ib-von Willebrand factor interactions activate tyrosine kinases in human platelets. Blood 1997; 90(12): 4789-98.
467. Nesbitt WS, Kulkarni S, Giuliano S, et al. Distinct glycoprotein Ib/V/IX and integrin alpha IIbbeta 3-dependent calcium signals cooperatively regulate platelet adhesion under flow. J Biol Chem 2002; 277(4): 2965-72.
468. Yin H, Liu J, Li Z, et al. Src family tyrosine kinase Lyn mediates VWF/GPIb-IX-induced platelet activation via the cGMP signaling pathway. Blood 2008; 112(4): 1139-46.
469. Alevriadou BR, Moake JL, Turner NA, et al. Real-time analysis of shear-dependent thrombus formation and its blockade by inhibitors of von Willebrand factor binding to platelets. Blood 1993; 81(5): 1263-76.
470. Chen J, Zhou H, Diacovo A, et al. Exploiting the kinetic interplay between GPIbα-VWF binding interfaces to regulate hemostasis and thrombosis. Blood 2014; 124(25): 3799-807.
471. Zhang Q, Zhou YF, Zhang CZ, et al. Structural specializations of A2, a force-sensing domain in the ultralarge vascular protein von Willebrand factor. Proc Natl Acad Sci U S A 2009; 106(23): 9226-31.
472. Luken BM, Winn LY, Emsley J, et al. The importance of vicinal cysteines, C1669 and C1670, for von Willebrand factor A2 domain function. Blood 2010; 115(23): 4910-3.
473. Xu AJ, Springer TA. Mechanisms by which von Willebrand disease mutations destabilize the A2 domain. J Biol Chem 2013; 288(9): 6317-24.
474. Lankhof H, Damas C, Schiphorst ME, et al. von Willebrand factor without the A2 domain is resistant to proteolysis. Thromb Haemost 1997; 77(5): 1008-13.
475. Suzuki M, Murata M, Matsubara Y, et al. Detection of von Willebrand factor-cleaving protease (ADAMTS-13) in human platelets. Biochem Biophys Res Commun 2004; 313(1): 212-6.

476. Liu L, Choi H, Bernardo A, et al. Platelet-derived VWF-cleaving metalloprotease ADAMTS-13. J Thromb Haemost 2005; 3(11): 2536-44.
477. Crawley JT, de Groot R, Xiang Y, et al. Unraveling the scissile bond: how ADAMTS13 recognizes and cleaves von Willebrand factor. Blood 2011; 118(12): 3212-21.
478. Goodall AH, Jarvis J, Chand S, et al. An immunoradiometric assay for human factor VIII/von Willebrand factor (VIII:vWF) using a monoclonal antibody that defines a functional epitope. Br J Haematol 1985; 59(4): 565-77.
479. Chand S, McCraw A, Hutton R, et al. A two-site, monoclonal antibody-based immunoassay for von Willebrand factor--demonstration that vWF function resides in a conformational epitope. Thromb Haemost 1986; 55(3): 318-24.
480. Lisman T, Raynal N, Groeneveld D, et al. A single high-affinity binding site for von Willebrand factor in collagen III, identified using synthetic triple-helical peptides. Blood 2006; 108(12): 3753-6.
481. Scaglione GL, Lancellotti S, Papi M, et al. The type 2B p.R1306W natural mutation of von Willebrand factor dramatically enhances the multimer sensitivity to shear stress. J Thromb Haemost 2013; 11(9): 1688-98.
482. Auton M, Sowa KE, Behymer M, et al. N-terminal flanking region of A1 domain in von Willebrand factor stabilizes structure of A1A2A3 complex and modulates platelet activation under shear stress. JBiolChem 2012; 287(18): 14579-85.
483. Fu X, Chen J, Gallagher R, et al. Shear stress-induced unfolding of VWF accelerates oxidation of key methionine residues in the A1A2A3 region. Blood 2011; 118(19): 5283-91.
484. Ganz PR, Atkins JS, Palmer DS, et al. Definition of the affinity of binding between human von Willebrand factor and coagulation factor VIII. Biochem Biophys Res Commun 1991; 180(1): 231-7.
485. Jacquemin M, Lavend'homme R, Benhida A, et al. A novel cause of mild/moderate hemophilia A: mutations scattered in the factor VIII C1 domain reduce factor VIII binding to von Willebrand factor. Blood 2000; 96(3): 958-65.
486. Fay PJ, Coumans JV, Walker FJ. von Willebrand factor mediates protection of factor VIII from activated protein C-catalyzed inactivation. J Biol Chem 1991; 266(4): 2172-7.
487. Nogami K, Shima M, Nishiya K, et al. A novel mechanism of factor VIII protection by von Willebrand factor from activated protein C-catalyzed inactivation. Blood 2002; 99(11): 3993-8.
488. Hill-Eubanks DC, Lollar P. von Willebrand factor is a cofactor for thrombin-catalyzed cleavage of the factor VIII light chain. J Biol Chem 1990; 265(29): 17854-8.
489. Fay PJ. Activation of factor VIII and mechanisms of cofactor action. Blood Rev 2004; 18(1): 1-15.
490. Regan LM, Fay PJ. Cleavage of factor VIII light chain is required for maximal generation of factor VIIIa activity. J Biol Chem 1995; 270(15): 8546-52.
491. Swami A, Kaur V. von Willebrand Disease: A Concise Review and Update for the Practicing Physician. Clin Appl Thromb Hemost 2016.

492. Peyvandi F, Garagiola I, Baronciani L. Role of von Willebrand factor in the haemostasis. Blood Transfus 2011; 9 Suppl 2: s3-8.
493. Mazurier C. Something new about type Normandy von Willebrand disease (type 2N VWD)? Thromb Haemost 2004; 92(1): 1-2.
494. Tuley EA, Gaucher C, Jorieux S, et al. Expression of von Willebrand factor "Normandy": an autosomal mutation that mimics hemophilia A. Proc Natl Acad Sci U S A 1991; 88(14): 6377-81.
495. Rodeghiero F. Von Willebrand disease: pathogenesis and management. Thromb Res 2013; 131 Suppl 1: S47-50.
496. Othman M, Chirinian Y, Brown C, et al. Functional characterization of a 13-bp deletion (c.-1522_-1510del13) in the promoter of the von Willebrand factor gene in type 1 von Willebrand disease. Blood 2010; 116(18): 3645-52.
497. Casonato A, Gallinaro L, Cattini MG, et al. Type 1 von Willebrand disease due to reduced von Willebrand factor synthesis and/or survival: observations from a case series. Transl Res 2010; 155(4): 200-8.
498. Eikenboom J, Hilbert L, Ribba AS, et al. Expression of 14 von Willebrand factor mutations identified in patients with type 1 von Willebrand disease from the MCMDM-1VWD study. J Thromb Haemost 2009; 7(8): 1304-12.
499. Haberichter SL, Castaman G, Budde U, et al. Identification of type 1 von Willebrand disease patients with reduced von Willebrand factor survival by assay of the VWF propeptide in the European study: molecular and clinical markers for the diagnosis and management of type 1 VWD (MCMDM-1VWD). Blood 2008; 111(10): 4979-85.
500. Smith NL, Chen MH, Dehghan A, et al. Novel associations of multiple genetic loci with plasma levels of factor VII, factor VIII, and von Willebrand factor: The CHARGE (Cohorts for Heart and Aging Research in Genome Epidemiology) Consortium. Circulation 2010; 121(12): 1382-92.
501. Rydz N, Swystun LL, Notley C, et al. The C-type lectin receptor CLEC4M binds, internalizes, and clears von Willebrand factor and contributes to the variation in plasma von Willebrand factor levels. Blood 2013; 121(26): 5228-37.
502. Souto JC, Almasy L, Soria JM, et al. Genome-wide linkage analysis of von Willebrand factor plasma levels: results from the GAIT project. Thromb Haemost 2003; 89(3): 468-74.
503. Jenkins PV, Pasi KJ, Perkins SJ. Molecular modeling of ligand and mutation sites of the type A domains of human von Willebrand factor and their relevance to von Willebrand's disease. Blood 1998; 91(6): 2032-44.
504. Flood VH, Lederman CA, Wren JS, et al. Absent collagen binding in a VWF A3 domain mutant: utility of the VWF:CB in diagnosis of VWD. J Thromb Haemost 2010; 8(6): 1431-3.
505. Flood VH, Gill JC, Christopherson PA, et al. Comparison of type I, type III and type VI collagen binding assays in diagnosis of von Willebrand disease. J Thromb Haemost 2012; 10(7): 1425-32.
506. Konstantopoulos K, Kamat SG, Schafer AI, et al. Shear-induced platelet aggregation is inhibited by in vivo infusion of an anti-glycoprotein IIb/IIIa antibody

fragment, c7E3 Fab, in patients undergoing coronary angioplasty. Circulation 1995; 91(5): 1427-31.
507. Hayward CP, Warkentin TE, Horsewood P, et al. Multimerin: a series of large disulfide-linked multimeric proteins within platelets. Blood 1991; 77(12): 2556-60.
508. Jeimy SB, Tasneem S, Cramer EM, et al. Multimerin 1. Platelets 2008; 19(2): 83-95.
509. Hayward CP, Hassell JA, Denomme GA, et al. The cDNA sequence of human endothelial cell multimerin. A unique protein with RGDS, coiled-coil, and epidermal growth factor-like domains and a carboxyl terminus similar to the globular domain of complement C1q and collagens type VIII and X. JBiolChem 1995; 270(31): 18246-51.
510. Hayward CP, Kelton JG. Multimerin: A Multimeric Protein Stored in Platelet Alpha-granules. Platelets 1995; 6(1): 1-10.
511. Specht CG, Schoepfer R. Deletion of multimerin-1 in alpha-synuclein-deficient mice. Genomics 2004; 83(6): 1176-8.
512. Leimeister C, Steidl C, Schumacher N, et al. Developmental expression and biochemical characterization of Emu family members. Dev Biol 2002; 249(2): 204-18.
513. Jeimy SB, Woram RA, Fuller N, et al. Identification of the MMRN1 binding region within the C2 domain of human factor V. J Biol Chem 2004; 279(49): 51466-71.
514. Jeimy SB, Fuller N, Tasneem S, et al. Multimerin 1 binds factor V and activated factor V with high affinity and inhibits thrombin generation. ThrombHaemost 2008; 100(6): 1058-67.
515. Lorenzon E, Colladel R, Andreuzzi E, et al. MULTIMERIN2 impairs tumor angiogenesis and growth by interfering with VEGF-A/VEGFR2 pathway. Oncogene 2012; 31(26): 3136-47.
516. Noy PJ, Lodhia P, Khan K, et al. Blocking CLEC14A-MMRN2 binding inhibits sprouting angiogenesis and tumour growth. Oncogene 2015; 34(47): 5821-31.
517. Christian S, Ahorn H, Novatchkova M, et al. Molecular cloning and characterization of EndoGlyx-1, an EMILIN-like multisubunit glycoprotein of vascular endothelium. J Biol Chem 2001; 276(51): 48588-95.
518. Torres MD, Van Tuinen P, Kroner PA. The human multimerin gene MMRN maps to chromosome 4q22. Cytogenet Cell Genet 2000; 88(3-4): 275-7.
519. Hayward CP. Platelet multimerin and its proteolytic processing. Thromb Haemost 1999; 82(6): 1779-80.
520. Carland TM, Gerwick L. The C1q domain containing proteins: Where do they come from and what do they do? Dev Comp Immunol 2010; 34(8): 785-90.
521. Doliana R, Bot S, Bonaldo P, et al. EMI, a novel cysteine-rich domain of EMILINs and other extracellular proteins, interacts with the gC1q domains and participates in multimerization. FEBS Lett 2000; 484(2): 164-8.
522. Colombatti A, Spessotto P, Doliana R, et al. The EMILIN/Multimerin family. Front Immunol 2011; 2: 93.
523. Colombatti A, Doliana R, Bot S, et al. The EMILIN protein family. Matrix Biol 2000; 19(4): 289-301.
524. Hayward CP, Fuller N, Zheng S, et al. Human platelets contain forms of factor V in disulfide-linkage with multimerin. Thromb Haemost 2004; 92(6): 1349-57.

525. Hayward CP, Rivard GE, Kane WH, et al. An autosomal dominant, qualitative platelet disorder associated with multimerin deficiency, abnormalities in platelet factor V, thrombospondin, von Willebrand factor, and fibrinogen and an epinephrine aggregation defect. Blood 1996; 87(12): 4967-78.
526. Jeimy SB, Quinn-Allen MA, Fuller N, et al. Location of the multimerin 1 binding site in coagulation factor V: an update. Thromb Res 2008; 123(2): 352-4.
527. Jeimy SB, Krakow EF, Fuller N, et al. An acquired factor V inhibitor associated with defective factor V function, storage and binding to multimerin 1. J Thromb Haemost 2008; 6(2): 395-7.
528. Hayward CP, Cramer EM, Kane WH, et al. Studies of a second family with the Quebec platelet disorder: evidence that the degradation of the alpha-granule membrane and its soluble contents are not secondary to a defect in targeting proteins to alpha-granules. Blood 1997; 89(4): 1243-53.
529. Sheth PM, Kahr WH, Haq MA, et al. Intracellular activation of the fibrinolytic cascade in the Quebec Platelet Disorder. Thromb Haemost 2003; 90(2): 293-8.
530. Diamandis M, Veljkovic DK, Maurer-Spurej E, et al. Quebec platelet disorder: features, pathogenesis and treatment. Blood Coagul Fibrinolysis 2008; 19(2): 109-19.
531. Kahr WH, Zheng S, Sheth PM, et al. Platelets from patients with the Quebec platelet disorder contain and secrete abnormal amounts of urokinase-type plasminogen activator. Blood 2001; 98(2): 257-65.
532. Diamandis M, Paterson AD, Rommens JM, et al. Quebec platelet disorder is linked to the urokinase plasminogen activator gene (PLAU) and increases expression of the linked allele in megakaryocytes. Blood 2009; 113(7): 1543-6.
533. Paterson AD, Rommens JM, Bharaj B, et al. Persons with Quebec platelet disorder have a tandem duplication of PLAU, the urokinase plasminogen activator gene. Blood 2010; 115(6): 1264-6.
534. Laszlo GS, Alonzo TA, Gudgeon CJ, et al. Multimerin-1 (MMRN1) as Novel Adverse Marker in Pediatric Acute Myeloid Leukemia: A Report from the Children's Oncology Group. Clin Cancer Res 2015; 21(14): 3187-95.
535. Huang Y, Zhang X, Jiang W, et al. Discovery of serum biomarkers implicated in the onset and progression of serous ovarian cancer in a rat model using iTRAQ technique. Eur J Obstet Gynecol Reprod Biol 2012; 165(1): 96-103.
536. Välk K, Vooder T, Kolde R, et al. Gene expression profiles of non-small cell lung cancer: survival prediction and new biomarkers. Oncology 2010; 79(3-4): 283-92.
537. Laszlo GS, Ries RE, Gudgeon CJ, et al. High expression of suppressor of cytokine signaling-2 predicts poor outcome in pediatric acute myeloid leukemia: a report from the Children's Oncology Group. Leuk Lymphoma 2014; 55(12): 2817-21.
538. Piao M, Mori D, Satoh T, et al. Inhibition of endothelial cell proliferation, in vitro angiogenesis, and the down-regulation of cell adhesion-related genes by genistein. Combined with a cDNA microarray analysis. Endothelium 2006; 13(4): 249-66.
539. Ross OA, Braithwaite AT, Skipper LM, et al. Genomic investigation of alpha-synuclein multiplication and parkinsonism. Ann Neurol 2008; 63(6): 743-50.

540. Park SM, Jung HY, Kim HO, et al. Evidence that alpha-synuclein functions as a negative regulator of Ca(++)-dependent alpha-granule release from human platelets. Blood 2002; 100(7): 2506-14.
541. Stefanis L. α-Synuclein in Parkinson's disease. Cold Spring Harb Perspect Med 2012; 2(2): a009399.
542. Wotjak CT. C57BLack/BOX? The importance of exact mouse strain nomenclature. Trends Genet 2003; 19(4): 183-4.
543. Specht CG, Schoepfer R. Deletion of the alpha-synuclein locus in a subpopulation of C57BL/6J inbred mice. BMC Neurosci 2001; 2: 11.
544. Chen PE, Specht CG, Morris RG, et al. Spatial learning is unimpaired in mice containing a deletion of the alpha-synuclein locus. Eur J Neurosci 2002; 16(1): 154-8.
545. George JM. The synucleins. Genome Biol 2002; 3(1): REVIEWS3002.
546. Hashimoto M, Yoshimoto M, Sisk A, et al. NACP, a synaptic protein involved in Alzheimer's disease, is differentially regulated during megakaryocyte differentiation. Biochem Biophys Res Commun 1997; 237(3): 611-6.
547. Tamo W, Imaizumi T, Tanji K, et al. Expression of alpha-synuclein, the precursor of non-amyloid beta component of Alzheimer's disease amyloid, in human cerebral blood vessels. Neurosci Lett 2002; 326(1): 5-8.
548. Laemmli UK. Cleavage of structural proteins during the assembly of the head of bacteriophage T4. Nature 1970; 227(5259): 680-5.
549. Mahmood T, Yang PC. Western blot: technique, theory, and trouble shooting. N Am J Med Sci 2012; 4(9): 429-34.
550. Nishio K, Anderson PJ, Zheng XL, et al. Binding of platelet glycoprotein Ibalpha to von Willebrand factor domain A1 stimulates the cleavage of the adjacent domain A2 by ADAMTS13. ProcNatlAcadSciUSA 2004; 101(29): 10578-83.
551. Lenting PJ, Westein E, Terraube V, et al. An experimental model to study the in vivo survival of von Willebrand factor. Basic aspects and application to the R1205H mutation. J Biol Chem 2004; 279(13): 12102-9.
552. Hulstein JJ, Lenting PJ, de Laat B, et al. beta2-Glycoprotein I inhibits von Willebrand factor dependent platelet adhesion and aggregation. Blood 2007; 110(5): 1483-91.
553. Zhang X, Halvorsen K, Zhang CZ, et al. Mechanoenzymatic cleavage of the ultralarge vascular protein von Willebrand factor. Science 2009; 324(5932): 1330-4.
554. Pruss CM, Golder M, Bryant A, et al. Pathologic mechanisms of type 1 VWD mutations R1205H and Y1584C through in vitro and in vivo mouse models. Blood 2011; 117(16): 4358-66.
555. Pruss CM, Golder M, Bryant A, et al. Use of a mouse model to elucidate the phenotypic effects of the von Willebrand factor cleavage mutants, Y1605A/M1606A and R1597W. JThrombHaemost 2012; 10(5): 940-50.
556. Zhang P, Pan W, Rux AH, et al. The cooperative activity between the carboxyl-terminal TSP1 repeats and the CUB domains of ADAMTS13 is crucial for recognition of von Willebrand factor under flow. Blood 2007; 110(6): 1887-94.

557. Drake AW, Myszka DG, Klakamp SL. Characterizing high-affinity antigen/antibody complexes by kinetic- and equilibrium-based methods. Anal Biochem 2004; 328(1): 35-43.
558. Katsamba PS, Navratilova I, Calderon-Cacia M, et al. Kinetic analysis of a high-affinity antibody/antigen interaction performed by multiple Biacore users. Anal Biochem 2006; 352(2): 208-21.
559. Szabo A, Stolz L, Granzow R. Surface plasmon resonance and its use in biomolecular interaction analysis (BIA). Curr Opin Struct Biol 1995; 5(5): 699-705.
560. Pattnaik P. Surface plasmon resonance: applications in understanding receptor-ligand interaction. Appl Biochem Biotechnol 2005; 126(2): 79-92.
561. Day YS, Baird CL, Rich RL, et al. Direct comparison of binding equilibrium, thermodynamic, and rate constants determined by surface- and solution-based biophysical methods. Protein Sci 2002; 11(5): 1017-25.
562. Mustard JF, Kinlough-Rathbone RL, Packham MA. Isolation of human platelets from plasma by centrifugation and washing. Methods Enzymol 1989; 169: 3-11.
563. Testa G, Schaft J, van der Hoeven F, et al. A reliable lacZ expression reporter cassette for multipurpose, knockout-first alleles. Genesis 2004; 38(3): 151-8.
564. Lo B, Li L, Gissen P, et al. Requirement of VPS33B, a member of the Sec1/Munc18 protein family, in megakaryocyte and platelet alpha-granule biogenesis. Blood 2005; 106(13): 4159-66.
565. Nichols WC, Cooney KA, Mohlke KL, et al. von Willebrand disease in the RIIIS/J mouse is caused by a defect outside of the von Willebrand factor gene. Blood 1994; 83(11): 3225-31.
566. Rand ML, Wang H, Pluthero FG, et al. Diannexin, an annexin A5 homodimer, binds phosphatidylserine with high affinity and is a potent inhibitor of platelet-mediated events during thrombus formation. JThrombHaemost 2012; 10(6): 1109-19.
567. Begbie ME, Mamdani A, Gataiance S, et al. An important role for the activation peptide domain in controlling factor IX levels in the blood of haemophilia B mice. ThrombHaemost 2005; 94(6): 1138-47.
568. Onley DJ, Knight CG, Tuckwell DS, et al. Micromolar Ca2+ concentrations are essential for Mg2+-dependent binding of collagen by the integrin alpha 2beta 1 in human platelets. J Biol Chem 2000; 275(32): 24560-4.
569. Nakamura T, Kambayashi J, Okuma M, et al. Activation of the GP IIb-IIIa complex induced by platelet adhesion to collagen is mediated by both alpha2beta1 integrin and GP VI. J Biol Chem 1999; 274(17): 11897-903.
570. Nesbitt WS, Giuliano S, Kulkarni S, et al. Intercellular calcium communication regulates platelet aggregation and thrombus growth. J Cell Biol 2003; 160(7): 1151-61.
571. Parker DN, Tasneem S, Farndale RW, et al. The functions of the A1A2A3 domains in von Willebrand factor include multimerin 1 binding. Thromb Haemost 2016; 116(1): 87-95.
572. Montoliu L. Mendel: a simple excel workbook to compare the observed and expected distributions of genotypes/phenotypes in transgenic and knockout mouse crosses involving up to three unlinked loci by means of a chi2 test. Transgenic Res 2012; 21(3): 677-81.

573. Baldauf C, Schneppenheim R, Stacklies W, et al. Shear-induced unfolding activates von Willebrand factor A2 domain for proteolysis. JThrombHaemost 2009; 7(12): 2096-105.
574. Feys HB, Anderson PJ, Vanhoorelbeke K, et al. Multi-step binding of ADAMTS-13 to von Willebrand factor. JThrombHaemost 2009; 7(12): 2088-95.
575. Shim K, Anderson PJ, Tuley EA, et al. Platelet-VWF complexes are preferred substrates of ADAMTS13 under fluid shear stress. Blood 2008; 111(2): 651-7.
576. Chen J, López JA. New light on an old story: von Willebrand factor binding to collagen. J Thromb Haemost 2006; 4(10): 2148-50.
577. Tischer A, Cruz MA, Auton M. The linker between the D3 and A1 domains of vWF suppresses A1-GPIbα catch bonds by site-specific binding to the A1 domain. Protein Sci 2013; 22(8): 1049-59.
578. Whittaker CA, Hynes RO. Distribution and evolution of von Willebrand/integrin A domains: widely dispersed domains with roles in cell adhesion and elsewhere. Mol Biol Cell 2002; 13(10): 3369-87.
579. Maita N, Nishio K, Nishimoto E, et al. Crystal structure of von Willebrand factor A1 domain complexed with snake venom, bitiscetin: insight into glycoprotein Ibalpha binding mechanism induced by snake venom proteins. JBiolChem 2003; 278(39): 37777-81.
580. Matsui T, Hamako J, Matsushita T, et al. Binding site on human von Willebrand factor of bitiscetin, a snake venom-derived platelet aggregation inducer. Biochemistry 2002; 41(25): 7939-46.
581. Furlan M. Von Willebrand factor: molecular size and functional activity. Ann Hematol 1996; 72(6): 341-8.
582. Federici AB, Bader R, Pagani S, et al. Binding of von Willebrand factor to glycoproteins Ib and IIb/IIIa complex: affinity is related to multimeric size. Br J Haematol 1989; 73(1): 93-9.
583. Mazzucato M, Spessotto P, Masotti A, et al. Identification of domains responsible for von Willebrand factor type VI collagen interaction mediating platelet adhesion under high flow. J Biol Chem 1999; 274(5): 3033-41.
584. McGrath RT, McRae E, Smith OP, et al. Platelet von Willebrand factor--structure, function and biological importance. Br J Haematol 2010; 148(6): 834-43.
585. Fukuda K, Doggett TA, Bankston LA, et al. Structural basis of von Willebrand factor activation by the snake toxin botrocetin. Structure 2002; 10(7): 943-50.
586. Gerritsen HE, Turecek PL, Schwarz HP, et al. Assay of von Willebrand factor (vWF)-cleaving protease based on decreased collagen binding affinity of degraded vWF: a tool for the diagnosis of thrombotic thrombocytopenic purpura (TTP). Thromb Haemost 1999; 82(5): 1386-9.
587. Golder M, Pruss CM, Hegadorn C, et al. Mutation-specific hemostatic variability in mice expressing common type 2B von Willebrand disease substitutions. Blood 2010; 115(23): 4862-9.
588. Wohner N, Legendre P, Casari C, et al. Shear stress-independent binding of von Willebrand factor-type 2B mutants p.R1306Q & p.V1316M to LRP1 explains their increased clearance. J Thromb Haemost 2015; 13(5): 815-20.

589. Lockyer S, Okuyama K, Begum S, et al. GPVI-deficient mice lack collagen responses and are protected against experimentally induced pulmonary thromboembolism. Thromb Res 2006; 118(3): 371-80.
590. Kato K, Kanaji T, Russell S, et al. The contribution of glycoprotein VI to stable platelet adhesion and thrombus formation illustrated by targeted gene deletion. Blood 2003; 102(5): 1701-7.
591. Bergmeier W, Schulte V, Brockhoff G, et al. Flow cytometric detection of activated mouse integrin alphaIIbbeta3 with a novel monoclonal antibody. Cytometry 2002; 48(2): 80-6.
592. Abeliovich A, Schmitz Y, Fariñas I, et al. Mice lacking alpha-synuclein display functional deficits in the nigrostriatal dopamine system. Neuron 2000; 25(1): 239-52.
593. Reininger AJ, Heijnen HF, Schumann H, et al. Mechanism of platelet adhesion to von Willebrand factor and microparticle formation under high shear stress. Blood 2006; 107(9): 3537-45.
594. Wang K, Zhou X, Zhou Z, et al. Platelet, not endothelial, P-selectin is required for neointimal formation after vascular injury. Arterioscler Thromb Vasc Biol 2005; 25(8): 1584-9.
595. Sun H, Yang TL, Yang A, et al. The murine platelet and plasma factor V pools are biosynthetically distinct and sufficient for minimal hemostasis. Blood 2003; 102(8): 2856-61.
596. Yang TL, Pipe SW, Yang A, et al. Biosynthetic origin and functional significance of murine platelet factor V. Blood 2003; 102(8): 2851-5.
597. Zaslavsky A, Baek KH, Lynch RC, et al. Platelet-derived thrombospondin-1 is a critical negative regulator and potential biomarker of angiogenesis. Blood 2010; 115(22): 4605-13.
598. Schoenwaelder SM, Jackson SP. Ferric chloride thrombosis model: unraveling the vascular effects of a highly corrosive oxidant. Blood 2015; 126(24): 2652-3.
599. Deutschbauer AM, Jaramillo DF, Proctor M, et al. Mechanisms of haploinsufficiency revealed by genome-wide profiling in yeast. Genetics 2005; 169(4): 1915-25.
600. Valastyan JS, Lindquist S. Mechanisms of protein-folding diseases at a glance. Dis Model Mech 2014; 7(1): 9-14.
601. Hillery CA, Mancuso DJ, Evan Sadler J, et al. Type 2M von Willebrand disease: F606I and I662F mutations in the glycoprotein Ib binding domain selectively impair ristocetin- but not botrocetin-mediated binding of von Willebrand factor to platelets. Blood 1998; 91(5): 1572-81.
602. Riddell AF, Gomez K, Millar CM, et al. Characterization of W1745C and S1783A: 2 novel mutations causing defective collagen binding in the A3 domain of von Willebrand factor. Blood 2009; 114(16): 3489-96.
603. Casaña P, Cabrera N, Haya S, et al. Von Willebrand's disease: a novel mutation, P1824H and the incidence of R1205H defect among families with dominant quantitative von Willebrand factor deficiency. Haematologica 2006; 91(8): 1130-3.

604. Strony J, Beaudoin A, Brands D, et al. Analysis of shear stress and hemodynamic factors in a model of coronary artery stenosis and thrombosis. Am J Physiol 1993; 265(5 Pt 2): H1787-96.
605. Siegel JM, Markou CP, Ku DN, et al. A scaling law for wall shear rate through an arterial stenosis. J Biomech Eng 1994; 116(4): 446-51.
606. Liu J, Pestina TI, Berndt MC, et al. Botrocetin/VWF-induced signaling through GPIb-IX-V produces TxA2 in an alphaIIbbeta3- and aggregation-independent manner. Blood 2005; 106(8): 2750-6.
607. Matsushita T, Meyer D, Sadler JE. Localization of von willebrand factor-binding sites for platelet glycoprotein Ib and botrocetin by charged-to-alanine scanning mutagenesis. J Biol Chem 2000; 275(15): 11044-9.
608. Rayes J, Hollestelle MJ, Legendre P, et al. Mutation and ADAMTS13-dependent modulation of disease severity in a mouse model for von Willebrand disease type 2B. Blood 2010; 115(23): 4870-7.
609. Massberg S, Gawaz M, Grüner S, et al. A crucial role of glycoprotein VI for platelet recruitment to the injured arterial wall in vivo. J Exp Med 2003; 197(1): 41-9.
610. Falati S, Patil S, Gross PL, et al. Platelet PECAM-1 inhibits thrombus formation in vivo. Blood 2006; 107(2): 535-41.
611. Westrick RJ, Winn ME, Eitzman DT. Murine models of vascular thrombosis (Eitzman series). Arterioscler Thromb Vasc Biol 2007; 27(10): 2079-93.
612. Sachs UJ, Nieswandt B. In vivo thrombus formation in murine models. CircRes 2007; 100(7): 979-91.
613. Dubois C, Panicot-Dubois L, Gainor JF, et al. Thrombin-initiated platelet activation in vivo is vWF independent during thrombus formation in a laser injury model. J Clin Invest 2007; 117(4): 953-60.
614. Rosen ED, Raymond S, Zollman A, et al. Laser-induced noninvasive vascular injury models in mice generate platelet- and coagulation-dependent thrombi. Am J Pathol 2001; 158(5): 1613-22.
615. Kalia N, Auger JM, Atkinson B, et al. Critical role of FcR gamma-chain, LAT, PLCgamma2 and thrombin in arteriolar thrombus formation upon mild, laser-induced endothelial injury in vivo. Microcirculation 2008; 15(4): 325-35.
616. Saniabadi AR, Umemura K, Matsumoto N, et al. Vessel wall injury and arterial thrombosis induced by a photochemical reaction. Thromb Haemost 1995; 73(5): 868-72.
617. Matsuno H, Uematsu T, Nagashima S, et al. Photochemically induced thrombosis model in rat femoral artery and evaluation of effects of heparin and tissue-type plasminogen activator with use of this model. J Pharmacol Methods 1991; 25(4): 303-17.
618. Matsuno H, Kozawa O, Okada K, et al. Plasmin generation plays different roles in the formation and removal of arterial and venous thrombus in mice. Thromb Haemost 2002; 87(1): 98-104.
619. Labat-gest V, Tomasi S. Photothrombotic ischemia: a minimally invasive and reproducible photochemical cortical lesion model for mouse stroke studies. J Vis Exp 2013(76).

620. Singh R, Pan S, Mueske CS, et al. Tissue factor pathway inhibitor deficiency enhances neointimal proliferation and formation in a murine model of vascular remodelling. Thromb Haemost 2003; 89(4): 747-51.
621. Kumar A, Lindner V. Remodeling with neointima formation in the mouse carotid artery after cessation of blood flow. Arterioscler Thromb Vasc Biol 1997; 17(10): 2238-44.
622. Sasaki T, Kuzuya M, Cheng XW, et al. A novel model of occlusive thrombus formation in mice. Lab Invest 2004; 84(11): 1526-32.
623. Mangin P, Yap CL, Nonne C, et al. Thrombin overcomes the thrombosis defect associated with platelet GPVI/FcRgamma deficiency. Blood 2006; 107(11): 4346-53.
624. Huang L, Lei D, Dong W, et al. Thrombosis Model in Mouse Carotid Induced by Guidewire. J Med Biol Eng 2016; 36(2): 236–44.
625. Konishi H, Katoh Y, Takaya N, et al. Platelets activated by collagen through immunoreceptor tyrosine-based activation motif play pivotal role in initiation and generation of neointimal hyperplasia after vascular injury. Circulation 2002; 105(8): 912-6.
626. Sata M, Maejima Y, Adachi F, et al. A mouse model of vascular injury that induces rapid onset of medial cell apoptosis followed by reproducible neointimal hyperplasia. J Mol Cell Cardiol 2000; 32(11): 2097-104.
627. DiMinno G, Silver MJ. Mouse antithrombotic assay: a simple method for the evaluation of antithrombotic agents in vivo. Potentiation of antithrombotic activity by ethyl alcohol. J Pharmacol Exp Ther 1983; 225(1): 57-60.
628. Verhenne S, Denorme F, Libbrecht S, et al. Platelet-derived VWF is not essential for normal thrombosis and hemostasis but fosters ischemic stroke injury in mice. Blood 2015; 126(14): 1715-22.